

UC Santa Barbara

UC Santa Barbara Electronic Theses and Dissertations

Title

Gold Catalysis Enabled Cascade Reactions from C-C Triple Bonds

Permalink

<https://escholarship.org/uc/item/3094v2mp>

Author

Zheng, Zhitong

Publication Date

2017

Peer reviewed|Thesis/dissertation

UNIVERSITY OF CALIFORNIA

Santa Barbara

Gold Catalysis Enabled Cascade Reactions from C-C Triple Bonds

A dissertation submitted in partial satisfaction of the
requirements for the degree Doctor of Philosophy
in Chemistry

by

Zhitong Zheng

Committee in Charge:

Professor Liming Zhang, Chair

Professor Bruce Lipshutz

Professor Daniel Little

Professor Norbert Reich

December 2017

The dissertation of Zhitong Zheng is approved.

Bruce Lipshutz

Daniel Little

Norbert Reich

Liming Zhang, Committee Chair

October 2017

Gold Catalysis Enabled Cascade Reactions from C-C Triple Bonds

Copyright © 2017

by

Zhitong Zheng

ACKNOWLEDGEMENTS

First, I would like to thank my advisor, Prof. Liming Zhang. During my five years' doctoral study, I was greatly inspired by Liming's great passion in organic chemistry. With his guidance and influence, I learned to maintain my work efficiency, pay attention to details, while keeping a prudent attitude towards the unknown world of science. Those traits would be invaluable in my future journey of organic chemistry research.

I would like to express my appreciation to my committee members: Professors Bruce Lipshutz, Daniel Little, and Norbert Reich. Their valuable advice after the candidacy exam really helped me to improve during the rest of the years of my doctoral study. Of course, I would also like to express my gratitude to my undergraduate research advisor, Prof. Jianbo Wang at Peking University. He lead me into the field and showed me the beauty of organic chemistry, which sparked my deep interest in scientific research.

I would also give my cheers to my fellow lab mates, both current and former, for our bond of brotherhood during the time working in the same lab. Lab work can get mundane from time to time, and it my wonderful lab mates that makes the everyday work in the lab so enjoyable and exciting.

Finally, I would thank my wife Mengya Tao and my parents Bingcheng Zheng and Yufen Liu, for their unconditional love and support. Pursuing a PhD degree in a different country is quite challenging, and there are moments of high and moments of low. No matter what happens, Mengya and my parents are always standing by my side, sharing my joy, and pulling me out of depression. Without them, I would never be able to reach this milestone in my life.

VITA OF ZHITONG ZHENG

September 2017

EDUCATION

- 2012-2017** Ph. D. in Chemistry, Department of Chemistry and Biochemistry, University of California, Santa Barbara.
- 2008-2012** Bachelor of Science, College of Chemistry and Molecular Engineering, Peking University.

PROFESSIONAL EMPLOYMENT

- 2012-2017** Teaching Assistant, Department of Chemistry and Biochemistry, University of California, Santa Barbara.
- 2012-2017** Graduate Student Researcher, Department of Chemistry and Biochemistry, University of California, Santa Barbara.
- 2010-2011** Undergraduate Student Researcher, College of Chemistry and Molecular Engineering, Peking University. Research advisor: Prof. Jianbo Wang

PUBLICATIONS

-- *Graduate Work (University of California, Santa Barbara, 2012-)*

- 10 Zheng, Z.; Wang, Z.; Wang, Y.; Zhang, L. "Au-Catalysed Oxidative Cyclisation" *Chem. Soc. Rev.*, **2016**, *45*, 4448-4458.
- 9 Zheng, Z.; Zhang, L. "C-H Insertions in Oxidative Gold Catalysis: Synthesis of Polycyclic 2*H*-Pyrans-3(6*H*)-ones via a Relay Strategy" *Org. Chem. Front.*, **2015**, *2*, 1556-1560.

- 8 Wang, Y.; Zheng, Z.; Zhang, L. "Intramolecular Insertions into Unactivated C(sp³)-H Bonds by Oxidatively Generated β -Diketone- α -Gold Carbenes: Synthesis of Cyclopentanones" *J. Am. Chem. Soc.*, **2015**, *137*, 5316-5319.
- 7 Ji, K.; Zheng, Z.; Wang Z.; Zhang, L. "Enantioselective Oxidative Gold Catalysis Enabled by a Designed Chiral *P,N*-Bidentate Ligand" *Angew. Chem. Int. Ed.*, **2015**, *54*, 1245-1249.
- 6 Wang, Y.; Zheng, Z.; Zhang, L. "Ruthenium-Catalyzed Oxidative Transformations of Terminal Alkynes to Ketenes by Using Tethered Sulfoxides: Access to β -Lactams and Cyclobutanones" *Angew. Chem. Int. Ed.*, **2014**, *53*, 9572-9576.
- 5 Zheng, Z.; Touve, M.; Barnes, J.; Reich, N.; Zhang, L. "Synthesis-Enabled Probing of Mitosene Structural Space Leads to Improved IC₅₀ over Mitomycin C" *Angew. Chem. Int. Ed.*, **2014**, *53*, 9302-9305.
- 4 Zheng, Z.; Tu, H.; Zhang, L. "One-Pot Synthesis of Fused Pyrroles through a Key Gold-Catalysis-Triggered Cascade" *Chem. Eur. J.*, **2014**, *20*, 2445-2448.

-- *Undergraduate Work (Peking University, 2010-2012)*

- 3 Qiu, D.; Jin, L.; Zheng, Z.; Meng, H.; Mo, F.; Wang, X.; Zhang, Y.; Wang, J. "Synthesis of Pinacol Arylboronates from Aromatic Amines: A Metal-Free Transformation" *J. Org. Chem.*, **2013**, *78*, 1923-1933.
- 2 Qiu, D.; Zheng, Z.; Mo, F.; Xiao, Q.; Tian, Y.; Zhang, Y.; Wang, J. "Gold(III)-Catalyzed Direct Acetoxylation of Arenes with Iodobenzene Diacetate" **Org. Lett.**, **2011**, *13*, 4988-4991.
- 1 Qiu, D.; Mo, F.; Zheng, Z.; Zhang, Y.; Wang, J. "Gold(III)-Catalyzed Halogenation of Aromatic Boronates with *N*-Halosuccinimides" *Org. Lett.*, **2010**, *12*, 5474-5477.

CONFERENCE PRESENTATIONS

- 3 "Gold Catalysis in the Synthesis of Polycyclic Structures" Short talk at 2016 DOC Graduate Research Symposium, Bryn Mawr PA, July 2016.

- 2 “C-H insertions in oxidative gold catalysis: Synthesis of Polycyclic Dihydropyran-3-ones via a Relay Strategy” Short talk at the 25th ISHC Congress, Santa Barbara CA, August 2015.
- 1 “C-H Insertions in Oxidative Gold Catalysis: Synthesis of Bicyclic Dihydropyran-3-ones from *in situ* Generated α -Oxo Gold Carbenes through the Relay of Vinyl Cation Intermediates” Poster at the 249th ACS National Meeting, Denver CO, March 2015.

AWARDS

- 2016** Graduate Division Dissertation Fellowship, UC Santa Barbara.
- 2015** Robert H. De Wolfe Graduate Teaching Award, UC Santa Barbara.
- 2013** Phi Lambda Upsilon Award, UC Santa Barbara.

ABSTRACT

Gold Catalysis Enabled Cascade Reactions from C-C Triple Bonds

by

Zhitong Zheng

Homogeneous gold catalysis has been a very hot topic in recent decades. With its unparalleled π -acidity, cationic gold complex exhibits a strong affinity to alkynes and promotes nucleophilic attack across C-C triple bonds. Such nucleophilic attacks lead to various reactive intermediates that trigger a wide range of cascade reactions, building molecular complexity readily in one step. My doctoral study is focused on the development and application of gold-catalyzed cascade reaction with alkyne substrates. In this dissertation, two methodology studies and two applications of gold-catalyzed cascades will be discussed. Namely: 1) one-pot synthesis of fused pyrroles from ketones and *N*-alkylhydroxylations via a gold catalysis-triggered cascade; 2) synthesis of polycyclic 2*H*-pyran-3(6*H*)-ones via a vinyl cation C(sp³)-H insertion triggered by oxidative gold catalysis; 3) streamlined synthesis of highly potent mitomycin C analogs with gold/platinum-catalyzed cycloisomerization cascade; and 4) gold-catalysis-activated stereoselective glycosylation reaction to construct 1,2-*cis* glycosyl linkage in glycoconjugates and oligosaccharides.

TABLE OF CONTENTS

Chapter 1 Introduction to Gold-Catalyzed Cascade Reactions of Alkynes	1
1.1 Gold Catalysis 101: History, Types of Catalyst, and Modes of Reactivity	1
1.2 Gold-Catalyzed Cascade Reactions of Alkynes	4
1.2.1 Cascades Initiated by Formation of Alkene Intermediates	4
1.2.1.1 Through Intramolecular Additions of Heteronucleophiles	5
1.2.1.2 Through Intermolecular Addition of Heteronucleophiles.....	9
1.2.1.3 Through Hydroarylation Reaction	14
1.2.1.4 Consecutive Nucleophilic Additions	15
1.2.2 Cascade Initiated by Formation of Gold Carbenoids	17
1.2.2.1 Through Enyne Cycloisomerization Reactions	17
1.2.2.2 Through 1,2-Acyloxy Migration of Propargylic Carboxylates/Acetals	22
1.2.2.3 Through Gold Vinylidenes and Related Intermediates.....	25
1.2.2.4 Through Oxidatively-Generated Gold Carbenes	30
1.3 Summary	34
1.4 References.....	34
Chapter 2 One-Pot Synthesis of Fused Pyrroles via a Gold Catalysis-Triggered Cascade	38
2.1 Design of a Gold Catalysis-Triggered Cascade	38
2.2 Condition Study, and Approaches to Achieve a One-Pot Reaction.....	40
2.3 Scope Study of the Cascade Reaction.....	42
2.4 Conclusion	45
2.5 Experimental Details.....	45
2.6 References.....	55

Chapter 3 Insertion into Unactivated C-H Bonds with Vinyl Cation Generated by Oxidative Gold Carbene Chemistry	57
3.1 Introduction of Metal Carbene C-H Insertion Chemistry	57
3.2 Our Strategy and Initial Study to a Relayed C-H Insertion Process	58
3.3 Scope Study of C-H Insertion with Vinyl Cation Generated by Oxidative Gold Chemistry	62
3.4 Mechanistic Studies that Supports a Concerted Pathway	65
3.5 Conclusion	67
3.6 Acknowledgements	68
3.7 Experimental Details	68
3.8 References	96
Chapter 4 Application of Gold-Catalyzed Cascade Reactions of Alkynes	98
4.1 Introduction	98
4.2 Streamlined Synthesis of New Mitosene Derivatives with Improved IC ₅₀ over Mitomycin C	98
4.2.1 A Brief History of Mitomycin C and Analogs	98
4.2.2 Our Preliminary Studies on a 7-Methoxymitosene Analog	99
4.2.3 MTSB-1: Evaluation of Potency and Mechanism	101
4.2.4 Synthesis of Derivatives Aiming at Higher Potency	105
4.2.5 Conclusion	108
4.2.6 Experimental Details	108
4.3 Gold-Catalyzed Stereoselective Glycosylation Reaction to Access 1,2-cis Glycosyl Linkage	123
4.3.1 Glycosylation: History and Challenges	123
4.3.2 Gold-Catalyzed Glycosylation with Thioglycoside Donors: Tackling the Problem	125

4.3.3 Condition Study, Scope Study, and Future Works	127
4.3.4 Conclusion	130
4.3.5 Experimental Details	131
4.4 References.....	140
Appendix: NMR Spectra for Selected Compounds	142
NMR Spectra for Compounds in Chapter 2.....	142
NMR Spectra for Compounds in Chapter 3.....	164
NMR Spectra for Compounds in Chapter 4.....	222

LIST OF SCHEMES, FIGURES, AND TABLES

Scheme 1. Early Reports of Homogeneous Gold Catalysis.....	1
Scheme 2. General Reactivities of Gold Activated Alkynes	4
Scheme 3. Gold-Catalyzed Tandem Cyclization-Isomerization or Cyclization-Dehydration Process	5
Scheme 4. Polycyclic Structures from Gold-Catalyzed Nucleophilic Addition Cascades ..	6
Scheme 5. Cascade Initiated by Ethers/Thioethers Attacking Gold-Activated Alkyne	7
Scheme 6. A Gold-Catalyzed Cyclization-Nucleophilic Addition Cascade.....	8
Scheme 7. Gold-Catalyzed Cyclization-Cycloaddition Cascade.....	8
Scheme 8. Etherification or Friedel-Crafts Reaction with 2-Alkynylbenzoates.....	9
Scheme 9. The Formation of Cyclic Acetals and Thioacetals from Diols and Dithiols....	10
Scheme 10. Synthesis of Azaisoflavanone Derivatives	10
Scheme 11. Double Hydroamination/Hydration of 1,3-Diynes	11
Scheme 12. Access to 1,2-Dihydroquinolines through Gold-Catalyzed Formal [4+2] Cycloaddition.....	12
Scheme 13. Claisen Rearrangement of Nucleophilic Addition Product.....	13
Scheme 14. A Novel Indole Synthesis from Aryl Hydroxylamine and Alkyne.....	13
Scheme 15. Transformation of Alkyne-Tethered Indoles.....	14
Scheme 16. Nucleophilic Trapping of Iminium Species in Gold-Catalyzed Hydroarylation	15
Scheme 17. Consecutive Nucleophilic Addition of Diynes.....	16
Scheme 18. Synthesis of Azahelicenes and S-Shaped Double Azahelicene	17
Scheme 19. Hashmi's First Report of Enyne Cycloisomerization	18
Scheme 20. Echavarren's Work on 1,6-Enyne Cycloisomerization.....	18
Scheme 21. Application of Echavarren's 1,6-Enyne Cycloisomerization.....	19
Scheme 22. Construction of a Fused 5,7,6-Tricyclic System	21
Scheme 23. Toste Group's Studies in 1,5-Enyne Cycloisomerization	21
Scheme 24. Reactivity of Propargylic Carboxylates/Acetals	22
Scheme 25. Synthesis of 2,5-Dihydrofurans from Propargyl Acetals	23

Scheme 26. Trapping of Gold Carbene Generated by 1,2-Migration of Propargylic Carboxylate	24
Scheme 27. Synthesis of (1 <i>Z</i> , 3 <i>E</i>)-1-Halo-2-carboxy-1,3-dienes	24
Scheme 28. Rautenstrauch Rearrangement of Propargylic Carboxylates	25
Scheme 29. From Benzene-1,2-diynes to Gold Vinylidene	26
Scheme 30. Hashmi's Studies on Benzene-1,2-diyne Chemistry	27
Scheme 31. Mechanistic Switch of Dual-Gold Catalysis	28
Scheme 32. Gold Vinylidenes from the Isomerization of Iodoalkynes	29
Scheme 33. Generation of Gold Vinylidenes with Terminal Alkynes	29
Scheme 34. Unactivated C(sp ³)-H Insertion of Gold Vinylidene	30
Scheme 35. Gold Carbenes Generated by an Oxidative Process	31
Scheme 36. Nucleophilic Trapping of Oxidatively-Generated Gold Carbenes	31
Scheme 37. Oxazole Synthesis with Oxidatively-Generated Gold Carbene	32
Scheme 38. Cyclopropanation of Oxidatively-Generated Gold Carbene	32
Scheme 39. Umpolung Chemistry of Oxidatively-Generated Gold Carbene	33
Scheme 40. Insertion of Oxidatively-Generated Gold Carbene into Unactivated C(sp ³)-H Bonds	34
Scheme 41. Pyrrole Synthesis from Oximes and Alkynes	38
Scheme 42. Examples of Pyrrole/Indole Synthesis Triggered by Gold-Catalyzed Nucleophilic Addition	39
Scheme 43. Design of a Cascade Approach towards 1,2-Fused Pyrroles	40
Scheme 44. Applying Acyclic 1,3-Dicarbonyl Compounds to the Reaction	43
Scheme 45. Direct C(sp ³)-H Insertion and Relayed C(sp ³)-H Insertion	59
Scheme 46. Results Supporting a Mostly Concerted C-H Insertion Mechanism	66
Scheme 47. Rationale for the Observed Diastereoselectivity	67
Scheme 48. Au/Pt-Catalyzed Synthesis of 7-Methoxymitosene Analogs	100
Scheme 49. Established Mechanism of DNA Cross-Linking by MMC and Hypothesized Mechanism of Action for MTSB-1	102
Scheme 50. Synthesis of Mechanistic Probes for MSTB-1	103
Scheme 51. Synthesis of Chloride Derivatives MTSB-5, MTSB-6, and MTSB-7	106
Scheme 52. Typical Pattern of Chemical Glycosylation	124

Scheme 53. Previous Studies on Gold-Catalyzed Glycosylation with Thioglycoside Donors	125
Scheme 54. Initial Results with the New Thioglycoside Donor	126
Scheme 55. Stereoselectivity Erosion Caused by Benzothiophene Side Product	130
Scheme 56. Synthesis of Disaccharide	130
Figure 1. Common Ligands and Counterions for Gold Catalysts.....	3
Figure 2. Structure of Mitomycin C.....	98
Figure 3. Bio-Active Natural Products Carrying Electrophilic Cyclopropane Rings.....	102
Figure 4. IC ₅₀ curves and values for MMC against PPC-1 cells and RWPE-1 cells, and MTSB-1 against PPC-1 cells and RWPE-1 cells.....	103
Figure 5. IC ₅₀ curves and values for MTSB-2 against PPC-1 cells and RWPE-1 cells, MTSB-3 against PPC-1 cells and RWPE-1 cells, and MTSB-4 against PPC-1 cells and RWPE-1 cells.....	105
Figure 6. IC ₅₀ curves and values for MTSB-5 against PPC-1 cells and RWPE-1 cells, MTSB-6 against PPC-1 cells and RWPE-1 cells, and MTSB-7 against PPC-1 cells and RWPE-1 cells.....	107
Figure 7. Design of a New Thioglycoside Donor for Stereoselective Glycosylation.....	126
Table 1. Reaction Discovery and Catalyst Optimization.....	41
Table 2. Optimizing the Condensation Step	42
Table 3. One-Pot Synthesis of Tricyclic Pyrroles from 1,3-Cyclodiketones.....	42
Table 4. Expanded Reaction Scope	44
Table 5. Initial reaction discovery and optimization	61
Table 6. Reaction Scope with Cyclohexanone-Derived Substrates.....	63
Table 7. Reaction Scope with Aldehyde-Based Substrates	64
Table 8. Condition Study	128
Table 9. Scope Study in Glycoconjugate Synthesis.....	129

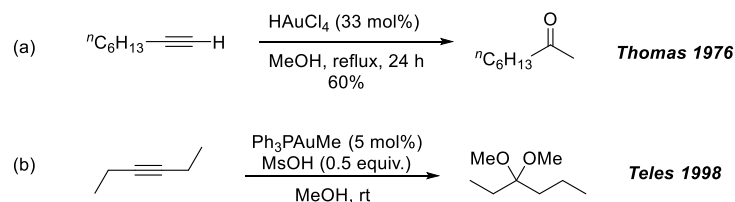
Chapter 1 Introduction to Gold-Catalyzed Cascade Reactions of Alkynes

1.1 Gold Catalysis 101: History, Types of Catalyst, and Modes of Reactivity

Gold has been recognized and valued by humans since ancient times. Despite its stoichiometric chemistry being thoroughly investigated,¹ gold has not been widely utilized in transition metal catalysis until recent decades.

One early milestone of homogeneous gold catalysis was reported by the Thomas group in 1976, where chloroauric acid was used to promote an alkyne hydration reaction (Scheme 1a).² Unfortunately, not realizing the catalytic potential of Au(III) salt, the author reported the transformation as a “gold(III) oxidation”. Apart from a few sporadic studies,³ cationic gold salts and its potent catalytic activity was largely neglected until the end of the last century.

Scheme 1. Early Reports of Homogeneous Gold Catalysis



In 1998, Teles group reported an Au(I)-catalyzed nucleophilic addition of methanol to internal alkynes, marking another milestone in the development of homogeneous gold catalysis (Scheme 1b).⁴ The highlight of this work is the first introduction of ligands on cationic gold(I) catalyst, which soon became broadly implemented in the emerging field of homogeneous gold catalysis.

Extensive studies in the last two decades' "gold rush" clearly showed that ligands play a crucial role in homogeneous gold catalysis. Ligands significantly stabilize the cationic gold center, extending the catalyst lifetime in the reaction media. Moreover, introduction of ligands with different steric, electronic, and chiral properties makes it possible to fine tune the catalytic activities of the gold center, leading to desirable controls of chemo-, regio-, and stereoselectivities in gold-catalyzed reactions.⁵ On the other hand, counterions have also been shown to affect reactivities of gold catalysts as well as selectivities of reactions, although the exact nature of "counterion effects" is yet to be fully rationalized.⁶ A summary of most frequently used gold catalysts is shown below in Figure 1.

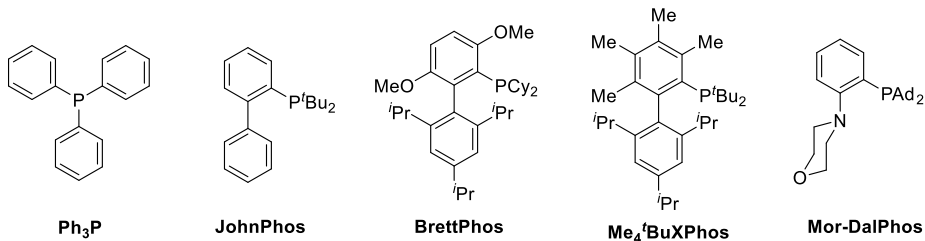
The most prominent advantage of cationic gold catalyst lies in its potent soft Lewis acidity, which leads to its strong affinity to π bonds, especially alkynes. The subsequent gold-alkyne complex is susceptible to attacks by a wide array of nucleophiles. Such nucleophilic attack, according to studies performed independently by Toste group⁷ and Hashmi group,⁸ is strictly following an *anti*-addition manner and affords an alkenylgold intermediate (i.e., **1-1**, Scheme 2).

1-1 can then undergo further transformations. When protic nucleophiles (Nu-H) are used, its protodeauration leads to an anti-addition of nucleophile over an unsaturated bond (Scheme 2, pathway A). Non-protic nucleophiles (Nu-E), apart from following a similar nucleophilic addition pathway A, is possible to undergo a competing pathway B, where the electrophile released could access the β -position of the alkenylgold intermediate, leading to a gold carbenoid species **1-4**. Such a gold carbenoid can exhibit reactivity either as "gold stabilized carbocation" or as gold carbene, depending on the electronic

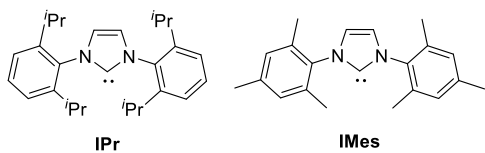
and plausibly the steric properties of the ligand used and the substituents to the carbene center.⁹

Figure 1. Common Ligands and Counterions for Gold Catalysts

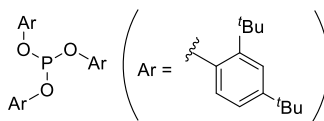
Examples of Phosphine Ligands



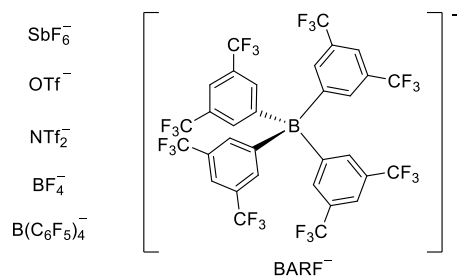
Examples of Carbene Ligands



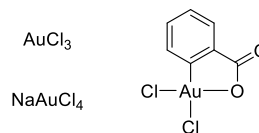
Example of Phosphite Ligands



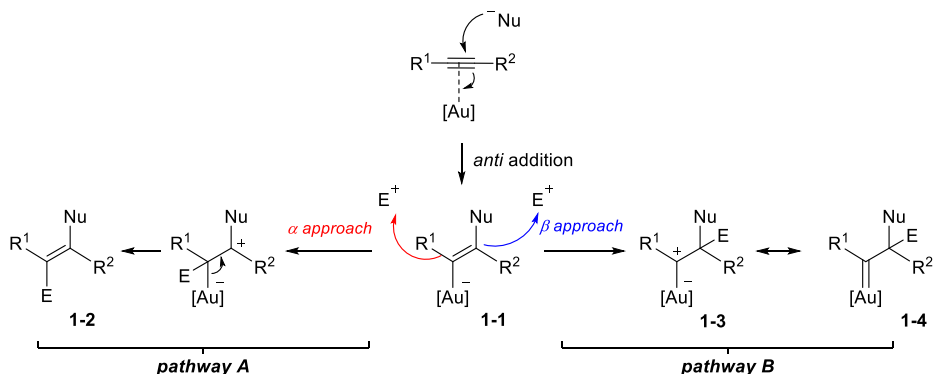
Examples of Counterions



Examples of Au(III) Catalysts



Scheme 2. General Reactivities of Gold Activated Alkynes



The vastly diverse range of transformations of gold-activated alkynes makes it a useful tool in assembly of molecular complexity.¹⁰ It has been extensively employed in cascade reactions, often setting up multiple rings or stereocenters in one step.¹¹ The following sections will focus on cascade reactions initiated/enabled by gold catalysis.

1.2 Gold-Catalyzed Cascade Reactions of Alkynes

Generally, gold-catalyzed cascade reactions are initiated by nucleophilic attacks of a C-C triple bond, followed by or resulting in the generations of reactive intermediates, and ended with their subsequent rearrangements or trappings. Typical reactive intermediates, as shown in Scheme 2, include alkene intermediate **1-2** and gold carbene **1-4**, which will be discussed in the following sections separately. For simplification, isomerization of alkynes into other unsaturated substrates (alkenes, allenes, and dienes) will not be reviewed.

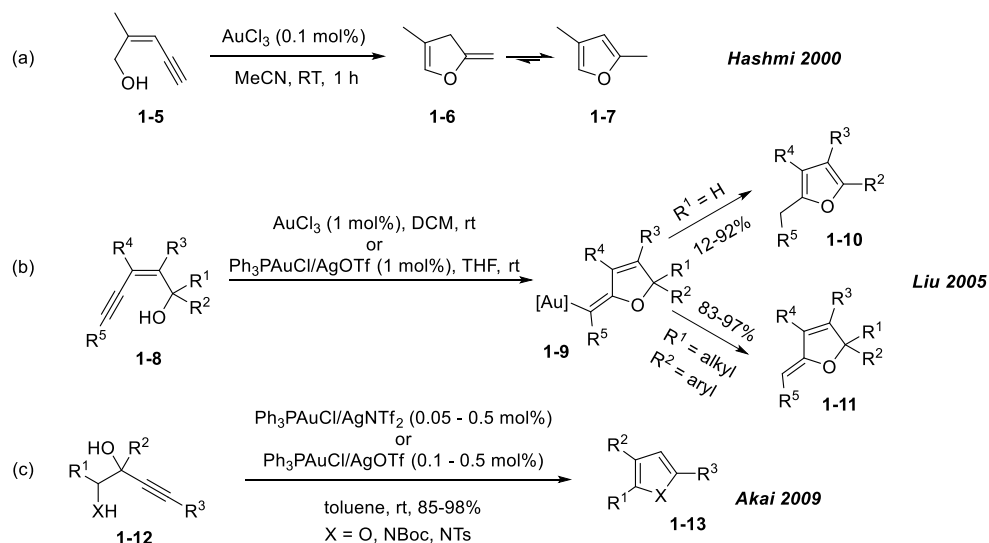
1.2.1 Cascades Initiated by Formation of Alkene Intermediates

The most straightforward way of generating alkene species **1-2** is the intramolecular addition of nucleophile across a C-C triple bond. The types of nucleophiles range from heteroatoms, enols, arenes, and heteroarenes.

1.2.1.1 Through Intramolecular Additions of Heteronucleophiles

One of the simplest examples of cascade reactions initiated by gold-catalyzed nucleophilic attack is the tandem cyclization-isomerization process. In 2000, Hashmi et al first demonstrated that (*Z*)-enynols **1-5** can undergo intramolecular addition to form **1-6**, which then quickly tautomerizes to furan **1-7**. Comparing with established methods with Pd, Ru or Ag catalysis, the efficiency of Au(III) catalyst is far more superior (Scheme 3a).¹² Shortly after, Liu et al utilized this method in a stereoselective synthesis fully substituted furans **1-10/1-11** by using either Au(I) or Au(III) catalysts (Scheme 3b).¹³ A similar approach to construct substituted furans and pyrroles was reported by Akai et al in 2009 using 1-amino-3-alkyn-2-ol (Scheme 3c, **1-12**) as substrate.¹⁴ Instead of tautomerization, a dehydration process occurs after the initial cyclization step.

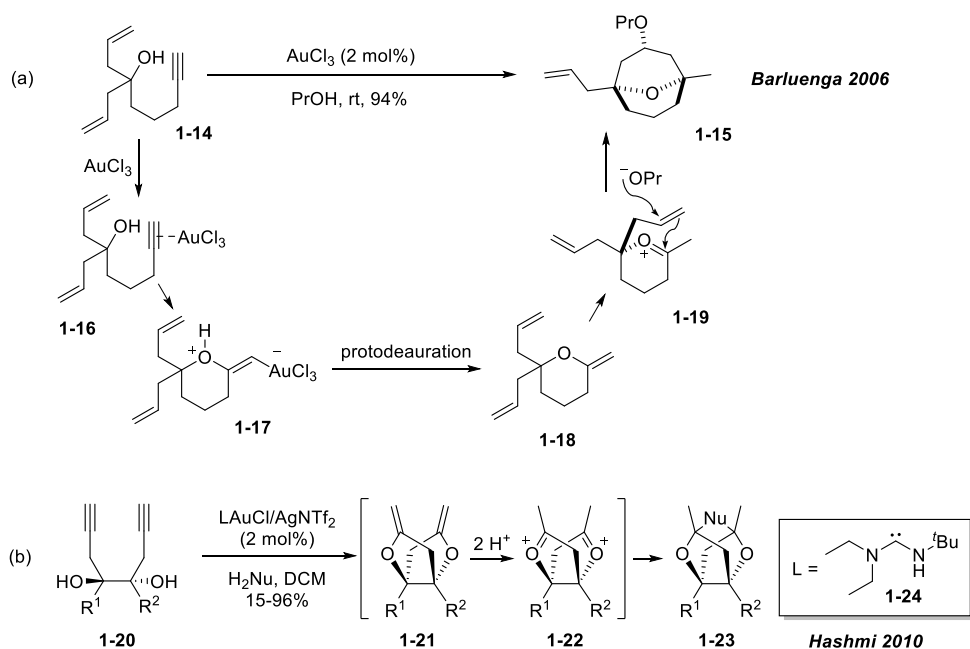
Scheme 3. Gold-Catalyzed Tandem Cyclization-Isomerization or Cyclization-Dehydration Process



More complicated polycyclic structures are synthesized when the alkene species formed in the initial nucleophilic addition are involved in further transformation. One early example was reported by Barluenga et al, where the enol ether **1-18** formed in the addition of alcohol

undergoes a subsequent Prins-type cyclization, generating bicyclic compounds **1-15** containing an eight-membered ring (Scheme 4a).¹⁵ With an external nucleophile, Hashmi group has successfully intercepted the enol intermediate in the dual nucleophilic addition of diynyl diol substrate **1-20** in a more recent study (Scheme 4b).¹⁶ The reaction produced a tricyclic cage-like structure **1-23** which showed extremely high structural rigidity. Notably, the reaction features **1-24**, a *N*-acyclic carbene as the ligand for the gold catalyst.

Scheme 4. Polycyclic Structures from Gold-Catalyzed Nucleophilic Addition Cascades

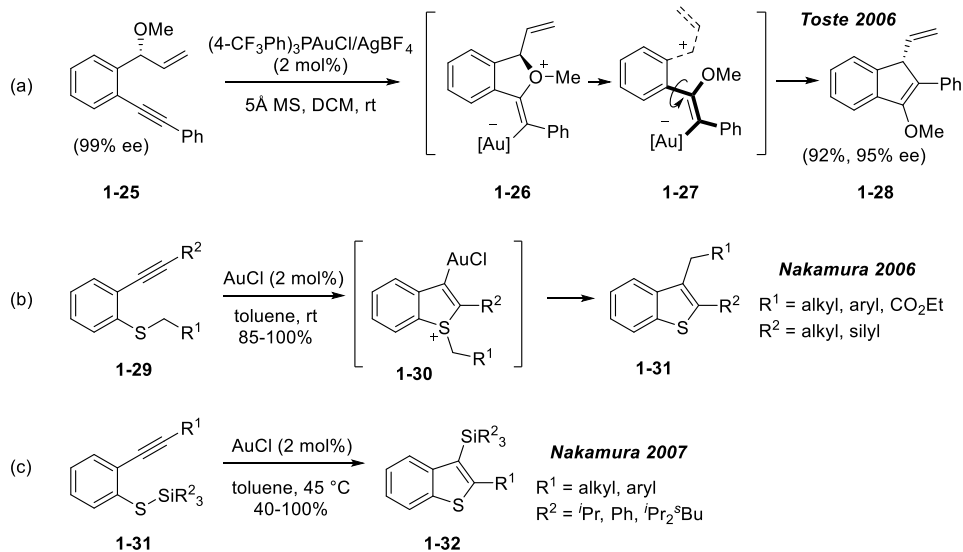


Apart from free alcohols, ethers/thioethers are also good nucleophiles towards gold-activated alkynes. Upon addition, the oxonium/sulfonium species (e.g. **1-26** and **1-30**) often fragment to a carbocation and trigger further rearrangement of the carbon backbone (Scheme 5a and b). Toste et al converted *o*-alkynylbenzyl methyl ether to indenyl ether with Au(I) -catalyzed intramolecular carboalkoxylation reaction.¹⁷ Double-labeled crossover experiment confirmed that the reaction is initiated by alkyne activation rather

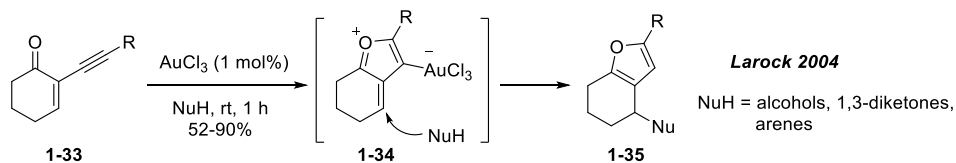
than ionization of benzyl ether. Notably, significant chirality conservation was observed with enantiomerically pure substrate. Nakamura et al first successfully employed Au(I) catalysis in the synthesis of 2,3-disubstituted thiophenols **1-29** from 2-alkynylaryl thioethers.¹⁸ Shortly after, this transformation was further expanded to aryl thiosilanes by the same research team to afford 3-silylbenzothiophenes in high yields (Scheme 5c).¹⁹

Another important type of intramolecular nucleophiles in gold-catalyzed cascade reactions is carbonyl compounds. Larock group used α -alkynyl enones to realize a cascade reaction, which is initiated by a gold-promoted intramolecular carbonyl addition and followed by intermolecular nucleophilic attack.²⁰ Highly substituted furans **1-35** were synthesized in moderate to good yields with a very wide range of external nucleophiles (Scheme 6).

Scheme 5. Cascade Initiated by Ethers/Thioethers Attacking Gold-Activated Alkyne



Scheme 6. A Gold-Catalyzed Cyclization-Nucleophilic Addition Cascade



Oxocarbenium species generated by initial carbonyl attack could also trigger a cycloaddition reaction with carbon-carbon multiple bonds. Yamamoto and co-workers first discovered an AuCl_3 -catalyzed benzannulation of *o*-alkynylbenzaldehydes **1-36** and alkynes (

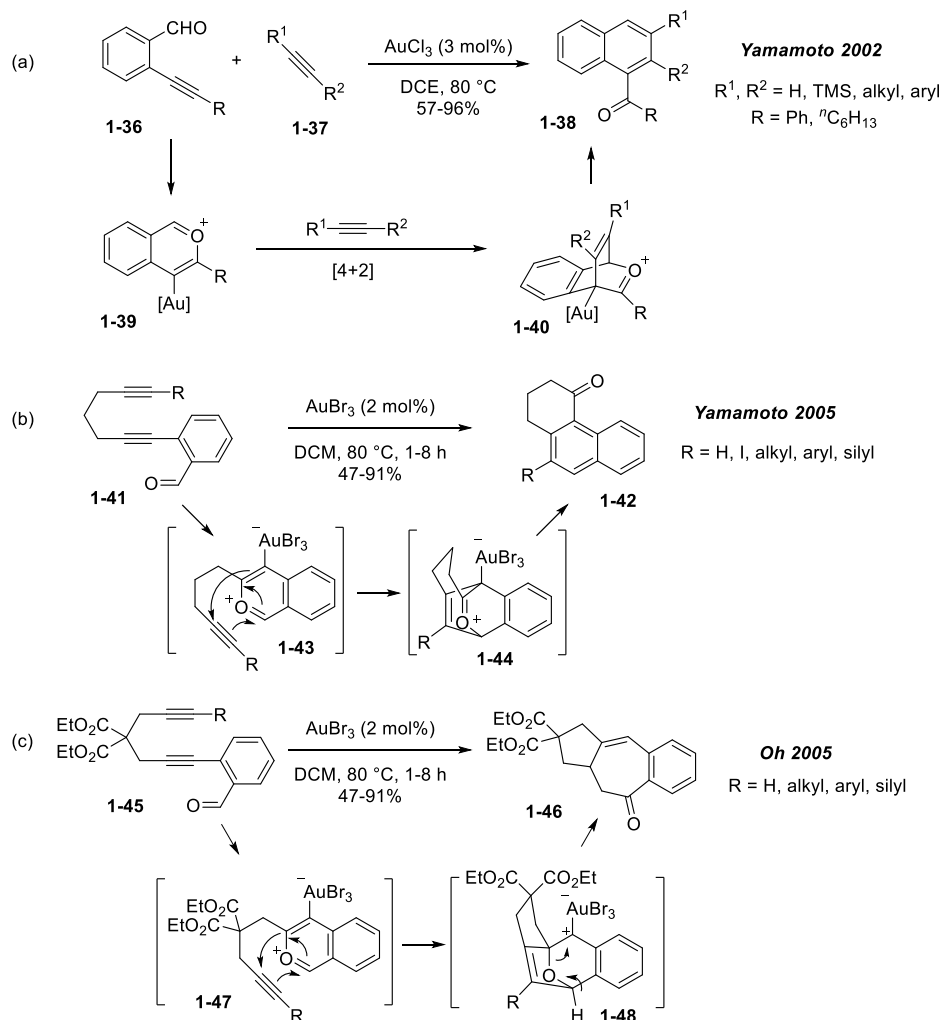
Scheme 7a).²¹ The cycloaddition intermediate **1-40** undergoes ring-opening aromatization to give α -naphthyl ketones **1-38**. A similar study with intramolecularly tethered alkyne was reported by Yamamoto et al in 2005 (

Scheme 7b).²² Furthermore, Oh group later observed a different [3+2] cycloaddition pattern with malonate-linked substrates **1-45** (

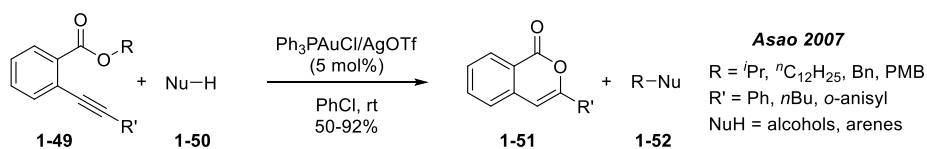
Scheme 7c).²³

2-Alkynylbenzoates **1-49** combined with the gold catalysis could become a powerful reagent for etherification or Friedel-Crafts alkylation with the formation of isocoumarin **1-51** as side product (Scheme 8). Such transformation was first realized by Asao et al in 2007.²⁴ The reaction features mild condition comparing to conventional etherification or Friedel-Crafts alkylation. Notably, experiment with chiral substrate suggests that the reaction involves a $\text{S}_{\text{N}}1$ mechanism with certain degree of $\text{S}_{\text{N}}2$ property.

Scheme 7. Gold-Catalyzed Cyclization-Cycloaddition Cascade



Scheme 8. Etherification or Friedel-Crafts Reaction with 2-Alkynylbenzoates

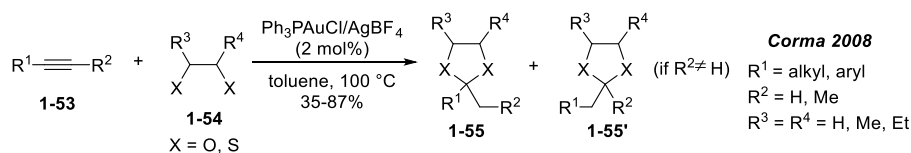


1.2.1.2 Through Intermolecular Addition of Heteronucleophiles

Intermolecular addition of nucleophile allows for a much broader selection of substrates and nucleophiles. Thus, cascade reactions initiated by gold-catalyzed intermolecular nucleophilic additions exhibit much higher diversity.

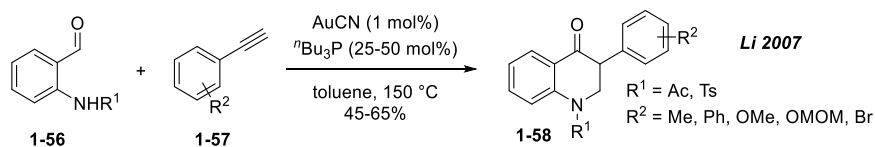
Cyclic acetals could be synthesized under a mild condition when diol undergoes two sequential nucleophilic addition to gold-activated alkynes. In one example reported by Corma et al, the reaction is general for a range of alkynes and diols or dithiols, and cyclic acetals/thioacetals were obtained with high regioselectivity (Scheme 9).²⁵

Scheme 9. The Formation of Cyclic Acetals and Thioacetals from Diols and Dithiols



Enol ethers or enamines generated by intermolecular nucleophilic addition of alcohols or amines could also engage in further attack as nucleophiles. Li et al reported a synthesis of azaisoflavanone derivatives **1-58** via a gold-catalyzed annulation of 2-aminobenzaldehyde and alkynes (Scheme 10).²⁶ The method is compatible with a good variety of aromatic alkynes, although non-aromatic alkynes show no reactivity.

Scheme 10. Synthesis of Azaisoflavanone Derivatives

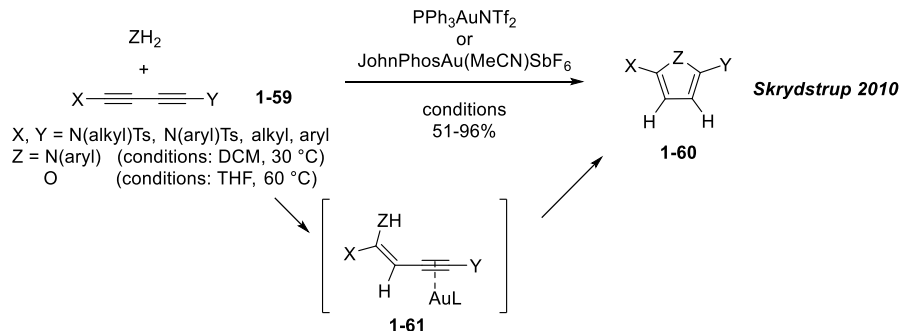


Another important type of cascade reactions with external nucleophiles is double hydroamination or hydration of 1,3-diynes **1-59** (Scheme 11). Cyclization of the intermediate **1-61**, which is formed in the first hydroalkoxylation/hydroamination step, gives the furan or pyrrole product **1-60**. Previously established approaches often require high temperatures or stoichiometric amounts of metal salt, making milder conditions enabled by gold catalysis quite appealing. Skrydstrup et al first reported such a

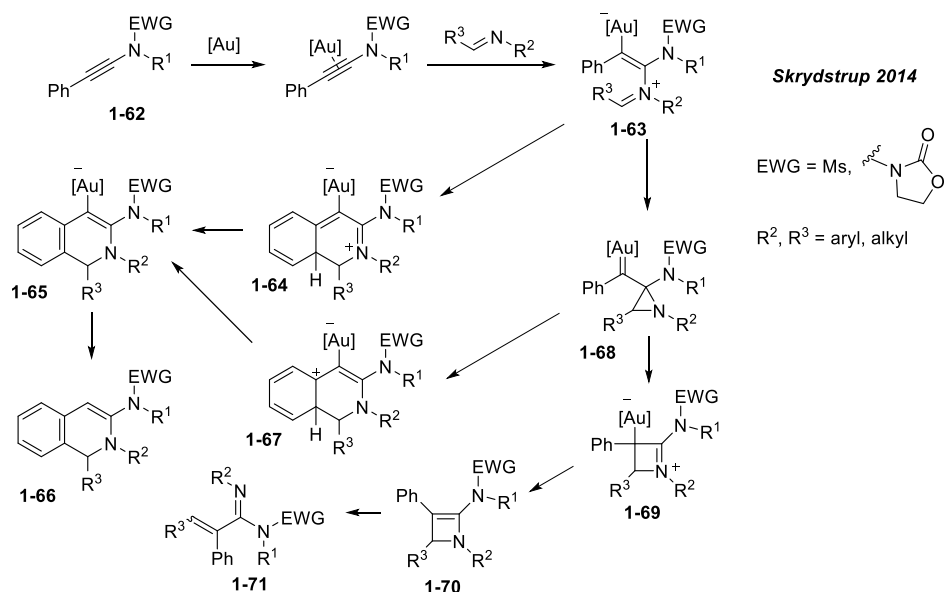
transformation with Au(I) catalyst under mild heating.²⁷ Substituted anilines and water aside, the author also showed one case affording a pyrazole by using phenylhydrazine as nucleophile.

A novel synthesis of 1,2-dihydroquinolines was also reported by Skrydstrup team, featuring a gold-catalyzed formal [4+2] cycloaddition between ynamide and imine (Scheme 12).²⁸ Notably, the aza-enyne metathesis byproducts **1-71** are observed for ynamides with unsubstituted phenyl rings. The author proposed the formation of the aziridine intermediate **1-68** after an initial nucleophilic attack, which is followed by either ring expansion to form the isoquinoline product **1-66**, or 1,2-migration to form the azetinium intermediate **1-69**, leading to the byproducts.

Scheme 11. Double Hydroamination/Hydration of 1,3-Diynes

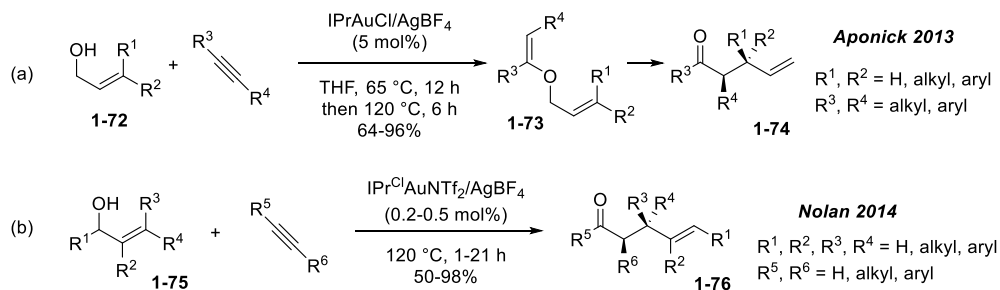


Scheme 12. Access to 1,2-Dihydroquinolines through Gold-Catalyzed Formal [4+2] Cycloaddition



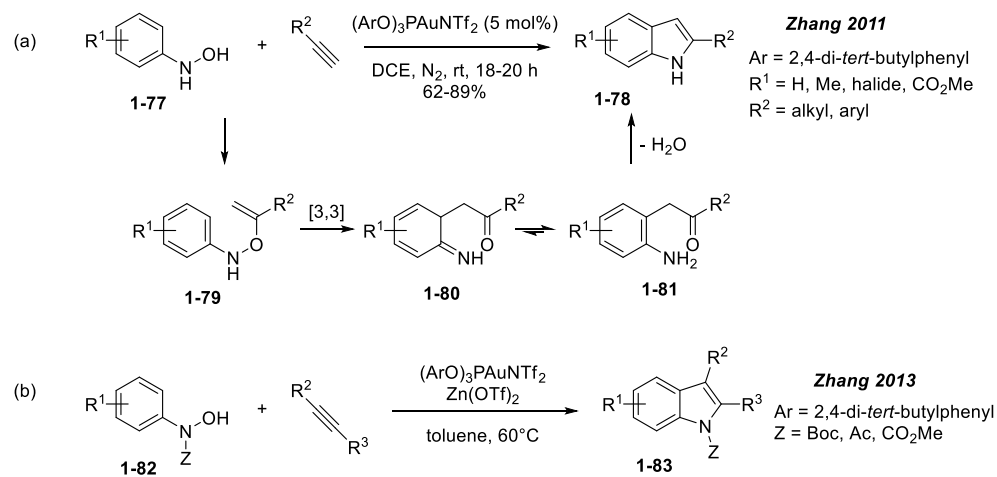
When allyl alcohol **1-72** is utilized in gold-catalyzed hydroalkoxylation of alkynes, the resulting allyl vinyl ether **1-73** undergoes a Claisen rearrangement when heated, affording γ,δ -unsaturated ketones **1-74** (Scheme 13). This new approach was first reported by Aponick's research team, who employed an NHC-gold complex IPrAuCl to achieve good yield and some degree of diastereoselectivity.²⁹ However, one major drawback of this method is relatively high reaction temperature and long reaction time. Shortly after, the method was further refined by Nolan and co-workers with a significantly lowered catalyst loading and better substrate compatibility.³⁰

Scheme 13. Claisen Rearrangement of Nucleophilic Addition Product



In 2011, our group published a synthesis of 2-alkylindoles through 3,3-rearrangement and subsequent dehydrative cyclization of *N*-aryl-*O*-alkenylhydroxylamine **1-79** (Scheme 14a).³¹ The cleavage of the weak N-O bond in intermediate **1-79** enables the reaction to proceed smoothly under room temperature. Soon afterwards, our group followed up this study with a cooperative Au/Zn catalysis featuring a much broader substrate scope (Scheme 14b).³² Notably, when internal alkynes are used, regioselectivity of the reaction could be controlled by the seemingly weak electronic effect of the tethered function groups on the alkynes.

Scheme 14. A Novel Indole Synthesis from Aryl Hydroxylamine and Alkyne

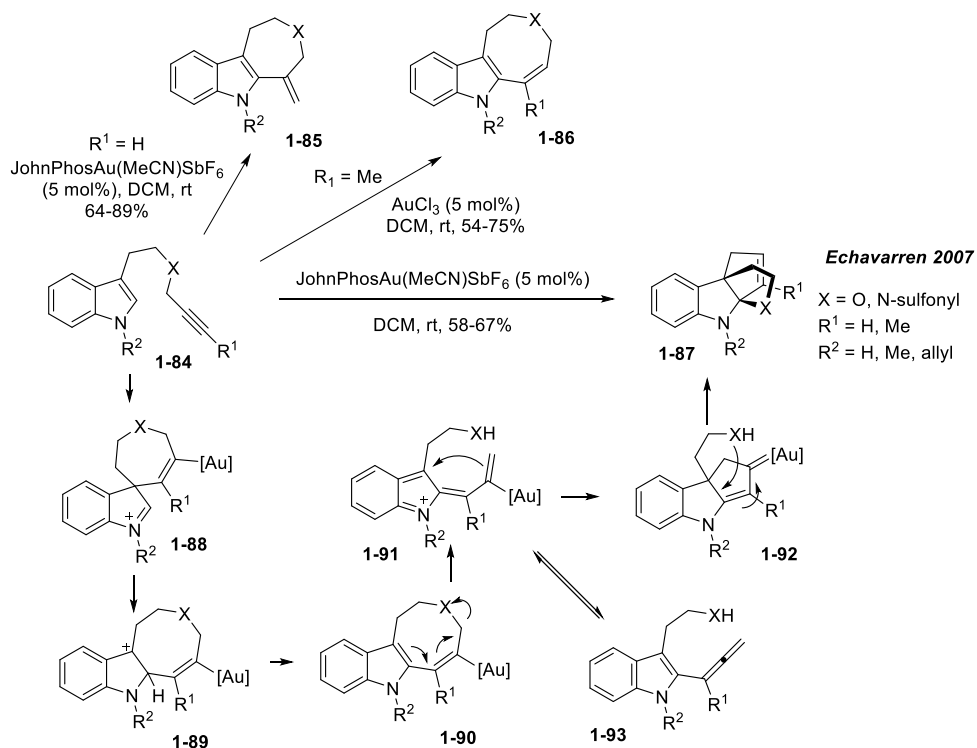


R² = H, R³ = alkyl, alkenyl: (ArO)₃PAuNTf₂ 5 mol%, Zn(OTf)₂ 5 mol%, 65-96%
 R² = alkyl, aryl, R³ = alkyl: (ArO)₃PAuNTf₂ 5 mol%, Zn(OTf)₂ 20 mol%, 52-86%,
 regioselectivity up to > 20:1

1.2.1.3 Through Hydroarylation Reaction

Gold-catalyzed hydroarylation of alkynes is a valuable method to synthesize alkenyl arenes or heteroarenes. The Echavarren group has reported a series of gold-catalyzed cascade reaction that transforms indole-type substrate **1-84** into six-, seven-, and eight-membered-ring products (see Scheme 15, **1-85**, **1-86**).³³ Additionally, allenes **1-93** and tetracyclic annulated products **1-87** are formed by the fragmentation of eight-membered ring intermediate **1-90**.

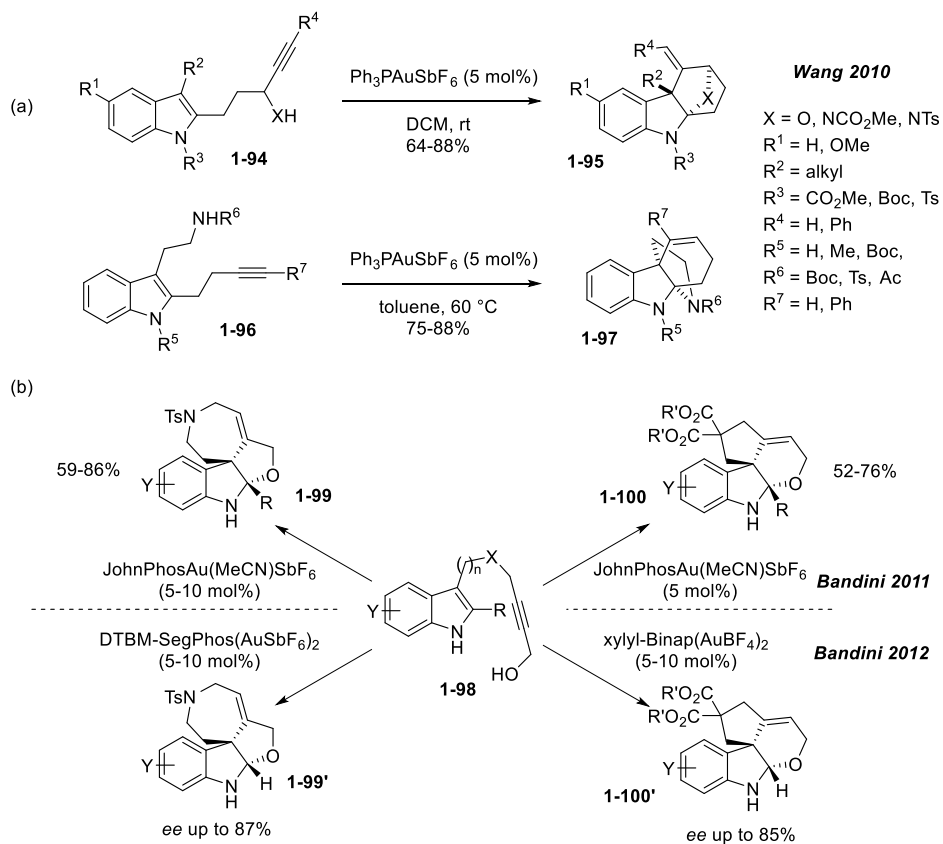
Scheme 15. Transformation of Alkyne-Tethered Indoles



Iminium species formed by hydroarylation on indole's 3-position (e.g. **1-88**) could also be trapped by a tethered nucleophile to afford polycyclic structures. Some selected reports are shown in Scheme 16. Depending on the position of tethered nucleophile, various bridged

compounds (e.g. **1-95**, **1-97**, **1-99/99'**, **1-100/100'**) could be synthesized under mild conditions.³⁴

Scheme 16. Nucleophilic Trapping of Iminium Species in Gold-Catalyzed Hydroarylation



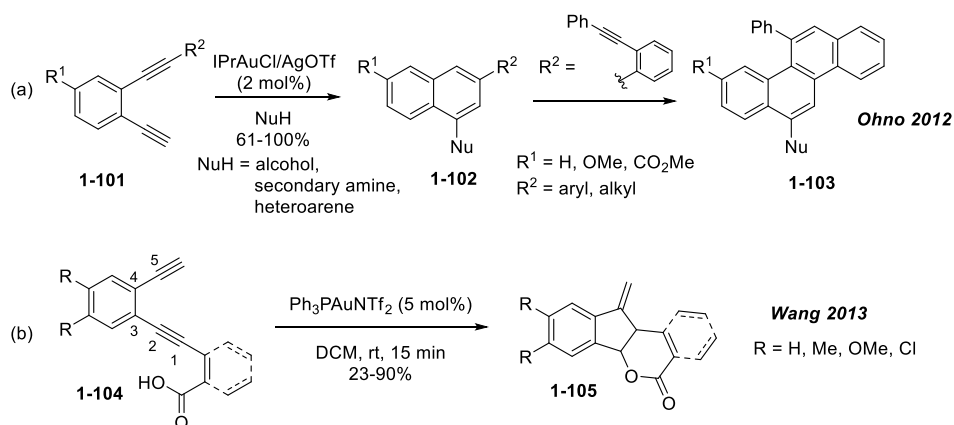
1.2.1.4 Consecutive Nucleophilic Additions

Consecutive addition of nucleophiles to diynes/poly-ynes is an important type of gold-catalyzed transformation that builds highly conjugated system in one step. Ohno et al has first reported this inter-/intramolecular addition cascade of diynes and triynes to make substituted naphthalene and chrysenes (Scheme 17a).³⁵ Types of nucleophile range from alcohols, amines to heteroarenes, making it a very flexible method building fused arene system. Shortly after, Wang and co-workers reported a different C1-C5 cyclization pattern

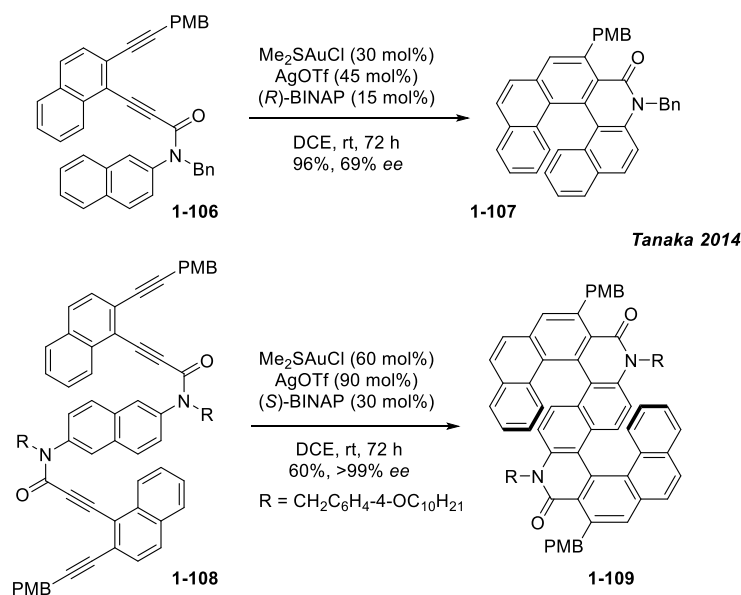
in a similar catalytic system (Scheme 17b).³⁶ To initiate the nucleophilic addition sequence, a carboxylic acid was used as the primary nucleophile.

Tanaka et al has reported an interesting application of this reaction in synthesizing chiral azahelicenes (Scheme 18).³⁷ Combining a gold-catalyzed sequential intramolecular hydroarylation with chiral BINAP ligands, the author synthesized azahelicene **1-107** and S-shaped double azahelicene **1-108** in high *ee*% value and synthetically useful yields. The author also noted that excess Ag salt towards the Au(I) complex is crucial for this transformation.

Scheme 17. Consecutive Nucleophilic Addition of Dienes



Scheme 18. Synthesis of Azahelicenes and S-Shaped Double Azahelicene



1.2.2 Cascade Initiated by Formation of Gold Carbenoids

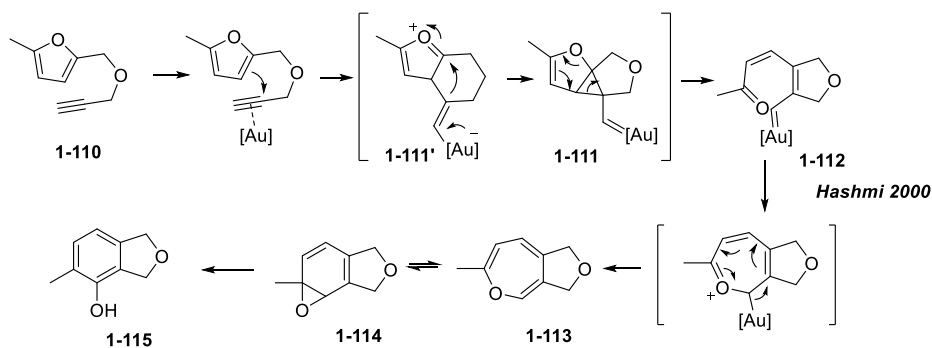
As shown in Scheme 2, pathway B, the transformation of gold-activated triple bond to gold carbenoid involves an electrophile accessing the β -position of alkenylgold species **1-1**. Careful selection of substrates and internal/external electrophiles enables a great variety of gold carbenoid with different electronic/steric properties being harnessed in building complicated structures.

1.2.2.1 Through Enyne Cycloisomerization Reactions

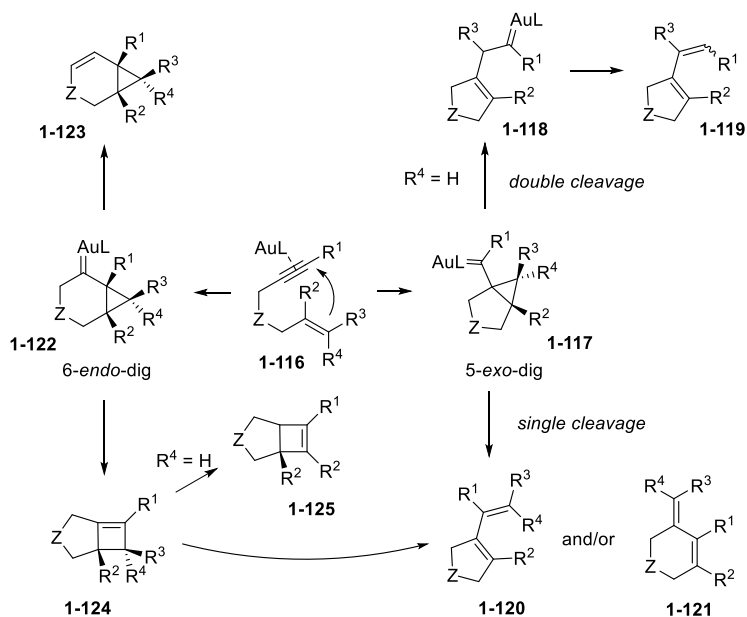
Gold-catalyzed enyne cycloisomerization is a very versatile reaction in synthesizing various types of cyclic compounds. The very first report in this field was Hashmi's phenol synthesis from furan-type substrate **1-110** (Scheme 19).³⁸ Initial hydroarylation reaction of **1-110** gives an oxocarbenium species **1-111'**, which was trapped intramolecularly by the alkenylgold moiety in proximity, affording exocyclic gold carbene **1-111**. **1-111** undergoes

skeletal rearrangement to form another gold carbene **1-112**. Subsequent cyclization, electrocyclization, and aromatization gives phenol product **1-115**.

Scheme 19. Hashmi's First Report of Enyne Cycloisomerization



Scheme 20. Echavarren's Work on 1,6-Enyne Cycloisomerization

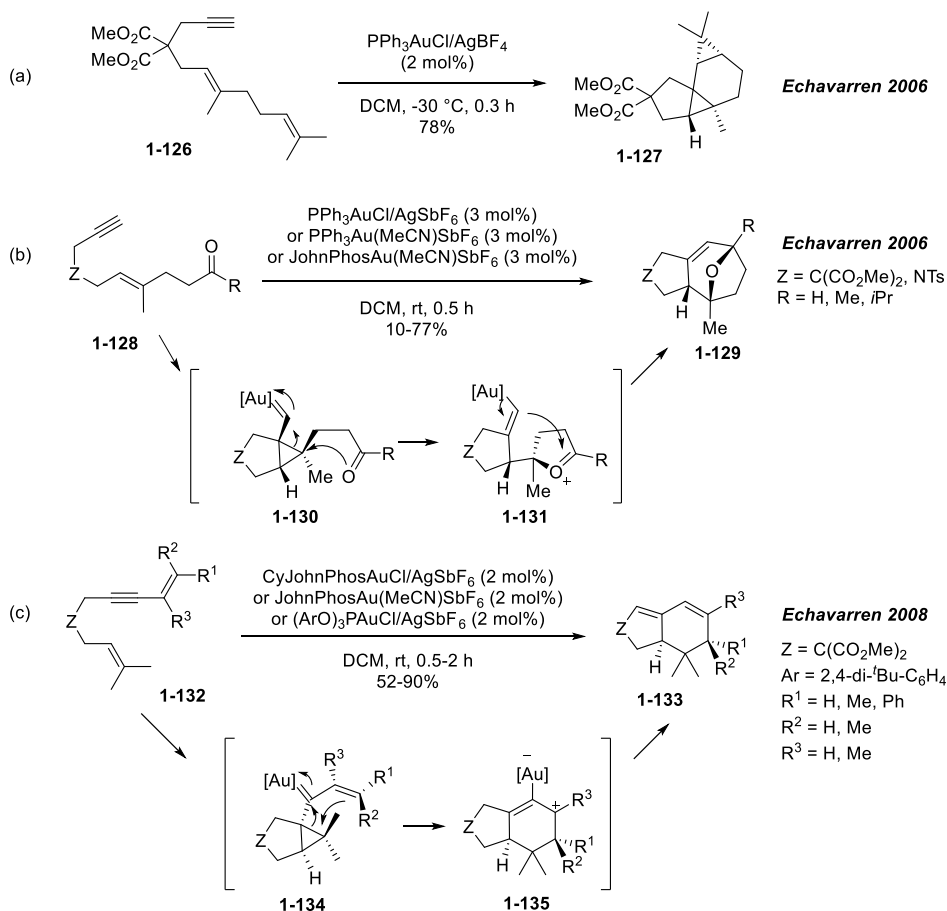


The Echavarren group has thoroughly studied this gold-catalyzed cycloisomerization system and demonstrated that a wide variety of (poly)cyclic products could be obtained.³⁹ As shown in Scheme 20, initial nucleophilic attack could proceed either in a 5-*exo*-dig or a 6-*endo*-dig manner. 5-*Exo*-dig cyclization of starting enyne **1-116** gives

exocyclic carbene intermediate **1-117**, which further undergoes single cleavage or double cleavage to form diene product **1-119**, **1-120**, or **1-121**. On the other hand, 6-*endo*-dig cyclization leads to endocyclic carbene **1-122**, followed by 1,2-*H*-shift or ring expansion to get product **1-123** or **1-125**.

Echavarren and co-workers further demonstrated that the gold carbene species generated by cycloisomerization of 1,6-enynes (i.e. **1-117** or **1-122**) can be utilized in various transformations, obtaining different polycyclic molecules in one pot. Examples include intramolecular cyclopropanation (Scheme 21a),⁴⁰ intramolecular Prins cyclization (Scheme 21b),⁴¹ and formal [4+2] cycloaddition (Scheme 21c).⁴²

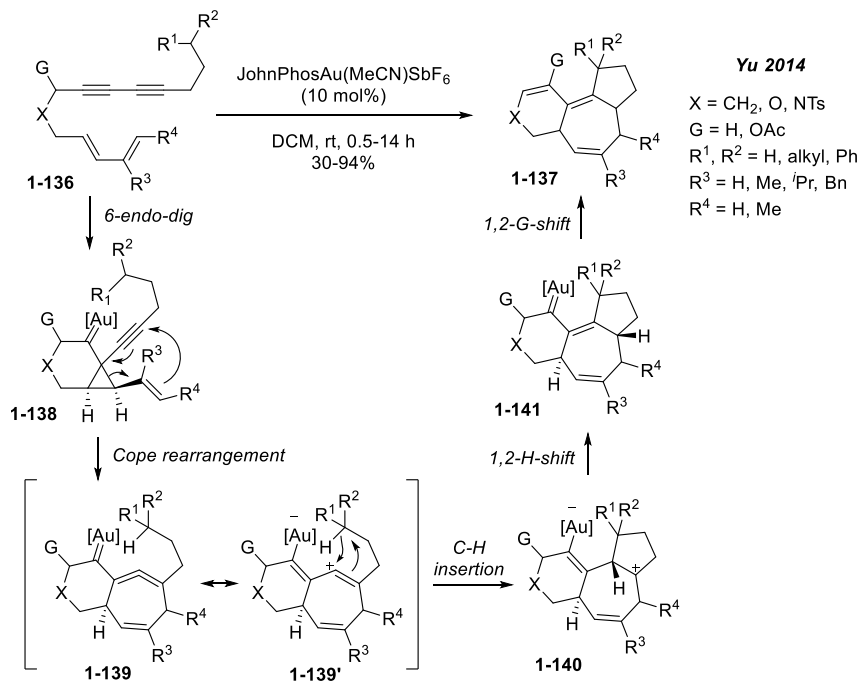
Scheme 21. Application of Echavarren's 1,6-Enyne Cycloisomerization



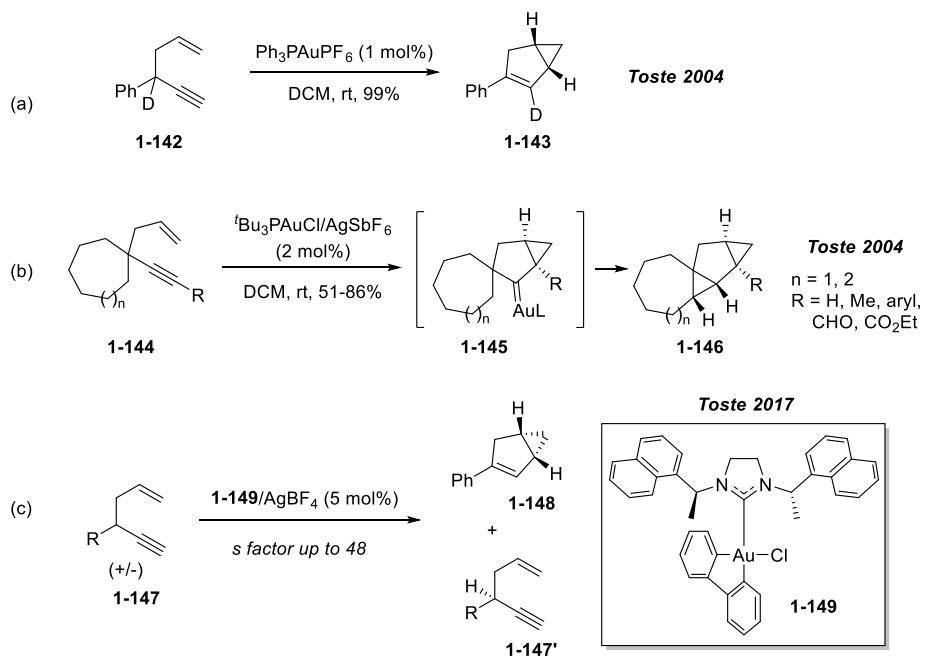
A more recent example was reported by Yu et al in 2014 (Scheme 22).⁴³ After the initial 6-*endo*-dig cyclization, the gold carbene intermediate **1-138** proceeds through a Cope rearrangement to afford a bent allene species **1-139**. The intermediate, which is in resonance with vinyl cation species **1-139**, then initiates a C-H insertion reaction to form a five-membered ring. A fused 5,7,6-tricyclic product **1-137** is obtained with high diastereoselectivity.

Besides 1,6-enyne, 1,5-enyne is also frequently used in gold-catalyzed cycloisomerizations. Generally, reaction of 1,5-enynes proceed in a 5-*endo*-dig pattern due to the higher stability of subsequent 5,3-fused system comparing to the 4,3-fused system formed by the 4-*exo*-dig pathway. As shown in Scheme 23a, bicyclo[3.1.0]hexane is formed almost exclusively in the cycloisomerization of 1,5-enyne **1-142**.⁴⁴ Toste group later discovered that the endocyclic gold carbene formed in the cycloisomerization (Scheme 23b, **1-145**) also inserts into the adjacent C-H bond.⁴⁵ Very recently, the same research team reported a rare enantioconvergent kinetic resolution of 1,5-enynes utilizing a structurally well-defined chiral gold(III) catalyst **1-149**, allowing access to a series of enantioenriched bicyclo[3.1.0]hexenes.⁴⁶

Scheme 22. Construction of a Fused 5,7,6-Tricyclic System



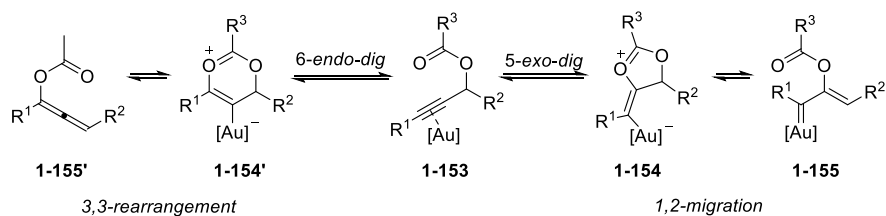
Scheme 23. Toste Group's Studies in 1,5-Enyne Cycloisomerization



1.2.2.2 Through 1,2-Acyloxy Migration of Propargylic Carboxylates/Acetals

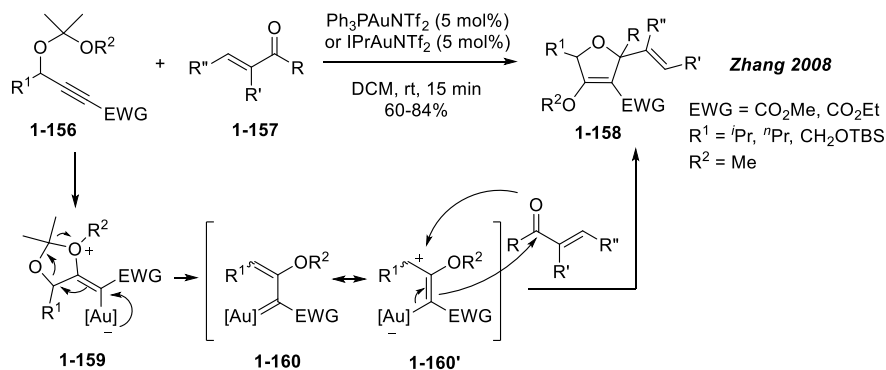
Propargylic carboxylates (e.g. Scheme 24, **1-153**) are easily-accessible substrates that enable construction of many complicated structures. The carbonyl group attacks the gold-activated C-C triple bond, leading to two different class of reactive intermediates. *6-Endo* attack, followed by Claisen-type rearrangement, gives an allenyl carboxylate **1-155'**; on the other hand, *5-exo* attack generates an alkenyl gold carbene **1-155**. The preference between 1,2-migration and 3,3-rearrangement could be regulated electronically or sterically on the propargyl ester substrate. In addition to propargyl carboxylates, propargyl acetals are also able to undergo similar 1,2-migration process.

Scheme 24. Reactivity of Propargylic Carboxylates/Acetals



Our group has published one of the earliest examples of 1,2-migration of propargyl acetals in a synthesis of substituted 2,5-dihydrofurans (Scheme 25, **1-158**).⁴⁷ To facilitate the initial *5-exo*-dig cyclization, strong electron-withdrawing groups are installed to the alkyne terminus of the propargyl moiety. Notably, the electron-withdrawing group also destabilizes alkenyl gold carbene intermediate **1-160** to harness its 1,3-dipole reactivity.

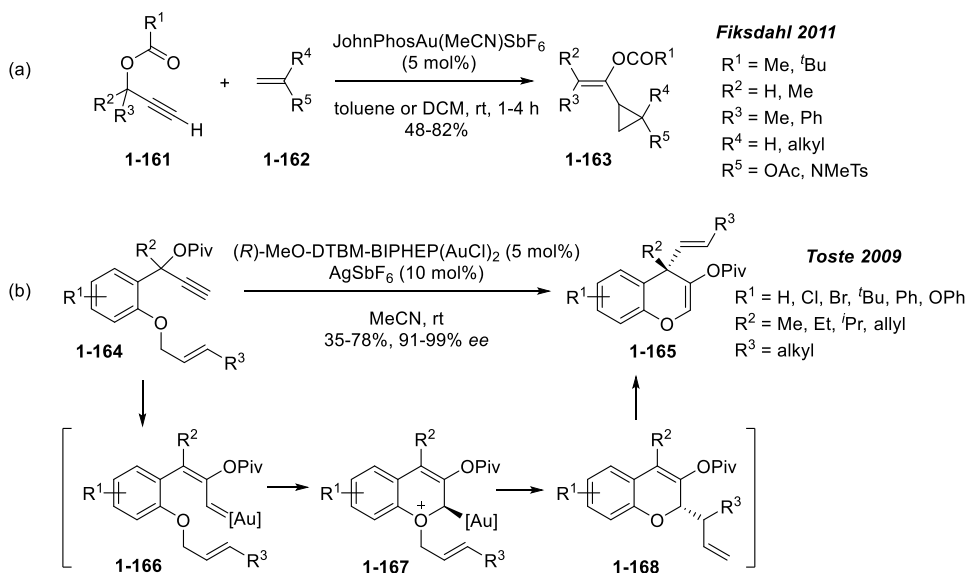
Scheme 25. Synthesis of 2,5-Dihydrofurans from Propargyl Acetals



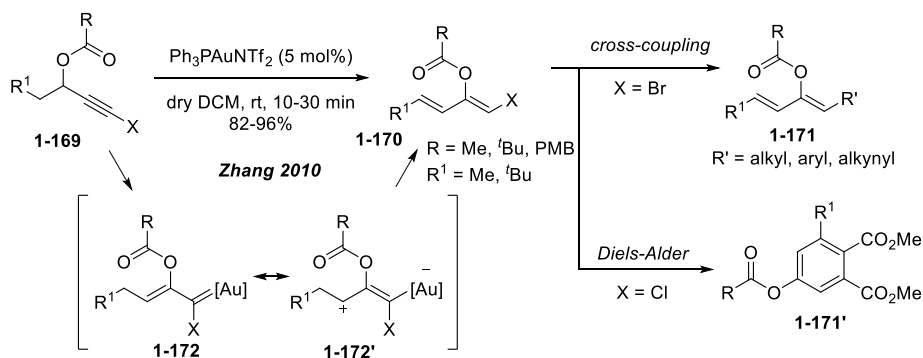
The alkenyl gold carbene generated from 1,2-migration of propargyl carboxylate can also be trapped by various internal or external nucleophiles. One example published by Fiksdahl et al is cyclopropanation with various terminal alkenes (Scheme 26a).⁴⁸ An earlier report by Toste group demonstrated an intramolecular trapping of gold carbene **1-166** by ethereal oxygen (Scheme 26b). The allyl group on the oxonium species **1-167** migrates subsequently to give benzopyran **1-165**.⁴⁹

Like other electron-withdrawing groups, chlorides and bromides installed at the alkyne terminus of propargyl carboxylate promote 1,2-migration effectively. Our group has utilized this property and developed a fast, efficient, and highly diastereoselective method to synthesize (1*Z*, 3*E*)-1-bromo/chloro-2-carboxy-1,3-dienes (Scheme 27, **1-170**).⁵⁰ Upon formation, the carbene intermediate **1-172** undergoes a δ -deprotonation to afford halodiene product. Synthetic flexibilities of the products have also been highlighted in the paper (see: Scheme 27, **1-171/171'**).

Scheme 26. Trapping of Gold Carbene Generated by 1,2-Migration of Propargylic Carboxylate

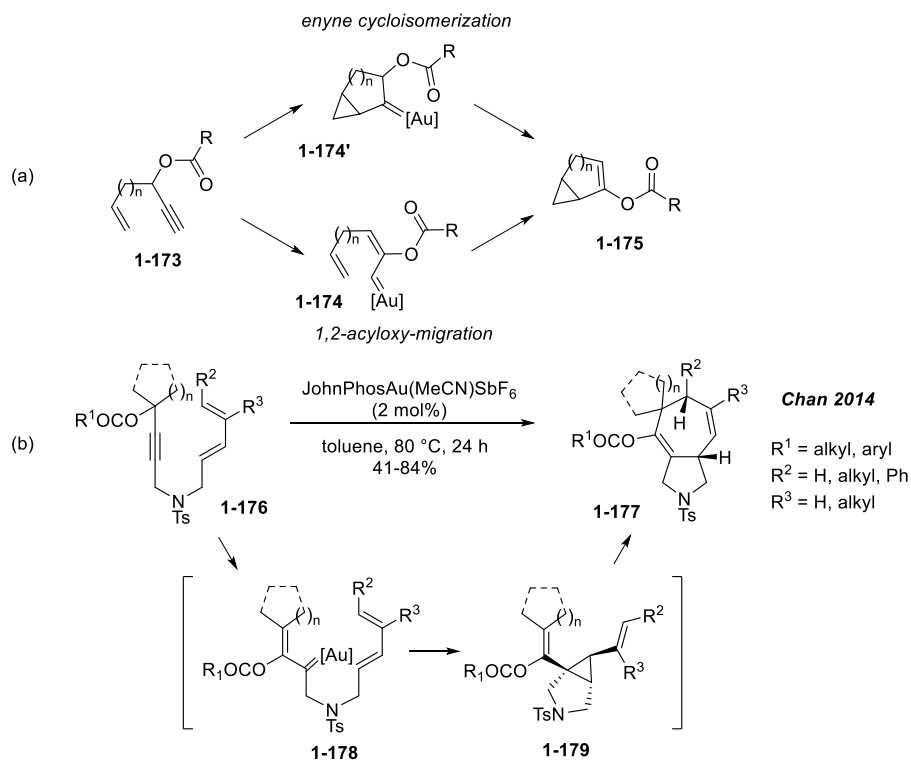


Scheme 27. Synthesis of (1Z, 3E)-1-Halo-2-carboxy-1,3-dienes



Another important gold-catalyzed cascade reaction of propargyl carboxylates is Rautenstrauch rearrangement, where enynes bearing propargylic α -acyloxy moiety (e.g. **1-173**) are involved. Notably, it is also possible that the reaction proceeds via enyne cycloisomerization to give the same product (see: Scheme 28a, the upper pathway). One cascade reaction initiated by Rautenstrauch rearrangement of dienyne **1-176** is shown below (Scheme 28b).⁵¹

Scheme 28. Rautenstrauch Rearrangement of Propargylic Carboxylates

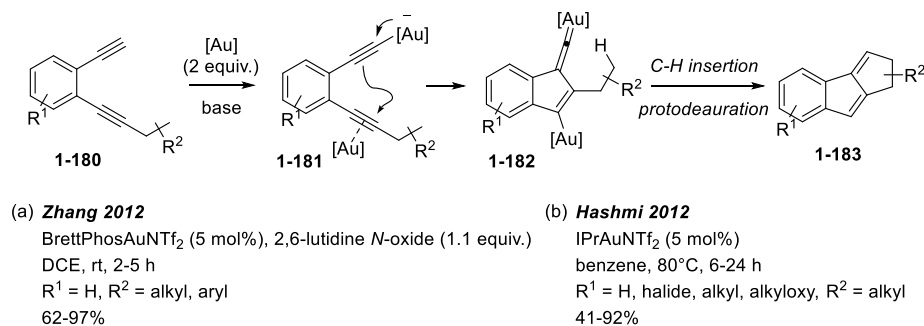


1.2.2.3 Through Gold Vinylidenes and Related Intermediates

Metal vinylidene is a reactive intermediate that leads to the formation of various carbon-carbon and carbon-heteroatom bonds. The first example of gold vinylidene generated by cycloisomerization of benzene-1,2-diynes was reported by our group in early 2012 (Scheme 29).⁵² Based on mechanistic experiments and DFT calculations, a dual-gold activation mechanism was proposed. Firstly, lutidine *N*-oxide extracts the proton from the terminal alkyne to generate alkynylgold complex **1-181**, while another molecule of gold complex activates the internal alkyne triple bond. A 5-endo-dig cyclization then happens to afford the gold vinylidene species **1-182**. The gold vinylidene is highly reactive and quickly undergoes an intramolecular C-H insertion to give the final tricyclic indene product

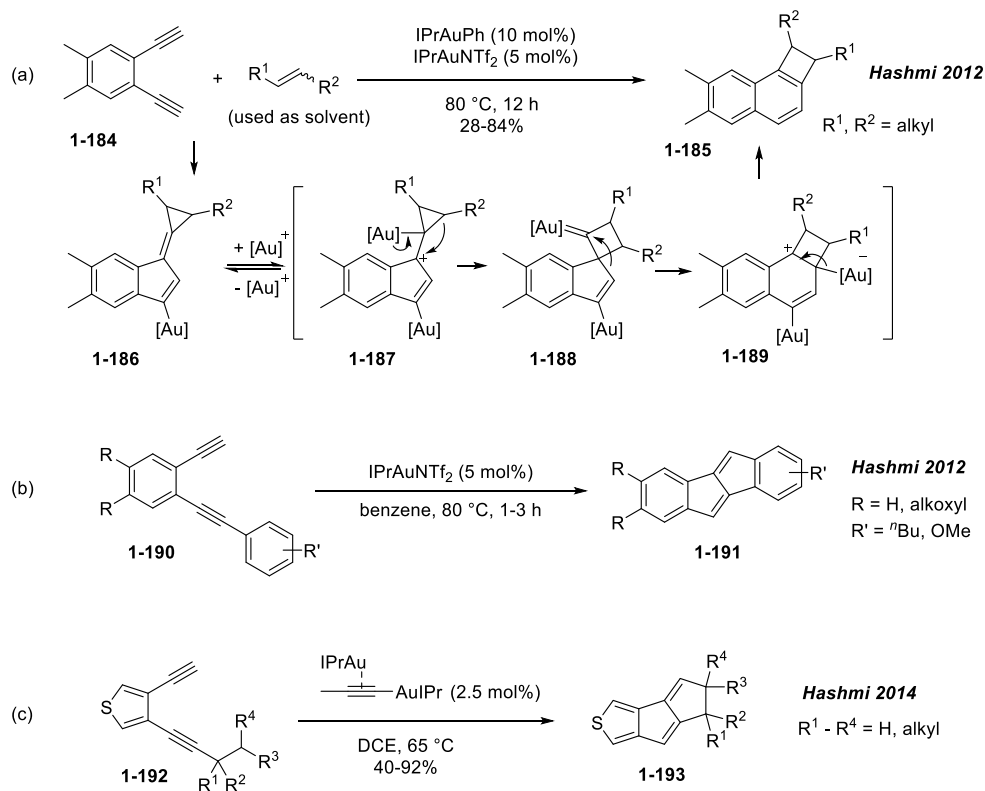
1-183. Shortly afterwards, a very similar approach was published independently by Hashmi et al.⁵³

Scheme 29. From Benzene-1,2-diynes to Gold Vinylidene



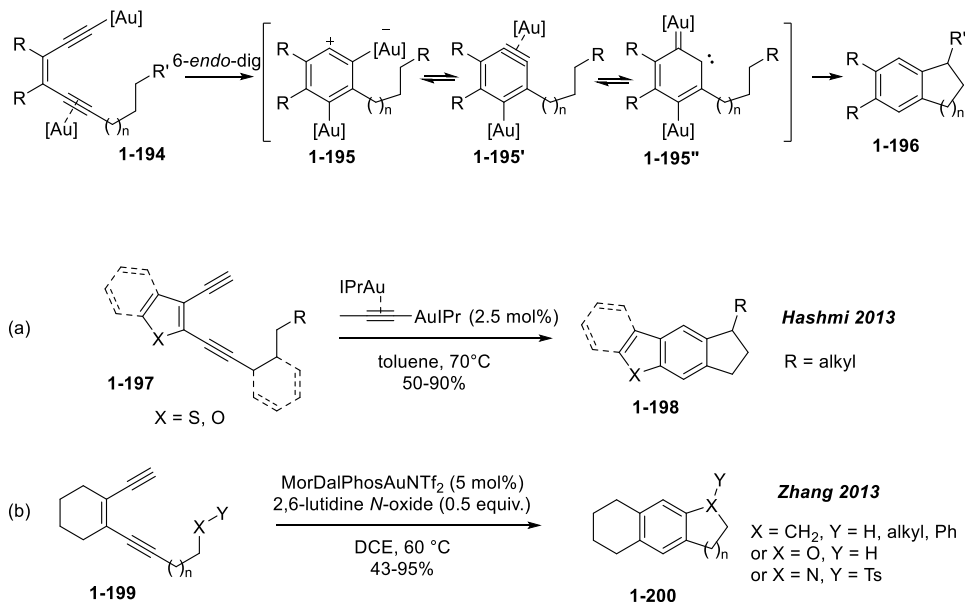
The Hashmi group continued studying on this type of reaction and revealed a series of interesting transformations of the gold vinylidene intermediate. Examples include a cyclopropanation-ring expansion sequence (Scheme 30a)⁵⁴ and intramolecular Friedel-Crafts reaction (Scheme 30b).⁵⁵ Additional to benzene-1,2-diynes, 3,4-Dialkynylthiophenes **1-192** are also suitable for this transformation (Scheme 30c).⁵⁶

Scheme 30. Hashmi's Studies on Benzene-1,2-diyne Chemistry



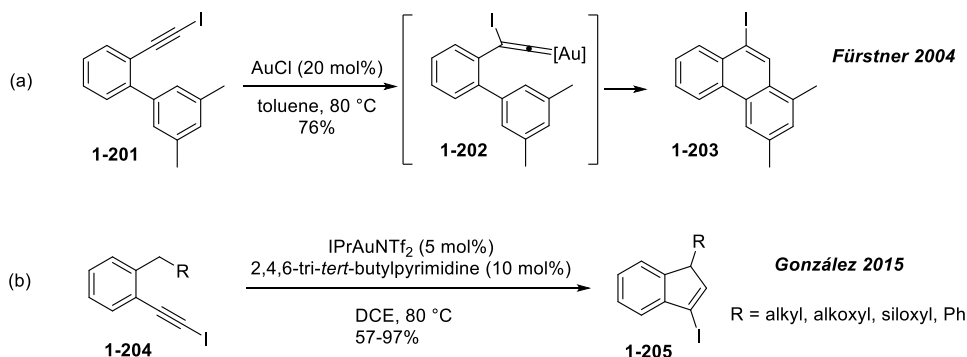
Interestingly, the mechanistic switch from 5-*exo*-dig to 6-*endo*-dig cyclization could be achieved by switching benzene ring with different alkenyl moiety (Scheme 31). In 2013, Hashmi group and our group independently reported two different types of substrates (i.e. **1-197**, **1-199**) that enables the mechanistic switch.⁵⁷ The increased gain in aromatic stabilization in cycloisomerization intermediate **1-195** is the key driving force of the divergence of initial cyclization step, as supported by DFT studies of both research teams. Additionally, a novel gold benzyne intermediate **1-195'** was suggested by mechanistic study.^{57b}

Scheme 31. Mechanistic Switch of Dual-Gold Catalysis



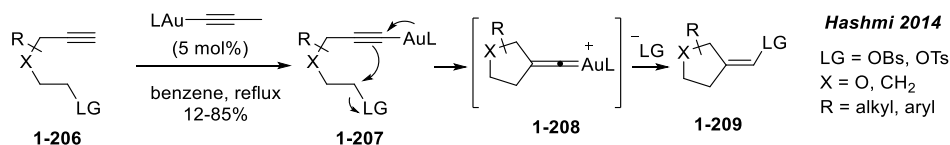
Another important way to generate gold vinylidene is direct isomerization of alkynes or haloalkynes. In 2004, Fürstner et al first reported an AuCl-catalyzed transformation of iodoalkyne to phenanthrenes (Scheme 32a).⁵⁸ The author suggested that gold(I) catalyst triggers the rearrangement of iodoalkyne **1-201** to form a gold vinylidene species **1-202**, which was subsequently trapped by the proximal aromatic ring. This gold-vinylidene intermediate was later supported by a DFT study published by Soriano et al.⁵⁹ Recently, González and co-workers also demonstrated a benzylic C(sp³)-H insertion of Fürstner-type gold vinylidenes (Scheme 32b).⁶⁰

Scheme 32. Gold Vinylidenes from the Isomerization of Iodoalkynes



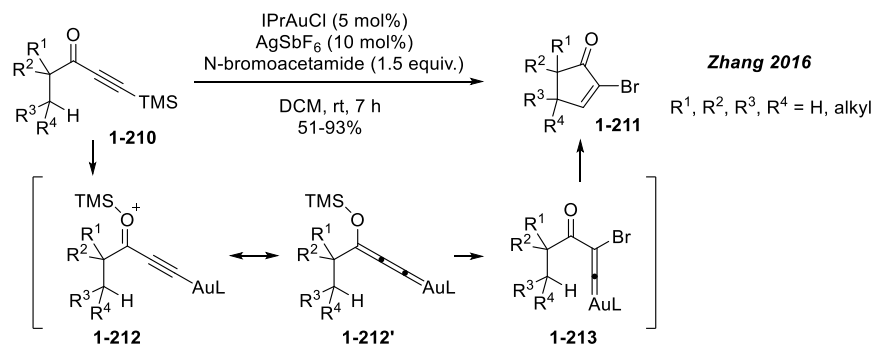
A similar way of generating gold vinylidenes from terminal alkyne was published by Hashmi et al in 2014 (Scheme 33).⁶¹ Deprotonative formation of alkynylgold species **1-207** triggers an intramolecular S_N2 reaction, generating the gold vinylidene species **1-208** by the expulsion of the leaving group. This work clearly demonstrates that the β -carbon of the alkynylgold species **1-207** is significantly nucleophilic.

Scheme 33. Generation of Gold Vinylidenes with Terminal Alkynes



An external electrophile could also trigger the S_N2 -type reaction of alkynylgold species. Recently, our group published an intermolecular generation of gold vinylidenes from TMS-protected ynones **1-210**, followed by insertion into unactivated $C(sp^3)$ -H bonds (Scheme 34).⁶² *N*-Bromoacetamide was added to facilitate the rearrangement of alkynylgold species **1-212** to gold vinylidene **1-213**. The method demonstrates a facile synthesis of 2-bromocyclopentenones with a broad substrate scope and synthetically desirable diastereoselectivities.

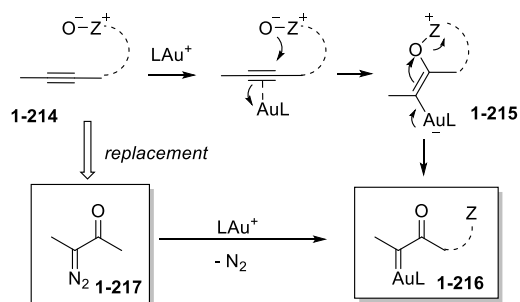
Scheme 34. Unactivated C(sp³)-H Insertion of Gold Vinylidene



1.2.2.4 Through Oxidatively-Generated Gold Carbenes

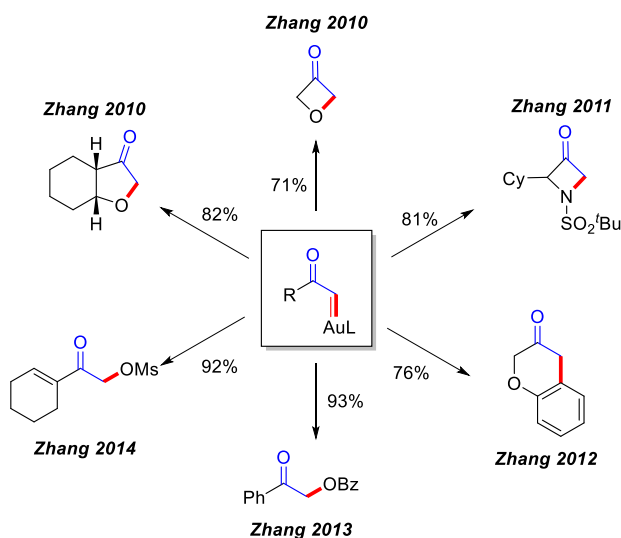
The methods described in previous sections focused on generation of gold carbenoids with isomerization reactions driven by the conversion of π -bonds to stronger σ -bonds. Another strategy of further strengthening the driving force is introducing an oxidant and thereby converting the alkynes into much more stable carbonyl compounds. Such protocol has only been developed and broadly applied in the very recent decade.⁶³ As shown in Scheme 35, the *O*-nucleophilic oxidant attacks the gold-activated alkyne moiety, affording an alkenylgold intermediate **1-215** bearing a weak O-Z bond. Subsequent expulsion of the Z leaving group leads to the formation of a highly electrophilic α -oxo gold carbene **1-216**. While similar α -oxo metal carbenoid could be accessed from the decomposition of diazoketones **1-217**, this gold-catalyzed process shows significant advantage of mild reaction condition, easily-accessible substrate, and higher degree of operational safety. It should be noted that the oxidant involved in such transformation could either be tethered to the substrate, or added to the reaction mixture as a reagent.^{10b}

Scheme 35. Gold Carbenes Generated by an Oxidative Process



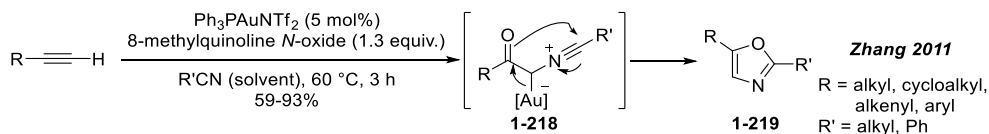
One simplest way of utilizing the highly reactive α -oxo gold carbene is trapping with a nucleophile. Our group has done substantial studies on this subject. Some selected transformations realized by our group are shown in Scheme 36.⁶⁴

Scheme 36. Nucleophilic Trapping of Oxidatively-Generated Gold Carbenes



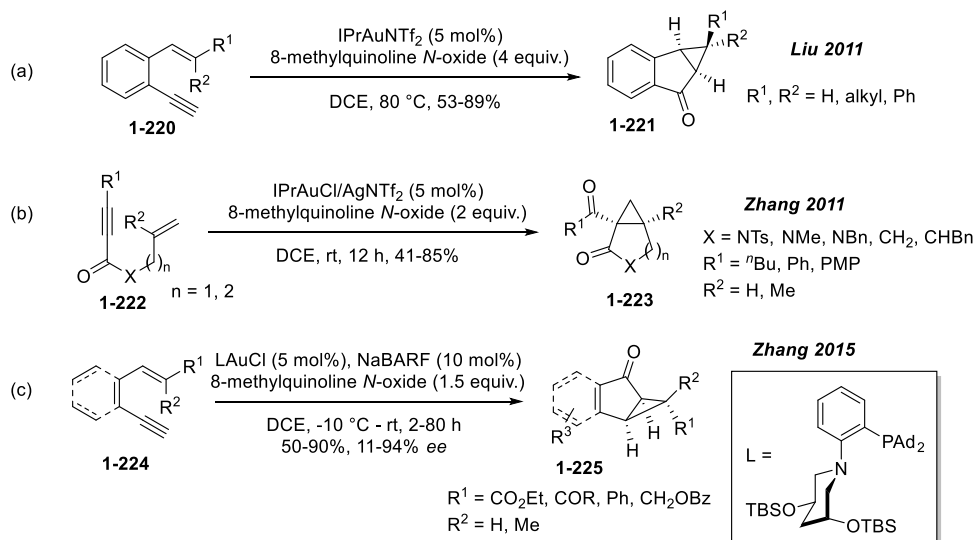
Nucleophilic trapping of α -oxo gold carbenes can also trigger additional transformations. As shown in Scheme 37, intermediate **1-218**, generated from trapping of α -oxo gold carbene with nitrile, undergoes a cyclization to form 2,5-disubstituted oxazole **1-219**.⁶⁵ The overall reaction is a [2+2+1]-type cyclization of an alkyne, a nitrile, and an oxygen atom from the oxidant.

Scheme 37. Oxazole Synthesis with Oxidatively-Generated Gold Carbene



Like gold carbenoid generated with other methods, α -oxo gold carbenes also undergo cyclopropanation reaction to further introduce molecular complexity. One typical case was given by Liu et al in 2011, where the gold carbene reacts intramolecularly with a tethered alkene moiety (Scheme 38a).⁶⁶ Shortly after, Zhang et al has reported a similar reaction using allyl 3-arylpropiolate (Scheme 38b, **1-222**), which leads to an even more reactive β -diketone- α -gold carbene species.⁶⁷ Our group has also reported an enantioselective cyclopropanation enable by a designed chiral *P,N*-bidentate ligand (Scheme 38c).⁶⁸

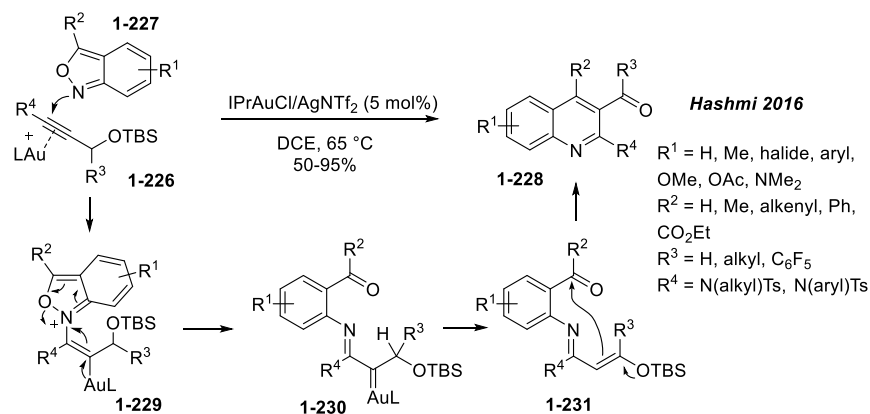
Scheme 38. Cyclopropanation of Oxidatively-Generated Gold Carbene



With carefully-designed substrate, α -oxo gold carbene undergoes 1,2-*H*-shift to give α,β -unsaturated ketones. One recent example was published by Hashmi and co-workers featuring an umpolung of the gold carbene center (Scheme 39).⁶⁹ The key design is putting

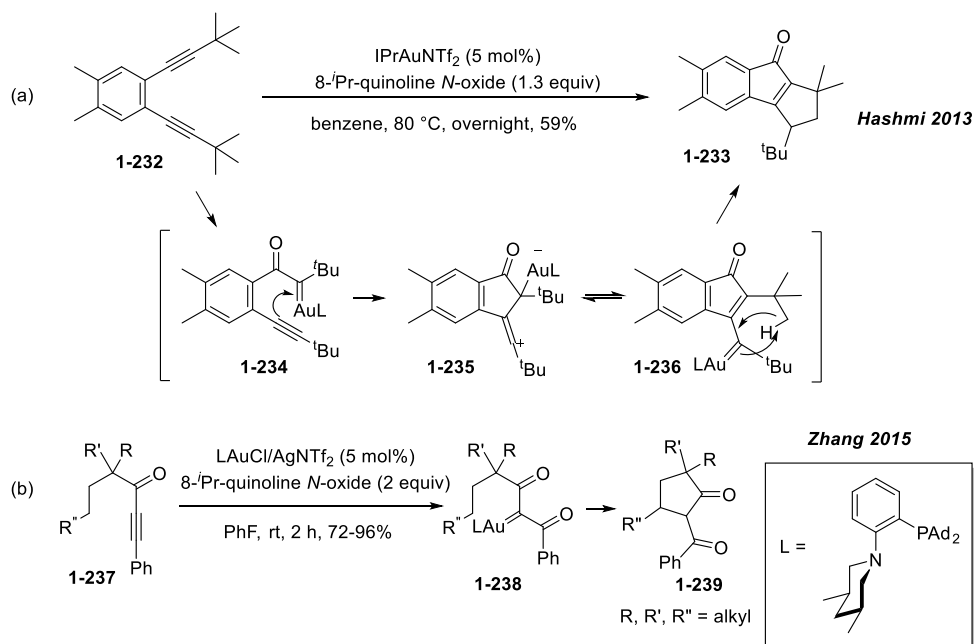
an OTBS group at the β -position of the gold carbene **1-230** so that 1,2-*H*-shift gives an enol ether intermediate **1-231**. Intermediate **1-231** then transforms into the quinoline product **1-228** through a Mukaiyama aldol condensation.

Scheme 39. Umpolung Chemistry of Oxidatively-Generated Gold Carbene



Finally, C-H insertion reaction has also been realized with the oxidative gold catalysis system. Early trials in this area were unsuccessful with unactivated $\text{C}(\text{sp}^3)\text{-H}$ bonds, possibly due to the α -oxo gold carbene being not reactive enough for this energy-demanding reaction. In 2013, Hashmi et al has reported one example of α -oxo gold carbene inserting into the C-H bond on a proximal tert-butyl group (Scheme 40a).⁷⁰ Two years later, our group reported a intramolecular insertion into unactivated $\text{C}(\text{sp}^3)\text{-H}$ bonds with β -diketone- α -gold carbenes (Scheme 40b).⁷¹ This method provides a versatile strategy of constructing cyclopentanones as well as various spiro-, bridged, and fused bicyclic ketones.

Scheme 40. Insertion of Oxidatively-Generated Gold Carbene into Unactivated C(sp³)-H Bonds



1.3 Summary

In summary, easily-available alkynes, combined with versatilities of homogeneous gold catalysis, provides endless possibilities in setting up cascade reaction that greatly increases molecular complexity. In the next three chapters, I will present my works on this topic during my doctoral study, which fall readily into the two categories discussed in the section above.

1.4 References

1. Wiberg, E., *Inorganic Chemistry*. 1 ed.; Academic Press: 2001; p 1884.
2. Norman, R. O. C.; Parr, W. J. E.; Thomas, C. B., *Journal of the Chemical Society, Perkin Transactions 1* **1976**, (18), 1983-1987.
3. (a) Fukuda, Y.; Utimoto, K.; Nozaki, H., *Heterocycles* **1987**, 25 (1), 297-300; (b) Fukuda, Y.; Utimoto, K., *Bulletin of the Chemical Society of Japan* **1991**, 64 (6), 2013-2015; (c) Fukuda, Y.; Utimoto, K., *Synthesis* **1991**, 1991 (11), 975-978; (d) Müller, T. E., *Tetrahedron Letters* **1998**, 39 (33), 5961-5962.

4. Teles, J. H.; Brode, S.; Chabanas, M., *Angewandte Chemie International Edition* **1998**, *37* (10), 1415-1418.
5. (a) Gorin, D. J.; Sherry, B. D.; Toste, F. D., *Chemical Reviews* **2008**, *108* (8), 3351-3378; (b) Clavier, H.; Nolan, S. P., *Chemical Communications* **2010**, *46* (6), 841-861; (c) Klahn, P.; Kirsch, S. F., *ChemCatChem* **2011**, *3* (4), 649-652; (d) Wang, W.; Hammond, G. B.; Xu, B., *Journal of the American Chemical Society* **2012**, *134* (12), 5697-5705.
6. Jia, M.; Bandini, M., *ACS Catalysis* **2015**, *5* (3), 1638-1652.
7. Kennedy-Smith, J. J.; Staben, S. T.; Toste, F. D., *Journal of the American Chemical Society* **2004**, *126* (14), 4526-4527.
8. Hashmi, A. S. K.; Weyrauch, J. P.; Frey, W.; Bats, J. W., *Organic Letters* **2004**, *6* (23), 4391-4394.
9. (a) Xi, Y.; Su, Y.; Yu, Z.; Dong, B.; McClain, E. J.; Lan, Y.; Shi, X., *Angewandte Chemie International Edition* **2014**, *53* (37), 9817-9821; (b) Yu, Z.; Ma, B.; Chen, M.; Wu, H.-H.; Liu, L.; Zhang, J., *Journal of the American Chemical Society* **2014**, *136* (19), 6904-6907.
10. (a) Dorel, R.; Echavarren, A. M., *Chem Rev* **2015**, *115* (17), 9028-907272; (b) Zheng, Z.; Wang, Z.; Wang, Y.; Zhang, L., *Chem Soc Rev* **2016**, *45* (16), 4448-4458; (c) Li, Y.; Li, W.; Zhang, J., *Chemistry* **2017**, *23* (3), 467-512.
11. Ohno, H., *Israel Journal of Chemistry* **2013**, *53* (11-12), 869-882.
12. Hashmi, A. S. K.; Schwarz, L.; Choi, J.-H.; Frost, T. M., *Angewandte Chemie International Edition* **2000**, *39* (13), 2285-2288.
13. Liu, Y.; Song, F.; Song, Z.; Liu, M.; Yan, B., *Organic Letters* **2005**, *7* (24), 5409-5412.
14. Egi, M.; Azechi, K.; Akai, S., *Organic Letters* **2009**, *11* (21), 5002-5005.
15. Barluenga, J.; Dieguez, A.; Fernandez, A.; Rodriguez, F.; Fananas, F. J., *Angewandte Chemie International Edition* **2006**, *45* (13), 2091-2093.
16. Hashmi, A. S.; Buhrlé, M.; Wolfle, M.; Rudolph, M.; Wietek, M.; Rominger, F.; Frey, W., *Chemistry - A European Journal* **2010**, *16* (32), 9846-9854.
17. Dubé, P.; Toste, F. D., *Journal of the American Chemical Society* **2006**, *128* (37), 12062-12063.
18. Nakamura, I.; Sato, T.; Yamamoto, Y., *Angewandte Chemie International Edition* **2006**, *45* (27), 4473-4475.
19. Nakamura, I.; Sato, T.; Terada, M.; Yamamoto, Y., *Organic Letters* **2007**, *9* (20), 4081-4083.
20. Yao, T.; Zhang, X.; Larock, R. C., *Journal of the American Chemical Society* **2004**, *126* (36), 11164-11165.
21. Asao, N.; Takahashi, K.; Lee, S.; Kasahara, T.; Yamamoto, Y., *Journal of the American Chemical Society* **2002**, *124* (43), 12650-12651.
22. Asao, N.; Sato, K.; Menggenbateer; Yamamoto, Y., *The Journal of Organic Chemistry* **2005**, *70* (9), 3682-3685.
23. Kim, N.; Kim, Y.; Park, W.; Sung, D.; Gupta, A. K.; Oh, C. H., *Organic Letters* **2005**, *7* (23), 5289-5291.
24. Asao, N.; Aikawa, H.; Tago, S.; Umetsu, K., *Organic Letters* **2007**, *9* (21), 4299-4302.
25. Santos, L. L.; Ruiz, V. R.; Sabater, M. J.; Corma, A., *Tetrahedron* **2008**, *64* (34), 7902-7909.
26. Li, C.-J.; Skouta, R., *Synlett* **2007**, *2007* (11), 1759-1762.
27. Kramer, S.; Madsen, J. L. H.; Rottländer, M.; Skrydstrup, T., *Organic Letters* **2010**, *12* (12), 2758-2761.
28. Xin, Z.; Kramer, S.; Overgaard, J.; Skrydstrup, T., *Chemistry - A European Journal* **2014**, *20* (26), 7926-7930.
29. Ketcham, J. M.; Biannic, B.; Aponick, A., *Chemical Communications* **2013**, *49* (39), 4157-4159.

30. Gómez-Suárez, A.; Gasperini, D.; Vummaleti, S. V. C.; Poater, A.; Cavallo, L.; Nolan, S. P., *ACS Catalysis* **2014**, *4* (8), 2701-2705.
31. Wang, Y.; Ye, L.; Zhang, L., *Chemical Communications* **2011**, *47* (27), 7815-7817.
32. Wang, Y.; Liu, L.; Zhang, L., *Chemical Science* **2013**, *4* (2), 739-746.
33. Ferrer, C.; Amijs, C. H.; Echavarren, A. M., *Chemistry - A European Journal* **2007**, *13* (5), 1358-1373.
34. (a) Liu, Y.; Xu, W.; Wang, X., *Organic Letters* **2010**, *12* (7), 1448-1451; (b) Cera, G.; Crispino, P.; Monari, M.; Bandini, M., *Chemical Communications* **2011**, *47* (27), 7803-7805; (c) Cera, G.; Chiarucci, M.; Mazzanti, A.; Mancinelli, M.; Bandini, M., *Organic Letters* **2012**, *14* (5), 1350-1353.
35. Naoe, S.; Suzuki, Y.; Hirano, K.; Inaba, Y.; Oishi, S.; Fujii, N.; Ohno, H., *The Journal of Organic Chemistry* **2012**, *77* (11), 4907-4916.
36. Hou, Q.; Zhang, Z.; Kong, F.; Wang, S.; Wang, H.; Yao, Z. J., *Chemical Communications* **2013**, *49* (7), 695-697.
37. Nakamura, K.; Furumi, S.; Takeuchi, M.; Shibuya, T.; Tanaka, K., *Journal of the American Chemical Society* **2014**, *136* (15), 5555-5558.
38. Hashmi, A. S. K.; Frost, T. M.; Bats, J. W., *Journal of the American Chemical Society* **2000**, *122* (46), 11553-11554.
39. (a) Nieto-Oberhuber, C.; Muñoz, M. P.; Buñuel, E.; Nevado, C.; Cárdenas, D. J.; Echavarren, A. M., *Angewandte Chemie International Edition* **2004**, *43* (18), 2402-2406; (b) Nieto-Oberhuber, C.; López, S.; Muñoz, M. P.; Cárdenas, D. J.; Buñuel, E.; Nevado, C.; Echavarren, A. M., *Angewandte Chemie International Edition* **2005**, *44* (38), 6146-6148; (c) Nieto-Oberhuber, C.; López, S.; Jiménez-Núñez, E.; Echavarren, A. M., *Chemistry - A European Journal* **2006**, *12* (23), 5916-5923; (d) Cabello, N.; Jiménez-Núñez, E.; Buñuel, E.; Cárdenas, D. J.; Echavarren, A. M., *European Journal of Organic Chemistry* **2007**, *2007* (25), 4217-4223.
40. Nieto-Oberhuber, C.; Lopez, S.; Munoz, M. P.; Jimenez-Nunez, E.; Bunuel, E.; Cardenas, D. J.; Echavarren, A. M., *Chemistry - A European Journal* **2006**, *12* (6), 1694-1702.
41. Jimenez-Nunez, E.; Claverie, C. K.; Nieto-Oberhuber, C.; Echavarren, A. M., *Angewandte Chemie International Edition* **2006**, *45* (33), 5452-5455.
42. Nieto-Oberhuber, C.; Pérez-Galán, P.; Herrero-Gómez, E.; Lauterbach, T.; Rodríguez, C.; López, S.; Bour, C.; Rosellón, A.; Cárdenas, D. J.; Echavarren, A. M., *Journal of the American Chemical Society* **2008**, *130* (1), 269-279.
43. Cai, P. J.; Wang, Y.; Liu, C. H.; Yu, Z. X., *Organic Letters* **2014**, *16* (22), 5898-5901.
44. Luzung, M. R.; Markham, J. P.; Toste, F. D., *Journal of the American Chemical Society* **2004**, *126* (35), 10858-10859.
45. Horino, Y.; Yamamoto, T.; Ueda, K.; Kuroda, S.; Toste, F. D., *Journal of the American Chemical Society* **2009**, *131* (8), 2809-2811.
46. Bohan, P. T.; Toste, F. D., *Journal of the American Chemical Society* **2017**, *139* (32), 11016-11019.
47. Zhang, G.; Zhang, L., *Journal of the American Chemical Society* **2008**, *130* (38), 12598-12599.
48. Sperger, C. A.; Tungen, J. E.; Fiksdahl, A., *European Journal of Organic Chemistry* **2011**, *2011* (20-21), 3719-3722.
49. Uemura, M.; Watson, I. D. G.; Katsukawa, M.; Toste, F. D., *Journal of the American Chemical Society* **2009**, *131* (10), 3464-3465.
50. Wang, Y.; Lu, B.; Zhang, L., *Chemical Communications* **2010**, *46* (48), 9179-9181.
51. Rao, W.; Sally; Berry, S. N.; Chan, P. W., *Chemistry - A European Journal* **2014**, *20* (41), 13174-13180.

52. Ye, L.; Wang, Y.; Aue, D. H.; Zhang, L., *Journal of the American Chemical Society* **2012**, *134* (1), 31-34.
53. Hashmi, A. S.; Braun, I.; Nosel, P.; Schadlich, J.; Wieteck, M.; Rudolph, M.; Rominger, F., *Angewandte Chemie International Edition* **2012**, *51* (18), 4456-4460.
54. Hashmi, A. S.; Wieteck, M.; Braun, I.; Rudolph, M.; Rominger, F., *Angewandte Chemie International Edition* **2012**, *51* (42), 10633-10637.
55. Hashmi, A. S. K.; Wieteck, M.; Braun, I.; Nösel, P.; Jongbloed, L.; Rudolph, M.; Rominger, F., *Advanced Synthesis & Catalysis* **2012**, *354* (4), 555-562.
56. Hansmann, M. M.; Tsupova, S.; Rudolph, M.; Rominger, F.; Hashmi, A. S., *Chemistry - A European Journal* **2014**, *20* (8), 2215-2223.
57. (a) Hansmann, M. M.; Rudolph, M.; Rominger, F.; Hashmi, A. S., *Angewandte Chemie International Edition* **2013**, *52* (9), 2593-2598; (b) Wang, Y.; Yepremyan, A.; Ghorai, S.; Todd, R.; Aue, D. H.; Zhang, L., *Angewandte Chemie International Edition* **2013**, *52* (30), 7795-7799.
58. Mamane, V.; Hannen, P.; Furstner, A., *Chemistry - A European Journal* **2004**, *10* (18), 4556-4575.
59. Soriano, E.; Marco-Contelles, J., *Organometallics* **2006**, *25* (19), 4542-4553.
60. Moran-Poladura, P.; Rubio, E.; Gonzalez, J. M., *Angewandte Chemie International Edition* **2015**, *54* (10), 3052-3055.
61. Bucher, J.; Wurm, T.; Nalivela, K. S.; Rudolph, M.; Rominger, F.; Hashmi, A. S., *Angewandte Chemie International Edition* **2014**, *53* (15), 3854-3858.
62. Wang, Y.; Zarca, M.; Gong, L. Z.; Zhang, L., *Journal of the American Chemical Society* **2016**, *138* (24), 7516-7519.
63. (a) Shapiro, N. D.; Toste, F. D., *Journal of the American Chemical Society* **2007**, *129* (14), 4160-4161; (b) Li, G.; Zhang, L., *Angewandte Chemie International Edition* **2007**, *46* (27), 5156-5159; (c) Lu, B.; Li, Y.; Wang, Y.; Aue, D. H.; Luo, Y.; Zhang, L., *Journal of the American Chemical Society* **2013**, *135* (23), 8512-8524.
64. (a) Ye, L.; Cui, L.; Zhang, G.; Zhang, L., *Journal of the American Chemical Society* **2010**, *132* (10), 3258-3259; (b) Ye, L.; He, W.; Zhang, L., *Journal of the American Chemical Society* **2010**, *132* (25), 8550-8551; (c) Ye, L.; He, W.; Zhang, L., *Angewandte Chemie International Edition* **2011**, *50* (14), 3236-3239; (d) Wang, Y.; Ji, K.; Lan, S.; Zhang, L., *Angewandte Chemie International Edition* **2012**, *51* (8), 1915-1918; (e) Ji, K.; Zhao, Y.; Zhang, L., *Angewandte Chemie International Edition* **2013**, *52* (25), 6508-6512; (f) Wu, G.; Zheng, R.; Nelson, J.; Zhang, L., *Advanced Synthesis & Catalysis* **2014**, *356* (6), 1229-1234.
65. He, W.; Li, C.; Zhang, L., *Journal of the American Chemical Society* **2011**, *133* (22), 8482-8485.
66. Vasu, D.; Hung, H. H.; Bhunia, S.; Gawade, S. A.; Das, A.; Liu, R. S., *Angewandte Chemie International Edition* **2011**, *50* (30), 6911-6914.
67. Qian, D.; Zhang, J., *Chemical Communications* **2011**, *47* (39), 11152-11154.
68. Ji, K.; Zheng, Z.; Wang, Z.; Zhang, L., *Angewandte Chemie International Edition* **2015**, *54* (4), 1245-1249.
69. Jin, H.; Tian, B.; Song, X.; Xie, J.; Rudolph, M.; Rominger, F.; Hashmi, A. S. K., *Angewandte Chemie International Edition* **2016**, *55* (41), 12688-12692.
70. Nösel, P.; dos Santos Comprido, L. N.; Lauterbach, T.; Rudolph, M.; Rominger, F.; Hashmi, A. S. K., *Journal of the American Chemical Society* **2013**, *135* (41), 15662-15666.
71. Wang, Y.; Zheng, Z.; Zhang, L., *Journal of the American Chemical Society* **2015**, *137* (16), 5316-5319.

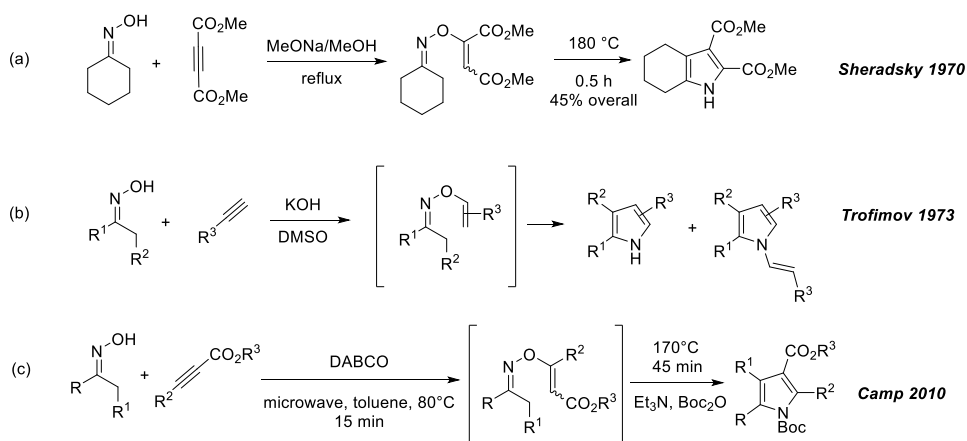
Chapter 2 One-Pot Synthesis of Fused Pyrroles via a Gold Catalysis-Triggered Cascade

2.1 Design of a Gold Catalysis-Triggered Cascade

Pyrrole and its derivatives makes up one of the largest family of organic compounds. It is also prevalent in various molecules of interest in pharmaceutical science¹ and polymer chemistry.² Although numerous methods of synthesizing pyrrole and its derivatives has been established,³ the development of new approaches, and particularly, methods featuring better functional group compatibility, milder conditions, and more readily accessible starting materials, is always in great demand.

One rather underutilized method in pyrrole synthesis is the rearrangement of *O*-vinyloximes, which is easily synthesized by addition of oxime over C-C triple bonds. Some of the earliest works in this area were done by Sheradsky in 1970, who demonstrated a two-step approach that involves a thermal 3,3-sigmatropic rearrangement of the *O*-vinyloxime intermediate (Scheme 41a).⁴ In 1973, a similar method was developed by Trofimov et al utilizing strongly basic conditions that allows unactivated alkynes to be used in the synthesis (Scheme 41b).⁵ Despite the harsh condition, Trofimov's method has been employed in synthesizing various pyrrole-containing molecules.⁶ More recently, a microwave-induced approach was developed by Camp et al (Scheme 41c).⁷ However, the reaction still requires alkynes with activating groups, limiting its synthetic versatility.

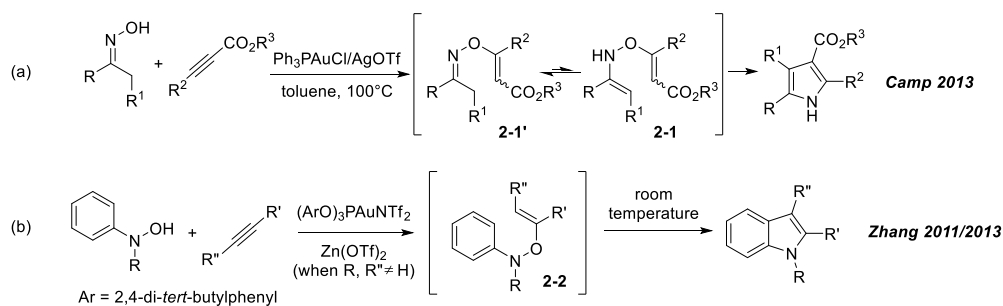
Scheme 41. Pyrrole Synthesis from Oximes and Alkynes



Homogeneous gold catalysts are known for their unique property of promoting nucleophilic addition over C-C triple bonds.⁸ Surprisingly, gold catalysis has only been utilized very recently in pyrrole synthesis. Camp et al. first achieved a regioselective synthesis of substituted pyrroles initiated by gold-catalyzed nucleophilic addition of oxime across activated alkynes (Scheme 42a).⁹ However, synthetic versatility of the method was limited by the rather high reaction temperatures.

During the same period, our group reported an efficient synthesis of 2-alkylindoles based on the rearrangement of *O*-vinyl-*N*-arylhydroxylamine generated via gold-catalyzed nucleophilic addition across an alkyne (Scheme 42b).¹⁰ Interestingly, the two seemingly similar reactions occur at vastly different temperatures (i.e., 100 °C versus room temperature). We reasoned that the difference in reaction temperature could be attributed to the different ways of generating key *N,O*-dialkenylhydroxamine species (i.e. intermediate **2-1** and **2-2**). In Camp's method, it takes a rather energy-demanding tautomerization to generate **2-2** from *O*-vinyloxime intermediate **2-1'**. We envision that if the tautomerization step could be facilitated by function groups on the substrate, the overall reaction should be very likely to occur under room temperature and exhibit much better synthetic versatility.

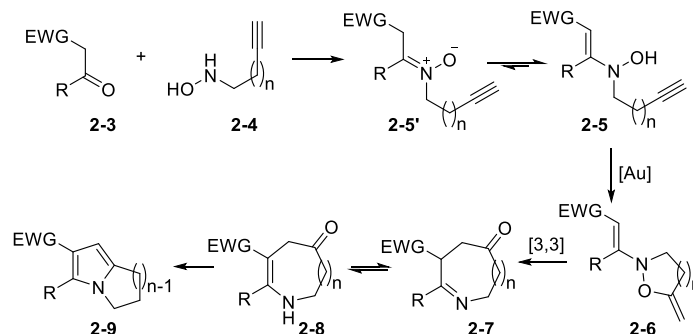
Scheme 42. Examples of Pyrrole/Indole Synthesis Triggered by Gold-Catalyzed Nucleophilic Addition



Our design based upon the reasoning above is shown in Scheme 43. We expected that the condensation between ketone **2-3** and *N*-monosubstituted hydroxylamine **2-4** would lead to the electronic neutral *N*-hydroxylenamine **2-5** instead of the charged nitron species **2-5'** with the aid of electron-withdrawing group at the ketone's α -position. With the C-C triple bond positioned on the alkyl group of the original hydroxylamine, **2-5** could undergo gold-catalyzed nucleophilic addition to deliver an *N,O*-dialkenylhydroxylamine **2-6**, which

should rearrange under room temperature in a similar way as the *O*-vinyl-*N*-aryhydroxyamine in our previously published indole synthesis. The subsequently formed cyclic iminoketone **2-7** could tautomerize to an enamine, which proceeds through dehydrative annulation to complete the cascade and deliver the product **2-9** as a 1,2-fused pyrrole.

Scheme 43. Design of a Cascade Approach towards 1,2-Fused Pyrroles



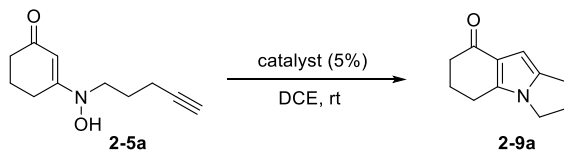
2.2 Condition Study, and Approaches to Achieve a One-Pot Reaction

To verify our hypothesis, we synthesized the *N*-hydroxylenamine **2-5a** by condensing *N*-(pent-4-yn-1-yl)hydroxylamine and 1,3-cyclohexanedione and treated it with various gold catalysts in dichloromethane (see Table 1). To our delight, the desired reaction occurred readily under room temperature in the presence of $\text{Ph}_3\text{PAuNTf}_2$, affording the desired tricyclic pyrrole **2-9a** in a moderate 50% yield (entry 1). Notably, neither of the eight-membered ring intermediates (i.e. **2-7** and **2-8**) was detected by ^1H NMR, suggesting that its subsequent transannular condensation was facile. This encouraging result was improved by using other gold catalysts (entries 2-5). Particularly, both BrettPhosAuNTf_2 (entry 3) and MorDalPhosAuNTf_2 (entry 4) led to NMR yields of more than 80%. Although the latter catalyst was slightly more effective, BrettPhosAuNTf_2 was preferred for the faster and cleaner reaction. On the other hand, AuCl_3 was less effective as a catalyst (entry 6), and the reaction was most likely not promoted by a Brønsted acid as CF_3COOH , even with a large excess amount, was incapable to promote the reaction (entry 7).

To improve the overall efficiency, we probed whether the synthesis of the *N*-hydroxylenamine precursor **2-5a** and the subsequent gold catalysis could be integrated into a one-pot process. First, we examined the synthesis of **2-5a** via the room temperature

condensation between *N*-(pent-4-yn-1-yl)-hydroxylammonium trifluoroacetates **2-4** and 1,3-cyclohexanedione **2-3a** in the presence of a base, under N₂ atmosphere. The protonated hydroxylamine was used as its free form is prone to oxidation. To avoid gold catalyst being poisoned by base, we limited the choices of bases to those of mild nature. As shown in Table 2, while K₂CO₃ (entry 1) worked poorly, the other bases including 8-methylquinoline (entry 2), sodium tosylate (entry 3), NaOAc (entry 4) and NaHCO₃ (entry 5) were all effective, with the last one affording the highest NMR yield of **2-5a**.

Table 1. Reaction Discovery and Catalyst Optimization



Entry	Catalyst	Time	Yield ^[a]
1	Ph ₃ PAuNTf ₂	4.5 h	50%
2	IPrAuNTf ₂	7 h	72%
3	BrettPhosAuNTf₂	0.5 h	82%
4	MorDalPhosAuNTf ₂	6 h	85%
5	PhosphiteAuNTf ₂	2 h	57%
6	AuCl ₃	12 h	42% ^c
7	CF ₃ COOH ^c	12 h	<1% ^c

[a] NMR yield, determined by using diethyl phthalate as the internal reference. [b] Not finished when stopped. [c] 10 equivalents used.

With the mild conditions (Table 2, entry 5) established, a gold catalysis-triggered cascade reaction using the optimized conditions in Table 1 in a one-pot manner was then performed. To our delight, the reaction proceeded smoothly although expectedly slower, and the overall isolated yield of **2-9a** was satisfactory (Table 3, entry 1).

2.3 Scope Study of the Cascade Reaction

Table 2. Optimizing the Condensation Step

Entry	Base	Time	Yield ^[a] (%)
1	K ₂ CO ₃ (1.5 eq.)	4 h	37
2	8-Methylquinoline (1.2 eq.)	3 h	88
3	TsONa (1.2 eq.)	2 h	80
4	NaOAc (1.2 eq.)	2.5 h	83
5	NaHCO ₃ (1.2 eq.)	1.5 h	93

[a] NMR yield, determined by using diethyl phthalate as the internal reference.

Table 3. One-Pot Synthesis of Tricyclic Pyrroles from 1,3-Cyclodiketones

Entry	Product	Yield ^[a]	Entry	Product	Yield ^[a]
1		2-9a , 75%, 4 h	5		2-9e , 57%, 3.5 h
2		2-9b , 55%, 4 h	6		2-9f , 63% ^[b] , 8 h
3		2-9c , 62% ^[b] , 4.5 h	7		2-9g , 50%, 7.5 h
4		2-9d , 52%, 4 h			

[a] One-pot overall isolated yield. Reaction time referring to the both steps. [b] Regiochemistry established by nOe experiments.

We then investigated the scope of the reaction by applying a series of readily available substituted 1,3-cyclohexanediones. To our delight, many of them underwent the reaction smoothly, affording substituted tricyclic pyrroles in mostly good yields (Table 3, entries 2-6). Interestingly, when the two carbonyl groups are sterically differentiated as in the case of **2-9c** or **2-9f**, the α -substituted one remained unchanged while the more hindered one was incorporated into the pyrrole ring (entries 3 and 6), indicating a high level of steric preference. In addition to cyclohexane-1,3-diones, cyclopentane-1,3-diones also participated in the reaction without accident, affording **2-9g** with an exquisite linear azatriquinane skeleton. While the overall yields in most cases are moderate, these one-pot reactions are serviceable considering the enhanced operational efficiency and, moreover, the average yield for each step is $>70\%$.

To further expand the reaction scope, we turned to acyclic 1,3-diketone compounds. Instead of the anticipated product, an acyl-substituted 1,2-fused pyrrole **2-10**, the isoxazonium side product was detected (Scheme 44, **2-11**). This heteroarene is likely formed by two consecutive condensation reactions during the first condensation step in the absence of the gold catalysis, as shown in the proposed mechanism (Scheme 44). Indeed, when the substrates were mixed without the presence of gold catalyst, **2-11** was formed in 60% NMR yield within similar period.

Scheme 44. Applying Acyclic 1,3-Dicarbonyl Compounds to the Reaction

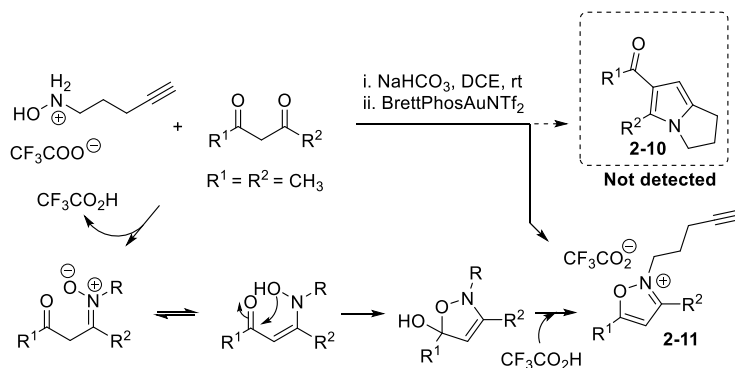


Table 4. Expanded Reaction Scope^[a]

entry	ketone	hydroxylamine	product	yield ^[b]
1				2-9h , 42% ^[c] , 4 h
2				2-9i , 37%, 4.5 h
3				2-9j , 61%, 4 h
4				2-9k , 56%, 6 h

[a] Reactions were run with the same condition as in Table 3. [b] Isolated yield. [c] Structure as shown, determined by nOe experiment.

To circumvent the formation of isoxazonium side product, we reasoned that a strong electron-withdrawing R¹ or R² group on **2-11** might hinder its formation due to the destabilization of the positively charged isoxazole ring. To our delight, when 1,1,1-trifluoropentane-2,4-dione was employed, the expected bicyclic pyrrole **2-9h** was obtained in 42% yield (Table 4, entry 1). Though with a relatively low efficiency, the reaction was highly selective toward the less electrophilic carbonyl group. An alternative approach to avoid the formation of isoxazonium intermediates is to replace one of the carbonyl group with other electron-withdrawing groups. For example, when a 4-nitrophenyl group was employed, a low yet serviceable yield of the substituted bicyclic pyrrole **2-9i** was obtained (entry 2). A few different *N*-alkynylhydroxylamine were also tested. A benzene-fused variant **2-4b** reacted without incident to afford the tetracyclic pyrrole **2-9j** in a good overall yield for the two-step sequence (entry 3), and a homolog of **2-4a** also participated in the

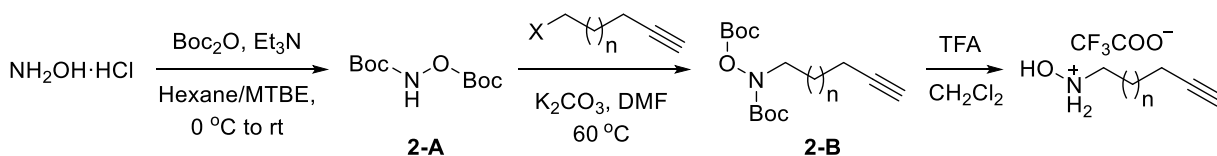
reaction smoothly, thus leading to the formation of a piperidine-fused tricyclic pyrrole **2-k** in a good overall yield (entry 4).

2.4 Conclusion

In summary, we have developed a facile two-step cascade reaction for the synthesis of fused pyrroles from *N*-alkynylhydroxylamines and readily enolizable ketones. By varying the substrates, fused pyrroles of different bicyclic, tricyclic, and tetracyclic skeletons can be readily access in moderate to good yields. This reaction employs a gold-catalyzed nucleophilic addition reaction to trigger a cascade process featuring a facile 3,3-sigmatropic rearrangement of *N,O*-dialkenylhydroxylamine intermediate, which is formed by the aforementioned nucleophilic addition. The method features mild condition and compatibility with different functional groups.

2.5 Experimental Details

General Procedure A: preparation of *N*-alkylhydroxylammonium trifluoroacetate

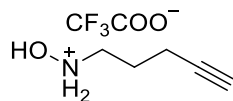


2-A was prepared using the method reported by Staszak et al¹¹ from hydroxylamine hydrochloride and di-*tert*-butyl dicarbonate.

2-A (1.165 g, 5 mmol), an alkyne (5.5 mmol, $n = 1$ or 2), K_2CO_3 (863 mg, 6.25 mmol) and DMF (5 mL) was mixed at room temperature. The mixture was then stirred vigorously and heated overnight at $60\text{ }^\circ\text{C}$. The resulting mixture was extracted with ethyl acetate and washed with water until most of the DMF is removed, dried with MgSO_4 and concentrated under reduced pressure to afford product **2-B** in 90% yield.

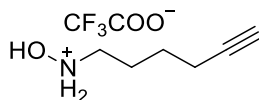
Trifluoroacetic acid (4.5 mL) was added dropwise into a solution of **2-B** (1.5 g, 5 mmol) in 10.5 mL dichloromethane at room temperature. The mixture was then stirred vigorously for 2.5 hours and TLC was used to monitor the reaction. Upon finished, the solvent and excess amount of trifluoroacetic acid was removed under vacuum to give the crude product as a yellow semi-solid. The crude product was further washed with cold hexanes to get rid of the trifluoroacetic acid impurities, affording the product in >90% yield as a light yellow solid.

***N*-(pent-4-ynyl)hydroxylammonium trifluoroacetate salt 2-4a**



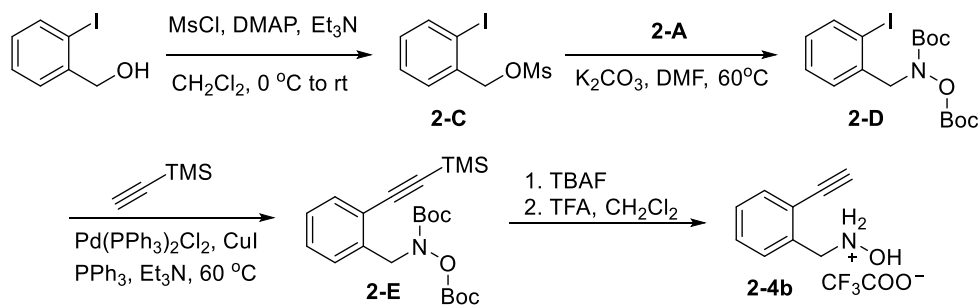
N-(pent-4-ynyl)hydroxylammonium trifluoroacetate salt was prepared following the general procedure A, using 5-chloro-1-pentyne in the second step. ¹H NMR (600 MHz, DMSO-*d*₆) δ 3.14 (t, *J* = 7.7 Hz, 2H), 2.81 (s, 1H), 2.26 (td, *J* = 7.0, 2.4 Hz, 2H), 1.76 (p, *J* = 7.3 Hz, 2H); ¹³C NMR (151 MHz, DMSO-*d*₆) δ 160.08 – 159.43 (q, ²*J*_{CF} = 32.5 Hz), 120.10 – 114.21 (q, ¹*J*_{CF} = 300.3 Hz), 83.32, 72.45, 49.66, 22.66, 15.44; IR (neat, cm⁻¹): 3301, 2122, 1672, 1440, 1198, 1141; ESI+ calculated for [C₅H₁₀NO]⁺: 100.08, found 100.07.

***N*-(hex-5-ynyl)hydroxylammonium trifluoroacetate salt 2-4c**



N-(hex-5-ynyl)hydroxylammonium trifluoroacetate salt (**2-4c**) was prepared following the general procedure A, using 6-bromo-1-hexyne in the second step. ¹H NMR (600 MHz, CDCl₃) δ 3.36 – 3.16 (m, 2H), 2.30 – 2.14 (t, *J* = 7.1 Hz, 2H), 2.02 – 1.94 (t, *J* = 3.3 Hz, 1H), 1.95 – 1.82 (p, *J* = 7.6 Hz, 2H), 1.68 – 1.51 (p, *J* = 7.1 Hz, 2H); ¹³C NMR (151 MHz, CDCl₃) δ 82.68, 69.49, 50.80, 24.96, 22.44, 17.83; IR (neat, cm⁻¹): 3304, 2956, 2122, 1673, 1439, 1201, 1144; ESI+ calculated for [C₆H₁₂NO]⁺: 114.09, found 114.08.

Preparation of *N*-(2-ethynylbenzyl)hydroxylammonium trifluoroacetate 2-4b



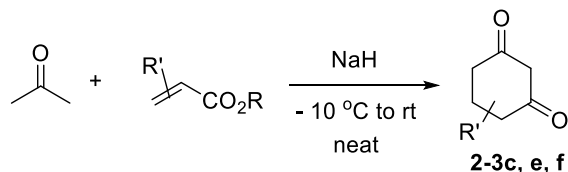
Methanesulfonyl chloride (0.58 mL, 7.5 mmol) was added dropwise to a solution of 2-Iodobenzyl alcohol (1.17 g, 5 mmol), triethylamine (3.5 mL, 25 mmol), and 4-(dimethylamino)pyridine in dichloromethane (10 mL) at 0 °C. The mixture was then allowed to stir at room temperature overnight. The reaction was quenched by 1 M HCl and extracted with ethyl acetate. The organic layer was washed with saturated NaHCO₃ and brine, dried over Na₂SO₄, and concentrated under reduced pressure. The crude product **2-C** was used directly in the next step.

A mixture of **2-C** (439 mg, 1.2 mmol), **2-A** (280 mg, 1.2 mmol) and K₂CO₃ (1.5 mmol, 207 mg) was mixed in 2 mL DMF and the mixture was heated overnight at 60 °C while stirred vigorously. The resulting mixture was extracted with ethyl acetate and washed with water until most of the DMF is removed, dried with MgSO₄ and concentrated under reduced pressure to afford crude product **2-D**, which was directly used in the next step.

To a N₂-flushed 50 mL Schlenk flask was added Pd(PPh₃)₂Cl₂ (84 mg, 0.12 mmol), CuI (45.7 mg, 0.24 mmol), triphenylphosphine (31.4 mg, 0.12 mmol), **2-D** (539 mg, 1.2 mmol), trimethylsilylacetylene (0.85 mL, 6 mmol) and triethylamine (5 mL). The mixture was stirred in N₂ at 60 °C, while TLC is used to monitor the reaction. Upon finished, the solvent is removed under reduced pressure and the residue was purified with flash column chromatography, affording product **2-E** in 82% yield.

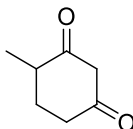
To a solution of **2-E** (419 mg, 1 mmol) in 5 mL dichloromethane was added a THF solution of tetrabutylammonium fluoride (1 M, 2 mL). The mixture was stirred at room temperature and TLC was used to monitor the reaction. Upon finished, the reaction was quenched by 1M HCl and washed with water, dried over Na₂SO₄, concentrated under reduced pressure. The resulting oil was dissolved in dichloromethane (2 mL) and trifluoroacetic acid (1 mL) was added dropwise while stirring vigorously. The mixture was allowed to stir at room temperature for 2 hours, then the solvent and excess amount of trifluoroacetic acid was removed under vacuum to give the product **2-4b** in 90% yield as a dark brown solid. ¹H NMR (500 MHz, CDCl₃) δ 7.67 – 7.55 (dd, *J* = 5.5, 3.5 Hz, 1H), 7.47 – 7.40 (m, 3H), 4.76 – 4.45 (s, 2H), 3.61 – 3.41 (s, 1H); ¹³C NMR (151 MHz, CDCl₃) δ 133.31, 131.37, 130.20, 130.05, 129.80, 122.71, 84.04, 79.95, 54.48; IR (neat, cm⁻¹): 3310, 1672, 1440, 1201, 1144; ESI+ calculated for [C₉H₁₀NO]⁺: 148.08, found 148.06.

General Procedure B: preparation of cyclic 1,3-diketones 2-3c, e, f



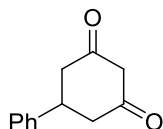
Cyclic 1,3-diketones were prepared using a slightly modified method reported by Das et al.¹² substituted esters (12 mmol) was mixed with NaH (60% dispersed in oil, 600 mg, 15 mmol) at $-10\text{ }^\circ\text{C}$ under N_2 protection. After stirring for 30 minutes, acetone (0.73 mL, 10 mmol) was added dropwise into the suspension. The mixture was stirred at $-10\text{ }^\circ\text{C}$ for 1 hour and was allowed to warm to room temperature and stir for another 2 hours (Caution! A lot of heat and H_2 gas may be generated during this process!). The resulting mixture was quenched by 1M HCl and extracted with ethyl acetate. The extract was washed with brine, dried with Na_2SO_4 , concentrated under reduced pressure, and purified by flash column chromatography.

4-Methylcyclohexane-1,3-dione (2-3c)



4-Methylcyclohexane-1,3-dione (**2c**) was prepared following the general procedure B using methyl methacrylate. Product is yellow semi-solid. Known compound. ESI+ calculated for $[\text{C}_7\text{H}_{11}\text{O}_2]^+$: 127.08, found 127.06.

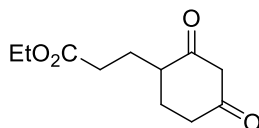
5-Phenylcyclohexane-1,3-dione (2-3e)



5-Phenylcyclohexane-1,3-dione (**2-3e**) was prepared following the general procedure B using ethyl cinnamate. Product is light yellow solid. (Known compound) ^1H NMR (600 MHz, CDCl_3) δ 7.04 – 6.96 (br, 1H), 5.47 (s, 1H), 3.49 – 3.33 (q, $J = 16.9$ Hz, 2H), 2.82 –

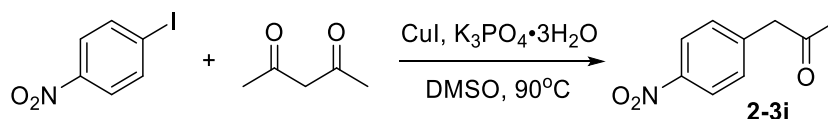
2.29 (m, 5H), 2.29 – 1.89 (m, 2H), 1.84 – 1.44 (m, 2H), 1.30 – 1.06 (m, 6H); ^{13}C NMR ; IR (neat, cm^{-1}): 1996, 1565, 1383, 1191, 1143; ESI+ calculated for $[\text{C}_{12}\text{H}_{13}\text{O}_2]^+$: 189.09, found 189.06.

Ethyl 3-(2,4-dioxocyclohexyl)propanoate (**2-3f**)



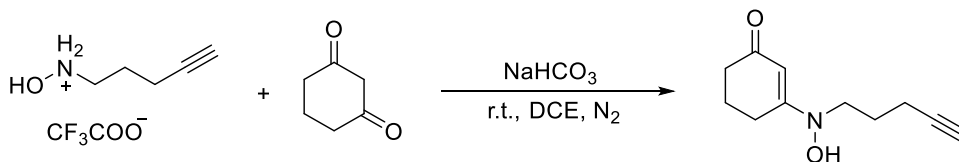
Ethyl 3-(2,4-dioxocyclohexyl)propanoate (**2-3f**) was prepared following the general procedure B using methyl crotonate. Product is light yellow oil. ^1H NMR (500 MHz, CDCl_3) δ 5.48 – 5.38 (s, 1H, tautomer), 4.19 – 4.09 (m, 2H), 3.52 – 3.34 (m, 1H), 2.75 – 2.04 (m, 7H), 1.83 – 1.67 (ddt, $J = 21.3, 14.0, 6.8$ Hz, 1H), 1.65 – 1.49 (qd, $J = 12.6, 4.6$ Hz, 1H), 1.32 – 1.22 (t, $J = 7.1$ Hz, 6H); ^{13}C NMR (151 MHz, CDCl_3) δ 203.92, 203.54, 173.14, 60.52, 58.36, 48.36, 39.77, 31.48, 24.69, 24.35, 14.18; IR (neat, cm^{-1}): 2928, 1730, 1603, 1457, 1195, 1031; ESI+ calculated for $[\text{C}_{11}\text{H}_{16}\text{O}_4\text{Na}]^+$: 235.09, found 235.06.

Preparation of substituted acyclic ketones **2-3i**



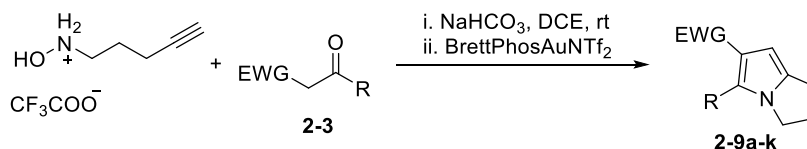
2-3i was prepared using the method reported by Lei:¹³ A mixture of 1-iodo-4-nitrobenzene (1.25 g, 5.0 mmol), acetylacetone (1.54 mL, 15 mmol), CuI (95.5 mg, 0.5 mmol), and $\text{K}_3\text{PO}_4 \cdot 3\text{H}_2\text{O}$ (3.18 g, 15 mmol) in DMSO (15 mL) was stirred in N_2 at 90 °C. After completion of the reaction, the mixture was quenched with 1 M HCl, extracted with ethyl acetate and dried over Na_2SO_4 . The solvent was removed under reduced pressure and the residue was purified by flash column chromatography to afford **2-3i** in 45% yield as a brown solid. (Known compound) ^1H NMR (500 MHz, CDCl_3) δ 8.19 (d, $J = 8.7$ Hz, 1H), 7.36 (d, $J = 8.6$ Hz, 1H), 3.85 (s, 1H), 2.24 (s, 2H); ^{13}C NMR (151 MHz, CDCl_3) δ 204.14, 147.05, 141.45, 130.46, 123.72, 50.01, 29.86; IR (neat, cm^{-1}): 1715, 1598, 1517, 1346, 1159; ESI+ calculated for $[\text{C}_9\text{H}_9\text{NO}_3\text{Na}]^+$: 202.05, found 202.03.

Preparation of 3-(hydroxy(pent-4-ynyl)amino)cyclohex-2-enone **2-5a**



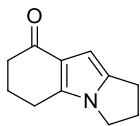
To a 50 mL round bottom flask was added **2-4a** (2.13 g, 10 mmol), 1,3-cyclohexanedione (1.35 g, 12 mmol) and NaHCO₃ (1 g, 12 mmol). The system was degassed with N₂ and 10 mL of anhydrous 1,2-dichloroethane was added. The mixture was allowed to stir at room temperature until TLC showed total consumption of the hydroxylammonium salt. The mixture was then concentrated under reduced pressure and the residue was purified by flash column chromatography and give the product in 90% yield as a light yellow to white solid. ¹H NMR (500 MHz, CDCl₃) δ 5.55 (s, 1H), 3.67 (t, *J* = 6.7 Hz, 2H), 2.50 (t, *J* = 6.3 Hz, 2H), 2.28 – 2.18 (m, 4H), 1.98 – 1.91 (m, 5H); ¹³C NMR (151 MHz, CDCl₃) δ 195.85, 165.18, 95.24, 83.23, 69.42, 51.02, 34.46, 25.64, 2

General procedure C: one-pot synthesis of fused pyrroles with the gold catalysis-triggered cascade



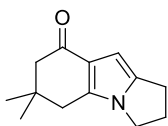
To a N₂-flushed vial with magnetic stirring bar was added **2-4a** (0.1 mmol), ketones **2-3** (1.2 equiv.), NaHCO₃ (1.2 equiv.) and 1,2-dichloroethane (2 mL). The system was degassed with N₂ and the mixture was stirred at room temperature. The reaction was monitored by TLC. Upon finished, the cap was opened and the BrettPhosAuNTf₂ (5 mol%) was added. The reaction was allowed to stir at room temperature until completion (monitored by TLC), and was concentrated under reduced pressure. The residue was purified by flash column chromatography to afford the product **2-9a-k**.

2,3,6,7-Tetrahydro-1H-pyrrolo[1,2-a]indol-8(5H)-one (2-9a)



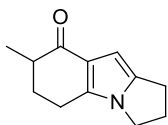
2,3,6,7-Tetrahydro-1H-pyrrolo[1,2-a]indol-8(5H)-one (**2-9a**) was prepared following the general procedure C. ^1H NMR (600 MHz, CDCl_3) δ 6.13 (s, 1H), 3.81 (t, $J = 7.1$ Hz, 2H), 2.78 (t, $J = 7.4$ Hz, 2H), 2.69 (t, $J = 6.2$ Hz, 2H), 2.48 (p, $J = 7.2$ Hz, 2H), 2.43 – 2.36 (m, 2H), 2.09 (p, $J = 6.3$ Hz, 2H); ^{13}C NMR (151 MHz, CDCl_3) δ 194.25, 138.86, 137.77, 124.23, 96.15, 44.02, 37.76, 27.77, 23.85, 23.55, 22.03; IR (neat, cm^{-1}): 2946, 1639, 1486, 1471, 1369, 1170; ESI+ calculated for $[\text{C}_{11}\text{H}_{13}\text{NONa}]^+$: 198.09, found 198.07.

6,6-Dimethyl-2,3,6,7-tetrahydro-1H-pyrrolo[1,2-a]indol-8(5H)-one (2-9b)



6,6-Dimethyl-2,3,6,7-tetrahydro-1H-pyrrolo[1,2-a]indol-8(5H)-one (**2-9b**) was prepared following the general procedure C. ^1H NMR (500 MHz, CDCl_3) δ 6.14 (s, 1H), 3.81 (t, $J = 7.1$ Hz, 2H), 2.81 (t, $J = 7.3$ Hz, 2H), 2.57 (s, 2H), 2.50 (p, $J = 7.2$ Hz, 2H), 2.30 (s, 2H), 1.10 (s, 6H); ^{13}C NMR (126 MHz, CDCl_3) δ 193.49, 137.91, 137.59, 123.10, 96.04, 52.00, 43.96, 36.14, 35.56, 28.75, 27.74, 23.60; IR (neat, cm^{-1}): 2959, 2931, 2094, 1644, 1470, 1368, 1274; ESI+ calculated for $[\text{C}_{13}\text{H}_{18}\text{NO}]^+$: 204.14, found 204.11.

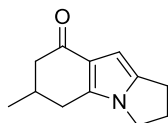
7-Methyl-2,3,6,7-tetrahydro-1H-pyrrolo[1,2-a]indol-8(5H)-one (2-9c)



7-Methyl-2,3,6,7-tetrahydro-1H-pyrrolo[1,2-a]indol-8(5H)-one (**2-9c**) was prepared following the general procedure C. ^1H NMR (500 MHz, CDCl_3) δ 6.14 (s, 1H), 3.81 (t, $J = 7.1$ Hz, 2H), 2.80 (t, $J = 7.3$ Hz, 2H), 2.77 – 2.67 (m, 2H), 2.53 – 2.39 (m, 3H), 2.18 (dq, $J = 14.4, 5.0$ Hz, 1H), 1.87 (dtd, $J = 13.6, 9.1, 6.1$ Hz, 1H), 1.20 (d, $J = 7.0$ Hz, 3H); ^{13}C NMR (126 MHz, CDCl_3) δ 196.71, 138.03, 137.82, 123.69, 96.39, 43.95, 41.07, 31.78,

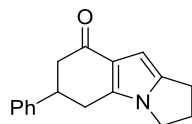
27.81, 23.63, 21.02, 15.54; IR (neat, cm^{-1}): 2962, 2932, 2103, 1644, 1470, 1372, 1149; ESI+ calculated for $[\text{C}_{12}\text{H}_{16}\text{NO}]^+$: 190.12, found 190.10.

6-Methyl-2,3,6,7-tetrahydro-1H-pyrrolo[1,2-a]indol-8(5H)-one (2-9d)



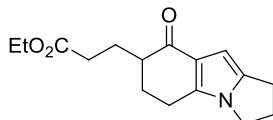
6-Methyl-2,3,6,7-tetrahydro-1H-pyrrolo[1,2-a]indol-8(5H)-one (**2-9d**) was prepared following the general procedure C. ^1H NMR (600 MHz, CDCl_3) δ 6.14 (s, 1H), 3.86 – 3.76 (m, 2H), 2.84 – 2.70 (m, 3H), 2.57 – 2.42 (m, 3H), 2.42 – 2.31 (m, 2H), 2.17 (dd, $J = 16.2, 11.5$ Hz, 1H), 1.12 (d, $J = 6.0$ Hz, 3H); ^{13}C NMR (151 MHz, CDCl_3) δ 193.83, 138.44, 137.88, 123.94, 96.11, 46.31, 43.98, 31.82, 30.30, 27.75, 23.57, 21.35; IR (neat, cm^{-1}): 2957, 2927, 2095, 1642, 1488, 1471, 1456, 1369; ESI+ calculated for $[\text{C}_{12}\text{H}_{15}\text{NONa}]^+$: 212.11, found 212.08.

6-Phenyl-2,3,6,7-tetrahydro-1H-pyrrolo[1,2-a]indol-8(5H)-one (2-9e)



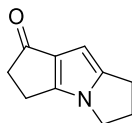
6-Phenyl-2,3,6,7-tetrahydro-1H-pyrrolo[1,2-a]indol-8(5H)-one (**2-9e**) was prepared following the general procedure C. ^1H NMR (600 MHz, CDCl_3) δ 7.33 (t, $J = 7.5$ Hz, 2H), 7.30 – 7.22 (m, 3H), 6.20 (s, 1H), 3.93 – 3.71 (m, 2H), 3.48 (tt, $J = 11.1, 4.9$ Hz, 1H), 3.02 – 2.86 (m, 2H), 2.82 (t, $J = 7.4$ Hz, 2H), 2.75 – 2.65 (m, 2H), 2.50 (p, $J = 7.2$ Hz, 2H); ^{13}C NMR (151 MHz, CDCl_3) δ 192.75, 143.52, 138.27, 137.86, 128.69, 126.90, 126.78, 124.03, 96.33, 44.94, 44.08, 42.49, 30.12, 27.79, 23.62; IR (neat, cm^{-1}): 2857, 1647, 1487, 1470, 1370, 1276; ESI+ calculated for $[\text{C}_{17}\text{H}_{17}\text{NONa}]^+$: 274.12, found 274.10.

Ethyl 3-(8-oxo-2,3,5,6,7,8-hexahydro-1H-pyrrolo[1,2-a]indol-7-yl)propanoate (2-9f)



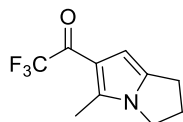
Ethyl 3-(8-oxo-2,3,5,6,7,8-hexahydro-1H-pyrrolo[1,2-a]indol-7-yl)propanoate (**2-9f**) was prepared following the general procedure C. ^1H NMR (600 MHz, CDCl_3) δ 6.10 (s, 1H), 4.08 (q, $J = 7.1$ Hz, 2H), 3.79 (t, $J = 7.1$ Hz, 2H), 2.84 – 2.62 (m, 4H), 2.54 – 2.29 (m, 5H), 2.21 – 2.08 (m, 2H), 1.90 (dtd, $J = 13.7, 8.8, 5.1$ Hz, 1H), 1.78 (dq, $J = 14.6, 6.9$ Hz, 1H), 1.21 (t, $J = 7.1$ Hz, 3H); ^{13}C NMR (126 MHz, CDCl_3) δ 195.42, 173.77, 137.97, 137.80, 123.76, 96.46, 60.24, 45.49, 43.98, 32.35, 29.13, 27.81, 25.24, 23.61, 20.74, 14.22; IR (neat): 2929, 1730, 1647, 1471, 1372, 1266, 1180; ESI+ calculated for $[\text{C}_{16}\text{H}_{21}\text{NO}_3\text{Na}]^+$: 298.14, found 298.12.

2,3,6,7-Tetrahydrocyclopenta[b]pyrrolizin-1(5H)-one (**2-9g**)



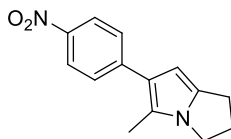
2,3,6,7-Tetrahydrocyclopenta[b]pyrrolizin-1(5H)-one (**2-9g**) was prepared following the general procedure C. ^1H NMR (600 MHz, CDCl_3) δ 5.96 (s, 1H), 3.86 (t, $J = 7.1$ Hz, 2H), 2.84 (m, 6H), 2.52 (p, $J = 7.2$ Hz, 2H); ^{13}C NMR (151 MHz, CDCl_3) δ 196.61, 153.88, 145.22, 131.06, 93.91, 44.20, 41.17, 28.15, 23.90, 20.36; IR (neat, cm^{-1}): 2932, 2858, 1647, 1498, 1355; ESI+ calculated for $[\text{C}_{10}\text{H}_{11}\text{NONa}]^+$: 184.07, found 184.06.

2,2,2-Trifluoro-1-(5-methyl-2,3-dihydro-1H-pyrrolizin-6-yl)ethanone (**2-9h**)



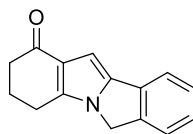
2,2,2-Trifluoro-1-(5-methyl-2,3-dihydro-1H-pyrrolizin-6-yl)ethanone (**2-9h**) was prepared following the general procedure C. ^1H NMR (500 MHz, CDCl_3) δ 6.24 (q, $J = 2.0$ Hz, 1H), 3.93 – 3.83 (m, 2H), 2.88 – 2.79 (m, 2H), 2.53 (m, 5H); ^{13}C NMR (151 MHz, CDCl_3) δ 176.31 – 175.39 (q, $^2J_{\text{CF}} = 33.9$ Hz), 136.53, 136.33, 117.38 (q, $^1J_{\text{CF}} = 291.9$ Hz), 117.34, 101.44 (q, $^3J_{\text{CF}} = 3.8$ Hz), 44.49, 27.53, 23.84, 13.09; IR (neat, cm^{-1}): 2102, 1644, 1361, 1275, 1197, 1132; ESI+ calculated for $[\text{C}_{10}\text{H}_{10}\text{F}_3\text{NONa}]^+$: 240.06, found 240.04.

5-Methyl-6-(4-nitrophenyl)-2,3-dihydro-1H-pyrrolizine (2-9i)



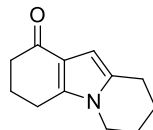
5-Methyl-6-(4-nitrophenyl)-2,3-dihydro-1H-pyrrolizine (**2-9i**) was prepared following the general procedure C. ^1H NMR (500 MHz, CDCl_3) δ 8.18 (d, $J = 8.5$ Hz, 2H), 7.49 (d, $J = 8.4$ Hz, 2H), 6.02 (s, 1H), 3.89 (t, $J = 7.0$ Hz, 2H), 2.88 (t, $J = 7.4$ Hz, 2H), 2.56 – 2.46 (m, 2H), 2.39 (s, 3H); ^{13}C NMR (151 MHz, CDCl_3) δ 144.89, 144.49, 135.78, 126.70, 123.94, 122.87, 121.86, 98.51, 44.66, 27.33, 24.33, 12.03; IR (neat, cm^{-1}): 2012, 1643, 1505, 1332, 1110; ESI+ calculated for $[\text{C}_{14}\text{H}_{14}\text{N}_2\text{O}_2\text{Na}]^+$: 265.10, found 265.08.

2,3,4,6-Tetrahydro-1H-isoindolo[2,1-a]indol-1-one (2-9j)



2,3,4,6-Tetrahydro-1H-isoindolo[2,1-a]indol-1-one (**2-9j**) was prepared following the general procedure C. ^1H NMR (500 MHz, CDCl_3) δ 7.51 (d, $J = 7.6$ Hz, 1H), 7.37 – 7.31 (m, 2H), 7.19 (t, $J = 7.5$ Hz, 1H), 6.61 (s, 1H), 4.77 (s, 2H), 2.75 (t, $J = 6.2$ Hz, 2H), 2.50 – 2.42 (m, 2H), 2.16 (p, $J = 6.3$ Hz, 2H); ^{13}C NMR (151 MHz, CDCl_3) δ 194.36, 140.86, 139.47, 138.59, 132.40, 128.36, 126.06, 124.33, 123.25, 119.73, 94.95, 77.24, 77.03, 76.82, 48.45, 37.73, 23.52, 22.02; IR (neat, cm^{-1}): 1642, 1483, 1432, 1412, 1352, 1191, 1170; ESI+ calculated for $[\text{C}_{15}\text{H}_{13}\text{NONa}]^+$: 246.09, found 246.07.

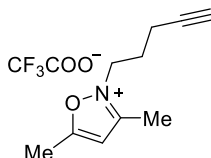
3,4,6,7,8,9-Hexahydropyrido[1,2-a]indol-1(2H)-one (2-9k)



3,4,6,7,8,9-Hexahydropyrido[1,2-a]indol-1(2H)-one (**2-9k**) was prepared following the general procedure C. ^1H NMR (500 MHz, CDCl_3) δ 6.18 (s, 1H), 3.78 (t, $J = 6.1$ Hz, 2H), 2.74 (t, $J = 6.4$ Hz, 2H), 2.67 (t, $J = 6.1$ Hz, 2H), 2.42 (t, $J = 6.3$ Hz, 2H), 2.11 (p, $J = 6.4$ Hz, 2H), 1.96 (p, $J = 6.1$ Hz, 2H), 1.79 (p, $J = 6.2$ Hz, 2H); ^{13}C NMR (126 MHz, CDCl_3)

δ 194.20, 142.36, 130.87, 119.71, 100.94, 43.15, 37.88, 23.66, 23.44, 23.21, 21.34, 20.82;
IR (neat, cm^{-1}): 1640, 1482, 1467, 1417, 1389, 1276, 1189; ESI+ calculated for $[\text{C}_{12}\text{H}_{16}\text{NO}]^+$: 190.12, found 190.11.

NMR identification of oxazonium species 2-11



2-11 was identified by crude NMR and ESI+ MS. Crude NMR is shown in the Appendix.
ESI+ calculated for $[\text{C}_{10}\text{H}_{14}\text{NO}]^+$: 164.11, found 164.08.

2.6 References

1. Baumann, M.; Baxendale, I. R.; Ley, S. V.; Nikbin, N., *Beilstein Journal of Organic Chemistry* **2011**, *7*, 442-495.
2. (a) Novák, P.; Müller, K.; Santhanam, K. S. V.; Haas, O., *Chemical Reviews* **1997**, *97* (1), 207-282; (b) Jadwiga, S.; Joanna, C.; Kamila, O.; Przemyslaw, D.; Mieczyslaw, L., *Current Organic Chemistry* **2013**, *17* (3), 283-295.
3. (a) Rubin, M.; Rubina, M.; Gevorgyan, V., *Chemical Reviews* **2007**, *107* (7), 3117-3179; (b) Estevez, V.; Villacampa, M.; Menendez, J. C., *Chem. Soc. Rev.* **2010**, *39* (11), 4402-4421; (c) Yamamoto, Y., *Chem. Soc. Rev.* **2014**, *43* (5), 1575-1600; (d) Tanoury, G. J., *Synthesis* **2016**, *48* (13), 2009-2025.
4. Sheradsky, T., *Tetrahedron Letters* **1970**, *11* (1), 25-26.
5. (a) Trofimov, B. A.; Atavin, A. S.; Mikhaleva, A. I.; Kalabin, G. A.; Chebotareva, E. G., *Zh. Org. Khim.* **1973**, *9*, 2205; (b) Trofimov, B. A.; Korostova, S. E.; Belabanova, L. N.; Mikhaleva, A. I., **1978**, *14*, 2182-2184; (c) Wang, Z., Trofimov Reaction. In *Comprehensive Organic Name Reactions and Reagents*, John Wiley & Sons, Inc.: 2010.
6. (a) Zaitsev, A. B.; Vasil'tsov, A. M.; Schmidt, E. Y.; Mikhaleva, A. I.; Afonin, A. V.; Il'icheva, L. N., *Russian Journal of Organic Chemistry* **2003**, *39* (10), 1406-1411; (b) Schmidt, E. Y.; Zorina, N. V.; Zaitsev, A. B.; Mikhaleva, A. b. I.; Vasil'tsov, A. M.; Audebert, P.; Clavier, G.; Méallet-Renault, R.; Pansu, R. B., *Tetrahedron Letters* **2004**, *45* (28), 5489-5491; (c) Voskressensky, L. G.; Borisova, T. N.; Varlamov, A. V., *Chemistry of Heterocyclic Compounds* **2004**, *40* (3), 326-333; (d) Zaitsev, A. B.; Schmidt, E. Y.; Mikhaleva, A. M.; Afonin, A. V.; Ushakov, I. A., *Chemistry of Heterocyclic Compounds* **2005**, *41* (6), 722-729.
7. Ngwerume, S.; Camp, J. E., *Chemical Communications* **2011**, *47* (6), 1857-1859.
8. (a) Hashmi, A. S.; Hutchings, G. J., *Angew Chem Int Ed Engl* **2006**, *45* (47), 7896-936; (b) Hashmi, A. S. K., *Chemical Reviews* **2007**, *107* (7), 3180-3211; (c) Ohno, H., *Israel Journal of*

- Chemistry* **2013**, 53 (11-12), 869-882; (d) Dorel, R.; Echavarren, A. M., *Chem Rev* **2015**, 115 (17), 9028-907272; (e) Asiri, A. M.; Hashmi, A. S., *Chem Soc Rev* **2016**, 45 (16), 4471-503.
9. Ngwerume, S.; Lewis, W.; Camp, J. E., *The Journal of Organic Chemistry* **2013**, 78 (3), 920-934.
10. (a) Wang, Y.; Ye, L.; Zhang, L., *Chemical Communications* **2011**, 47 (27), 7815-7817; (b) Wang, Y.; Liu, L.; Zhang, L., *Chemical Science* **2013**, 4 (2), 739-746.
11. Staszak, M. A.; Doecke, C. W., *Tetrahedron Letters* **1993**, 34 (44), 7043-7044.
12. Sharma, D.; Bandna; Shil, A. K.; Singh, B.; Das, P., *Synlett* **2012**, 2012 (08), 1199-1204.
13. He, C.; Guo, S.; Huang, L.; Lei, A., *Journal of the American Chemical Society* **2010**, 132 (24), 8273-8275.

Chapter 3 Insertion into Unactivated C-H Bonds with Vinyl Cation Generated by Oxidative Gold Carbene Chemistry

3.1 Introduction of Metal Carbene C-H Insertion Chemistry

With its unparalleled potential of carrying out late-stage modification in complex molecule synthesis, C(sp³)-H functionalization has always been a hot topic in the past decades. Of particular challenge is the insertion into unactivated C(sp³)-H bonds as 1) they have relatively high bond dissociation energies (range from 95-110 kcal/mol); b) their prevalence in any organic molecule makes regio-/stereoselective functionalization a daunting challenge.

Since its earliest observation 60 years ago,¹ the insertion of a carbene into a C(sp³)-H bond has aroused great interest because of its potential in facile construction of C-C bond. Nevertheless, it is not until a few decades later that its synthetic applications, especially those featuring transition metal-carbene complexes, were reported. The Teyssie group discovered that when a transition metal complex was employed, the yield and selectivity of carbene C-H insertion could be greatly influenced by altering the properties of ligands on the transition metal.² Follow-up studies on intramolecular reactions³ further demonstrated the synthetic advantages of transition metal catalysts, while a later study⁴ focused on the regioselectivity of such C(sp³)-H insertion reaction. Up to now, hundreds of papers as well as several books have been published on the topic of metal carbene C(sp³)-H insertions.⁵

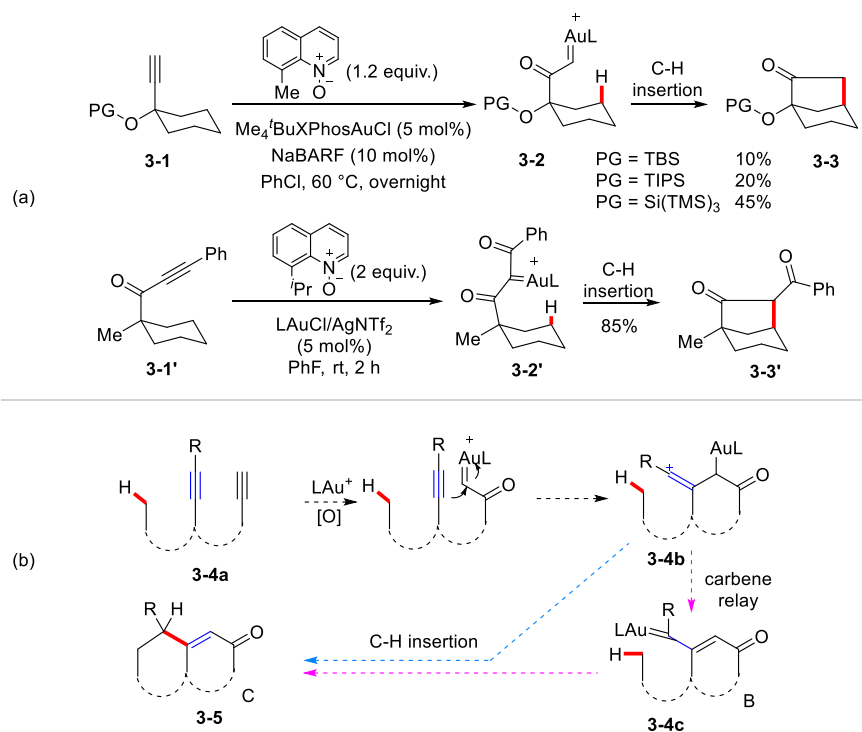
3.2 Our Strategy and Initial Study to a Relayed C-H Insertion Process

In 2010, our research group developed a general strategy to accessing α -oxo gold carbenes via gold-catalyzed intermolecular oxidations of alkynes.⁶ Comparing to commonly used copper, ruthenium, or rhodium carbenes, gold carbenes are considerably more reactive,⁷ enabling a wider range of challenging transformations. Moreover, the mild reaction conditions and the use of benign alkyne substrates make the strategy a much safer and highly efficient surrogate of the typical metal carbene generation, where toxic and potentially explosive diazo compounds are used as precursors.

Exploiting this oxidative gold carbene strategy, our group has developed a great variety of transformations leading to numerous valuable molecules and structures.^{6b,c,8} However, this strategy has never been applied to functionalization of unactivated C(sp³)-H bonds, which is quite surprising since the high reactivity of α -oxo gold carbenes clearly suggests the feasibility of such reaction. To this end, our lab launched two parallel projects aiming at exploring the utilities of our oxidatively-generated gold carbenes in intramolecular C-H insertion chemistry.

Firstly, we considered possibilities of direct C(sp³)-H insertion by oxidatively-generated gold carbenes (Scheme 45a). It soon became clear that despite the Thorpe-Ingold effect enhances the probability of the carbene center encountering the target C(sp³)-H bond, mono-substituted α -oxo gold carbenes are still prone to side reactions, which diminishes the reaction yield. As a solution, we introduced an additional carbonyl group on the carbene center (i.e. intermediate **3-2'**), further increasing its reactivity while suppressing intermolecular side reactions by its steric hindrance. The strategy was proved to be very effective, and the work was later published in JACS.⁹

Scheme 45. Direct C(sp³)-H Insertion and Relayed C(sp³)-H Insertion

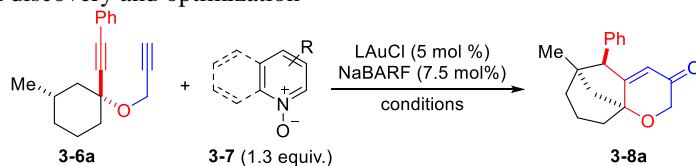


While working on the direct C-H insertion strategy, we came up with a different and relayed approach, where an oxidatively generated gold carbene is transformed into another reactive species that undergoes C-H insertion process (Scheme 45b). Alkynes are known to be reactive towards metal carbenes.¹⁰ We envisioned that with an electrophilic α -oxo gold carbene, the reaction product would be a highly reactive vinyl cation. It has been reported that such a vinyl cation undergoes insertion into unactivated C(sp³)-H bonds in a concerted manner.¹¹ As such, we proposed that with a diyne substrate **3-4a**, the α -oxo gold carbene generated upon selective oxidation of the terminal alkyne would be trapped by the internal alkyne to form a vinyl cation intermediate (i.e., **3-4b**). **3-4b** would either undergo a concerted C(sp³)-H insertion to afford the cyclic product **3-5**, or isomerize into the gold carbene intermediate **3-4c**, followed by carbene C-H insertion to give the same product. The latter scenario has been suggested by Hashmi and Ji respectively.¹² We surmised that

this relay strategy would allow a facile access to polycyclic products with limited prior functionalization.

We started the reaction discovery and then condition optimization with the diyne substrate **3-6a** as substrate, which was readily accessed by a two-step synthesis from 3-methylcyclohexanone. While several initial trials with common gold catalysts including Ph₃PAuCl, IPrAuCl and JohnPhosAuCl led to complicated mixtures (Table 5, entries 1-3), we achieved a 24% yield of desired tricyclic product **3-8a** with a combination of BrettPhosAuCl and 2,6-dichloropyridine *N*-oxide (entry 4). Improved yields (40% and 41%) were observed when switching to sterically more hindered Me₄'BuXPhos (entry 5) or the *P,N*-bidentate ligand MorDalPhos (entry 6). Due to a shorter reaction time, Me₄'BuXPhosAuCl was chosen for further optimization. A brief screening showed that fluorobenzene was the solvent of choice, giving a 50% yield of the desired product (entries 5, 7, 8). A series of *N*-oxides with different steric and electronic properties were also tested (entries 8-12), and 8-isopropylquinoline *N*-oxide **3-7e** turned out to be the most effective with a 70% yield. To our surprise, the reaction efficiency was somewhat independent to the reaction temperature except a slight increase in side reactions (entries 12-15). It is noteworthy that the reaction was highly regioselective and diastereoselective: methine C-H bond is preferred over the methylene counterpart, and 2D NMR studies showed that the *endo*-Ph isomer was formed in >20:1 ratio over the *exo* isomer.

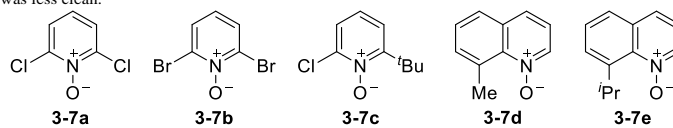
Table 5. Initial reaction discovery and optimization



entry	catalyst	<i>N</i> -oxide	conditions	yield
1	Ph ₃ PAuCl	3-7a	DCE, rt, 18 h	trace ^b
2	IPrAuCl	3-7a	DCE, rt, 18 h	trace ^b
3	JohnPhosAuCl	3-7a	DCE, rt, 18 h	trace ^b
4	BrettPhosAuCl	3-7a	DCE, rt, 3 h	24%
5	Me ₄ ^t BuXPhosAuCl	3-7a	DCE, rt, 2 h	40%
6	MorDalPhosAuCl	3-7a	DCE, rt, 7 h	41%
7	Me ₄ ^t BuXPhosAuCl	3-7a	PhMe, rt, 1 h	46%
8	Me ₄ ^t BuXPhosAuCl	3-7a	PhF, rt, 1 h	50%
9	Me ₄ ^t BuXPhosAuCl	3-7b	PhF, rt, 1 h	49%
10	Me ₄ ^t BuXPhosAuCl	3-7c	PhF, rt, 1.5 h	60%
11	Me ₄ ^t BuXPhosAuCl	3-7d	PhF, rt, 1 h	58%
12	Me ₄ ^t BuXPhosAuCl	3-7e	PhF, rt, 1 h	70%
13	Me ₄ ^t BuXPhosAuCl	3-7e	PhF, 50 °C, 5 min	70% ^c
14	Me ₄ ^t BuXPhosAuCl	3-7e	PhF, 0 °C, 7 h	66%
15	Me ₄ ^t BuXPhosAuCl	3-7e	PhF, -20 °C, 36 h	65%

^a Reaction is run in vial. ^b Complicated mixture formed, and no desired product detected. ^c

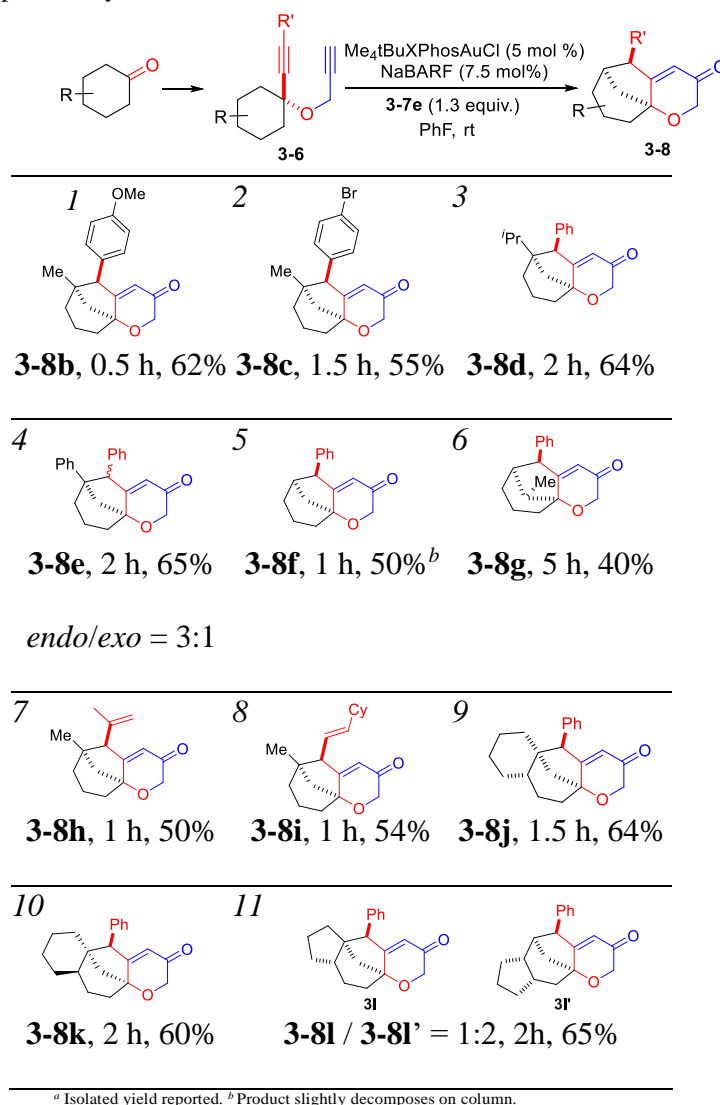
Reaction was less clean.



3.3 Scope Study of C-H Insertion with Vinyl Cation Generated by Oxidative Gold Chemistry

With the optimal reaction condition in hand, the scope of the reaction was further explored with a series of substrates derived from substituted cyclohexanones, as shown in Table 6. First, we altered the electronic properties of the phenyl group in **3-8a**, installing 4-OMe (entry 1) and 4-Br (entry 2) respectively. In either case, the desired product was formed in satisfactory yield. The methyl group on the cyclohexane ring was then modified. With either isopropyl group (entry 3) or phenyl group (entry 4), the reaction worked smoothly, affording tricyclic ketone **3-8d** and **3-8e** in 64% and 65% respectively. Even with the substituting group on the cyclohexane ring removed (entry 5), the C-H insertion product **3-8f** was still formed in a decent 50% yield, while the lowered yield (comparing to **3-8a**) is in accordance to the apparent preference of inserting into tertiary C-H bonds.⁴ Substrate **3-6g** prepared from 2-methylcyclohexanone, although giving only a modest 40% yield, showed an unexpected regioselectivity: the methylene C-H bond vicinal to the methyl group is selectively functionalized. To our delight, the phenyl group at the alkyne terminus of **3-6a** could also be replaced by alkenyl groups such as 2-propenyl (entry 7) and cyclohexylvinyl (entry 8), and the tricyclic products **3-8h** and **3-8i** were isolated in fair yields.

Table 6. Reaction Scope with Cyclohexanone-Derived Substrates^a

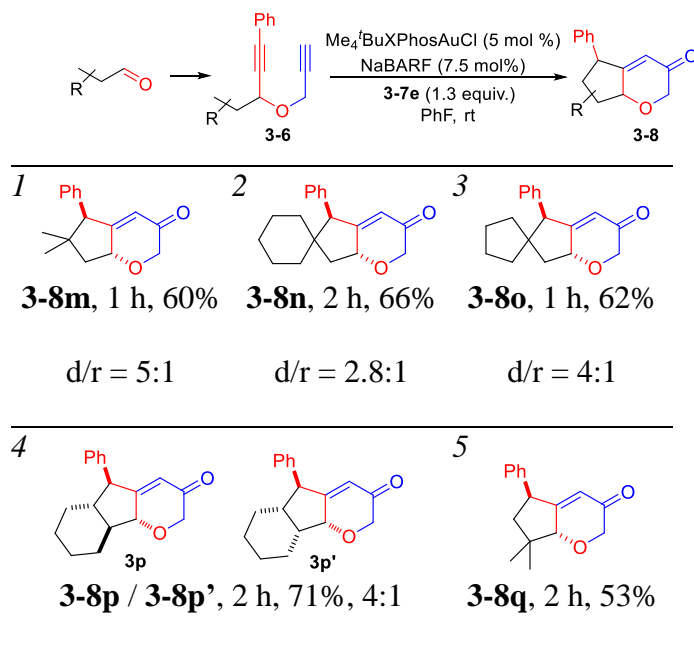


^a Isolated yield reported. ^b Product slightly decomposes on column.

To further test the synthetic utility of this relayed C-H insertion strategy, substrates from readily available *cis*- and *trans*-2-decalones were also employed (Table 6, entries 9-11). Both cases reacted smoothly, affording tetracyclic products **3-8j** and **3-8k** in satisfactory yields. On the other hand, the substrate derived from *cis*-hexahydro-1*H*-inden-5(6*H*)-one ended up with two regioisomeric products in a combined yield of 65% (i.e. **3-8l** and **3-8l'**). The major isomer **3-8l'** came from the insertion into a secondary C-H bond, while the minor isomer **3-8l** is the result of a typically favored insertion into tertiary C-H bond. This

inconsistency in reaction outcome is likely caused by the higher energy barrier for *cis*-fused cyclopentane ring to achieve optimal conformation for tertiary C-H insertion. Moreover, the conformation impact on the reaction was further supported by the fact that the diastereomer of **3-6a**, where methyl is *cis* to phenylethynyl moiety, lead to no desired product despite the full consumption of substrate. In this case, it is possible that the insertion into the available methylene C-H bond was hampered by the energetic impact of the axial methyl group on the conformation that allows for such insertion. Another interesting observation is that except **3-8e**, all the other polycyclic products were formed as single diastereomers, with the R' group positioned on the *endo* side of the bicyclo[3.2.1]octane skeleton.

Table 7. Reaction Scope with Aldehyde-Based Substrates^a



^a Isolated yield reported.

With the success of cyclohexanone-derived substrates, we then investigated substrates prepared from various aldehydes. The C-H insertion reaction worked well on a series of substrates bearing properly positioned methine C-H bonds, affording the desired products

in good yields and modest diastereoselectivities (Table 7, entries 1-3). Methylene C-H bond on a cyclohexane ring could also be inserted under the same condition, giving a good combined yield (Table 7, **3-8p** and **3-8p'**). Extensive 2D-NMR studies revealed that the two diastereomeric products differed at the ring fusion, and the *trans*-fused **3-8p** was moderately favored over the *cis*-fused **3p'**. Finally, insertion into methyl C-H bond was achieved on substrate prepared from pivalaldehyde, affording **3q** with serviceable yield and excellent diastereoselectivity. This result highlighted the high reactivity of the putative vinyl cation intermediate **3-4b** or gold carbene **3-4c**. Notably, in all these cases, the reaction favors the diastereomer that displays *trans* relationship between the phenyl group and the ethereal oxygen.

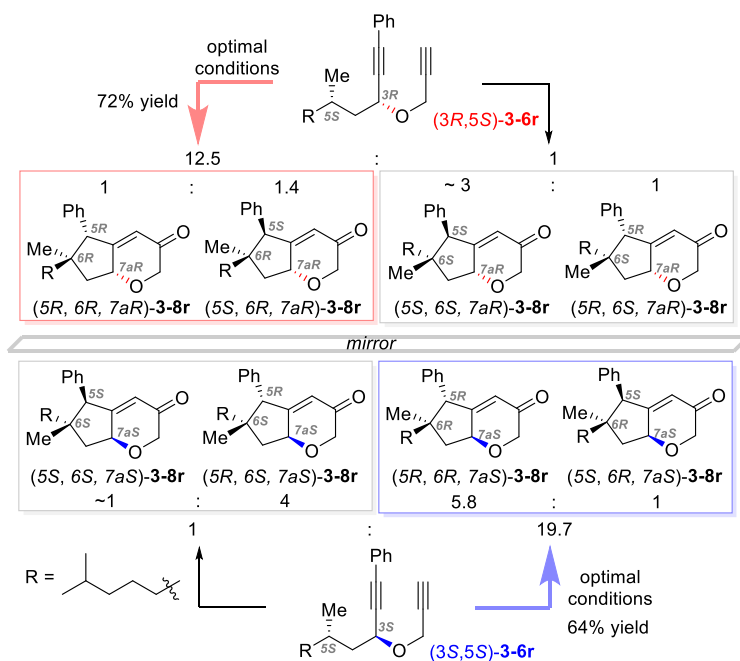
3.4 Mechanistic Studies that Supports a Concerted Pathway

As mentioned previously, on most of the substrates tested, the reaction exhibits excellent diastereoselectivity. Additionally, substrates derived from substituted cyclohexanones almost always give the thermodynamically less-favored diastereomer, with bulky phenyl group pointing into the concave face of the molecule. Those interesting results prompted us to further investigate the reaction mechanism.

To probe whether the C-H insertion in our system is concerted or not, we prepared the diastereomers (*3R*, *5S*)-**3-6r** and (*3S*, *5S*)-**3-6r** from (*S*)-dihydrocitronellal (95% ee) and subjected each of them to the optimal reaction conditions. As shown in Scheme 46, both reactions were efficient, and more importantly, the insertions were confirmed to be mostly concerted with both substrates. For (*3R*, *5S*)-**3-6r**, the pair of diastereomers, i.e., (*5S*, *6R*, *7aR*)-**3-8r** and (*5R*, *6R*, *7aR*)-**3-8r** differing only at the benzylic position, is formed in a 12.5:1 ratio to the other pair, i.e., (*5S*, *6S*, *7aR*)-**3-8r** and (*5R*, *6S*, *7aR*)-**3-8r**, which again

differ at the benzylic position. The major pair has a quaternary carbon center exhibiting the same three dimensional orientations of the original non-hydrogen substituents, reflecting the conservation of original chirality and a concerted C-H insertion; on the other hand, the minor pair is the result of stereochemical inversion, which is only slightly more than what has been reported by Gaunt (~2%).^{11b} With (3*S*, 5*S*)-**3-6r** as the substrate, the conservation is even more pronounced as the corresponding ratio is now 19.5:1. Additionally, although the involvement of gold carbene could not be totally ruled out at this point, previous studies of related donor/acceptor-type gold carbenes showed little reactivity of C(sp³)-H insertion.¹³ Therefore, it is more likely that this C-H insertion reaction is enabled by the vinyl cation intermediates.

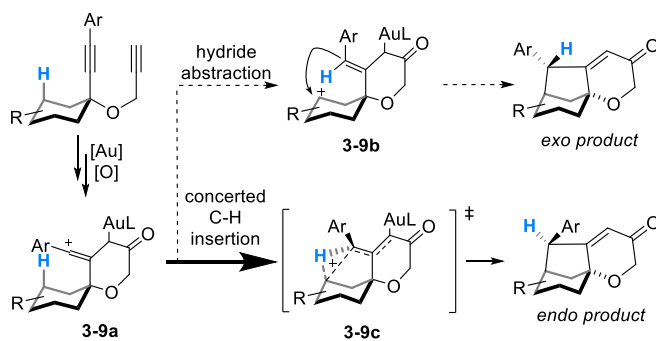
Scheme 46. Results Supporting a Mostly Concerted C-H Insertion Mechanism



Upon establishing the concerted nature of the vinyl cation C-H insertion, the unique stereoselectivities of the reaction can be readily rationalized. As shown in Scheme 47, the

vinyl cation intermediate **3-9a** formed by oxidative gold chemistry would have its linear vinyl cation moiety bisecting the cyclohexane ring. In a concerted C-H insertion scenario, the H atom would be delivered to the developing *exo* face of the bicyclo[3.2.1]octane system, while pushing the phenyl group into the *endo* face (see Scheme 47, **3-9c**). On the other hand, if the reaction proceeds through a hydride abstraction-cyclization process, the cationic intermediate **3-9b** would lead to formation of the unobserved *exo* product due to the approach of the cationic moiety to the back side of the alkene. Therefore, we proposed that the concerted pathway would be predominant under our reaction condition. Additionally, this rationale can also account for the formation of significant amounts of the *exo*-product in the case of **3-8e**, where the benzylic hydrogen is much more susceptible to hydride abstraction.

Scheme 47. Rationale for the Observed Diastereoselectivity



3.5 Conclusion

We have achieved an expedient synthesis of bicyclic/polycyclic *2H*-pyran-3(*6H*)-ones from bis-propargyl ethers derived conveniently in two steps from aldehydes/cyclic ketones. In this oxidative gold catalysis-triggered cascade, an α -oxo gold carbene intermediate is initially formed and subsequently trapped by the tethered internal C-C triple bond,

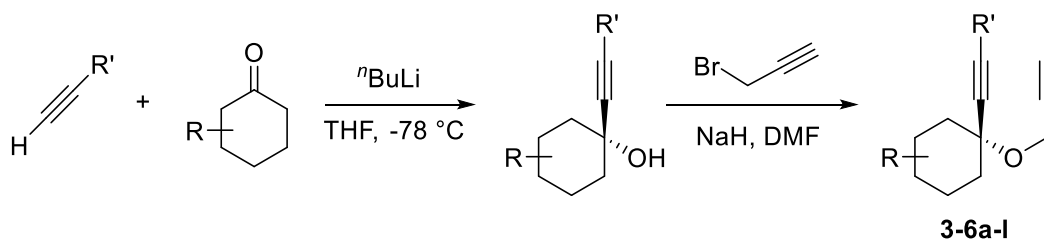
affording a putative vinyl cation intermediate and realizing a relay of electrophilic site. Subsequently, the highly reactive intermediate undergoes an intramolecular insertion into unactivated C(sp³)-H bond, the mostly concerted nature of which is established by the reactions of chiral substrates. This relay strategy opens a new venue for the application of oxidative gold catalysis in the development of novel and synthetically streamlining C-H insertions.

3.6 Acknowledgements

Reproduced from *Org. Chem. Front.*, **2015**, 2, 1556-1560, with permission from the Royal Society of Chemistry.

3.7 Experimental Details

General Procedure A: preparation of substrates 3-6a-l

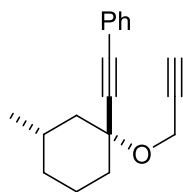


A terminal alkyne (6 mmol) and tetrahydrofuran (10 mL) was mixed in a flame-dried Schlenk flask under N₂ atmosphere. The mixture was cooled to -78 °C in a dry ice-acetone bath, to which ⁿBuLi (2.5 M in hexane, 2.4 mL) was added slowly. The mixture was stirred at the same temperature for 0.5 h before a cyclohexanone (5 mmol) was added in one portion. The reaction was allowed to warm to room temperature and stirred for an additional hour. Upon completion, the reaction was carefully quenched by 5 mL saturated NH₄Cl aqueous solution and the resulting mixture was extracted by diethyl ether. The

organic layers are combined, washed with brine, dried with MgSO₄, filtered, and concentrated under vacuum. The crude residue was purified by silica gel chromatography, and the major diastereomer was collected.

The desired tertiary alcohol (1 mmol) thus obtained was dissolved in DMF (5 mL). The solution was cooled down to 0 °C, and NaH (50 mg, 60% dispersion in mineral oil) was added. The mixture was stirred at 0 °C for 20 min and propargyl bromide (1.2 mmol) was added in one portion. The mixture was then allowed to stir at room temperature until TLC showed completion of reaction. The reaction was poured into a mixture of ice and saturated NH₄Cl solution, and was subsequently extracted with diethyl ether. The organic layer was washed with water and brine, dried with MgSO₄, and concentrated under vacuum. The residue was purified by silica gel chromatography to give the substrates **3-6a-l**.

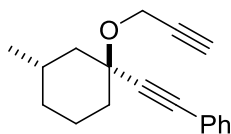
((*trans*-3-methyl-1-(prop-2-ynoxy)cyclohexyl)ethynyl)benzene 3-6a



3-6a was synthesized following **General Procedure A** with an overall yield of 40%. ¹H NMR (500 MHz, CDCl₃) δ 7.50 – 7.39 (m, 2H), 7.34 – 7.28 (m, 3H), 4.41 (d, *J* = 2.4 Hz, 2H), 2.42 (dd, *J* = 4.9, 2.4 Hz, 1H), 2.22 – 2.12 (m, 2H), 1.85 – 1.61 (m, 4H), 1.46 (td, *J* = 12.8, 3.8 Hz, 1H), 1.22 (dd, *J* = 15.4, 9.1 Hz, 1H), 0.96 (d, *J* = 6.6 Hz, 3H), 0.92 – 0.82 (m, 1H); ¹³C NMR (126 MHz, CDCl₃) δ 131.71, 128.34, 128.26, 122.69, 89.16, 87.68, 81.25, 76.56, 73.46, 51.76, 45.92, 37.36, 34.26, 30.30, 23.41, 22.16; IR (neat, cm⁻¹): 2930, 2861,

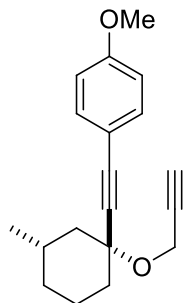
2119, 1490, 1457, 1443, 1303, 1166, 1063; ESI+ calculated for $[C_{18}H_{20}NaO]^+$: 275.14, found 275.06.

((*cis*-3-methyl-1-(prop-2-ynyloxy)cyclohexyl)ethynyl)benzene 3-6a'



3-6a' was synthesized following **General Procedure A** with an overall yield of 26%. ¹H NMR (500 MHz, CDCl₃) δ 7.42 (ddd, *J* = 4.6, 2.9, 1.3 Hz, 2H), 7.32 – 7.27 (m, 3H), 4.34 – 4.27 (m, 2H), 2.47 – 2.35 (m, 1H), 2.18 (d, *J* = 14.0 Hz, 2H), 1.84 (dd, *J* = 6.2, 3.0 Hz, 1H), 1.67 (dd, *J* = 18.0, 7.4 Hz, 2H), 1.61 – 1.56 (m, 1H), 1.32 (t, *J* = 13.1 Hz, 1H), 0.95 – 0.84 (m, 4H); ¹³C NMR (126 MHz, CDCl₃) δ 131.69, 128.25, 128.23, 122.70, 90.85, 84.85, 81.11, 73.67, 73.27, 51.93, 44.66, 35.71, 33.93, 26.92, 22.07, 20.88; IR (neat, cm⁻¹): 2949, 2865, 2118, 1491, 1456, 1444, 1352, 1262, 1152, 1066; ESI+ calculated for $[C_{18}H_{20}NaO]^+$: 275.14, found 275.11.

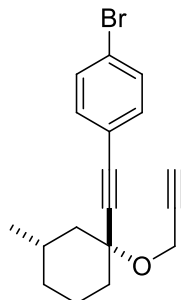
1-Methoxy-4-((*trans*-3-methyl-1-(prop-2-ynyloxy)cyclohexyl)ethynyl)benzene 3-6b



3-6b was synthesized following **General Procedure A** with an overall yield of 45%. ¹H NMR (500 MHz, CDCl₃) δ 7.38 (d, *J* = 8.8 Hz, 2H), 6.84 (d, *J* = 8.8 Hz, 2H), 4.41 – 4.38 (m, 2H), 3.81 (s, 3H), 2.41 (t, *J* = 2.2 Hz, 1H), 2.15 (t, *J* = 8.5 Hz, 2H), 1.82 – 1.55 (m, 4H), 1.45 (td, *J* = 12.8, 3.7 Hz, 1H), 1.20 (t, *J* = 12.2 Hz, 1H), 0.93 (t, *J* = 11.5 Hz, 3H),

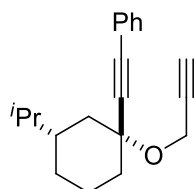
0.91 – 0.82 (m, 1H); ^{13}C NMR (126 MHz, CDCl_3) δ 159.60, 133.14, 114.75, 113.85, 87.61, 87.52, 81.29, 76.59, 73.38, 55.31, 55.26, 51.66, 45.93, 37.38, 34.25, 30.26, 23.40, 22.16; IR (neat, cm^{-1}): 3295, 2929, 2860, 2218, 1606, 1509, 1458, 1288, 1248, 1165, 1098, 1061, 1032; ESI+ calculated for $[\text{C}_{19}\text{H}_{22}\text{NaO}_2]^+$: 305.15, found 305.11.

1-Bromo-4-((*trans*-3-methyl-1-(prop-2-ynyloxy)cyclohexyl)ethynyl)benzene 3-6c



3-6c was synthesized following **General Procedure A** with an overall yield of 37%. ^1H NMR (500 MHz, CDCl_3) δ 7.44 (d, $J = 8.4$ Hz, 2H), 7.30 (d, $J = 8.4$ Hz, 2H), 4.38 (d, $J = 2.4$ Hz, 2H), 2.42 (t, $J = 2.4$ Hz, 1H), 2.15 (dd, $J = 12.9, 5.8$ Hz, 2H), 1.83 – 1.55 (m, 4H), 1.45 (td, $J = 12.7, 3.7$ Hz, 1H), 1.28 – 1.15 (m, 1H), 0.95 (d, $J = 6.6$ Hz, 3H), 0.92 – 0.82 (m, 1H); ^{13}C NMR (126 MHz, CDCl_3) δ 133.15, 131.53, 122.59, 121.60, 90.44, 86.56, 81.12, 76.52, 73.56, 51.80, 45.78, 37.25, 34.20, 30.30, 23.39, 22.14; IR (neat, cm^{-1}): 3303, 2949, 2931, 2861, 2221, 2119, 1901, 1649, 1588, 1486, 1458, 1301, 1062, 823; ESI+ calculated for $[\text{C}_{18}\text{H}_{19}\text{BrNaO}]^+$: 353.05, 355.05, found 353.01, 355.01.

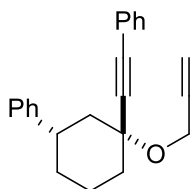
((*trans*-3-isopropyl-1-(prop-2-ynyloxy)cyclohexyl)ethynyl)benzene 3-6d



3-6d was synthesized following **General Procedure A** with an overall yield of 39%. ^1H NMR (500 MHz, CDCl_3) δ 7.45 (dt, $J = 7.3, 3.6$ Hz, 2H), 7.32 (dd, $J = 9.2, 5.6$ Hz, 3H),

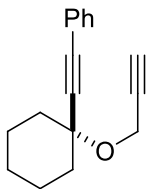
4.41 (dt, $J = 14.4, 7.2$ Hz, 2H), 2.43 (t, $J = 2.4$ Hz, 1H), 2.17 (dd, $J = 16.2, 5.9$ Hz, 2H), 1.84 – 1.78 (m, 1H), 1.72 – 1.43 (m, 5H), 1.29 (t, $J = 12.1$ Hz, 1H), 1.01 – 0.86 (m, 7H); ^{13}C NMR (126 MHz, CDCl_3) δ 131.73, 128.34, 128.27, 122.74, 89.16, 87.77, 81.23, 77.01, 73.47, 51.77, 41.38, 41.23, 37.61, 32.45, 28.64, 23.41, 19.73, 19.63; IR (neat, cm^{-1}): 2928, 2853, 2223, 2117, 1490, 1444, 1331, 1072; ESI+ calculated for $[\text{C}_{20}\text{H}_{24}\text{NaO}]^+$: 303.17, found 303.12.

((*trans*-3-phenyl-1-(prop-2-ynoxy)cyclohexyl)ethynyl)benzene 3-6e



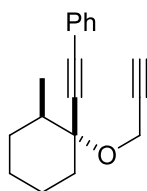
3-6e was synthesized following **General Procedure A** with an overall yield of 54%. ^1H NMR (500 MHz, CDCl_3) δ 7.53 – 7.44 (m, 2H), 7.38 – 7.29 (m, 5H), 7.27 – 7.19 (m, 3H), 4.49 – 4.38 (m, 2H), 3.01 – 2.93 (m, 1H), 2.45 – 2.36 (m, 2H), 2.29 (d, $J = 12.8$ Hz, 1H), 1.93 (d, $J = 12.0$ Hz, 2H), 1.89 – 1.74 (m, 2H), 1.67 – 1.59 (m, 1H), 1.46 – 1.36 (m, 1H); ^{13}C NMR (126 MHz, CDCl_3) δ 145.77, 131.82, 128.54, 128.46, 128.35, 126.92, 126.25, 122.55, 88.66, 88.29, 81.09, 76.69, 73.62, 51.92, 44.44, 41.67, 37.47, 33.70, 23.73; IR (neat, cm^{-1}): 3082, 3061, 3029, 2933, 2859, 2223, 2126, 1599, 1491, 1444, 1335, 1308, 1067, 1014; ESI+ calculated for $[\text{C}_{23}\text{H}_{22}\text{NaO}]^+$: 337.16, found 337.11.

((1-(Prop-2-ynoxy)cyclohexyl)ethynyl)benzene 3-6f



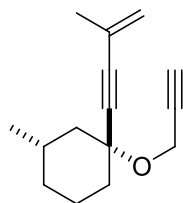
3-6f was synthesized following **General Procedure A** with an overall yield of 70%. ^1H NMR (500 MHz, CDCl_3) δ 7.45 (dt, $J = 7.3, 3.6$ Hz, 2H), 7.34 – 7.27 (m, 3H), 4.38 (d, $J = 2.4$ Hz, 2H), 2.42 (t, $J = 2.4$ Hz, 1H), 2.06 – 1.97 (m, 2H), 1.80 – 1.67 (m, 4H), 1.67 – 1.50 (m, 3H), 1.32 (dt, $J = 12.7, 10.0$ Hz, 1H); ^{13}C NMR (126 MHz, CDCl_3) δ 131.72, 128.32, 128.26, 122.72, 89.46, 87.03, 81.23, 75.52, 73.41, 51.77, 37.35, 25.38, 23.02; IR (neat, cm^{-1}): 2936, 2858, 2117, 1489, 1443, 1303, 1146; ESI+ calculated for $[\text{C}_{17}\text{H}_{18}\text{NaO}]^+$: 261.13, found 261.09.

((cis-2-methyl-1-(prop-2-ynyloxy)cyclohexyl)ethynyl)benzene 3-6g



3-6g was synthesized following **General Procedure A** with an overall yield of 35%. ^1H NMR (500 MHz, CDCl_3) δ 7.52 – 7.37 (m, 2H), 7.38 – 7.30 (m, 3H), 4.47 – 4.27 (m, 2H), 2.41 (t, $J = 2.4$ Hz, 1H), 2.29 (dt, $J = 11.8, 2.8$ Hz, 1H), 1.79 – 1.70 (m, 2H), 1.69 – 1.61 (m, 2H), 1.57 (tdd, $J = 10.5, 6.8, 3.8$ Hz, 1H), 1.53 – 1.45 (m, 1H), 1.44 – 1.35 (m, 1H), 1.30 – 1.21 (m, 1H), 1.10 (d, $J = 6.5$ Hz, 3H); ^{13}C NMR (126 MHz, CDCl_3) δ 131.74, 128.31, 128.27, 122.82, 89.14, 87.06, 81.53, 80.25, 73.22, 52.08, 41.79, 36.78, 32.23, 25.28, 23.84, 16.59; IR (neat, cm^{-1}): 2931, 2857, 2119, 1643, 1444, 1373, 1344, 1286, 1072; ESI+ calculated for $[\text{C}_{18}\text{H}_{20}\text{NaO}]^+$: 275.14, found 275.08.

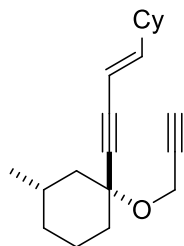
trans-3-Methyl-1-(3-methylbut-3-en-1-ynyl)-1-(prop-2-ynyloxy)cyclohexane 3-6h



3-6h was synthesized following **General Procedure A** with an overall yield of 40%. ^1H NMR (500 MHz, CDCl_3) δ 5.30 – 5.27 (m, 1H), 5.24 – 5.21 (m, 1H), 4.34 – 4.30 (m, 2H), 2.42 – 2.38 (m, 1H), 2.11 – 2.04 (m, 2H), 1.90 (t, $J = 1.3$ Hz, 3H), 1.75 – 1.64 (m, 3H), 1.60 – 1.50 (m, 1H), 1.43 – 1.36 (m, 1H), 1.14 (t, $J = 12.2$ Hz, 1H), 0.93 (d, $J = 6.5$ Hz, 3H), 0.88 – 0.78 (m, 1H); ^{13}C NMR (126 MHz, CDCl_3) δ 126.32, 121.83, 88.90, 88.11, 81.26, 76.40, 73.36, 51.61, 45.85, 37.31, 34.23, 30.21, 23.54, 23.35, 22.13; IR (neat, cm^{-1}): 2930, 2867, 2118, 1457, 1373, 1305, 1099, 1063; ESI+ calculated for $[\text{C}_{15}\text{H}_{20}\text{NaO}]^+$: 239.14, found 239.09.

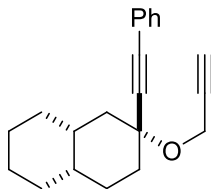
trans-1-((E)-4-Cyclohexylbut-3-en-1-ynyl)-3-methyl-1-(prop-2-ynyloxy)cyclohexane

3-6i



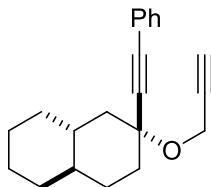
3-6i was synthesized following **General Procedure A** with an overall yield of 30%. ^1H NMR (500 MHz, CDCl_3) δ 6.09 (dt, $J = 15.3, 7.7$ Hz, 1H), 5.46 (dd, $J = 16.1, 1.4$ Hz, 1H), 4.32 (d, $J = 2.5$ Hz, 2H), 2.41 – 2.38 (m, 1H), 2.11 – 1.98 (m, 3H), 1.79 – 1.63 (m, 8H), 1.62 – 1.51 (m, 1H), 1.42 – 1.35 (m, 1H), 1.31 – 1.22 (m, 2H), 1.20 – 1.04 (m, 4H), 0.92 (d, $J = 6.5$ Hz, 3H), 0.82 (ddd, $J = 24.8, 12.8, 3.8$ Hz, 1H); ^{13}C NMR (126 MHz, CDCl_3) δ 150.50, 106.59, 87.61, 86.55, 81.37, 76.56, 73.27, 51.57, 45.92, 41.20, 37.36, 34.26, 32.21, 30.17, 26.00, 25.82, 23.34, 22.12; IR (neat, cm^{-1}): 3021, 2927, 2852, 2201, 1448, 1332, 1295, 1278, 1184, 1098, 1064, 957; ESI+ calculated for $[\text{C}_{20}\text{H}_{28}\text{NaO}]^+$: 307.20, found 307.16.

***trans*-2-(phenylethynyl)-2-(prop-2-ynoxy)-*cis*-decahydronaphthalene 3-6j**



3-6j was synthesized following **General Procedure A** with an overall yield of 33%. ^1H NMR (500 MHz, CDCl_3) δ 7.48 – 7.39 (m, 2H), 7.35 – 7.28 (m, 3H), 4.41 (d, $J = 2.4$ Hz, 2H), 2.43 (dd, $J = 5.5, 3.1$ Hz, 1H), 2.13 – 2.05 (m, 1H), 1.97 – 1.80 (m, 3H), 1.80 – 1.65 (m, 4H), 1.65 – 1.53 (m, 3H), 1.47 – 1.40 (m, 1H), 1.39 – 1.19 (m, 4H); ^{13}C NMR (126 MHz, CDCl_3) δ 131.73, 128.33, 128.26, 122.70, 89.18, 87.51, 81.20, 73.49, 51.72, 46.71, 44.65, 42.75, 40.09, 37.75, 37.31, 34.93, 33.56, 33.10, 32.52, 31.43, 31.02, 26.49, 21.17 (aliphatic carbon signals are messy due to rapid conformation change); IR (neat, cm^{-1}): 2924, 2857, 2126, 1489, 1443, 1371, 1304, 1275, 1144, 1068; ESI+ calculated for $[\text{C}_{21}\text{H}_{24}\text{NaO}]^+$: 315.17, found 315.12.

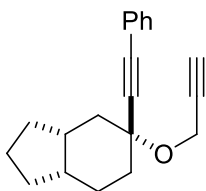
***trans*-2-(phenylethynyl)-2-(prop-2-ynoxy)-*trans*-decahydronaphthalene 3-6k**



3-6k was synthesized following **General Procedure A** with an overall yield of 40%. ^1H NMR (500 MHz, CDCl_3) δ 7.45 (dt, $J = 7.2, 3.0$ Hz, 2H), 7.37 – 7.28 (m, 3H), 4.40 (d, $J = 2.4$ Hz, 2H), 2.42 (t, $J = 2.4$ Hz, 1H), 2.19 (ddd, $J = 11.7, 6.0, 2.8$ Hz, 1H), 2.13 – 2.03 (m,

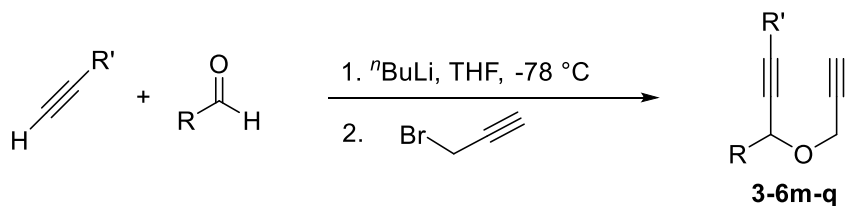
1H), 1.75 – 1.55 (m, 6H), 1.46 – 1.18 (m, 5H), 1.09 – 0.85 (m, 3H); ¹³C NMR (126 MHz, CDCl₃) δ 131.74, 128.34, 128.27, 122.74, 89.39, 87.47, 81.24, 76.49, 73.46, 51.80, 44.65, 42.75, 40.10, 37.76, 33.51, 33.11, 31.02, 26.49, 26.24; IR (neat, cm⁻¹): 2923, 2854, 2221, 2127, 1598, 1489, 1444, 1321, 1068; ESI+ calculated for [C₂₁H₂₄NaO]⁺: 315.17, found 315.12.

***trans*-5-(phenylethynyl)-5-(prop-2-ynoxy)octahydro-1H-indene 3-6l**



3-6l was synthesized following **General Procedure A** with an overall yield of 27%. ¹H NMR (500 MHz, CDCl₃) δ 7.47 – 7.41 (m, 2H), 7.32 (dd, *J* = 5.0, 1.6 Hz, 3H), 4.40 (d, *J* = 2.4 Hz, 2H), 2.42 (t, *J* = 2.4 Hz, 1H), 2.29 – 2.15 (m, 1H), 2.01 – 1.89 (m, 4H), 1.81 – 1.67 (m, 4H), 1.67 – 1.51 (m, 3H), 1.48 – 1.39 (m, 2H); ¹³C NMR (500 MHz, CDCl₃) δ 80.88, 80.64, 80.63, 80.24, 77.82, 77.76, 77.30, 76.97, 76.75, 75.21, 74.28, 74.23, 74.23, 73.82, 73.79, 73.43, 73.27, 73.11; IR (neat, cm⁻¹): 2949, 2874, 2117, 1643, 1489, 1444, 1371, 1312, 1070; ESI+ calculated for [C₂₀H₂₂NaO]⁺: 301.16, found 301.12.

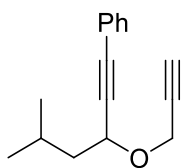
General Procedure B: preparation of substrates from aldehydes



A terminal alkyne (6 mmol) and tetrahydrofuran (10 mL) was mixed in a flame-dried

Schlenk flask under N₂ atmosphere. The mixture was then cooled to -78 °C in a dry ice-acetone bath, and ⁿBuLi (2.5 M in hexane, 2.4 mL) was added slowly. The mixture was stirred at the same temperature for 0.5 h before the corresponding aldehyde (5 mmol) was added in one portion. The reaction was allowed to warm to room temperature and stirred for an additional hour. Upon completion, propargyl bromide (1.2 mmol) was added in one portion, and the mixture was stirred at room temperature. The reaction was monitored by TLC until the complete consumption of the tertiary alcohol. If no product is forming after the addition of propargyl bromide, tetrabutylammonium iodide (20 mol%) and DMF (1 mL) could be added to accelerate the reaction. Upon completion, the reaction was quenched by saturated NH₄Cl and extracted with diethyl ether. The combined organic layers were washed with water and brine, dried with MgSO₄, and concentrated under vacuum. The residue was purified by silica gel chromatography to give the substrates **3-6m-q**.

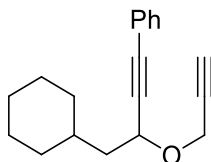
(5-methyl-3-(prop-2-ynoxy)hex-1-ynyl)benzene 3-6m



3-6m was synthesized following **General Procedure B** with an overall yield of 80%. ¹H NMR (500 MHz, CDCl₃) δ 7.50 – 7.41 (m, 2H), 7.37 – 7.28 (m, 3H), 4.57 (d, *J* = 6.8 Hz, 1H), 4.38 (ddd, *J* = 15.7, 10.8, 2.4 Hz, 2H), 2.45 – 2.44 (m, 1H), 2.00 – 1.90 (m, 1H), 1.80 (dt, *J* = 14.2, 7.2 Hz, 1H), 1.67 (dt, *J* = 13.7, 6.9 Hz, 1H), 0.98 (t, *J* = 6.3 Hz, 6H); ¹³C NMR (126 MHz, CDCl₃) δ 131.74, 128.38, 128.26, 122.63, 87.54, 86.15, 79.72, 74.33,

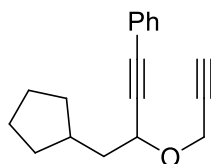
67.38, 55.73, 44.57, 24.72, 22.71, 22.35; IR (neat, cm^{-1}): 2958, 2870, 2118, 1644, 1490, 1468, 1443, 1331, 1127, 1081; ESI+ calculated for $[\text{C}_{16}\text{H}_{18}\text{NaO}]^+$: 249.13, found 249.02.

(4-Cyclohexyl-3-(prop-2-ynoxy)but-1-ynyl)benzene 3-6n



3-6n was synthesized following **General Procedure B** with an overall yield of 72%. ^1H NMR (500 MHz, CDCl_3) δ 7.45 (dtt, $J = 5.5, 2.9, 1.4$ Hz, 2H), 7.34 – 7.30 (m, 3H), 4.60 (dd, $J = 7.8, 6.4$ Hz, 1H), 4.37 (ddd, $J = 15.7, 12.4, 2.4$ Hz, 2H), 2.44 (t, $J = 2.4$ Hz, 1H), 1.88 – 1.75 (m, 3H), 1.75 – 1.60 (m, 5H), 1.34 – 1.22 (m, 2H), 1.22 – 1.15 (m, 1H), 1.02 – 0.92 (m, 2H); ^{13}C NMR (126 MHz, CDCl_3) δ 131.75, 128.36, 128.30, 128.26, 122.67, 87.68, 86.11, 79.73, 74.32, 66.89, 55.73, 43.21, 34.03, 33.44, 32.99, 26.53, 26.21, 26.13; IR (neat, cm^{-1}): 3081, 3057, 3034, 2924, 2852, 2226, 2118, 1742, 1599, 1490, 1447, 1336, 1261, 1074; ESI+ calculated for $[\text{C}_{19}\text{H}_{22}\text{NaO}]^+$: 289.16, found 289.12.

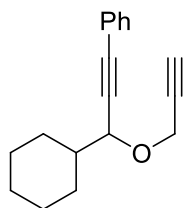
(4-Cyclopentyl-3-(prop-2-ynoxy)but-1-ynyl)benzene 3-6o



3-6o was synthesized following **General Procedure B** with an overall yield of 75%. ^1H NMR (600 MHz, CDCl_3) δ 7.45 – 7.41 (m, 2H), 7.34 – 7.27 (m, 3H), 4.50 (t, $J = 6.9$ Hz, 1H), 4.35 (qd, $J = 15.7, 2.4$ Hz, 2H), 2.43 (t, $J = 2.4$ Hz, 1H), 2.08 (dt, $J = 15.3, 7.7$ Hz, 1H), 1.92 – 1.79 (m, 4H), 1.65 – 1.58 (m, 2H), 1.58 – 1.48 (m, 2H), 1.21 – 1.11 (m, 2H); ^{13}C NMR (126 MHz, CDCl_3) δ 131.74, 128.37, 128.25, 122.65, 87.61, 86.16, 79.74, 74.30,

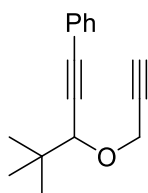
68.44, 55.75, 41.95, 36.52, 32.72, 32.63, 25.12, 24.98; IR (neat, cm^{-1}): 2950, 2867, 2117, 1643, 1490, 1443, 1333, 1075; ESI+ calculated for $[\text{C}_{18}\text{H}_{20}\text{NaO}]^+$: 275.14, found 275.10.

(3-Cyclohexyl-3-(prop-2-ynoxy)prop-1-ynyl)benzene 3-6p



3-6p was synthesized following **General Procedure B** with an overall yield of 82%. ^1H NMR (500 MHz, CDCl_3) δ 7.46 (dd, $J = 6.7, 3.1$ Hz, 2H), 7.32 (dd, $J = 4.6, 2.0$ Hz, 3H), 4.46 – 4.29 (m, 3H), 2.44 (t, $J = 2.3$ Hz, 1H), 1.98 – 1.89 (m, 2H), 1.83 – 1.62 (m, 4H), 1.33 – 1.13 (m, 5H); ^{13}C NMR (126 MHz, CDCl_3) δ 131.77, 128.32, 128.25, 122.74, 87.02, 86.45, 79.83, 74.22, 73.66, 55.95, 42.66, 29.06, 28.50, 26.43, 25.94, 25.91; IR (neat, cm^{-1}): 2927, 2853, 2117, 1643, 1490, 1444, 1331, 1261, 1072; ESI+ calculated for $[\text{C}_{18}\text{H}_{20}\text{NaO}]^+$: 275.14, found 275.11.

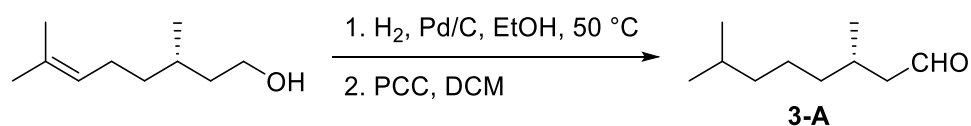
(4,4-Dimethyl-3-(prop-2-ynoxy)pent-1-ynyl)benzene 3-6q



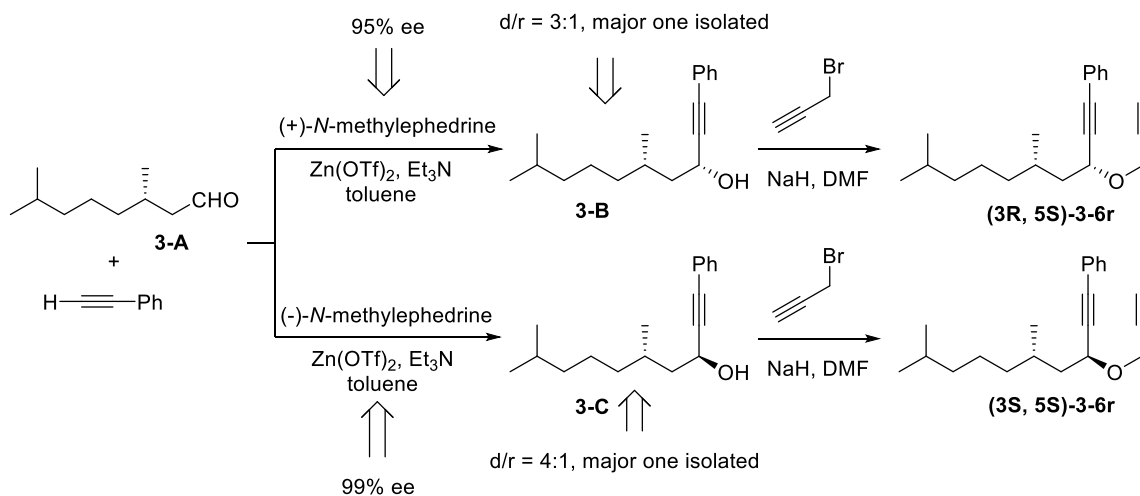
3-6q was synthesized following **General Procedure B** with an overall yield of 81%. ^1H NMR (500 MHz, CDCl_3) δ 7.48 – 7.42 (m, 2H), 7.34 – 7.28 (m, 3H), 4.38 (ddd, $J = 19.5, 16.0, 2.4$ Hz, 2H), 4.16 (s, 1H), 2.44 – 2.41 (m, 1H), 1.08 (s, 9H); ^{13}C NMR (126 MHz, CDCl_3) δ 131.75, 128.27, 128.25, 122.84, 86.81, 86.39, 79.87, 77.51, 74.16, 56.28, 35.56,

25.91 IR (neat, cm^{-1}): 3082, 3035, 2958, 2906, 2869, 2219, 2118, 1599, 1490, 1394, 1364, 1321, 1246, 1195, 1073; ESI+ calculated for $[\text{C}_{16}\text{H}_{18}\text{NaO}]^+$: 249.13, found 249.10.

Preparation of chiral substrates 3-6r

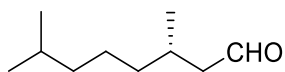


Pd/C (150 mg, 10% on carbon) was added to a dry round-bottom flask flushed with H_2 . To the flask was added ethanol (10 mL), (-)-citronellol (50 mmol, 95% ee), and concentrated HCl (12 M, 0.05 mL). The mixture was stirred at 50 °C under H_2 atmosphere and monitored by TLC. Upon completion, Pd/C was filtered off by a Celite plug, and the filtrate was concentrated under vacuum. The residue was dissolved in DCM (20 mL) and Celite was added to make the solution into a slurry. Pyridinium chlorochromate (60 mmol) was added to the slurry, and the mixture was stirred overnight at room temperature. The reaction mixture was then filtered through a silica pad to remove the chromium salts. The filtrate was concentrated under vacuum, and purified by silica gel chromatography to give the dihydrocitronellal **3-A**.



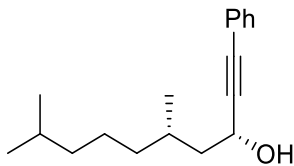
The asymmetric nucleophilic addition to **3-A** (2 mmol) was performed using Carreira's method.¹⁴ (+)-*N*-methylephedrine (95% ee) and (-)-*N*-methylephedrine (99% ee) were used to prepare the chiral tertiary alcohols **3-B** and **3-C**, respectively. After careful column chromatography, **3-B** and **3-C** were isolated pure in 69% and 60% yield, respectively.

(S)-3,7-Dimethyloctanal 3-A



¹H NMR (500 MHz, CDCl₃) δ 9.76 (t, *J* = 2.3 Hz, 1H), 2.43 – 2.35 (m, 1H), 2.22 (ddd, *J* = 16.0, 7.8, 2.6 Hz, 1H), 2.06 (dt, *J* = 12.5, 5.7 Hz, 1H), 1.52 (dq, *J* = 13.3, 6.7 Hz, 1H), 1.36 – 1.12 (m, 6H), 0.96 (d, *J* = 6.7 Hz, 3H), 0.87 (d, *J* = 6.6 Hz, 6H); ¹³C NMR (126 MHz, CDCl₃) δ 203.11, 51.09, 38.98, 37.13, 28.18, 27.89, 24.65, 22.62, 22.54, 19.97; IR (neat, cm⁻¹): 2956, 2929, 2871, 2714, 1728, 1465, 1383, 1367, 1238, 1170, 1015; ESI+ calculated for [C₁₀H₂₀NaO]⁺: 179.14, found 179.07.

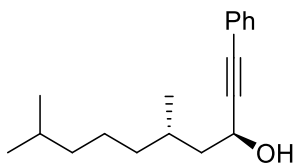
(3R, 5S)-5,9-dimethyl-1-phenyldec-1-yn-3-ol 3-B



¹H NMR (500 MHz, CDCl₃) δ 7.45 – 7.40 (m, 2H), 7.30 (ddd, *J* = 10.8, 7.1, 2.7 Hz, 3H), 4.66 (dt, *J* = 8.0, 5.6 Hz, 1H), 1.89 – 1.82 (m, 1H), 1.82 – 1.73 (m, 2H), 1.61 – 1.55 (m, 1H), 1.53 – 1.49 (m, 1H), 1.39 – 1.25 (m, 3H), 1.21 – 1.13 (m, 3H), 0.97 (d, *J* = 6.6 Hz,

3H), 0.87 (d, $J = 6.6$ Hz, 6H); ^{13}C NMR (126 MHz, CDCl_3) δ 131.63, 128.31, 128.25, 122.69, 90.61, 84.65, 61.23, 45.38, 39.20, 37.26, 29.34, 27.96, 24.54, 22.69, 22.58, 19.49; IR (neat, cm^{-1}): 2954, 2928, 2869, 1490, 1466, 1443, 1366, 1028; ESI+ calculated for $[\text{C}_{18}\text{H}_{26}\text{NaO}]^+$: 281.19, found 281.04.

(3*S*, 5*S*)-5,9-dimethyl-1-phenyldec-1-yn-3-ol 3-C

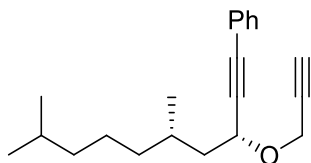


^1H NMR (500 MHz, CDCl_3) δ 7.46 – 7.40 (m, 2H), 7.36 – 7.29 (m, 3H), 4.70 – 4.65 (m, 1H), 1.84 – 1.74 (m, 2H), 1.69 – 1.62 (m, 1H), 1.54 – 1.51 (m, 1H), 1.41 – 1.25 (m, 4H), 1.22 – 1.14 (m, 2H), 0.97 (d, $J = 6.5$ Hz, 3H), 0.87 (d, $J = 6.6$ Hz, 6H); ^{13}C NMR (126 MHz, CDCl_3) δ 131.65, 128.32, 128.25, 122.70, 90.30, 84.94, 61.74, 45.25, 39.19, 37.23, 29.74, 27.96, 24.53, 22.68, 22.58, 19.82; IR (neat, cm^{-1}): 2958, 2932, 2100, 1643, 1489, 1465, 1445, 1382, 1364, 1140; ESI+ calculated for $[\text{C}_{18}\text{H}_{26}\text{NaO}]^+$: 281.19, found 281.15.

The chiral tertiary alcohol **3-B** or **3-C** (1 mmol) obtained from last step was dissolved in DMF (5 mL). The solution was cooled down to 0 °C and NaH (50 mg, 60% dispersion in mineral oil) was added. The mixture was stirred at 0 °C for 20 min and propargyl bromide (1.2 mmol) was added in one portion. The mixture was then allowed to stir at room temperature until TLC showed completion of reaction. The reaction was poured into a mixture of ice and saturated NH_4Cl solution, and was subsequently extracted with diethyl ether. The combined organic layers were washed with water and brine, dried with MgSO_4 , and concentrated under vacuum. The residue was purified by silica gel chromatography to

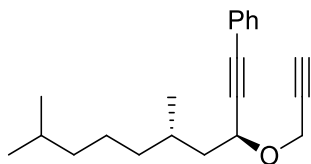
give the chiral substrates **3-6r**.

((3*R*, 5*S*)-5,9-dimethyl-3-(prop-2-ynoxy)dec-1-ynyl)benzene (3*R*, 5*S*)-3-6r



^1H NMR (500 MHz, CDCl_3) δ 7.49 – 7.40 (m, 2H), 7.34 – 7.30 (m, 3H), 4.60 (dd, $J = 8.4$, 5.5 Hz, 1H), 4.43 – 4.33 (m, 2H), 2.45 (t, $J = 2.4$ Hz, 1H), 1.92 (ddd, $J = 13.8$, 8.4, 5.4 Hz, 1H), 1.81 (h, $J = 6.6$ Hz, 1H), 1.63 – 1.56 (m, 1H), 1.54 – 1.50 (m, 1H), 1.36 – 1.26 (m, 3H), 1.22 – 1.14 (m, 3H), 0.97 (d, $J = 6.6$ Hz, 3H), 0.87 (d, $J = 6.6$ Hz, 6H); ^{13}C NMR (126 MHz, CDCl_3) δ 131.72, 128.35, 128.24, 122.65, 87.76, 86.00, 79.73, 74.30, 67.02, 55.71, 42.99, 39.24, 37.32, 29.22, 27.95, 24.53, 22.69, 22.58, 19.36; IR (neat, cm^{-1}): 2955, 2929, 2118, 1490, 1466, 1365, 1081; ESI+ calculated for $[\text{C}_{21}\text{H}_{28}\text{NaO}]^+$: 319.20, found 319.16.

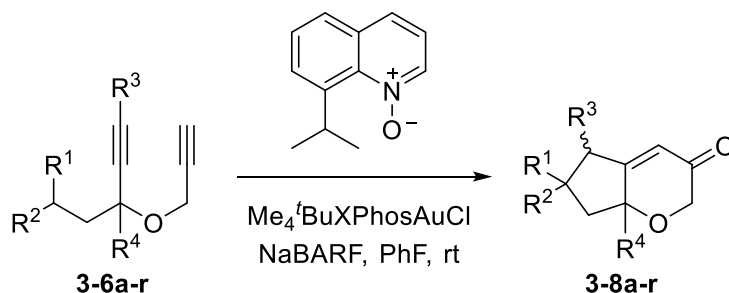
(3*S*, 5*S*)-5,9-dimethyl-3-(prop-2-ynoxy)dec-1-ynyl)benzene (3*S*, 5*S*)-3-6r



^1H NMR (500 MHz, CDCl_3) δ 7.47 – 7.41 (m, 2H), 7.35 – 7.28 (m, 3H), 4.58 (t, $J = 7.0$ Hz, 1H), 4.37 (qd, $J = 15.7$, 2.4 Hz, 2H), 2.44 (dd, $J = 2.4$, 1.9 Hz, 1H), 1.85 – 1.73 (m, 2H), 1.73 – 1.63 (m, 1H), 1.51 (dd, $J = 13.3$, 6.6 Hz, 1H), 1.40 – 1.24 (m, 3H), 1.19 – 1.12 (m, 3H), 0.96 (d, $J = 6.4$ Hz, 3H), 0.86 (d, $J = 6.6$ Hz, 6H); ^{13}C NMR (126 MHz, CDCl_3) δ 131.75, 128.37, 128.25, 122.64, 87.44, 86.32, 79.71, 74.31, 67.68, 55.76, 42.75, 39.19, 37.05, 29.59, 27.93, 24.45, 22.68, 22.59, 19.84; IR (neat, cm^{-1}): 2954, 2928, 2869, 2118,

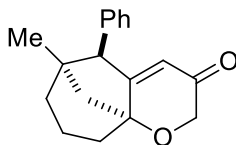
1490, 1465, 1365, 1334, 1130, 1078; ESI+ calculated for $[C_{21}H_{28}NaO]^+$: 319.20, found 319.16.

General procedure C: C-H insertion reactions



Substrate **3-6a-r** (0.05 mmol), 8-isopropylquinoline *N*-oxide (12.2 mg, 0.065 mmol), and fluorobenzene (1 mL) were mixed in a dry, clean vial with a magnetic string bar. The solution was stirred briefly before NaBARF (3.3 mg, 7.5 mol%) and $\text{Me}_4^t\text{BuXPhosAuCl}$ (1.8 mg, 5 mol%) were sequentially added. The reaction was then allowed to stir at room temperature until TLC showed complete consumption of the substrate. Fluorobenzene was then removed under vacuum and the residue was purified by silica gel chromatography to give the products **3-8a-r**.

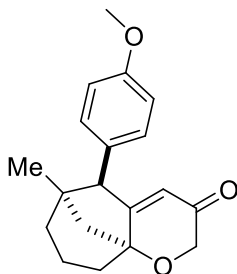
3-8a



3-8a was prepared following **General Procedure C** in 70% yield. $^1\text{H NMR}$ (500 MHz, CDCl_3) δ 7.39 – 7.30 (m, 4H), 7.30 – 7.26 (m, 1H), 5.99 (d, $J = 2.2$ Hz, 1H), 4.38 (dd, $J = 141.2, 17.9$ Hz, 2H), 3.89 (s, 1H), 2.64 – 2.36 (m, 1H), 1.96 (dt, $J = 10.8, 2.5$ Hz, 1H), 1.74

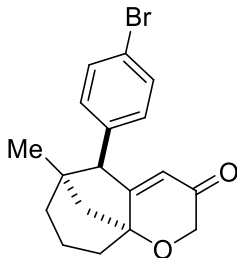
(d, $J = 10.7$ Hz, 1H), 1.70 – 1.64 (m, 3H), 1.30 – 1.22 (m, 4H), 1.18 – 1.10 (m, 1H); ^{13}C NMR (126 MHz, CDCl_3) δ 194.84, 175.07, 135.50, 128.87, 128.38, 127.11, 120.51, 80.59, 67.51, 58.16, 51.39, 44.88, 32.96, 32.88, 26.65, 19.78; IR (neat, cm^{-1}): 2954, 2874, 1669, 1495, 1450, 1386, 1317, 1260, 1186, 1105; HRMS (ES+) calculated for $[\text{C}_{18}\text{H}_{20}\text{O}_2]^+$: 268.1463, found 268.1469.

3-8b



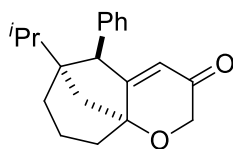
3-8b was prepared following **General Procedure C** in 62% yield. ^1H NMR (400 MHz, CDCl_3) δ 7.24 (d, $J = 8.6$ Hz, 2H), 6.87 (d, $J = 8.8$ Hz, 2H), 5.97 (d, $J = 2.2$ Hz, 1H), 4.52 (d, $J = 17.9$ Hz, 1H), 4.23 (d, $J = 17.9$ Hz, 1H), 3.83 (s, 1H), 3.81 (s, 3H), 2.51 – 2.43 (m, 1H), 1.95 – 1.90 (m, 1H), 1.76 – 1.71 (m, 1H), 1.71 – 1.52 (m, 4H), 1.29 – 1.18 (m, 4H), 1.14 (dd, $J = 13.7, 4.6$ Hz, 1H); ^{13}C NMR (151 MHz, CDCl_3) δ 175.72, 158.53, 129.88, 127.34, 120.28, 113.71, 80.57, 67.54, 57.54, 55.23, 51.22, 44.74, 32.90, 32.87, 26.55, 19.80; IR (neat, cm^{-1}): 2932, 1731, 1696, 1511, 1456, 1236, 1172, 1103, 1030; HRMS (ES+) calculated for $[\text{C}_{19}\text{H}_{22}\text{O}_3]^+$: 298.1569, found 298.1571.

3-8c



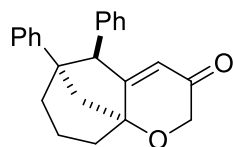
3-8c was prepared following **General Procedure C** in 55% yield. ^1H NMR (600 MHz, CDCl_3) δ 7.47 (d, $J = 8.4$ Hz, 2H), 7.21 (d, $J = 8.4$ Hz, 2H), 5.95 (d, $J = 2.0$ Hz, 1H), 4.51 (d, $J = 17.9$ Hz, 1H), 4.24 (d, $J = 17.9$ Hz, 1H), 3.84 (s, 1H), 2.51 – 2.44 (m, 1H), 1.95 (d, $J = 10.8$ Hz, 1H), 1.77 – 1.64 (m, 3H), 1.62 – 1.56 (m, 1H), 1.31 – 1.20 (m, 4H), 1.12 (dd, $J = 14.1, 5.5$ Hz, 1H); ^{13}C NMR (126 MHz, CDCl_3) δ 194.69, 174.31, 134.55, 131.55, 130.48, 121.08, 120.62, 80.50, 67.48, 57.55, 51.29, 44.85, 32.90, 32.79, 26.56, 19.78; IR (neat, cm^{-1}): 2956, 2870, 1672, 1489, 1457, 1261, 1101, 1074, 1010; HRMS (ES+) calculated for $[\text{C}_{18}\text{H}_{19}\text{BrO}_2]^+$: 346.0568, found 346.0572.

3-8d



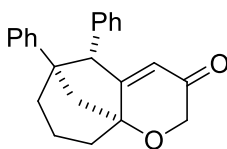
3-8d was prepared following **General Procedure C** in 64% yield. ^1H NMR (600 MHz, CDCl_3) δ 7.31 (t, $J = 4.3$ Hz, 4H), 7.27 – 7.25 (m, 1H), 5.94 (d, $J = 2.2$ Hz, 1H), 4.50 (d, $J = 17.8$ Hz, 1H), 4.22 (d, $J = 17.8$ Hz, 1H), 4.25 (s, 1H), 2.47 (dd, $J = 6.6, 3.2$ Hz, 1H), 1.96 – 1.88 (m, 2H), 1.70 – 1.59 (m, 5H), 1.10 (d, $J = 6.8$ Hz, 3H), 0.92 (d, $J = 6.8$ Hz, 3H); ^{13}C NMR (126 MHz, CDCl_3) δ 194.80, 175.69, 136.22, 128.98, 128.41, 126.97, 120.42, 80.65, 67.54, 53.17, 51.21, 43.24, 33.34, 32.25, 29.79, 19.77, 18.63, 17.54; IR (neat, cm^{-1}): 2962, 2877, 1671, 1497, 1449, 1372, 1317, 1261, 1112, 1087; HRMS (ES+) calculated for $[\text{C}_{20}\text{H}_{24}\text{O}_2]^+$: 296.1776, found 296.1779.

3-8e



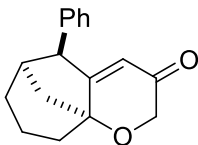
3-8e was prepared following **General Procedure C** in 53% yield. ^1H NMR (600 MHz, CDCl_3) δ 7.42 – 7.35 (m, 4H), 7.30 (dd, $J = 9.7, 4.3$ Hz, 1H), 7.22 – 7.13 (m, 3H), 6.86 (d, $J = 7.5$ Hz, 2H), 6.08 (d, $J = 1.9$ Hz, 1H), 4.54 (s, 1H), 4.56 (d, $J = 17.8$ Hz, 1H), 4.29 (d, $J = 17.8$ Hz, 1H), 2.63 (d, $J = 11.2$ Hz, 1H), 2.55 (s, 1H), 1.96 (d, $J = 11.1$ Hz, 1H), 1.76 (ddd, $J = 20.6, 18.4, 6.8$ Hz, 5H); ^{13}C NMR (126 MHz, CDCl_3) δ 194.71, 173.38, 145.00, 135.11, 128.62, 128.18, 128.13, 127.07, 126.81, 126.17, 121.25, 80.89, 67.46, 58.80, 51.62, 50.46, 32.72, 30.15, 19.38; IR (neat, cm^{-1}): 2962, 1669, 1501, 1446, 1259, 1156, 1102; HRMS (ES+) calculated for $[\text{C}_{23}\text{H}_{22}\text{O}_2]^+$: 330.1620, found 330.1625.

3-8e'



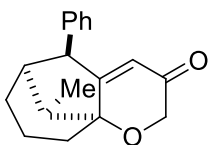
3-8e' was prepared following **General Procedure C** in 17% yield. ^1H NMR (500 MHz, CDCl_3) δ 7.07 (dd, $J = 7.9, 7.5$ Hz, 2H), 7.05 – 6.94 (m, 6H), 6.88 (d, $J = 6.9$ Hz, 2H), 5.59 (d, $J = 1.9$ Hz, 1H), 4.48 (d, $J = 17.7$ Hz, 1H), 4.23 (d, $J = 17.7$ Hz, 1H), 4.06 (s, 1H), 2.89 (dt, $J = 11.0, 2.6$ Hz, 1H), 2.54 – 2.44 (m, 1H), 2.18 (dd, $J = 13.7, 2.5$ Hz, 1H), 2.14 (dd, $J = 11.1, 1.8$ Hz, 1H), 2.07 – 2.01 (m, 1H), 1.87 – 1.67 (m, 3H); ^{13}C (126 MHz, CDCl_3) δ 194.91, 176.78, 144.11, 140.85, 128.00, 127.72, 126.90, 126.42, 125.84, 121.66, 80.89, 67.25, 57.03, 51.89, 46.66, 42.68, 31.89, 20.35; IR (neat, cm^{-1}): 2958, 1671, 1494, 1452, 1314, 1263, 1121, 1097; HRMS (ES+) calculated for $[\text{C}_{23}\text{H}_{22}\text{O}_2]^+$: 330.1620, found 330.1625.

3-8f



3-8f was prepared following **General Procedure C** in 50% yield. The product slightly decomposes on silica gel column. ^1H NMR (500 MHz, CDCl_3) δ 7.37 – 7.31 (m, 4H), 7.25 (d, $J = 2.5$ Hz, 1H), 6.17 (d, $J = 2.2$ Hz, 1H), 4.40 (dd, $J = 6.7, 1.8$ Hz, 1H), 4.52 (d, $J = 17.8$ Hz, 1H), 4.24 (d, $J = 17.8$ Hz, 1H), 2.84 (s, 1H), 2.46 (d, $J = 11.7$ Hz, 1H), 2.14 – 2.09 (m, 1H), 1.90 (d, $J = 10.7$ Hz, 1H), 1.69 (td, $J = 12.4, 5.8$ Hz, 1H), 1.54 – 1.50 (m, 1H), 1.43 – 1.26 (m, 6H); ^{13}C NMR (126 MHz, CDCl_3) δ 194.88, 172.60, 136.51, 128.53, 127.89, 126.67, 121.65, 81.36, 67.09, 51.09, 44.18, 39.53, 33.20, 26.00, 19.12; IR (neat, cm^{-1}): 2937, 2587, 1678, 1494, 1448, 1314, 1256, 1130, 1084, 1033; HRMS (ES+) calculated for $[\text{C}_{17}\text{H}_{18}\text{O}_2]^+$: 254.1307, found 254.1302.

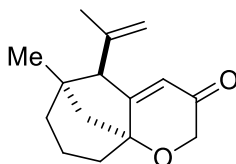
3-8g



3-8g was prepared following **General Procedure C** in 40% yield. ^1H NMR (500 MHz, CDCl_3) δ 7.35 – 7.30 (m, 4H), 7.25 – 7.20 (m, 1H), 6.24 (d, $J = 2.1$ Hz, 1H), 4.46 (d, $J = 7.1$ Hz, 1H), 4.50 (d, $J = 17.7$ Hz, 1H), 4.24 (d, $J = 17.7$ Hz, 1H), 2.54 – 2.43 (m, 2H), 2.12 (q, $J = 7.0$ Hz, 1H), 1.69 – 1.60 (m, 1H), 1.50 – 1.27 (m, 5H), 1.08 (d, $J = 7.0$ Hz, 3H); ^{13}C NMR (151 MHz, CDCl_3) δ 194.91, 171.80, 136.79, 128.43, 127.91, 126.45, 123.63, 83.44, 66.91, 48.04, 47.69, 45.71, 33.83, 27.55, 19.24, 13.31; IR (neat, cm^{-1}): 2930, 2860, 1674,

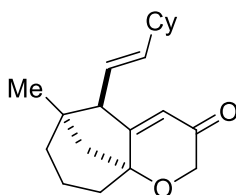
1494, 1449, 1264, 1134, 1099, 1023; HRMS (ES⁺) calculated for [C₁₈H₂₀O₂]⁺: 268.1463, found 268.1465.

3-8h



3-8h was prepared following **General Procedure C** in 50% yield. ¹H NMR (500 MHz, CDCl₃) δ 5.91 (d, *J* = 2.1 Hz, 1H), 5.11 – 5.04 (m, 1H), 4.96 (d, *J* = 0.6 Hz, 1H), 4.44 (d, *J* = 17.7 Hz, 1H), 4.17 (d, *J* = 17.8 Hz, 1H), 2.41 – 2.32 (m, 1H), 1.88 (d, *J* = 0.6 Hz, 3H), 1.86 – 1.82 (m, 1H), 1.70 – 1.55 (m, 5H), 1.40 – 1.34 (m, 1H), 1.24 (s, 3H); ¹³C NMR (126 MHz, CDCl₃) δ 194.94, 174.81, 139.49, 121.13, 115.21, 80.43, 67.25, 59.37, 52.17, 43.44, 33.82, 32.45, 27.58, 24.32, 19.83; IR (neat, cm⁻¹): 2952, 2872, 1668, 1457, 1316, 1286, 1267, 1214, 1099, 1028; HRMS (ES⁺) calculated for [C₁₅H₂₀O₂]⁺: 232.1463, found 232.1463.

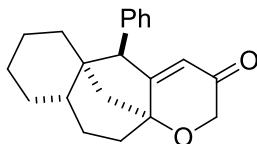
3-8i



3-8i was prepared following **General Procedure C** in 54% yield. ¹H NMR (500 MHz, CDCl₃) δ 5.84 (d, *J* = 2.2 Hz, 1H), 5.60 (dt, *J* = 15.9, 8.0 Hz, 1H), 5.36 – 5.27 (m, 1H), 4.42 (d, *J* = 17.9 Hz, 1H), 4.17 (d, *J* = 17.9 Hz, 1H), 2.98 (d, *J* = 8.1 Hz, 1H), 2.30 (dd, *J* = 7.3, 4.5 Hz, 1H), 2.03 – 1.96 (m, 1H), 1.76 – 1.68 (m, 5H), 1.68 – 1.63 (m, 1H), 1.58 (d, *J* = 6.3 Hz, 1H), 1.56 – 1.51 (m, 1H), 1.44 – 1.24 (m, 4H), 1.19 – 1.07 (m, 3H), 1.04 (d, *J* =

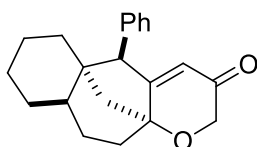
2.4 Hz, 3H); ^{13}C NMR (126 MHz, CDCl_3) δ 195.00, 177.17, 143.03, 120.28, 118.87, 80.94, 67.55, 55.94, 50.57, 43.09, 40.92, 33.53, 33.21, 33.11, 32.68, 26.09, 25.93, 25.92, 25.31, 20.29; IR (neat, cm^{-1}): 2926, 2852, 1678, 1449, 1315, 1284, 1259, 1076; HRMS (ES+) calculated for $[\text{C}_{20}\text{H}_{28}\text{O}_2]^+$: 300.2089, found 300.2090.

3-8j



3-8j was prepared following **General Procedure C** in 64% yield. ^1H NMR (600 MHz, CDCl_3) δ 7.34 – 7.30 (m, 4H), 7.30 – 7.26 (m, 1H), 5.95 (d, $J = 1.7$ Hz, 1H), 4.50 (d, $J = 17.9$ Hz, 1H), 4.22 (d, $J = 17.9$ Hz, 1H), 3.79 (s, 1H), 2.37 – 2.29 (m, 2H), 1.94 (tt, $J = 13.8, 6.8$ Hz, 1H), 1.82 – 1.71 (m, 2H), 1.69 – 1.60 (m, 2H), 1.57 (dd, $J = 14.5, 10.6$ Hz, 1H), 1.53 – 1.49 (m, 2H), 1.40 – 1.24 (m, 3H), 1.11 – 0.99 (m, 2H); ^{13}C NMR (126 MHz, CDCl_3) δ 194.95, 175.19, 135.05, 129.42, 128.32, 127.25, 119.97, 81.27, 67.54, 60.52, 49.48, 43.40, 37.03, 35.53, 30.43, 29.59, 26.60, 26.11, 23.35; IR (neat, cm^{-1}): 2929, 2859, 1672, 1497, 1449, 1320, 1263, 1241, 1105, 1034; HRMS (ES+) calculated for $[\text{C}_{21}\text{H}_{24}\text{O}_2]^+$: 308.1776, found 308.1781.

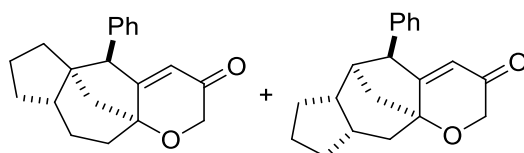
3-8k



3-8k was prepared following **General Procedure C** in 60% yield. ^1H NMR (500 MHz, CDCl_3) δ 7.42 – 7.37 (m, 2H), 7.32 – 7.27 (m, 3H), 5.80 (d, $J = 2.5$ Hz, 1H), 4.49 (d, $J = 17.9$ Hz, 1H), 4.21 (d, $J = 17.9$ Hz, 1H), 2.59 – 2.53 (m, 1H), 1.92 (dd, $J = 10.7, 3.1$ Hz,

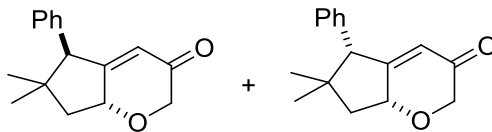
2H), 1.86 – 1.76 (m, 3H), 1.74 – 1.67 (m, 1H), 1.64 – 1.54 (m, 3H), 1.46 (dd, $J = 13.8, 4.6$ Hz, 3H), 1.15 – 1.05 (m, 2H), 0.61 – 0.51 (m, 1H); ^{13}C NMR (126 MHz, CDCl_3) δ 194.84, 177.84, 138.03, 129.03, 128.12, 127.41, 118.35, 79.92, 67.51, 60.65, 54.20, 48.53, 45.26, 38.65, 34.04, 28.20, 27.94, 26.50, 22.52; IR (neat, cm^{-1}): 2931, 2856, 1673, 1452, 1319, 1284, 1253, 1107, 102; HRMS (ES⁺) calculated for $[\text{C}_{21}\text{H}_{24}\text{O}_2]^+$: 308.1776, found 308.1770.

3-81, 3-81'



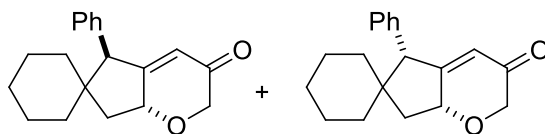
3-81 and **3-81'** were prepared following **General Procedure C** as an inseparable 1:2 mixture, overall yield is 65%. ^1H NMR (500 MHz, CDCl_3) δ 7.36 – 7.28 (m, 3H), 7.25 – 7.21 (m, 2H), 6.11 (**3-81'**, d, $J = 2.2$ Hz, 1H), 5.94 (**3-81**, d, $J = 2.2$ Hz, 1H), 4.45 (**3-81'**, dd, $J = 6.7, 1.7$ Hz, 1H), 4.51 (**3-81**, d, $J = 17.9$ Hz, 1H), 4.49 (**3-81'**, d, $J = 17.9$ Hz, 1H), 4.23 (**3-81**, d, $J = 17.8$ Hz, 1H), 4.22 (**3-81'**, d, $J = 17.8$ Hz, 1H), 4.09 (**3-81**, d, $J = 2.1$ Hz, 1H), 2.76 – 2.73 (**3-81'**, m, 1H), 2.50 – 2.43 (**3-81'**, m, 1H), 2.35 (ddd, $J = 11.9, 7.0, 3.7$ Hz, 1H), 2.04 (dd, $J = 12.4, 6.9$ Hz, 2H), 1.98 – 1.90 (m, 1H), 1.85 – 1.73 (m, 1H), 1.68 – 1.56 (m, 5H), 1.51 – 1.44 (m, 2H), 1.37 – 1.31 (m, 1H); ^{13}C NMR (126 MHz, CDCl_3) δ 195.02, 194.95, 175.85, 173.00, 136.88, 135.79, 129.32, 128.62, 128.40, 128.04, 127.22, 126.82, 121.55, 120.85, 81.30, 80.42, 67.75, 67.19, 55.91, 54.18, 53.42, 43.94, 43.56, 39.48, 38.81, 38.30, 37.84, 34.15, 34.12, 33.00, 31.37, 29.85, 28.72, 23.61, 22.45, 21.46; IR (neat, cm^{-1}): 2947, 2870, 1673, 1496, 1449, 1314, 1122, 1100; HRMS (ES⁺) calculated for $[\text{C}_{20}\text{H}_{22}\text{O}_2]^+$: 294.1620, found 294.1620.

3-8m, 3-8m'



3-8m and **3-8m'** were prepared following **General Procedure C** as a 5:1 mixture, overall yield is 60%. ^1H NMR (500 MHz, CDCl_3) δ 7.36 – 7.28 (m, 3H), 7.16 – 7.12 (**3-8m**, m, 2H), 7.12 – 7.08 (**3-8m'**, m, 2H), 5.90 (**3-8m**, d, $J = 1.9$ Hz, 1H), 5.30 (**3-8m'**, s, 1H), 4.84 – 4.78 (**3-8m'**, m, 1H), 4.78 – 4.72 (**3-8m**, m, 1H), 4.33 (**3-8m'**, d, $J = 16.6$ Hz, 1H), 4.32 (**3-8m**, d, $J = 9.6$ Hz, 1H), 4.15 (**3-8m'**, dd, $J = 16.8, 1.8$ Hz, 1H), 4.09 (**3-8m**, dd, $J = 16.7, 1.7$ Hz, 2H), 3.89 – 3.87 (**3-8m'**, m, 1H), 3.59 (**3-8m**, d, $J = 2.3$ Hz, 1H), 2.19 (dt, $J = 11.6, 7.6$ Hz, 1H), 1.84 (**3-8m**, dd, $J = 13.7, 6.1$ Hz, 1H), 1.77 (**3-8m'**, t, $J = 11.5$ Hz, 1H), 1.22 (**3-8m'**, s, 3H), 1.14 (**3-8m**, s, 3H), 0.82 (**3-8m**, s, 3H), 0.68 (**3-8m'**, s, 3H); ^{13}C NMR (126 MHz, CDCl_3) δ 195.43, 195.06, 174.14, 173.20, 137.70, 136.50, 130.25, 129.15, 128.36, 128.24, 127.28, 127.14, 122.33, 121.14, 78.02, 77.20, 72.91, 72.89, 60.12, 59.94, 44.79, 44.10, 42.54, 41.34, 29.63, 28.66, 25.84, 24.45; IR (neat, cm^{-1}): 2961, 2867, 1683, 1494, 1451, 1334, 1289, 1260, 1236, 1110, 1026; HRMS (ES+) calculated for $[\text{C}_{16}\text{H}_{18}\text{O}_2]^+$: 242.1307, found 242.1308.

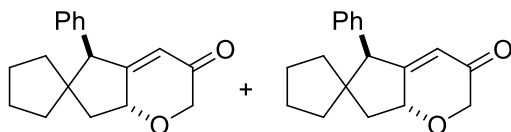
3-8n, 3-8n'



3-8n and **3-8n'** were prepared following **General Procedure C** as an inseparable 2.8:1 mixture, overall yield is 66%. ^1H NMR (500 MHz, CDCl_3) δ 7.37 – 7.26 (m, 3H), 7.13 (**3-8n'**, d, $J = 7.4$ Hz, 2H), 7.06 (**3-8n**, d, $J = 7.2$ Hz, 2H), 5.88 (**3-8n**, s, 1H), 5.84 (**3-8n'**, s, 1H), 4.81 – 4.69 (m, 1H), 4.32 (**3-8n**, d, $J = 16.7$ Hz, 1H), 4.30 (**3-8n'**, d, $J = 16.8$ Hz, 1H),

4.13 (**3-8n**, dd, $J = 16.8, 2.0$ Hz, 1H), 4.08 (**3-8n'**, dd, $J = 16.7, 1.8$ Hz, 1H), 3.79 (**3-8n**, t, $J = 2.3$ Hz, 1H), 3.59 (**3-8n'**, d, $J = 2.2$ Hz, 1H), 2.65 (**3-8n**, dd, $J = 12.3, 7.7$ Hz, 1H), 2.27 (**3-8n'**, dd, $J = 13.7, 9.2$ Hz, 1H), 1.92 (**3-8n'**, dd, $J = 13.7, 7.2$ Hz, 1H), 1.67 – 1.22 (m, 10H), 1.00 – 0.92 (m, 1H), 0.60 (**3-8n**, td, $J = 13.3, 3.9$ Hz, 1H); ^{13}C NMR (126 MHz, CDCl_3) δ 195.37, 195.15, 174.20, 137.41, 130.69, 129.60, 128.29, 128.12, 127.21, 127.12, 121.91, 121.07, 120.70, 115.26, 77.93, 76.68, 72.87, 72.66, 61.49, 60.37, 45.87, 45.25, 38.79, 38.59, 38.14, 33.94, 31.78, 25.53, 25.51, 23.56, 23.40, 22.40, 22.27; IR (neat, cm^{-1}): 2928, 2854, 1667, 1497, 1452, 1424, 1332, 1258, 1232, 1118, 1014; HRMS (ES $^+$) calculated for $[\text{C}_{19}\text{H}_{22}\text{O}_2]^+$: 282.1620, found 282.1616.

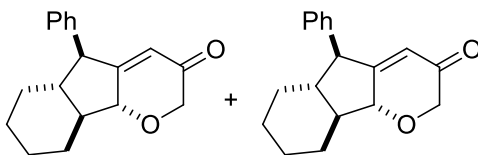
3-8o, 3-8o'



3-8o and **3-8o'** were prepared following **General Procedure C** as an inseparable 4:1 mixture, overall yield is 62%. ^1H NMR (400 MHz, CDCl_3) δ 7.34 – 7.25 (m, 3H), 7.08 (t, $J = 5.8$ Hz, 2H), 5.86 (**3-8o**, s, 1H), 5.74 (**3-8o'**, s, 1H), 4.77 – 4.66 (m, 1H), 4.31 (**3-8o**, d, $J = 16.7$ Hz, 1H), 4.28 (**3-8o'**, d, $J = 16.7$ Hz, 1H), 4.13 (**3-8o**, dd, $J = 16.7, 1.9$ Hz, 1H), 4.08 (**3-8o'**, dd, $J = 16.7, 1.8$ Hz, 1H), 4.05 (**3-8o**, s, 1H), 3.68 (**3-8o'**, s, 1H), 2.27 (**3-8o**, dd, $J = 11.8, 7.4$ Hz, 1H), 2.14 (**3-8o'**, dd, $J = 12.7, 8.2$ Hz, 1H), 1.96 (**3-8o'**, dd, $J = 12.7, 9.6$ Hz, 1H), 1.85 – 1.76 (m, 1H), 1.73 – 1.42 (m, 5H), 1.27 – 1.08 (m, 3H); ^{13}C NMR (126 MHz, CDCl_3) δ 195.24, 195.04, 174.61, 174.27, 139.59, 138.15, 129.99, 129.54, 128.39, 128.34, 127.13, 127.06, 121.81, 121.80, 78.32, 77.11, 72.75, 72.42, 57.50, 57.48, 52.90, 52.25, 42.96, 42.55, 41.02, 38.38, 34.96, 33.34, 24.46, 23.48, 23.47, 22.97; IR (neat, cm^{-1}

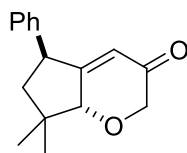
¹): 3029, 2957, 2867, 1675, 1494, 1452, 1333, 1259, 1233, 1112, 1049, 1032; HRMS (ES+) calculated for [C₁₈H₂₀O₂]⁺: 268.1463, found 268.1461.

3-8p, 3-8p'



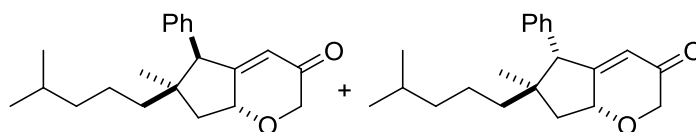
3-8p and **3-8p'** were prepared following **General Procedure C** as an inseparable 4:1 mixture, overall yield is 71%. ¹H NMR (500 MHz, CDCl₃) δ 7.33 (dd, *J* = 10.2, 4.7 Hz, 2H), 7.28 – 7.24 (m, 1H), 7.14 – 7.09 (m, 2H), 5.93 (**3-8p'**, s, 1H), 5.86 (**3-8p**, t, *J* = 2.0 Hz, 1H), 4.79 – 4.74 (**3-8p'**, m, 1H), 4.31 (d, *J* = 16.6 Hz, 1H), 4.29 – 4.26 (**3-8p**, m, 1H), 4.11 (**3-8p'**, dd, *J* = 16.5, 2.2 Hz, 1H), 4.10 (**3-8p**, dd, *J* = 16.6, 1.9 Hz, 1H), 3.90 (**3-8p'**, d, *J* = 11.0 Hz, 1H), 3.51 (**3-8p**, dt, *J* = 10.9, 2.5 Hz, 1H), 2.42 (**3-8p'**, td, *J* = 11.9, 5.4 Hz, 1H), 2.25 (**3-8p'**, dd, *J* = 13.8, 9.1 Hz, 1H), 2.20 (**3-8p**, dd, *J* = 8.1, 4.0 Hz, 1H), 1.93 – 1.88 (**3-8p**, m, 1H), 1.88 – 1.73 (m, 2H), 1.59 – 1.45 (m, 2H), 1.31 – 1.16 (m, 4H); ¹³C NMR (126 MHz, CDCl₃) δ 195.18, 194.89, 174.30, 173.25, 141.79, 140.58, 128.82, 128.76, 128.21, 128.07, 127.02, 126.97, 123.64, 122.32, 82.95, 81.97, 72.37, 72.22, 54.18, 49.32, 48.59, 48.47, 43.54, 41.02, 29.74, 29.36, 25.78, 25.39, 24.25, 23.75, 21.98, 20.43; IR (neat, cm⁻¹): 3085, 3061, 3028, 2928, 2855, 1682, 1495, 1450, 1318, 1271, 1259, 1235, 1154, 1012; HRMS (ES+) calculated for [C₁₈H₂₀O₂]⁺: 268.1463, found 268.1464.

3-8q



3-8q was prepared following **General Procedure C** in 53% yield. ^1H NMR (600 MHz, CDCl_3) δ 7.30 (t, $J = 6.7$ Hz, 2H), 7.22 (t, $J = 7.3$ Hz, 1H), 7.13 (d, $J = 7.3$ Hz, 2H), 5.93 (s, 1H), 4.30 (d, $J = 2.5$ Hz, 1H), 4.29 (d, $J = 16.3$ Hz, 1H), 4.08 (dd, $J = 16.4, 2.0$ Hz, 1H), 4.00 (dd, $J = 10.7, 8.7$ Hz, 1H), 2.15 (dd, $J = 13.2, 8.7$ Hz, 1H), 1.74 – 1.69 (m, 1H), 1.24 (s, 3H), 0.98 (s, 3H); ^{13}C NMR (151 MHz, CDCl_3) δ 194.94, 173.16, 142.18, 128.85, 127.41, 126.89, 123.30, 86.06, 71.85, 46.56, 45.28, 40.56, 26.20, 20.15; IR (neat, cm^{-1}): 2962, 2868, 1675, 1495, 1455, 1268, 1228, 1136, 1031; HRMS (ES $^+$) calculated for $[\text{C}_{16}\text{H}_{18}\text{O}_2]^+$: 242.1307, found 242.1306.

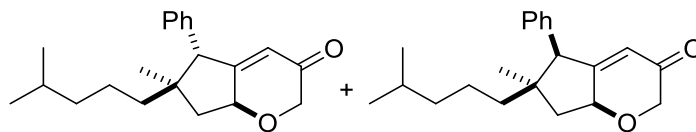
(5S, 6R, 7aR)-3-8r, (5R, 6R, 7aR)-3-8r



^1H NMR (500 MHz, CDCl_3) δ 7.37 – 7.27 (m, 3H), 7.14 (**5R**, d, $J = 7.5$ Hz, 2H), 7.11 (**5S**, d, $J = 7.5$ Hz, 2H), 5.92 (**5S**, s, 1H), 5.89 (**5R**, s, 1H), 4.75 – 4.67 (m, 1H), 4.34 (**5S**, d, $J = 8.0$ Hz, 1H), 4.30 (**5R**, d, $J = 8.0$ Hz, 1H), 4.14 (**5S**, d, $J = 16.7$ Hz, 1H), 4.08 (**5R**, d, $J = 16.7$ Hz, 1H), 3.91 (**5S**, s, 1H), 3.64 (**5R**, s, 1H), 2.38 (**5S**, dd, $J = 12.3, 7.5$ Hz, 1H), 2.27 (**5R**, dd, $J = 13.9, 9.5$ Hz, 1H), 1.74 (**5R**, dd, $J = 13.9, 6.0$ Hz, 1H), 1.61 – 1.50 (m, 2H), 1.34 (pt, $J = 13.9, 6.1$ Hz, 3H), 1.15 (p, $J = 6.5, 6.1$ Hz, 1H), 1.09 – 0.92 (m, 1H), 0.87 (**5S**, dd, $J = 6.7, 3.0$ Hz, 6H), 0.81 (s, 3H), 0.79 (**5R**, t, $J = 7.1$ Hz, 6H), 0.63 (**5S**, t, $J = 12.2$ Hz, 1H); ^{13}C NMR (126 MHz, CDCl_3) δ 195.43, 195.12, 173.97, 173.23, 137.01, 136.39, 130.40, 129.33, 128.35, 128.22, 127.25, 127.16, 122.16, 121.01, 77.71, 76.58, 72.96, 72.86, 61.86, 59.06, 45.76, 44.30, 42.46, 41.87, 40.71, 39.63, 39.60, 35.98, 27.95, 27.88, 25.58, 23.38, 22.64, 22.62, 22.55, 22.47, 22.43, 21.98; IR (neat, cm^{-1}): 2956, 2932, 2868,

1678, 1495, 1453, 1381, 1333, 1259, 1233, 1115; HRMS (ES⁺) calculated for [C₂₁H₂₈O₂]⁺: 312.2089, found 312.2086.

(5R, 6R, 7aS)-3-8r, (5S, 6R, 7aS)-3-8r



¹H NMR (500 MHz, CDCl₃) δ 7.30 (q, *J* = 9.5, 8.3 Hz, 3H), 7.12 (**5S**, d, *J* = 7.7 Hz, 2H), 7.08 (**5R**, d, *J* = 7.5 Hz, 2H), 5.89 (**5R**, s, 1H), 5.84 (**5S**, s, 1H), 4.84 – 4.74 (m, 1H), 4.33 (**5R**, d, *J* = 16.7 Hz, 1H), 4.31 (**5S**, d, *J* = 16.8 Hz, 1H), 4.14 (**5R**, d, *J* = 16.7 Hz, 1H), 4.09 (**5S**, d, *J* = 16.7 Hz, 1H), 3.92 (**5R**, d, *J* = 2.9 Hz, 1H), 3.64 (**5S**, d, *J* = 2.3 Hz, 1H), 2.16 (**5R**, dd, *J* = 11.9, 7.5 Hz, 1H), 2.09 (**5S**, dd, *J* = 13.4, 8.8 Hz, 1H), 1.92 (**5S**, dd, *J* = 13.4, 7.7 Hz, 1H), 1.74 (**5R**, t, *J* = 11.4 Hz, 1H), 1.54 (dq, *J* = 21.6, 7.6 Hz, 2H), 1.46 – 1.38 (m, 1H), 1.32 (p, *J* = 7.6 Hz, 2H), 1.25 – 1.15 (m, 2H), 0.88 (**5R**, dd, *J* = 6.8, 2.8 Hz, 6H), 0.77 (**5S**, d, *J* = 6.6 Hz, 6H), 0.68 (s, 3H); ¹³C NMR (126 MHz, CDCl₃) δ 195.06, 195.05, 174.20, 171.10, 137.90, 137.43, 130.45, 129.39, 128.29, 128.17, 127.16, 127.08, 122.34, 121.61, 89.23, 78.08, 72.89, 72.73, 60.72, 60.37, 59.37, 45.12, 44.47, 42.05, 41.99, 41.51, 39.61, 39.58, 38.23, 27.89, 27.23, 22.64, 22.54, 22.51, 22.38, 22.08, 21.03, 14.19; IR (neat, cm⁻¹): 2958, 2868, 1674, 1495, 1453, 1383, 1334, 1287, 1259, 1118; HRMS (ES⁺) calculated for [C₂₁H₂₈O₂]⁺: 312.2089, found 312.2089.

3.8 References

1. von E. Doering, W.; Buttery, R. G.; Laughlin, R. G.; Chaudhuri, N., *Journal of the American Chemical Society* **1956**, *78* (13), 3224-3224.
2. Demonceau, A.; Noels, A. F.; Hubert, A. J.; Teyssie, P., *Journal of the Chemical Society, Chemical Communications* **1981**, (14), 688-689.
3. (a) Wenkert, E.; Davis, L. L.; Mylari, B. L.; Solomon, M. F.; Da Silva, R. R.; Shulman, S.; Warnet, R. J.; Ceccherelli, P.; Curini, M.; Pellicciari, R., *The Journal of Organic Chemistry* **1982**, *47*

- (17), 3242-3247; (b) Taber, D. F.; Petty, E. H., *The Journal of Organic Chemistry* **1982**, *47* (24), 4808-4809.
4. Taber, D. F.; Ruckle, R. E., *Journal of the American Chemical Society* **1986**, *108* (24), 7686-7693.
5. (a) Davies, H. M. L.; Dick, A. R., *Top. Curr. Chem.* **2010**, *292* (Copyright (C) 2015 American Chemical Society (ACS). All Rights Reserved.), 303-345; (b) Yu, J.-Q.; Shi, Z.; Editors, *C-H Activation. [In: Top. Curr. Chem., 2010; 292]*. Springer GmbH: 2010; p 384 pp; (c) Perez, P. J.; Editor, *Alkane C-H Activation by Single-Site Metal Catalysis. [In: Catal. Met. Complexes, 2012; 38]*. Springer: 2012; p 269 pp; (d) Doyle, M. P.; Liu, Y.; Ratnikov, M., *Org. React.* **2013**, *80* (Copyright (C) 2015 American Chemical Society (ACS). All Rights Reserved.), 1-131.
6. (a) Lu, B.; Li, C.; Zhang, L., *Journal of the American Chemical Society* **2010**, *132* (40), 14070-14072; (b) Ye, L.; Cui, L.; Zhang, G.; Zhang, L., *Journal of the American Chemical Society* **2010**, *132* (10), 3258-3259; (c) Ye, L.; He, W.; Zhang, L., *Journal of the American Chemical Society* **2010**, *132* (25), 8550-8551.
7. Tresca, J. P.; Fourrey, J. L.; Polonsky, J.; Wenkert, E., *Tetrahedron Letters* **1973**, *14* (12), 895-897.
8. (a) He, W.; Li, C.; Zhang, L., *Journal of the American Chemical Society* **2011**, *133* (22), 8482-8485; (b) Ye, L.; He, W.; Zhang, L., *Angewandte Chemie International Edition* **2011**, *50* (14), 3236-3239; (c) Wang, Y.; Ji, K.; Lan, S.; Zhang, L., *Angewandte Chemie International Edition* **2012**, *51* (8), 1915-1918; (d) Ji, K.; Zhao, Y.; Zhang, L., *Angewandte Chemie International Edition* **2013**, *52* (25), 6508-6512; (e) Wu, G.; Zheng, R.; Nelson, J.; Zhang, L., *Advanced Synthesis & Catalysis* **2014**, *356* (6), 1229-1234; (f) Ji, K.; Zheng, Z.; Wang, Z.; Zhang, L., *Angewandte Chemie International Edition* **2015**, *54* (4), 1245-1249.
9. Wang, Y.; Zheng, Z.; Zhang, L., *Journal of the American Chemical Society* **2015**, *137* (16), 5316-5319.
10. (a) Bunz, U. H. F.; Kloppenburg, L., *Angewandte Chemie International Edition* **1999**, *38* (4), 478-481; (b) Fürstner, A., *Angewandte Chemie International Edition* **2000**, *39* (17), 3012-3043; (c) Connon, S. J.; Blechert, S., *Angewandte Chemie International Edition* **2003**, *42* (17), 1900-1923; (d) Fernandez-Rodriguez, M. A.; Garcia-Garcia, P.; Aguilar, E., *Chemical Communications* **2010**, *46* (41), 7670-7687.
11. (a) Biermann, U.; Koch, R.; Metzger, J. O., *Angewandte Chemie International Edition* **2006**, *45* (19), 3076-3079; (b) Zhang, F.; Das, S.; Walkinshaw, A. J.; Casitas, A.; Taylor, M.; Suero, M. G.; Gaunt, M. J., *Journal of the American Chemical Society* **2014**, *136*, 8851-8854.
12. (a) Nösel, P.; dos Santos Comprido, L. N.; Lauterbach, T.; Rudolph, M.; Rominger, F.; Hashmi, A. S. K., *Journal of the American Chemical Society* **2013**, *135* (41), 15662-15666; (b) Ji, K.; Liu, X.; Du, B.; Yang, F.; Gao, J., *Chemical Communications* **2015**, *51* (51), 10318-10321.
13. (a) Li, C.-W.; Lin, G.-Y.; Liu, R.-S., *Chemistry – A European Journal* **2010**, *16* (19), 5803-5811; (b) Dateer, R. B.; Pati, K.; Liu, R.-S., *Chemical Communications* **2012**, *48* (57), 7200-7202; (c) Li, L.; Shu, C.; Zhou, B.; Yu, Y.-F.; Xiao, X.-Y.; Ye, L.-W., *Chemical Science* **2014**, *5*, 4057-4064; (d) Xi, Y.; Su, Y.; Yu, Z.; Dong, B.; McClain, E. J.; Lan, Y.; Shi, X., *Angewandte Chemie International Edition* **2014**, *53* (37), 9817-9821; (e) Yu, Z.; Ma, B.; Chen, M.; Wu, H.-H.; Liu, L.; Zhang, J., *Journal of the American Chemical Society* **2014**, *136* (19), 6904-6907.
14. (a) Frantz, D. E.; Fässler, R.; Carreira, E. M., *Journal of the American Chemical Society* **2000**, *122* (8), 1806-1807; (b) Boyall, D.; Frantz, D. E.; Carreira, E. M., *Organic Letters* **2002**, *4* (15), 2605-2606.

Chapter 4 Application of Gold-Catalyzed Cascade Reactions of Alkynes

4.1 Introduction

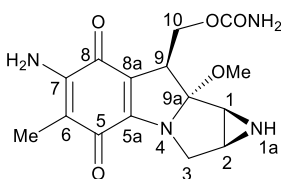
In this chapter, I will present my works on the application of gold-catalyzed cascade reactions. The first project, done in collaboration with the Reich group from Chemistry Department, is mainly focused on applying gold/platinum-catalyzed cycloisomerization to synthesize novel mitomycin C analogs with promising anticancer potency. The second project, which is still ongoing, is focused on utilizing gold-catalyzed nucleophilic addition across C-C triple bond to activate a glycosyl donor, thereby achieving stereoselective construction of 1,2-*cis* linkages in glycoconjugate and oligosaccharide synthesis.

4.2 Streamlined Synthesis of New Mitosene Derivatives with Improved IC₅₀ over Mitomycin C

4.2.1 A Brief History of Mitomycin C and Analogs

Mitomycin C (MMC, Figure 2), a chemotherapeutic agent isolated from extracts of genus *Streptomyces*,¹ cross links DNA and possesses potent antitumor and antibiotic activities.² It has been used since the 1960s to treat many types of soft and solid tumors,³ but is approved only for gastric and pancreatic adenocarcinoma. Its restricted use is mainly due to dose-limiting toxicity and delayed myelosuppression, as well as other significant side effects.^{2c}

Figure 2. Structure of Mitomycin C

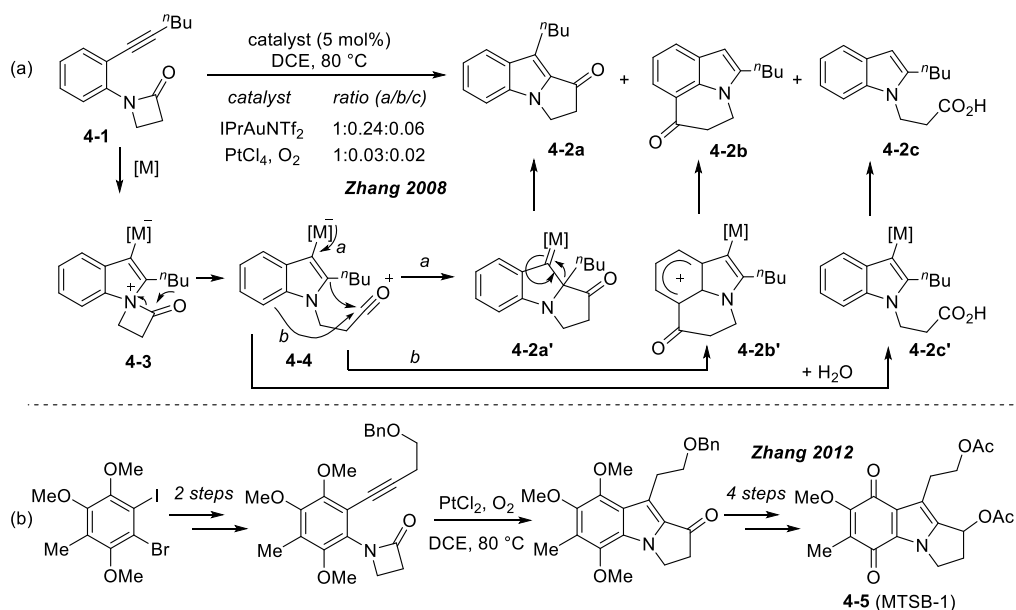


Although MMC is readily available via fermentation,^{1, 4} efforts to improve its pharmaceutical potency via direct modification have been largely limited to C7,⁵ C6,⁶ C10, and N1a⁷ positions and minor structural perturbation due to the sensitive structure, especially under acidic conditions. To date, there have been only a few derivatives with improved efficacy and/or decreased toxicity,^{5a, c, 6} but none has reached the market. On the other hand, the chemical synthesis of MMC,⁸ due to the densely organized functional groups and the strained aziridine ring, is a great challenge. While several elegant total syntheses⁹ have been achieved, access to new structural spaces has been limited by long synthetic sequences and low overall yields. In addition, analogous quinone-containing agents with simplified structures while maintaining reductive alkylating capacities have also failed due to high toxicities or lost anticancer activity *in vivo*.¹⁰

4.2.2 Our Preliminary Studies on a 7-Methoxymitosene Analog

In 2008, our group has published a cycloisomerization of *N*-(2-alkynylphenyl)lactams targeting the key tricyclic pyrrolo-[1,2-*a*]indole skeleton of MMC (Scheme 48a).¹¹ The initial nucleophilic attack of the nitrogen atom triggers a fragmentation of the lactam ring to give acylium species **4-4**, which subsequently undergoes a series of migrations to afford the desired product **4-2a**. Side reactions include the Friedel-Crafts-type product **4-2b** and hydration product **4-2c**. Notably, PtCl₄ demonstrates much better selectivity against its Au(I) counterpart. Based upon this work, our group realized a formal synthesis of 7-methoxymitosene as well as one novel analogs **4-5**, later renamed MTSB-1, with an overall yield of 27% over seven steps (Scheme 48b).¹² With the streamlined, versatile synthetic route to access the molecule of interest, I took over the project and endeavored into investigation of the new analog's anticancer activity.

Scheme 48. Au/Pt-Catalyzed Synthesis of 7-Methoxymitosene Analogs



Comparing to the original MMC, the structural alterations of our MTSB-1 include replacing the strained aziridine ring with a readily installable 1-OAc group and inserting an additional CH₂Bu group at the C9 side chain. We proposed that the structural deviations and simplifications from MMC would give rise to unique mechanism of action and biological activity. The established mechanism of action for MMC (Scheme 49A) is initiated by a cellular reduction of the quinone moiety, followed by the formation of 7-aminoleucoaziridinomitosenes **4-6** upon elimination of MeOH, and terminated with mono- or bis-alkylation of DNA. Bis-alkylation most often results in cross-linking of complementary DNA strands and is the major cause of the irreversible damage. Meanwhile, MTSB-1, as shown in Scheme 49B, can also undergo an initial reduction of its quinone moiety to trigger the monoalkylation of DNA at the same electrophilic site. However, what distinguishes MTSB-1 mechanistically from MMC is the second alkylation. Instead of an eniminium intermediate **4-7**, the expulsion of the second leaving group would generate an

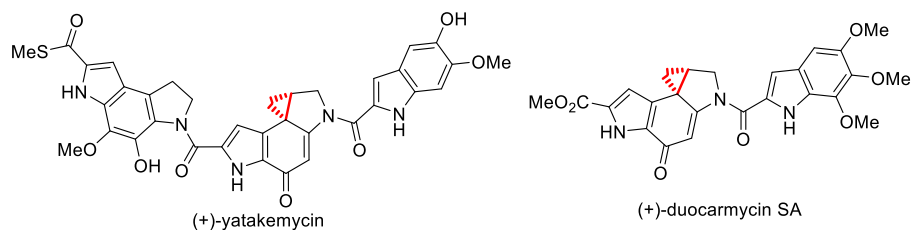
electrophilic spirocyclopropane species (i.e., **4-7'**). We reasoned that the strained three-membered ring could behave like a Michael-type receptor and react with DNA molecule, thereby realizing the bis-alkylation. It needs to be pointed out that the order of these two alkylation events could be reversed.¹³ Nevertheless, we believed the introduction of a new alkylation mechanism would make unexplored chemical space around the MMC/mitosene skeleton available for addressing the issues associated with MMC. Notably, DNA monoalkylations by electrophilic cyclopropane rings have already been reported in exceptionally potent natural products such as (+)-yatakemycin¹⁴ and (+)-duocarmycin SA¹⁵ (see Figure 3).

4.2.3 MTSB-1: Evaluation of Potency and Mechanism

To evaluate the efficacy of MTSB-1, thereby test and verify our proposed mechanism, we worked in collaboration with the Reich group and carried out cell toxicity experiments. We chose the prostate cancer cell line (PPC-1) and the normal prostate cell line (RWPE-1), which are frequently used to study the potency and toxicity of chemotherapeutics, respectively.¹⁶ We selected RWPE-1 because these immortalized normal cells divide more slowly than cancer cell lines and can provide information about a compound's off-target toxicity. Much to our delight, MTSB-1 inhibits proliferation of the PPC-1 prostate cancer cell at reasonably low concentrations (IC_{50} : $16.6 \pm 1.8 \mu\text{M}$, Figure 4C), while its IC_{50} against the RWPE-1 normal prostate cell line ($74.1 \pm 6.3 \mu\text{M}$, Figure 4D) is more than 4 times higher. In comparison, MMC is over an order more potent against the PPC-1 prostate cancer cell line with an IC_{50} value of $0.8 \pm 0.2 \mu\text{M}$ (Figure 4), which is similar to other reported values.¹⁷ However, little difference could be observed for MMC against the

normal RWPE-1 prostate cells (IC_{50} : $0.9 \pm 0.2 \mu\text{M}$, Figure 4B), which is consistent with the considerable off-target toxicity demonstrated by MMC *in vivo*.

Figure 3. Bio-Active Natural Products Carrying Electrophilic Cyclopropane Rings



Scheme 49. Established Mechanism of DNA Cross-Linking by MMC and Hypothesized Mechanism of Action for MTSB-1

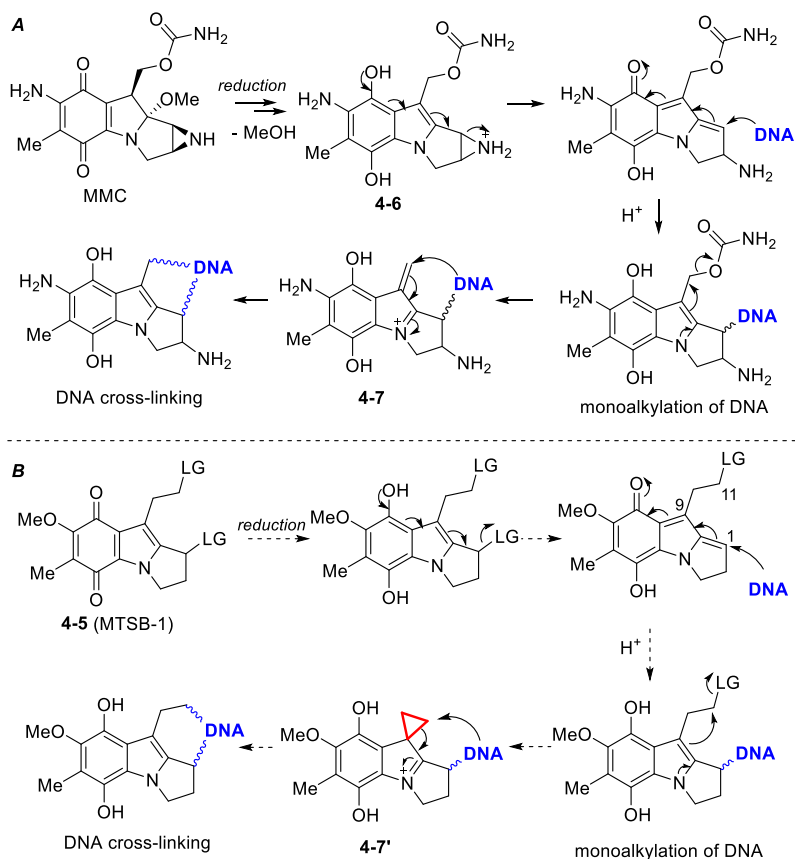
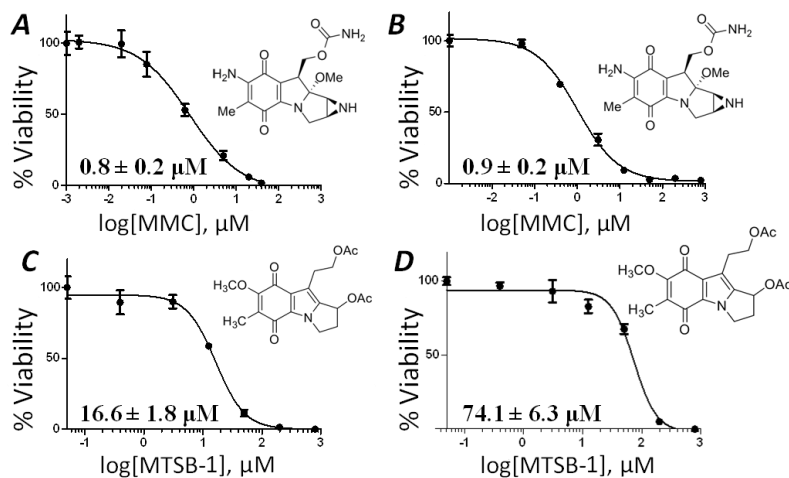
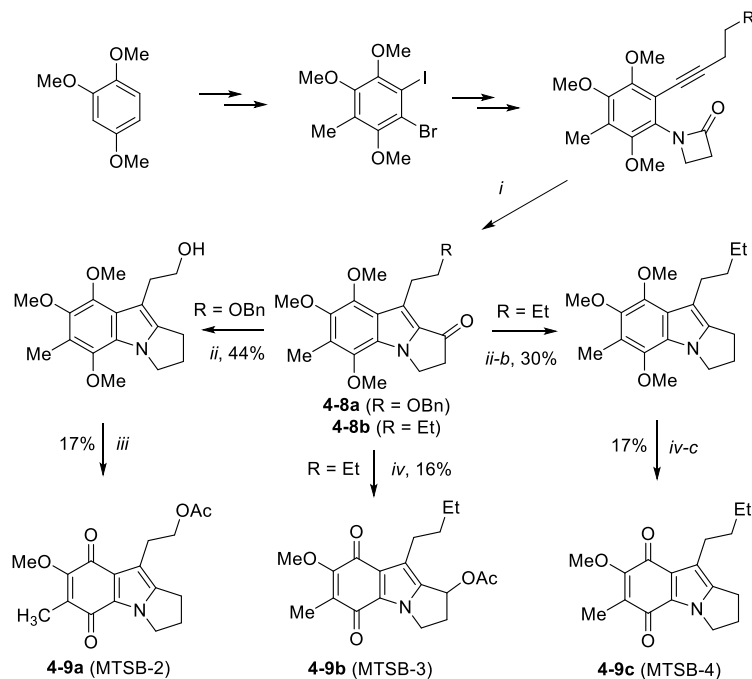


Figure 4. IC₅₀ curves and values for MMC against PPC-1 cells (**A**) and RWPE-1 cells (**B**), and MTSB-1 against PPC-1 cells (**C**) and RWPE-1 cells (**D**)



Scheme 50. Synthesis of Mechanistic Probes for MSTB-1



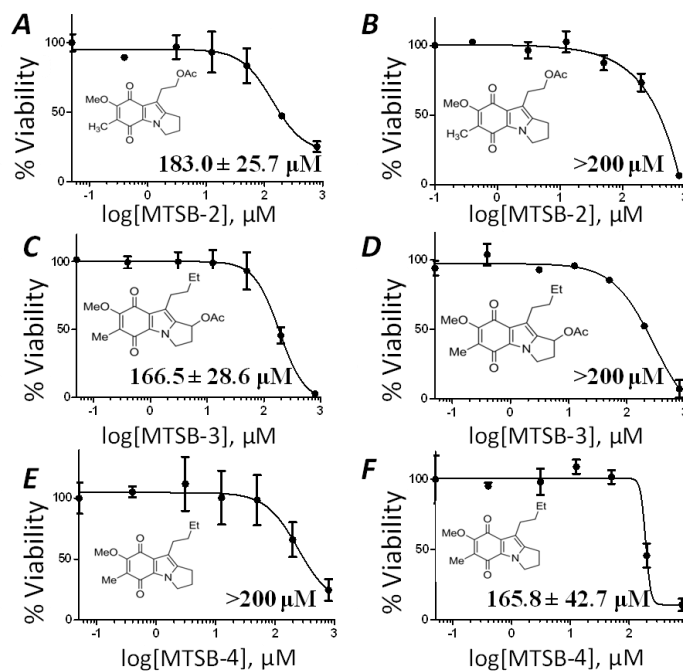
Conditions: *i*. PtCl₂ (0.3 equiv.), O₂ (1 atm), DCE, 80 °C, 12 h. *ii*. a) Pd/C, H₂ (1 atm), THF, rt, 12 h, 88%; b) N₂H₄ (2 equiv.), K₂CO₃ (15 equiv.), ethylene glycol, 180 °C, 6 h, 50%. *iii*. a) AcCl (1.5 equiv.), Et₃N (3 equiv.), DCM, 0 °C to rt, 83%; b) NaNO₂ (1.5 equiv.), HCl (1 M), CHCl₃/H₂O, rt, 16 h, 20%. *iv*. a) NaBH₄ (2 equiv.), MeOH, rt, 2 h, 91%; b) AcCl (1.5 equiv.), Et₃N (3 equiv.), DCM, 0 °C to rt, 84%. *c*) Ag₂O (3 equiv.), HNO₃ (6 M), THF, rt, 5 min.

Considering the substantially lower off-target cytotoxicity, these encouraging initial results on MTSB-1 strongly supported the proposed mechanism (see: Scheme 49B). To further probe the mechanism of action of MTSB-1, and thereby lay the foundation for improving its efficacy, we synthesized three of its structural variants, i.e., MTSB-2, MTSB-3, and MTSB-4, as mechanistic probes, following a similar synthetic strategy (Scheme 50).¹² MTSB-2, which has the OAc group at C1 removed, was prepared from the previously reported tricyclic fully substituted indole **4-8a**¹² via a four-step sequence: debenzoylation, Wolff-Kishner deoxygenation, acetylation of the free OH group, and finally oxidative quinone formation; MTSB-3, which has a *n*-butyl group replacing the OAc at C9 side chain, was readily prepared from the requisite tricyclic indole **4-8b** upon sequential reduction, acetylation and oxidative quinone formation; and MTSB-4, which does not have any OAc leaving group, was accessed in two steps from **4-8b**. Notably, in all the preparations, the final oxidation of the electron-rich benzene ring suffered from very low efficiencies due to a myriad of side reactions despite many efforts to improve it.

We reasoned that if MTSB-1 exhibits its cytotoxicity by cross-linking DNA (as proposed in Scheme 49B), these mechanistic probes would be much less cytotoxic due to the removal of one or both alkylating site(s). The IC₅₀ values of the three analogs were determined against the PPC-1 prostate cancer cell line. As shown in Figure 5, MTSB-2, MTSB-3, and MTSB-4 have IC₅₀ values of 166.5 ± 28.6 μM, 183.0 ± 25.7 μM, and >200 μM, respectively, which are all ten-fold down less potent than MTSB-1, and hence are all largely ineffective in decreasing cell viability. Likewise, they were ineffective against the RWPE-1 normal prostate cell line, with IC₅₀ values close to or over 200 μM (Figure 5B, D, F). These data suggest that MTSB-1 most likely double alkylates DNA, which in turn

supports our hypothesis that the cyclopropane species **4-7'** would be a key intermediate in DNA alkylation.

Figure 5. IC₅₀ curves and values for MTSB-2 against PPC-1 cells (**A**) and RWPE-1 cells (**B**), MTSB-3 against PPC-1 cells (**C**) and RWPE-1 cells (**D**), and MTSB-4 against PPC-1 cells (**E**) and RWPE-1 cells (**F**)

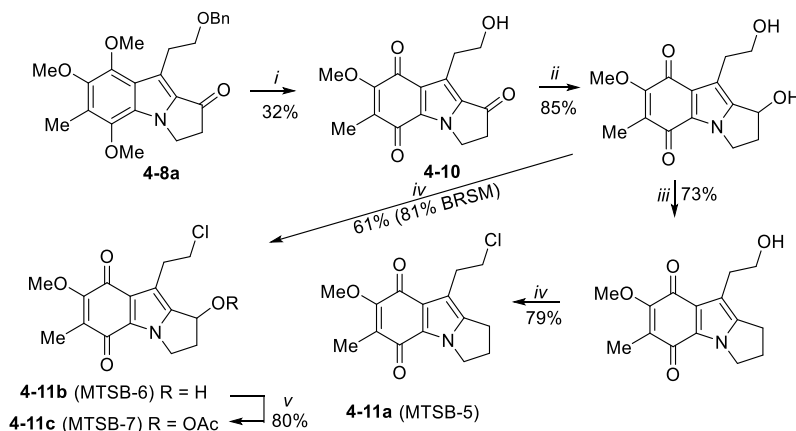


4.2.4 Synthesis of Derivatives Aiming at Higher Potency

To provide further support for the involvement of the cyclopropane species **4-7'** in DNA alkylation, we designed a chloro analog, i.e., MTSB-5, which has the OAc at C1 of MTSB-1 removed and the other OAc at C10 replaced by a chloride. Its synthesis is outlined in Scheme 51. To improve the low efficiencies encountered in the previous synthetic routes, we performed it upon the debenzoylation of the common intermediate **4-8a** and before manipulation of the electron-withdrawing C1 carbonyl group. An improved 40% isolated yield of the corresponding indoloquinone **4-10** was achieved. Subsequent two-step

reductive deoxygenation of the ketone moiety followed by the treatment of triphosgene smoothly delivered the target molecule.

Scheme 51. Synthesis of Chloride Derivatives MTSB-5, MTSB-6, and MTSB-7

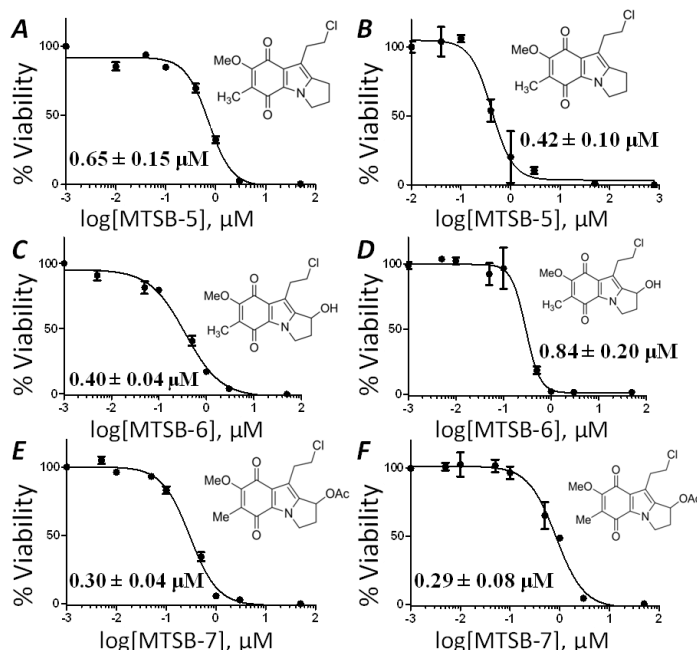


Conditions: *i.* a) Pd/C, H₂ (1 atm), THF, rt, 80%; b) NaNO₂ (1.5 equiv.), HCl (1 M), CHCl₃/H₂O, rt, 16 h, 40%; *ii*) NaBH₄ (3 equiv.), MeOH, rt, 2 h, then add NH₄Cl/H₂O, stir in air. *iii.* Et₃SiH (2 equiv.), CF₃COOH (5 equiv.), DCM, 0 °C, 1 h, then TBAF, 73%. *iv.* Triphosgene (0.5 equiv.), Et₃N (2.5 equiv.), DCM, 0 °C to rt. *v.* AcCl (1.5 equiv.), pyridine (3 equiv.), DCM, 0 °C to rt, 80%.

As chloride is a better leaving group than acetate, an alkylating species of that in Scheme 49B would be formed more readily if in accordance to our hypothesis. Hence, MTSB-5 should at least show a lower IC₅₀ value than that of MTSB-2. Much to our delight, MTSB-5 has a low IC₅₀ value of 0.65 ± 0.15 μM against PPC-1 prostate cancer cells (Figure 6A), showing much higher potency than MTSB-2 and even slightly improved potency over MMC. While monoalkylation of DNA by an alkylating reagent may be repaired and thus non-lethal, this result is nevertheless in line with the high anticancer potency of (+)-yatakemyin¹⁸ and (+)-duocarmycin SA¹⁹ (see Figure 3 for the structures of natural products involved), which monoalkylate DNA via a reactive spirocyclopropane ring. This in turn is consistent with the involvement of a spirocyclopropane intermediate **4-7'** in the hypothesized mechanism of action (see Scheme 49B) and implicates a DNA alkylating site

different from those of MMC. Like MMC, MTSB-5, shows similar potencies against both PPC-1 and RPWE-1 cell lines (Figure 6B).

Figure 6. IC₅₀ curves and values for MTSB-5 against PPC-1 cells (A) and RWPE-1 cells (B), MTSB-6 against PPC-1 cells (C) and RWPE-1 cells (D), and MTSB-7 against PPC-1 cells (E) and RWPE-1 cells (F)



Because DNA cross-linking may be more lethal to cells than the related monoalkylation in the cases of MMC and MTSB-1, installation of an additional alkylating site to MTSB-5 could enhance cytotoxicity. Two such compounds, MTSB-6 and MTSB-7, with an OH group and an OAc group at C1 of the MTSB-5 structure, respectively, were readily prepared (Scheme 51).

Indeed, MTSB-6 and MTSB-7 demonstrated increasing efficacy against PPC-1 cells with improved IC₅₀ values of $0.40 \pm 0.04 \mu\text{M}$ and $0.30 \pm 0.04 \mu\text{M}$, respectively (Figure 6C and E). Contrary to MTSB-7, which showed no difference in potency against the RWPE-1 cell

line (IC_{50} of $0.29 \pm 0.08 \mu\text{M}$, Figure 6F), MTSB-6 was 2-fold less cytotoxic against RWPE-1 (IC_{50} : $0.84 \pm 0.20 \mu\text{M}$, Figure 6D) than against PPC-1. These results may form the basis of rationally improving the potency of these analogs while lowering the toxicity, as scored in these cell-based assays.

4.2.5 Conclusion

In conclusion, we have advanced a hypothesis that, different from the mode of DNA double alkylation by mitomycin C, structurally related yet novel mitosene derivatives could likewise cross link DNA via a novel electrophilic spirocyclopropane intermediate. Rational design and substantial structural simplification permits rapid access to some preliminary examples of the mitosenes, i.e., MTSB-1 - MTSB-7. Their cytotoxicity assays against the PPC-1 prostate cancer cell line and the RWPE-1 normal cell line yield IC_{50} values that are consistent with the hypothesis. Among them, MTSB-6 exhibits twice as high potency against PPC-1 as mitomycin C but similar toxicity against RPWE-1. The facile synthesis of these mitosenes and the promising potency and toxicity data open novel mitosene structural space for systematic optimization and thus the potential for developing a new class of anticancer drugs.

4.2.6 Experimental Details

Cell Lines and Cell Culture

The human prostate cancer cells (PPC-1) were a generous gift from Erkki Ruoslahti (Sanford-Burnham Medical Research Institute, La Jolla, San Diego, CA). PPC-1 cells were maintained in Dulbecco's Modified Eagle Medium (DMEM) high glucose medium (Hyclone) supplemented with 10% fetal bovine serum (Hyclone). Noncancerous prostate

epithelial cells (RWPE-1) (ATCC) were grown in keratinocyte serum free medium (Invitrogen) supplemented with bovine pituitary extract (0.05 ng/mL) and recombinant EGF (5 ng/mL). Both cell lines were maintained at 37 °C in atmospheric 5% CO₂ and grown in 96-well plates (BD Falcon) for experiments.

Cell Treatment with Compounds

MMC (O Chem Incorporation) was dissolved in nuclease-free water (IDT Technologies) and standard serial dilutions using cell growth media were performed to yield concentrations of 40- 0.002 μM.²⁰ For MTSB-1 and its analogs, each compound was dissolved in DMSO (Fischer Scientific) and standard serial dilutions of each compound were performed using cell growth media to yield concentrations of 800- 0.001 μM. DMSO concentration was kept below 0.1% to ensure no carrier-induced decrease in cell viability. Controls of PPC-1 and RWPE-1 cells growing in drug-free cell growth media, and in cell growth media containing 0.1% DMSO, were used.

100 μL aliquots of PPC-1 and RWPE-1 cells in cell growth media were seeded in separate 96-well plates to a cell density of 3,000 cells per well and cells were allowed to adhere to wells for 24 hours at 37°C in 5% CO₂. After 24 hours, cell growth media was removed and replaced with cell growth media supplemented with increasing concentrations of the given compound (MMC, MTSB-1 – MTSB-7). All compound concentrations were tested in triplicates.

PPC-1 and RWPE-1 cells were incubated with media supplemented with the desired compound concentrations for 24 hours and then the media was removed. Each well was subsequently washed twice and then fully replaced with 100μL of compound-free cell

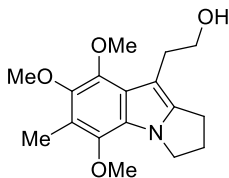
growth medium. Cells were allowed to incubate for an additional 48 hours at 37°C in 5% CO₂, and then cell viability assays were performed.

Viability Assay and IC₅₀ Value Determination

After 48 hours of incubation with compound-free cell growth medium, 10 µL PrestoBlue Cell Viability Reagent²¹ (Invitrogen) was added to each well of the 96-well plate and allowed to incubate with cells for 1 hour at 37°C in atmospheric 5% CO₂. The fluorescence signal was recorded in a Tecan Infinite 200 Pro reader in bottom-read mode with excitation and emission wavelengths of 560 nm (9 nm bandwidth) and 590 nm (20 nm bandwidth), respectively. Fluorescence values for each treatment were averaged and converted to percent viability by comparison to the control fluorescence value (PPC-1 or RWPE-1 cells not treated with any compound, 100% viable). Percent viability data was plotted to create triplicate IC₅₀ curves for the given compound. A log(dose)-response curve formulated by GraphPad Prism 5 software was fitted to each data set to yield triplicate IC₅₀ values, reported as mean ± standard deviation (SD). The same procedure was carried out for every compound on at least two separate occasions.

Synthesis of Mitosene Derivatives MTSB-2 to MTSB-4

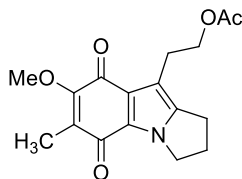
2-(5,7,8-Trimethoxy-6-methyl-2,3-dihydro-1H-pyrrolo[1,2-a]indol-9-yl)ethanol (4-A)



To 9-(2-(benzyloxy)ethyl)-5,7,8-trimethoxy-6-methyl-2,3-dihydro-1H-pyrrolo[1,2-a]-indol-1-one (**4-8a**)¹² (41 mg, 0.1 mmol) in 2 mL THF was added Pd/C (10 mg), and the

mixture was then stirred in H₂ atmosphere at room temperature for 12 h. After TLC showed complete conversion of the starting material, the mixture was filtered through a Celite pad and concentrated under vacuum. The crude product was charged with K₂CO₃ (207 mg, 1.5 mmol), N₂H₄·H₂O (32 μL) and ethylene glycol (4 mL) under N₂ atmosphere. The mixture was then heated at 180 °C for 6 h. Upon completion, the system was washed with water and extracted with ethyl acetate. The extract was washed with brine continuously and was then dried over MgSO₄, concentrated under vacuum and purified by column chromatography to furnish **4-A** in 44% yield (two steps). ¹H NMR (500 MHz, CDCl₃) δ 4.22 (t, *J* = 7.0 Hz, 2H), 3.95 (s, 3H), 3.86 (t, *J* = 6.1 Hz, 2H), 3.82 (s, 3H), 3.81 (s, 3H), 3.01 (t, *J* = 6.1 Hz, 2H), 2.90 (t, *J* = 7.4 Hz, 2H), 2.56 (p, *J* = 7.1 Hz, 2H), 2.29 (s, 3H); ¹³C NMR (151 MHz, CDCl₃) δ 143.88, 142.59, 141.94, 139.85, 124.82, 124.57, 117.05, 101.65, 63.85, 62.24, 61.11, 60.62, 45.87, 29.27, 27.80, 22.76, 9.15; IR (neat, cm⁻¹): 3425, 2937, 1493, 1448, 1426, 1379, 1274, 1093, 1027; ESI+ calculated for [C₁₇H₂₃NNaO₄]⁺: 328.15, found: 328.17.

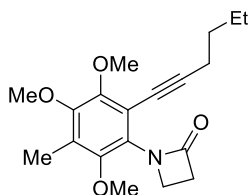
2-(7-Methoxy-6-methyl-5,8-dioxo-2,3,5,8-tetrahydro-1H-pyrrolo[1,2-a]indol-9-yl)ethyl acetate 4-9a (MTSB-2)



To **4-A** (16 mg, 0.05 mmol) in 1 mL dry CH₂Cl₂ was added triethylamine (15 mg, 0.15 mmol), the mixture was then stirred at 0 °C while acetyl chloride (5.5 μL, 0.075 mmol) was added. The reaction was then allowed to stir in room temperature for 1 h until TLC

showed the complete conversion of the starting material. Additional acetyl chloride may be added if the reaction did not show complete conversion after 1 h. The mixture was washed with saturated NaHCO₃ and brine, and dried over Na₂SO₄. After removing the solvent under reduced pressure, the residue was dissolved in 2.5 mL chloroform and 3 M HCl (2.0 mL) was added. The mixture was stirred vigorously while sodium nitrite (4.0 mg, 0.06 mmol) in water (0.6 mL) was added dropwise over the course of 1 h. The reaction was then stirred for another 15 h or until TLC showed no starting material left. The layers were separated and the aqueous phase was further extracted with chloroform until the extract becomes colorless. Combined organic phase was dried with Na₂SO₄. After removing the solvent under reduced pressure, the residue was purified by flash chromatography to furnish **4-9a (MTSB-2)** in 17% yield (two steps). ¹H NMR (600 MHz, CDCl₃) δ 4.25 (t, *J* = 6.8 Hz, 2H), 4.22 (t, *J* = 7.3 Hz, 2H), 3.97 (s, 3H), 3.01 (t, *J* = 6.8 Hz, 2H), 2.80 (t, *J* = 7.4 Hz, 2H), 2.58 – 2.52 (m, 2H), 2.02 (s, 3H), 1.94 (s, 3H); ¹³C NMR (151 MHz, CDCl₃) δ 186.81, 179.88, 178.23, 170.93, 156.87, 143.53, 128.12, 126.17, 125.08, 113.36, 63.90, 61.05, 46.93, 27.23, 24.76, 22.73, 21.03, 8.49; IR (neat, cm⁻¹): 2926, 2091, 1640, 1481, 1370, 1244, 1108; ESI+ calculated for [C₁₇H₁₉NNaO₅]⁺: 340.12, found: 340.12.

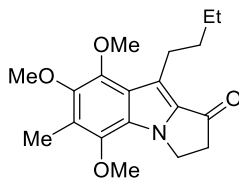
1-(2-(Hex-1-ynyl)-3,4,6-trimethoxy-5-methylphenyl)azetidin-2-one (**4-B**)



Compound **4-B** was prepared from 1-bromo-2-iodo-3,4,6-trimethoxy-5-methylbenzene using our previously reported procedure^[3]. 1-bromo-2-iodo-3,4,6-trimethoxy-5-methyl-

benzene (188 mg, 0.5 mmol), CuI (19.3 mg, 0.1 mmol), Pd(PPh₃)₂Cl₂ (35 mg, 0.05 mmol), triphenylphosphine (13.1 mg, 0.05 mmol), 1-hexyne (205 mg, 2.5 mmol) were mixed in 2 mL Et₃N under N₂. After being heated at 60 °C for 4 h, the solvent was removed under vacuum, and the residue was filtered through a silica gel pad using hexanes/ethyl acetate 10:1. The filtrate was concentrated under. The crude product was directly charged with CuI (24 mg, 0.125 mmol), K₂CO₃ (138 mg, 1 mmol), *N,N*-dimethylcyclohexane-1,2-diamine (37.5 μL, 0.125 mmol), 2-azetidinone (50 mg, 0.7 mmol) and 6 mL 1,4-dioxane under N₂. After being heated at 125 °C for 13 h, the solvent was removed under vacuum, and the residue was purified by flash chromatography to furnish **4-B** in 60% yield (two steps). ¹H NMR (400 MHz, CDCl₃) δ 3.88 (s, 3H), 3.82 (s, 3H), 3.76 – 3.68 (m, 5H), 3.11 (t, *J* = 4.3 Hz, 2H), 2.49 (t, *J* = 7.0 Hz, 2H), 2.18 (s, 3H), 1.65 – 1.57 (m, 2H), 1.55 – 1.43 (m, 2H), 0.95 (t, *J* = 7.3 Hz, 3H); ¹³C NMR (151 MHz, CDCl₃) δ 166.36, 151.66, 151.63, 150.59, 127.16, 126.41, 115.81, 99.35, 72.77, 61.08, 60.89, 60.52, 41.57, 36.99, 30.75, 21.95, 19.47, 13.59, 9.62; IR (neat, cm⁻¹): 2959, 2936, 2229, 1761, 1644, 1466, 1411, 1195, 1123, 1100; ESI+ calculated for [C₁₉H₂₅NNaO₄]⁺: 354.17, found: 354.18.

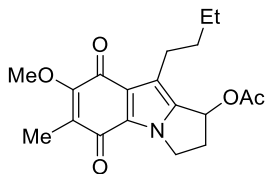
9-Butyl-5,7,8-trimethoxy-6-methyl-2,3-dihydro-1H-pyrrolo[1,2-a]indol-1-one (4-8b)



To **4-B** (100 mg, 0.3 mmol) in 10 mL DCE was added PtCl₂ (30 mg, 0.1 mmol) under O₂ atmosphere, the mixture was then stirred at 80 °C for 11 h. After removing the solvent under reduced pressure, the residue was purified by flash chromatography to furnish **4-8b**

in 80% yield. ^1H NMR (500 MHz, CDCl_3) δ 4.52 (t, $J = 6.4$ Hz, 2H), 3.96 (s, 3H), 3.85 (s, 6H), 3.13 (t, $J = 6.3$ Hz, 2H), 3.09 (t, $J = 7.6$ Hz, 2H), 2.31 (s, 3H), 1.73 – 1.64 (m, 2H), 1.47 – 1.36 (m, 2H), 0.94 (t, $J = 7.4$ Hz, 3H); ^{13}C NMR (126 MHz, CDCl_3) δ 192.64, 144.80, 144.63, 140.61, 131.98, 127.74, 124.81, 123.17, 118.59, 62.37, 60.87, 60.56, 41.72, 40.09, 34.04, 24.59, 22.66, 13.97, 9.61; IR (neat, cm^{-1}): 2957, 2932, 1704, 1564, 1501, 1452, 1395, 1295, 1260, 1112, 1161, 1086, 1024; ESI+ calculated for $[\text{C}_{19}\text{H}_{25}\text{NNaO}_4]^+$: 354.17, found: 354.19.

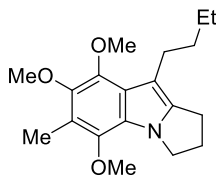
9-Butyl-7-methoxy-6-methyl-5,8-dioxo-2,3,5,8-tetrahydro-1H-pyrrolo[1,2-a]indol-1-yl acetate 4-9b (MTSB-3)



To **4-8b** (66 mg, 0.2 mmol) in 2 mL MeOH was added NaBH_4 (15.2 mg, 0.4 mmol). The mixture was stirred at room temperature for 2 h and quenched by saturated NH_4Cl . The solution was then extracted with ethyl acetate and washed with brine, dried over MgSO_4 and concentrated under vacuum. The residue was dissolved in 1 mL dry CH_2Cl_2 with triethylamine (15 mg, 0.15 mmol), and was then stirred at 0 °C while acetyl chloride (5.5 μL , 0.075 mmol) was added. The reaction was allowed to stir in room temperature for 1 h until TLC showed the complete conversion of the starting material. Additional acetyl chloride may be added if the reaction did not show complete conversion. The mixture was washed with saturated NaHCO_3 and brine, dried over Na_2SO_4 , and concentrated under vacuum. The product was used directly without further purification.

To the crude product above in 2 mL THF was added silver (II) oxide (52 mg, 0.42 mmol). The mixture was stirred vigorously at room temperature while 6 M HNO₃ (0.16 mL) was added dropwise. The reaction was stirred for 5 min and quenched by 2 mL water. The resulting solution was extracted with CH₂Cl₂ until the extract was colorless. The extract was combined and dried over Na₂SO₄. After removing the solvent under reduced pressure, the residue was purified by flash chromatography to furnish **4-9b (MTSB-3)** in 16% overall yield. ¹H NMR (600 MHz, CDCl₃) δ 6.10 (dd, *J* = 6.7, 1.5 Hz, 1H), 4.36 – 4.24 (m, 2H), 4.00 (s, 3H), 2.91 (dt, *J* = 15.2, 8.5 Hz, 1H), 2.76 – 2.67 (m, 2H), 2.56 – 2.50 (m, 1H), 2.07 (s, 3H), 1.95 (s, 3H), 1.56 (ddd, *J* = 23.1, 15.4, 7.6 Hz, 1H), 1.52 – 1.45 (m, 1H), 1.35 (dq, *J* = 14.7, 7.3 Hz, 2H), 0.91 (t, *J* = 7.3 Hz, 3H); ¹³C NMR (151 MHz, CDCl₃) δ 179.42, 178.79, 170.22, 157.57, 138.76, 128.11, 126.84, 124.85, 121.98, 77.19, 76.98, 76.77, 67.66, 61.13, 45.19, 35.72, 32.29, 24.67, 22.54, 20.98, 13.94, 8.45; IR (neat, cm⁻¹): 2959, 2926, 2096, 1639, 1487, 1457, 1374, 1224, 1124; ESI+ calculated for [C₁₉H₂₃NNaO₅]⁺: 368.15, found: 368.18.

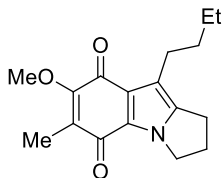
9-Butyl-5,7,8-trimethoxy-6-methyl-2,3-dihydro-1H-pyrrolo[1,2-a]indole (4-C)



4-8b (100 mg, 0.3 mmol) was charged with K₂CO₃ (621 mg, 4.5 mmol), N₂H₄·H₂O (0.1 mL) and ethylene glycol (12 mL) under N₂ atmosphere. The mixture was then heated at 180 °C for 6 h. Upon completion, the system was washed with water and extracted with ethyl acetate. The extract was washed with brine continuously and was then dried over

MgSO₄, concentrated under vacuum and purified by column chromatography to furnish **4-C** in 30% yield. ¹H NMR (500 MHz, CDCl₃) δ 4.20 (t, *J* = 6.9 Hz, 2H), 3.93 (d, *J* = 0.5 Hz, 3H), 3.84 (d, *J* = 0.5 Hz, 3H), 3.81 (d, *J* = 0.5 Hz, 3H), 2.88 (t, *J* = 7.4 Hz, 2H), 2.77 (t, *J* = 7.6 Hz, 2H), 2.54 (p, *J* = 7.2 Hz, 2H), 2.29 (s, 3H), 1.70 – 1.61 (m, 2H), 1.45 – 1.36 (m, 2H), 0.95 (t, *J* = 7.4 Hz, 3H); ¹³C NMR (151 MHz, CDCl₃) δ 143.80, 142.64, 141.10, 139.57, 124.66, 124.38, 116.61, 106.46, 62.20, 61.10, 60.64, 45.63, 33.67, 27.91, 25.61, 22.98, 22.77, 14.04, 9.16; IR (neat, cm⁻¹): 2955, 2932, 2872, 2857, 1986, 1563, 1493, 1448, 1379, 1272, 1106, 1082, 1032; ESI+ calculated for [C₁₉H₂₇NNaO₃]⁺: 340.19, found: 340.21.

9-Butyl-7-methoxy-6-methyl-2,3-dihydro-1H-pyrrolo[1,2-a]indole-5,8-dione 4-9c (MTSB-4)

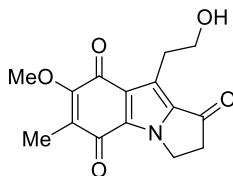


To **C** (47 mg, 0.15 mmol) in 2 mL THF was added silver (II) oxide (55.8 mg, 0.45 mmol). The mixture was stirred vigorously at room temperature while 6 M HNO₃ (0.16 mL) was added dropwise. The reaction was stirred for 5 min and quenched by 1 mL water. The resulting solution was extracted with CH₂Cl₂ until the extract was colorless. The extract was combined and dried over Na₂SO₄. After removing the solvent under reduced pressure, the residue was purified by flash chromatography to furnish **4-9c (MTSB-4)** in 17% yield. ¹H NMR (600 MHz, CDCl₃) δ 4.20 (t, *J* = 7.3 Hz, 2H), 3.97 (s, 3H), 2.79 (t, *J* = 7.4 Hz, 2H), 2.68 (t, *J* = 7.6 Hz, 2H), 2.58 – 2.51 (m, 2H), 1.94 (s, 3H), 1.58 – 1.53 (m, 2H), 1.38

– 1.31 (m, 2H), 0.92 (t, $J = 7.4$ Hz, 3H); ^{13}C NMR (151 MHz, CDCl_3) δ 179.89, 178.15, 156.95, 142.69, 128.06, 125.84, 125.03, 118.98, 61.02, 46.79, 31.89, 27.21, 24.96, 22.89, 22.55, 13.93, 8.48; IR (neat, cm^{-1}): 2957, 2854, 2103, 1639, 1480, 1371, 1317; ESI+ calculated for $[\text{C}_{17}\text{H}_{21}\text{NNaO}_3]^+$: 310.14, found: 310.15.

Synthesis of Mitosene Derivatives MTSB-5 to MTSB-7

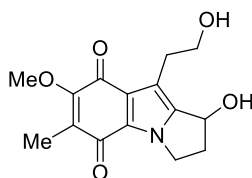
9-(2-Hydroxyethyl)-7-methoxy-6-methyl-2,3-dihydro-1H-pyrrolo[1,2-a]indole-1,5,8-trione (4-10)



To 9-(2-(benzyloxy)ethyl)-5,7,8-trimethoxy-6-methyl-2,3-dihydro-1H-pyrrolo[1,2-a]-indol-1-one (**4-8a**)^[3] (41 mg, 0.1 mmol) in 2 mL THF was added Pd/C (10 mg), and the mixture was then stirred in H_2 atmosphere at room temperature for 12 h. After TLC showed complete conversion of the starting material, the mixture was filtered through a Celite pad and concentrated under vacuum. The crude product was dissolved in chloroform, 3 M HCl (5.0 mL) was added. The mixture was stirred vigorously while sodium nitrite (10 mg, 0.15 mmol) in water (1.5 mL) was added dropwise over the course of 1 h. The reaction was left to stir overnight at room temperature. Upon completion, the layers were separated and the aqueous phase was extracted with chloroform until the extract becomes colorless. Combined organic phase was dried with Na_2SO_4 . After removing the solvent under reduced pressure, the residue was purified through flash chromatography to give **4-10** in 32% yield (two steps). ^1H NMR (500 MHz, CDCl_3) δ 4.55 (t, $J = 6.1$ Hz, 2H), 4.08 (s, 3H), 3.92 (t, J

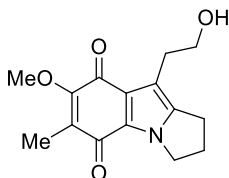
= 5.9 Hz, 2H), 3.28 (t, $J = 5.9$ Hz, 2H), 3.15 (t, $J = 6.1$ Hz, 2H), 1.99 (s, 3H); ^{13}C NMR (126 MHz, CDCl_3) δ 191.53, 179.72, 179.04, 158.59, 133.83, 130.27, 129.44, 125.68, 124.15, 62.57, 61.37, 43.16, 39.19, 28.32, 8.60; IR (neat, cm^{-1}): 2927, 1713, 1662, 1489, 1436, 1318, 1117; ESI+ calculated for $[\text{C}_{15}\text{H}_{15}\text{NNaO}_5]^+$: 312.08, found: 312.10.

1-Hydroxy-9-(2-hydroxyethyl)-7-methoxy-6-methyl-2,3-dihydro-1H-pyrrolo[1,2-a]indole-5,8-dione (4-D)



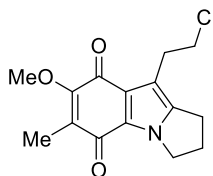
4-10 (28.9 mg, 0.1 mmol) was dissolved in 1 mL methanol, NaBH_4 (11.1 mg, 0.3 mmol) was then added. The mixture was stirred at room temperature for 2 h and quenched by saturated NH_4Cl . The solution was then extracted with ethyl acetate and washed with brine, dried over MgSO_4 and concentrated under vacuum to give **4-D** in 85% yield. ^1H NMR (400 MHz, CDCl_3) δ 5.13 (dd, $J = 6.4, 1.6$ Hz, 1H), 4.34 – 4.27 (m, 2H), 4.07 – 3.99 (m, 1H), 3.98 (s, 3H), 3.77 (tt, $J = 6.9, 3.5$ Hz, 2H), 3.39 – 3.31 (m, 1H), 2.84 – 2.69 (m, 2H), 2.56 – 2.49 (m, 1H), 1.94 (d, $J = 8.3$ Hz, 3H); ^{13}C NMR (126 MHz, CDCl_3) δ 180.14, 178.71, 157.27, 145.32, 128.55, 126.31, 124.63, 115.69, 65.16, 62.22, 61.09, 45.73, 36.98, 27.49, 8.55; IR (neat, cm^{-1}): 3421, 2927, 1639, 1489, 1373, 1317, 1228, 1103; ESI+ calculated for $[\text{C}_{15}\text{H}_{17}\text{NNaO}_5]^+$: 314.10, found: 314.11.

9-(2-Hydroxyethyl)-7-methoxy-6-methyl-2,3-dihydro-1H-pyrrolo[1,2-a]indole-5,8-dione (4-E)



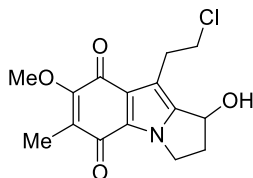
Et₃SiH (11.7 mg, 0.1 mmol) was added to a solution of **4-D** (14.6 mg, 0.05 mmol) in 3 mL dry dichloromethane. The solution was stirred at 0 °C while trifluoroacetic acid (28.5 mg, 0.25 mmol) in 1 mL dry dichloromethane was added dropwise. The solution was kept at 0 °C for 1 h and was then allowed to rise to room temperature. Upon complete conversion of the starting material (the 1° OH group might be protected by triethylsilyl group as well), which was indicated by TLC, the mixture was washed with NaHCO₃ and treated with tetrabutylammonium fluoride (0.1 mL, 1.0 M solution in THF). The mixture was then washed with 1 M HCl, brine, dried over Na₂SO₄, and concentrated under vacuum. The residue was purified by column chromatography to give **4-E** in 73% yield. ¹H NMR (400 MHz, CDCl₃) δ 4.21 (t, *J* = 7.2 Hz, 2H), 3.96 (s, 3H), 3.84 (t, *J* = 6.1 Hz, 2H), 2.93 (t, *J* = 6.1 Hz, 2H), 2.81 (t, *J* = 7.4 Hz, 2H), 2.60 – 2.51 (m, 2H), 1.94 (s, 3H); ¹³C NMR (126 MHz, CDCl₃) δ 180.56, 178.12, 157.03, 143.69, 128.41, 126.32, 125.45, 114.51, 63.07, 61.08, 47.03, 28.78, 27.17, 22.65, 8.54; IR (neat, cm⁻¹): 2930, 2854, 2092, 1639, 1481, 1373, 1315, 1100; ESI+ calculated for [C₁₅H₁₅NNaO₄]⁺: 298.11, found: 298.14.

9-(2-Chloroethyl)-7-methoxy-6-methyl-2,3-dihydro-1H-pyrrolo[1,2-a]indole-5,8-dione 4-11a (MTSB-5)



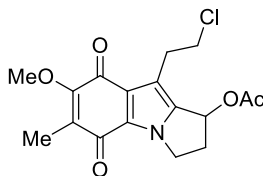
4-11a (MTSB-5) was prepared from **4-E** following Kartika's method.²² **4-E** (5.5 mg, 0.02 mmol) was dissolved in 1 mL dry DCM and was cooled down to 0 °C in an ice bath. Et₃N (7 μL, 0.05 mmol) was then added, and triphosgene (3 mg, 0.01 mmol) was added slowly. The system was kept at 0 °C for another 5 min and was allowed to stir at room temperature for another 2 h. The reaction was quenched by saturated NaHCO₃ and extracted with dichloromethane. The organic phase was combined, dried over Na₂SO₄ and concentrated in vacuum. The residue was purified by column chromatography to give **4-11a (MTSB-5)** in 70% yield. ¹H NMR (600 MHz, CDCl₃) δ 4.23 (t, *J* = 7.3 Hz, 2H), 3.97 (s, 3H), 3.79 (t, *J* = 6.5 Hz, 2H), 3.10 (t, *J* = 6.5 Hz, 2H), 2.85 (t, *J* = 7.4 Hz, 2H), 2.60 – 2.53 (m, 2H), 1.95 (s, 3H); ¹³C NMR (151 MHz, CDCl₃) δ 179.94, 178.24, 156.82, 144.14, 128.31, 124.87, 113.74, 61.05, 47.03, 44.72, 28.90, 27.17, 22.82, 8.51; IR (neat, cm⁻¹): 2923, 1637, 1479, 1372, 1276, 1092; ESI+ calculated for [C₁₅H₁₆ClNNaO₃]⁺: 316.07, 318.07, found: 316.08, 318.10.

9-(2-Chloroethyl)-1-hydroxy-7-methoxy-6-methyl-2,3-dihydro-1H-pyrrolo[1,2-a]indole-5,8-dione 4-11b (MTSB-6)



4-11b (MTSB-6) was prepared from **4-D** following Kartika's method.²² **4-D** (5.8 mg, 0.02 mmol) was dissolved in 1 mL dry DCM and was cooled down to 0 °C in an ice bath. Et₃N (7 μL, 0.05 mmol) was then added, and triphosgene (3 mg, 0.01 mmol) was added slowly. The system was kept at 0 °C for another 5 min and was allowed to stir at room temperature for another 2 h. The reaction was quenched by saturated NaHCO₃ and extracted with dichloromethane. The organic phase was combined, dried over Na₂SO₄ and concentrated in vacuum. The residue was purified by column chromatography to give **4-11b (MTSB-6)** in 61% yield. The yield based on recovered starting material is 81%. ¹H NMR (400 MHz, CDCl₃) δ 5.23 (dd, *J* = 6.6, 2.2 Hz, 1H), 4.42 – 4.22 (m, 2H), 3.99 (s, 3H), 3.88 (dd, *J* = 6.9, 5.3 Hz, 2H), 3.33 (dt, *J* = 14.4, 5.3 Hz, 1H), 3.09 (dt, *J* = 14.3, 6.8 Hz, 1H), 2.80 (dtd, *J* = 14.4, 8.3, 6.4 Hz, 1H), 2.53 (ddt, *J* = 13.6, 7.1, 3.0 Hz, 1H), 2.24 (s, 1H), 1.96 (s, 3H); ¹³C NMR (126 MHz, CDCl₃) δ 179.77, 178.79, 157.24, 144.34, 128.59, 126.76, 124.64, 114.94, 65.93, 61.15, 45.53, 44.95, 37.93, 28.48, 8.55; IR (neat, cm⁻¹): 2926, 2855, 1642, 1484, 1373, 1318, 1229, 1153, 1096; ESI+ calculated for [C₁₅H₁₆ClNNaO₄]⁺: 332.07, 334.06, found: 332.09, 334.09.

9-(2-Chloroethyl)-7-methoxy-6-methyl-5,8-dioxo-2,3,5,8-tetrahydro-1H-pyrrolo[1,2-a]indol-1-yl acetate 4-11c (MTSB-7)



To **4-11b (MTSB-6)** (3.1 mg, 0.01 mmol) in 1 mL dry CH_2Cl_2 was added pyridine (2.4 mg, 0.03 mmol). The mixture was then stirred at 0 °C while acetyl chloride (1 μL , 0.015 mmol) was added. The reaction was then allowed to stir in room temperature for 1 h until TLC showed the complete conversion of the starting material. Additional acetyl chloride may be added if the reaction did not show complete conversion after 1 h. The mixture was washed with saturated NaHCO_3 and brine, and dried over Na_2SO_4 . After removing the solvent under reduced pressure, the residue was purified by column chromatography to give **4-11c (MTSB-7)** in 80% yield. ^1H NMR (600 MHz, CDCl_3) δ 6.13 (d, $J = 5.8$ Hz, 1H), 4.39 – 4.28 (m, 2H), 4.00 (s, 3H), 3.84 – 3.73 (m, 2H), 3.25 – 3.12 (m, 2H), 2.56 (dd, $J = 14.3, 6.7$ Hz, 1H), 2.07 (s, 3H), 1.96 (s, 3H); ^{13}C NMR (126 MHz, CDCl_3) δ 179.55, 178.79, 170.27, 157.44, 140.37, 128.39, 127.26, 124.77, 116.57, 67.57, 61.18, 45.43, 44.05, 35.66, 28.29, 21.04, 8.52; IR (neat, cm^{-1}): 2927, 2848, 1742, 1645, 1494, 1372, 1230, 1095; ESI+ calculated for $[\text{C}_{17}\text{H}_{18}\text{ClNNaO}_5]^+$: 374.08, 376.07, found: 374.10, 376.09.

4.3 Gold-Catalyzed Stereoselective Glycosylation Reaction to Access 1,2-*cis* Glycosyl Linkage

4.3.1 Glycosylation: History and Challenges

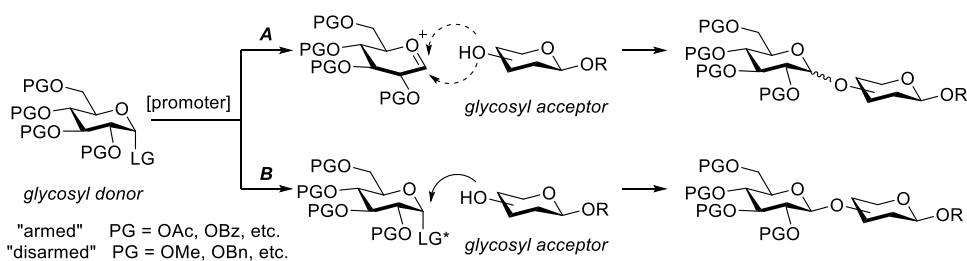
Glycans, including monosaccharides, oligosaccharides, polysaccharides, and their conjugates are important families of molecules that involve in a wide range of biological processes. Great efforts have been spent on unraveling the key role of glycans, particularly oligosaccharides and glycoconjugates, in numerous life activities.²³ Recently, oligosaccharides and glycoconjugates have also shown huge potential in disease diagnosis, immunotherapies, and bioimaging.²⁴

Structurally defined, isomerically pure glycoconjugates and oligosaccharides are critical for the study and application of glycans. Extracting those compounds from natural sources is often unrealistic because of their structural microheterogeneity significantly reduces the efficiency of the isolation process. Chemical synthesis, on the other hand, addresses this problem by providing precise, reproducible, and scalable methods to obtain naturally occurring glycans as well as their unnatural counterparts. To this end, numerous methods for chemical synthesis of glycans have been developed in the past decades.²⁵

The chemical synthesis of glycans mainly focuses on formation of glycosyl bond with the aid of a chemical promoter. As shown in Scheme 52, a donor monosaccharide with a leaving group at the anomeric position, when activated by a promoter, would undergo substitution reaction with a nucleophilic acceptor. However, the seemingly simple pattern obscures the true complexity of the reaction. The leaving group, on one hand, should be sufficiently easy to be expelled by a relatively weak nucleophile (e.g., OH group from a saccharide acceptor); on the other hand, it cannot be so reactive that an oxocarbenium

species forms upon the donor molecule, diminishing the stereoselectivity of the reaction (see: Scheme 52, pathway A). Therefore, the intrinsic properties of the leaving group, along with the method of activation, have a substantial impact on the stereoselectivity of the reaction. Additionally, the protecting groups on the donor also affect the outcome of corresponding glycosylation reactions by promoting or inhibiting the formation of the cationic intermediates, also known as the “armed” and “disarmed” effect.²⁶

Scheme 52. Typical Pattern of Chemical Glycosylation

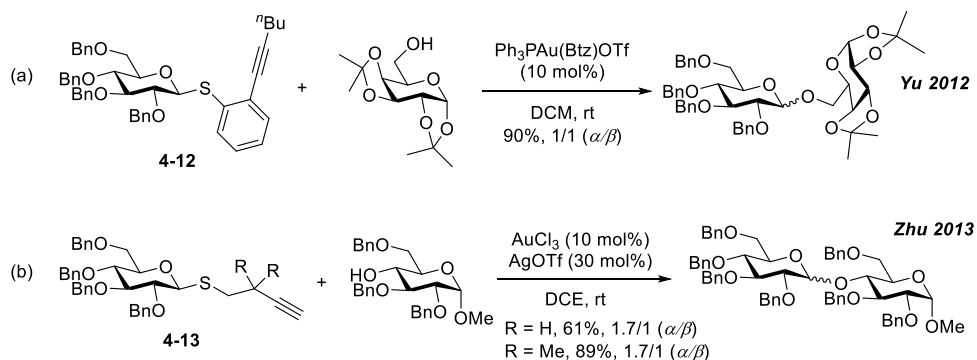


Those effects, often intertwined with influences from properties of the acceptor, solvent effect, and substrate conformation, pose daunting challenges to the stereoselectivity of chemical glycosylation. Although several specific types of glycosyl linkages, for instance, 1,2-*trans*, can be reliably accessed, there are still more types (e.g. 1,2-*cis*) that requires general methods for stereoselective construction.²⁷ Moreover, most glycosyl donor developed need to be activated with stoichiometric amount of chemical promoter, thereby undermining the versatility and scalability of the method.^{25e, 28} To date, there is still a continuous effort to develop novel chemical glycosylation systems that improve upon those criteria to meet the need of an ever demanding glycobiology research community.

4.3.2 Gold-Catalyzed Glycosylation with Thioglycoside Donors: Tackling the Problem

Thioglycosides have been extensively used as donor in glycosylation due to ease of access, relative high stability, and abundance of thiophilic activating reagents.²⁹ Combined with versatile gold catalysis, thioglycoside donors carry great potential in achieving an efficient, selective glycosylation approach that works under a broad range of scenarios. Nevertheless, only limited studies have been done in this field. In 2002, Yu et al first realized a gold(I)-catalyzed *O*-glycosylation reaction with *ortho*-alkynylphenyl thioglycosides **4-12** as the donor (Scheme 53a).³⁰ Although the reaction was very efficient, the author was only able to get 1:1 anomeric mixture of the disaccharide. Shortly afterwards, a similar 1.7:1 selectivity was observed by the Zhu group with aliphatic thioglycosides **4-13** and AuCl₃ catalyst (Scheme 53b).³¹ In addition, the synthetic utilities of those methods are hampered by relatively high catalyst loadings (at least 10 mol% Au salt).

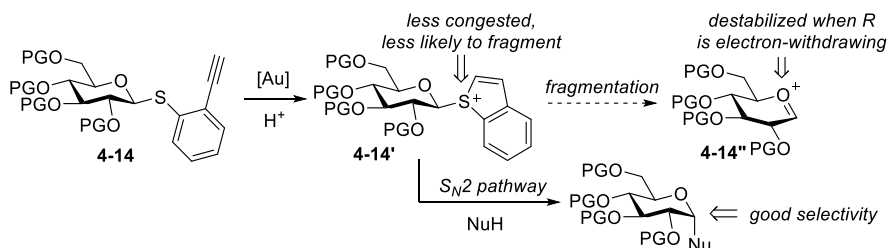
Scheme 53. Previous Studies on Gold-Catalyzed Glycosylation with Thioglycoside Donors



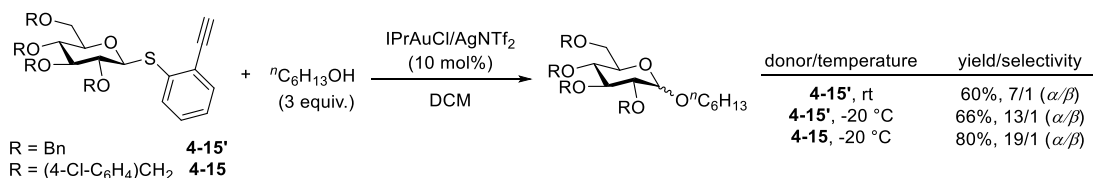
The deficiencies of those preliminary results prompted us to come up with an improved system. We reasoned that the low stereoselectivity is caused by the activated donor, a thiophenium species (e.g. **4-14'** in Figure 7), being so reactive that fragments to give an oxocarbenium species before the acceptor could approach (see: Scheme 52, pathway A).

To address this problem, we designed the donor **4-14** shown in Figure 7. On one hand, introduction of electron-withdrawing effect on the donor's protecting groups should destabilize the oxocarbenium species (i.e. **4-14''**) and suppress its formation; on the other hand, application of terminal alkyne could reduce the steric congestion at the anomeric position of **4-14'**, thereby further discouraging its spontaneous fragmentation. To verify our reasoning, we synthesized donors **4-15** and **4-15'** and tested them side by side with *n*-hexanol as acceptor (Scheme 54). To our delight, a much better 7:1 selectivity was obtained with donor **4-15'**, whose only difference from Yu's donor is the terminal alkyne moiety. With the same donor used, lowering down the reaction temperature enhanced the selectivity to 13:1 while maintaining a similar yield. Finally, an outstanding 19:1 selectivity with good yield was achieved with donor **4-15** bearing electron-withdrawing protecting groups. It should also be noted that the usually difficult-to-access 1,2-*cis* glycosyl linkage is constructed reliably in all cases, signifying the synthetic utility of the method.

Figure 7. Design of a New Thioglycoside Donor for Stereoselective Glycosylation



Scheme 54. Initial Results with the New Thioglycoside Donor



4.3.3 Condition Study, Scope Study, and Future Works

With the encouraging results, we performed a brief condition study with the combination of donor **4-15a** and *n*-hexanol (Table 8). With molecular sieve added to suppress hydrolysis of the donor, we can still maintain high efficiency and stereoselectivity while lowering down the catalyst loading to 5 mol% (Table 8, entry 1). A brief screening of the counterion (Table 8, entries 1-4) revealed that AgNTf₂ provides the best stereoselectivity and excellent yield. Notably, a very poor selectivity was observed when AgOTf was used, indicating that the thiophenium intermediate (see: **4-14'**) is reactive enough to be attacked by the weakly coordinating triflate ion and racemizes. Formation of similar glycosyl triflates has also been reported in other glycosylation methods with various donors.³² Surprisingly, significant solvent effect was observed in the reaction (Table 8, entries 4-6). While the reaction exhibited slight higher efficiency in trifluorotoluene and fluorobenzene, its stereoselectivity saw a significant drop to 7:1 and 12:1, respectively.

To begin our scope study, we tested the gold-catalyzed glycosylation system in synthesizing different glycoconjugates (Table 9). Like *n*-hexanol, benzyl alcohol was converted to corresponding benzyl glycoside **4-16b** in excellent efficiency and stereoselectivity (entry 2). When secondary alcohol was used, a slight drop in yield and selectivity was observed (entries 3, 4), indicating steric hindrance has an impact on the reaction. Nevertheless, *tert*-butyl alcohol was successfully employed with yield and selectivity similar to those of secondary alcohols (entry 5). Benzoic acid is also applicable in the reaction, although with an even lower 10:1 selectivity (entry 6). Despite its similarity to a primary alcohol, *L*-serine-derived acceptor only showed a 3.5:1 selectivity despite a decent 67% yield. We also applied our gold-catalyzed glycosylation in the synthesis of

cholesterol glucosides. To our delight, we were able to obtain the desired product **4-16h** at a decent 63% yield with 5:1 ratio of both anomers, marking a significant improvement to the similar synthesis reported by Yu et al.³⁰

Table 8. Condition Study^a

entry	Additive (5 mol%)	solvent	yield, selectivity (α/β) ^b
1	AgNTf ₂	DCM	84%, 19/1
2	AgOTf	DCM	80%, 0.8/1
3	AgSbF ₆	DCM	90%, 15/1
4	NaBARF	DCM	65%, 16/1
5	NaBARF	C ₆ H ₅ CF ₃	72% ^c , 7/1
6	NaBARF	C ₆ H ₅ F	74%, 12/1

^a Concentration: 0.05M. Reaction was stirred in a cooling bath for 6 hours before being quenched by ⁿBu₄NCl. ^b Combined yield and anomeric ratio determined by NMR with internal references. ^c Yield based on recovered donor.

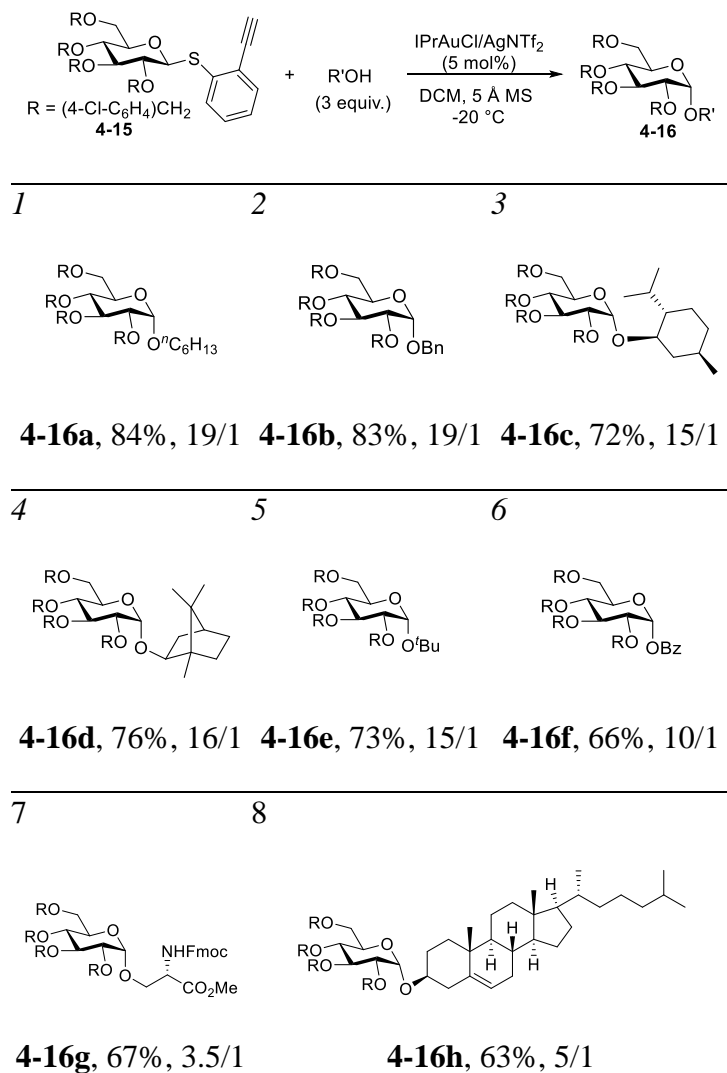
The glycoconjugate synthesis clearly demonstrated that nucleophilicity and steric hindrance of the acceptor play important roles in achieving a stereoselective reaction. Namely, when the proposed S_N2 attack was hampered by a less nucleophilic acceptor, the activated donor proceeds through an alternative pathway and loses the stereospecificity at the anomeric position. With a closer examination of the reaction system, we hypothesized that the said pathway may involve the benzothiophene side product (Finally, we performed a synthesis of disaccharide with our thioglycoside donor and 1,2;3,4-di-*O*-isopropylidene- α -D-galactopyranoside **4-18** (Scheme 56). To our delight, the reaction gave disaccharide **4-19** in a synthetically useful 73% yield based on recovered starting material. Although

only a modest 3:1 stereoselectivity was observed, this unoptimized result marks a two-fold improvement over similar methods reported by Yu³⁰ and Zhu³¹. Our future work in this area will be focused on optimizing the reaction to achieve a general and efficient way to synthesize various disaccharides.

Scheme 55A). As the reaction proceeds, benzothiophene accumulated in the system reacts with the activated donor **4-17** as a nucleophile, causing racemization at the anomeric position. Therefore, the less nucleophilic the acceptor is, the more anomeric racemization would be observed, which is in accordance with the results of stereoelectronically different acceptors in Table 9. Moreover, the stereoselectivity of the reaction saw a sharp decrease when one equivalent of benzothiophene was added (Finally, we performed a synthesis of disaccharide with our thioglycoside donor and 1,2;3,4-di-*O*-isopropylidene- α -D-galactopyranoside **4-18** (Scheme 56). To our delight, the reaction gave disaccharide **4-19** in a synthetically useful 73% yield based on recovered starting material. Although only a modest 3:1 stereoselectivity was observed, this unoptimized result marks a two-fold improvement over similar methods reported by Yu³⁰ and Zhu³¹. Our future work in this area will be focused on optimizing the reaction to achieve a general and efficient way to synthesize various disaccharides.

Scheme 55B). Possible ways of addressing this problem (e.g., altering the electronic effect on the thiophene ring or trapping the benzothiophene with Lewis acid) is still under our exploration.

Table 9. Scope Study in Glycoconjugate Synthesis^a



^a Reactions were stirred in cooling bath for 10 hours. All yields are combined isolated yield.

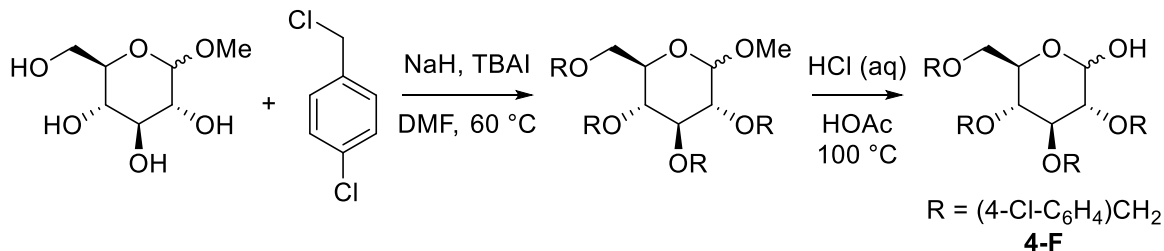
Anomeric ratio was determined by NMR.

Finally, we performed a synthesis of disaccharide with our thioglycoside donor and 1,2;3,4-di-*O*-isopropylidene- α -D-galactopyranoside **4-18** (Scheme 56). To our delight, the reaction gave disaccharide **4-19** in a synthetically useful 73% yield based on recovered starting material. Although only a modest 3:1 stereoselectivity was observed, this unoptimized result marks a two-fold improvement over similar methods reported by Yu³⁰ and Zhu³¹.

achieving a reliable, efficient, and selective approach to construct 1,2-*cis* linkage in glycoconjugates and oligosaccharides.

4.3.5 Experimental Details

Preparation of 2,3,4,6-tetra-*O*-(4-chlorobenzyl)-*D*-glucopyranose (**4-F**)

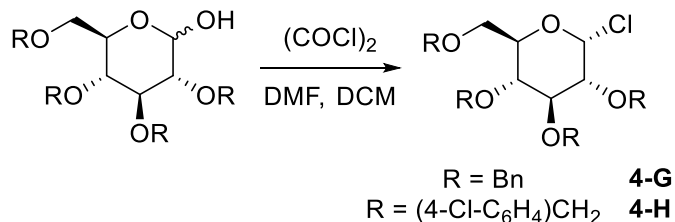


To a cooled (0 °C) mixture of 1-methyl-*D*-glucopyranose (1.94 g, 10 mmol), TBAI (369 mg, 1 mmol), and DMF (25 mL) was added NaH (60% in mineral oil, 2 g, 5 equiv.). The mixture was then stirred vigorously for 20 min, and 4-chlorobenzyl chloride (8 g, 5 equiv.) was added in small portions. The reaction was warmed up to room temperature gradually, heated at 60 °C for 12 hours, and quenched by careful addition of saturated NH₄Cl solution at 0 °C. The crude product was extracted by DCM, washed with water and brine, and concentrated under vacuum.

To the crude product of the first step was added HOAc (50 mL) and HCl (6M, 10 mL), and the mixture was stirred at 100 °C until TLC showed complete transformation of the starting material. The reaction was concentrated under vacuum, dissolved by DCM, washed with saturated NaHCO₃, and dried with MgSO₄. Upon removal of DCM under vacuum, the crude product was purified by silica gel column chromatography to give **4-F** as a colorless oil (4.1 g, 61%). ¹H NMR (not very pure) ¹H NMR (400 MHz, CDCl₃) δ 7.30 – 7.27 (m, 4H), 7.25 – 7.15 (m, 12H), 7.01 (dd, *J* = 8.3, 4.4 Hz, 2H), 5.25 (d, *J* = 3.4 Hz, 1H), 4.93 –

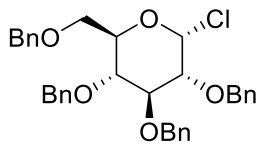
4.77 (m, 2H), 4.76 – 4.62 (m, 6H), 4.58 – 4.51 (m, 1H), 4.42 (d, $J = 12.2$ Hz, 2H), 4.00 (d, $J = 9.9$ Hz, 1H), 3.91 (t, $J = 9.3$ Hz, 1H), 3.70 – 3.48 (m, 6H).

Preparation of Glucopyranosyl Chlorides (4-G and 4-H)



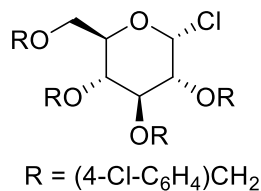
5 mmol of corresponding D-glucopyranose and 10 mmol of oxalyl chloride was mixed in DCM (20 mL) at room temperature, and 5 drops of DMF was added into the solution. Gas evolution was observed immediately, and the reaction was stirred at room temperature for 2 hours. The reaction was then concentrated under vacuum and purified with silica gel column chromatography to give the corresponding glucopyranosyl chlorides as colorless oil.

2,3,4,6-tetra-*O*-benzyl-D-glucopyranosyl chloride (4-G)



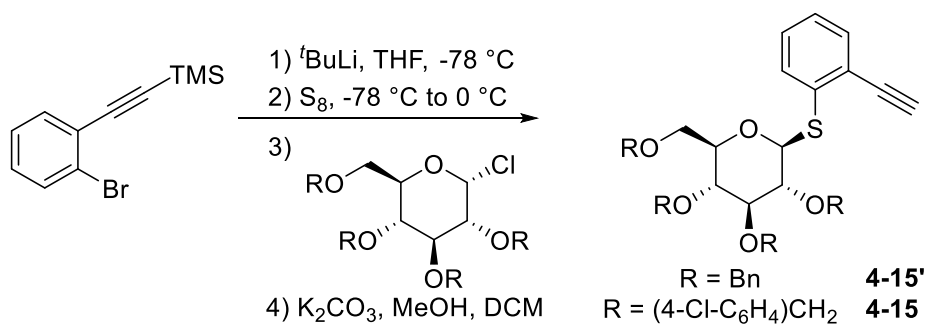
Prepared in 70% yield from 2,3,4,6-tetra-*O*-benzyl-D-glucopyranose. Its NMR data is in accordance with those reported by Takeo et al.³³

2,3,4,6-tetra-*O*-(4-chlorobenzyl)-D-glucopyranosyl chloride (4-H)



Prepared in 59% yield from 2,3,4,6-tetra-*O*-(4-chlorobenzyl)-*D*-glucopyranose. ¹H NMR (400 MHz, CDCl₃) δ 7.34 – 7.20 (m, 10H), 7.17 (d, *J* = 8.3 Hz, 2H), 7.02 (d, *J* = 8.3 Hz, 2H), 6.09 (d, *J* = 3.7 Hz, 1H), 4.86 (d, *J* = 11.3 Hz, 1H), 4.71 (d, *J* = 10.1 Hz, 2H), 4.63 (q, *J* = 11.8 Hz, 2H), 4.54 (d, *J* = 12.3 Hz, 1H), 4.47 – 4.37 (m, 2H), 4.05 (d, *J* = 10.0 Hz, 1H), 3.96 (t, *J* = 9.2 Hz, 1H), 3.7ff5 – 3.57 (m, 4H).

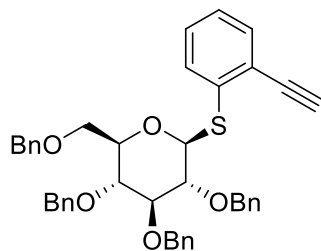
Preparation of Glycosyl Donors (4-15 and 4-15')



2-Bromo-1-(trimethylsilylethynyl)benzene was synthesized quantitatively according to method reported by Ohno Group (OL 2012 326). A solution of 2-bromo-1-(trimethylsilylethynyl)benzene (860 mg, 3.4 mmol) in THF (10 mL) was cooled to -78 °C, and ^tBuLi (1.7 M in hexanes, 4 mL, 6.8 mmol) was added dropwise. The solution was stirred at -78 °C for another 30 minutes, and sulfur (109 mg, 3.4 mmol) was added in one portion at -78 °C. The reaction was then kept at 0 °C for 1 hour and cooled down again to -78 °C before a solution of corresponding glucopyranosyl chloride (2.5 mmol) in THF (5

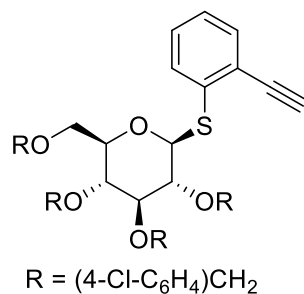
mL) was added in one portion. The reaction was then warmed up to room temperature and stirred for 10 hours or until complete consumption of the glucopyranosyl chloride. The mixture was quenched by water, concentrated under vacuum, dissolved in a mixture of methanol and DCM (1:1, 10 mL in total), added K_2CO_3 (200 mg), and stirred for 2 hours. Upon completion, the mixture was partitioned in DCM and water, extracted by additional DCM, dried with $MgSO_4$, and concentrated under vacuum. Column chromatography with silica gel gave the desired product **4-15** and **4-15'**.

4-15



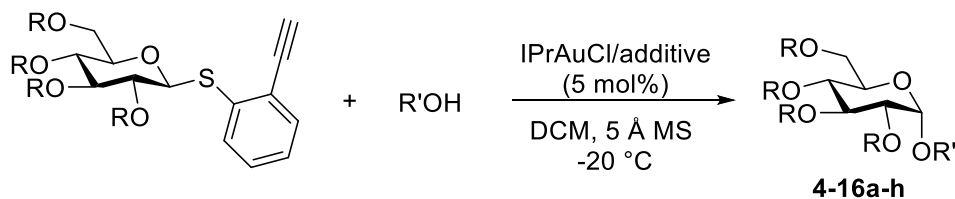
Prepared in 72% overall yield from **4-G**. 1H NMR (400 MHz, $CDCl_3$) δ 7.71 – 7.65 (m, 1H), 7.48 (dd, $J = 5.8, 3.3$ Hz, 1H), 7.45 – 7.39 (m, 2H), 7.36 – 7.25 (m, 12H), 7.23 – 7.18 (m, 2H), 7.18 – 7.11 (m, 2H), 4.95 (dd, $J = 12.9, 10.5$ Hz, 2H), 4.89 – 4.79 (m, 3H), 4.73 (d, $J = 10.0$ Hz, 1H), 4.64 – 4.50 (m, 3H), 3.84 – 3.51 (m, 6H), 3.37 (s, 1H).

4-15'

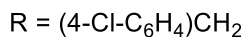
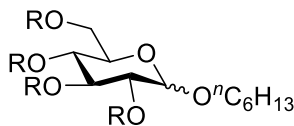


Prepared in 60% overall yield from **4-H**. ¹H NMR (500 MHz, CDCl₃) δ 7.63 – 7.58 (m, 1H), 7.52 – 7.46 (m, 1H), 7.30 – 7.21 (m, 11H), 7.20 – 7.13 (m, 4H), 7.07 (d, *J* = 8.3 Hz, 2H), 4.91 (d, *J* = 10.5 Hz, 1H), 4.81 – 4.68 (m, 4H), 4.61 (d, *J* = 10.5 Hz, 1H), 4.57 – 4.51 (m, 2H), 4.46 (d, *J* = 12.1 Hz, 1H), 3.73 (dd, *J* = 10.9, 1.8 Hz, 1H), 3.69 – 3.48 (m, 5H), 3.36 (s, 1H).

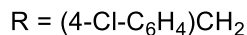
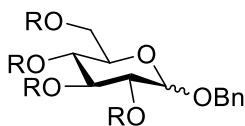
General Procedure for Glycosylation Reaction



To a vial equipped with septum screw cap was added corresponding glycosyl acceptor (3 equiv.), IPrAuCl (5 mol %), additive (5 mol %), 5 Å molecular sieve (10 mg per 0.5 mmol donor), and dry DCM (0.5 mL per 0.5 mmol donor). The mixture was stirred at room temperature for 15 minutes, and was cooled down to -20 °C before a cold solution of glycosyl donor in DCM (0.5 mL per 0.5 mmol donor) was added with syringe. The reaction was stirred at -20 °C until completion, and was then concentrated under vacuum and purified by silica gel column chromatography. Anomeric ratio was determined by ¹H NMR.

4-16a

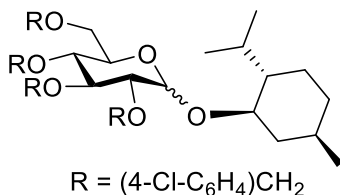
Prepared in 84% yield from **4-15**. α -anomer: $^1\text{H NMR}$ (500 MHz, CDCl_3) δ 7.30 – 7.21 (m, 12H), 7.19 (d, $J = 8.4$ Hz, 2H), 7.01 (d, $J = 8.3$ Hz, 2H), 4.88 (d, $J = 11.4$ Hz, 1H), 4.79 (d, $J = 3.6$ Hz, 1H), 4.70 (d, $J = 11.1$ Hz, 2H), 4.68 – 4.54 (m, 3H), 4.40 (dd, $J = 11.8, 2.9$ Hz, 2H), 3.92 (t, $J = 9.3$ Hz, 1H), 3.75 (dd, $J = 10.7, 2.6$ Hz, 1H), 3.70 – 3.53 (m, 4H), 3.50 (dd, $J = 9.6, 3.6$ Hz, 1H), 3.41 (dt, $J = 9.8, 6.7$ Hz, 1H), 1.62 (p, $J = 6.9$ Hz, 2H), 1.38 – 1.25 (m, 6H), 0.89 (t, $J = 6.9$ Hz, 3H). β -anomer: $^1\text{H NMR}$ (500 MHz, CDCl_3) δ 7.30 – 7.18 (m, 12H), 7.13 (d, $J = 8.4$ Hz, 2H), 7.03 (d, $J = 8.3$ Hz, 2H), 4.89 (d, $J = 11.4$ Hz, 1H), 4.80 (d, $J = 11.4$ Hz, 1H), 4.71 – 4.54 (m, 4H), 4.47 (dd, $J = 14.3, 11.9$ Hz, 2H), 4.35 (d, $J = 7.8$ Hz, 1H), 3.93 (dt, $J = 9.4, 6.5$ Hz, 1H), 3.66 (qd, $J = 10.8, 3.2$ Hz, 2H), 3.58 – 3.46 (m, 3H), 3.44 – 3.33 (m, 2H), 1.62 (dtd, $J = 9.5, 6.6, 3.2$ Hz, 2H), 1.40 – 1.20 (m, 6H), 0.88 (t, $J = 6.9$ Hz, 3H).

4-16b

Prepared in 83% yield from **4-15**. $^1\text{H NMR}$ (α -anomer) (500 MHz, CDCl_3) δ 7.42 – 7.09 (m, 19H), 7.15 (d, $J = 8.3$ Hz, 2H), 7.02 (d, $J = 8.3$ Hz, 2H), 4.93 – 4.84 (m, 2H), 4.72 (dd, $J = 11.6, 2.7$ Hz, 3H), 4.56 (t, $J = 11.8$ Hz, 3H), 4.48 (d, $J = 12.1$ Hz, 1H), 4.44 – 4.38 (m,

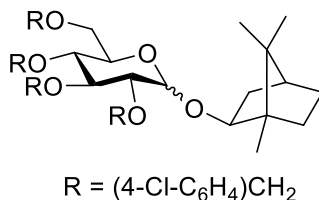
2H), 3.98 (t, $J = 9.3$ Hz, 1H), 3.79 (d, $J = 9.6$ Hz, 1H), 3.67 (dd, $J = 10.6, 3.3$ Hz, 1H), 3.63 – 3.47 (m, 3H).

4-16c



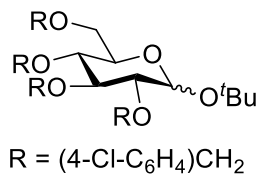
Prepared in 72% yield from **4-15**. ^1H NMR (α -anomer) (500 MHz, CDCl_3) δ 7.29 – 7.18 (m, 12H), 7.15 (d, $J = 8.5$ Hz, 2H), 7.01 (d, $J = 8.4$ Hz, 2H), 5.02 (d, $J = 3.6$ Hz, 1H), 4.86 (d, $J = 11.4$ Hz, 1H), 4.71 (d, $J = 10.8$ Hz, 2H), 4.66 – 4.55 (m, 3H), 4.43 – 4.35 (m, 2H), 4.00 – 3.89 (m, 2H), 3.70 (dd, $J = 10.5, 3.7$ Hz, 1H), 3.62 – 3.52 (m, 2H), 3.47 (dd, $J = 9.7, 3.6$ Hz, 1H), 3.33 (td, $J = 10.6, 4.4$ Hz, 1H), 2.36 (ddd, $J = 11.6, 6.9, 3.4$ Hz, 1H), 2.12 (d, $J = 12.4$ Hz, 1H), 1.68 – 1.56 (m, 2H), 1.41 – 1.28 (m, 3H), 1.09 – 0.90 (m, 2H), 0.84 (q, $J = 7.1, 6.6$ Hz, 6H), 0.69 (d, $J = 6.9$ Hz, 2H).

4-16d



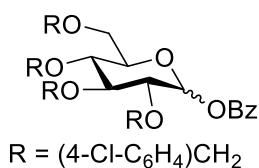
Prepared in 76% NMR yield from **4-15**. Purification not successful, characteristic peaks for both anomers are shown. ^1H NMR (400 MHz, CDCl_3) δ 4.94 (d, $J = 3.4$ Hz, 1H, α -anomer), 4.35 (d, $J = 7.8$ Hz, 1H, β -anomer).

4-16e



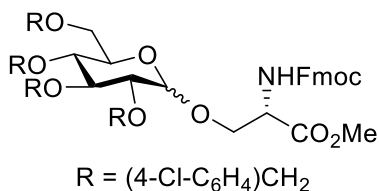
Prepared in 73% NMR yield from **4-15**. Purification not successful, characteristic peaks for both anomers are shown. ¹H NMR (500 MHz, CDCl₃) δ 5.16 (d *J* = 3.4 Hz, 1H, α-anomer), 1.31 (s, 9H, β-anomer), 1.27 (s, 9H, α-anomer).

4-16f



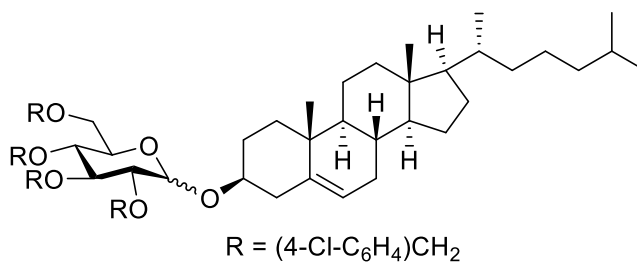
Prepared in 66% yield from **4-15**. ¹H NMR (α-anomer) (500 MHz, CDCl₃) δ 8.07 – 8.04 (m, 2H), 7.61 (t, *J* = 7.4 Hz, 1H), 7.48 (t, *J* = 7.8 Hz, 2H), 7.32 – 7.16 (m, 14H), 7.04 (d, *J* = 8.4 Hz, 2H), 6.61 (d, *J* = 3.5 Hz, 1H), 4.88 (d, *J* = 11.4 Hz, 1H), 4.78 – 4.67 (m, 4H), 4.57 (d, *J* = 11.9 Hz, 2H), 4.48 (d, *J* = 11.0 Hz, 1H), 4.42 (d, *J* = 12.3 Hz, 1H), 3.97 (q, *J* = 10.8, 10.1 Hz, 2H), 3.74 (ddd, *J* = 11.1, 8.1, 4.0 Hz, 3H), 3.61 (d, *J* = 1.9 Hz, 1H).

4-16g



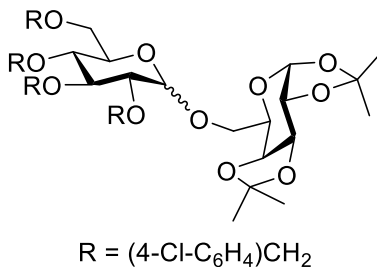
Prepared in 67% yield from **4-15**. Separation of anomeric mixture failed, characteristic peaks for both anomers reported. ^1H NMR (600 MHz, CDCl_3) δ 5.97 (d, $J = 8.5$ Hz, 1H, α -anomer), 5.72 (d, $J = 8.0$ Hz, 1H, β -anomer).

4-16h



Prepared in 63% NMR yield from **4-15**. Purification not successful, crude NMR with characteristic peaks for both anomers are shown. ^1H NMR (500 MHz, CDCl_3) δ 5.36 – 5.32 (m, 1H, α -anomer), 5.31 – 5.28 (m, 1H, β -anomer), 5.06 (d, $J = 3.6$ Hz, 1H, α -anomer).

4-19



Not purified, characteristic peaks for both anomers are shown. ^1H NMR (500 MHz, CDCl_3) δ 5.54 (d, $J = 5.0$ Hz, 1H, β -anomer), 5.51 (d, $J = 5.0$ Hz, 1H, α -anomer).

4.4 References

1. Wakaki, S.; Marumo, H.; Tomioka, K.; Shimizu, G.; Kato, E.; Kamada, H.; Kudo, S.; Fujimoto, Y., *Antibiot. Chemother.* **1958**, *8*, 228-40.

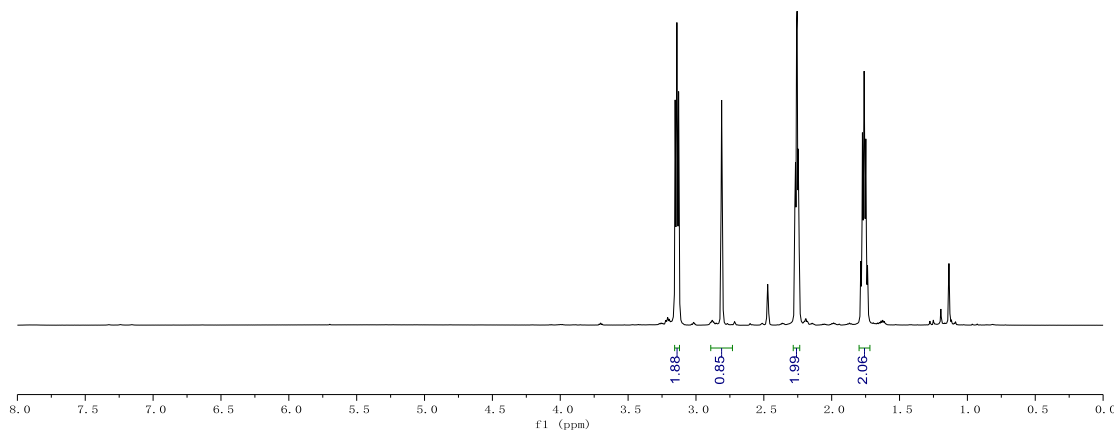
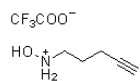
2. (a) Galm, U.; Hager, M. H.; Van Lanen, S. G.; Ju, J. H.; Thorson, J. S.; Shen, B., *Chemical Reviews* **2005**, *105* (2), 739-758; (b) Tomasz, M., *Chem. & Biol.* **1995**, *2* (9), 575-579; (c) Crooke, S. T.; Bradner, W. T., *Cancer Treat. Rev.* **1976**, *3* (3), 121-139.
3. Bradner, W. T., *Cancer Treat. Rev.* **2001**, *27* (1), 35-50.
4. Gourevitch, A.; Chertow, B.; Lein, J. Mitomycin recovery. US3042582, 1962.
5. (a) Bradner, W. T.; Rose, W. C.; Schurig, J. E.; Florczyk, A. P.; Huftalen, J. B.; Catino, J. J., *Cancer Res.* **1985**, *45* (12 Part 1), 6475-6481; (b) Doyle, T. W.; Vyas, D. M., *Cancer Treat. Rev.* **1990**, *17* (2-3), 127-131; (c) Masters, J. R. W.; Know, R. J.; Hartley, J. A.; Kelland, L. R.; Hendriks, H. R.; Connors, T., *Biochem. Pharm.* **1997**, *53* (3), 279-285.
6. Arai, H.; Kanda, Y.; Ashizawa, T.; Morimoto, M.; Gomi, K.; Kono, M.; Kasai, M., *J. Med. Chem.* **1994**, *37* (12), 1794-1804.
7. Fujimoto, Y.; Nakano, K.; Urakawa, C. 1a-Acylmitomycin C compounds. DE2459616A1, 1975.
8. Andrez, J. C., *Beilstein J. Org. Chem.* **2009**, *5*, 1-36.
9. (a) Fukuyama, T.; Nakatsubo, F.; Cocuzza, A. J.; Kishi, Y., *Tetrahedron Letters* **1977**, (49), 4295-4298; (b) Fukuyama, T.; Yang, L. H., *Journal of the American Chemical Society* **1987**, *109* (25), 7881-7882; (c) Benbow, J. W.; McClure, K. F.; Danishefsky, S. J., *Journal of the American Chemical Society* **1993**, *115* (26), 12305-12314; (d) Wang, Z.; Jimenez, L. S., *Tetrahedron Letters* **1996**, *37* (34), 6049-6052.
10. (a) Beall, H.; Winski, S., *Frontiers Biosci.* **2000**, *5*, d639-648; (b) Loadman, P. M.; Bibby, M. C.; Phillips, R. M., *Brit. J. Pharm.* **2002**, *137* (5), 701-709.
11. Li, G.; Huang, X.; Zhang, L., *Angewandte Chemie International Edition* **2008**, *47* (2), 346-349.
12. Liu, L.; Wang, Y.; Zhang, L., *Organic Letters* **2012**, *14* (14), 3736-3739.
13. Maliepaard, M.; de Mol, N. J.; Janssen, L. H. M.; Hoogvliet, J. C.; van der Neut, W.; Verboom, W.; Reinhoudt, D. N., *J. Med. Chem.* **1993**, *36* (15), 2091-2097.
14. Igarashi, Y.; Futamata, K.; Fujita, T.; Sekine, A.; Senda, H.; Naoki, H.; Furumai, T., *The Journal of Antibiotics* **2003**, *56* (2), 107-113.
15. Allen, G. R.; Poletto, J. F.; Weiss, M. J., *Journal of the American Chemical Society* **1964**, *86* (18), 3877-3878.
16. (a) Brothman, A. R.; Lesho, L. J.; Somers, K. D.; Jr., J. L. W.; Merchant, D. J., *Int. J. Chem.* **1989**, *44*, 898-903; (b) Bello, D.; Webber, M. M.; Kleinman, H. K.; Waringer, D. D.; Rhim, J. S., *Carcinogenesis* **1997**, *18*, 1215-1223.
17. Dusre, L.; Rajagopalan, S.; Eliot, H. M.; Covey, J. M.; Sinha, B. K., *Cancer Res.* **1990**, *50*, 648-652.
18. Parrish, J. P.; Kastrinsky, D. B.; Wolkenberg, S. E.; Igarashi, Y.; Boger, D. L., *Journal of the American Chemical Society* **2003**, *125* (36), 10971-10976.
19. Boger, D. L.; Johnson, D. S., *Proc. Nat. Acad. Sci.* **1995**, *92* (9), 3642-3649.
20. Kim, J.-I.; Choi, H.-J.; Lee, J.-S., *Journal of Applied Biological Chemistry* **2013**, *56* (1), 49-51.
21. Lall, N.; Henley-Smith, C. J.; De Canha, M. N.; Oosthuizen, C. B.; Berrington, D., *International Journal of Microbiology* **2013**, *2013*, 5.
22. Ayala, C. E.; Villalpando, A.; Nguyen, A. L.; McCandless, G. T.; Kartika, R., *Organic Letters* **2012**, *14* (14), 3676-3679.
23. (a) Rademacher, T.; Parekh, R.; Dwek, R., *Annual review of biochemistry* **1988**, *57* (1), 785-838; (b) Paulson, J. C., *Trends in biochemical sciences* **1989**, *14* (7), 272-276; (c) Kobata, A., *The FEBS Journal* **1992**, *209* (2), 483-501; (d) Varki, A., *Glycobiology* **1993**, *3* (2), 97-130; (e) Varki, A.; Marth, J. In *Oligosaccharides in vertebrate development*, Seminars in developmental Biology, Elsevier: 1995; pp 127-138; (f) Ohtsubo, K.; Marth, J. D., *Cell* **2006**, *126* (5), 855-867.

24. (a) Dube, D. H.; Bertozzi, C. R., *Nat Rev Drug Discov* **2005**, *4* (6), 477-488; (b) Nahálka, J.; Shao, J.; Gemeiner, P., *Biotechnology and Applied Biochemistry* **2007**, *46* (1), 1-12; (c) Niederhafner, P.; Reiniš, M.; Šebestík, J.; Ježek, J., *Journal of Peptide Science* **2008**, *14* (5), 556-587; (d) Oppenheimer, S. B.; Alvarez, M.; Nnoli, J., *Acta Histochemica* **2008**, *110* (1), 6-13; (e) Fukase, K.; Tanaka, K., *Current Opinion in Chemical Biology* **2012**, *16* (5), 614-621; (f) Ulrich, S.; Dumy, P.; Boturyn, D.; Renaudet, O., *Journal of Drug Delivery Science and Technology* **2013**, *23* (1), 5-16.
25. (a) Galonic, D. P.; Gin, D. Y., *Nature* **2007**, *446* (7139), 1000-1007; (b) Seeberger, P. H.; Werz, D. B., *Nature* **2007**, *446* (7139), 1046-1051; (c) Bernardes, G. J. L.; Castagner, B.; Seeberger, P. H., *ACS Chemical Biology* **2009**, *4* (9), 703-713; (d) Boltje, T. J.; Buskas, T.; Boons, G.-J., *Nat Chem* **2009**, *1* (8), 611-622; (e) Zhu, X.; Schmidt, R. R., *Angewandte Chemie International Edition* **2009**, *48* (11), 1900-1934; (f) Kiessling, L. L.; Splain, R. A., *Annual Review of Biochemistry* **2010**, *79* (1), 619-653.
26. Mootoo, D. R.; Konradsson, P.; Udodong, U.; Fraser-Reid, B., *Journal of the American Chemical Society* **1988**, *110* (16), 5583-5584.
27. (a) Kong, F., *Carbohydrate Research* **2007**, *342* (3), 345-373; (b) Shino, M.; Yukishige, I., *Current Bioactive Compounds* **2008**, *4* (4), 258-281; (c) Nigudkar, S. S.; Demchenko, A. V., *Chemical Science* **2015**, *6* (5), 2687-2704.
28. Wang, L.-X.; Davis, B. G., *Chemical Science* **2013**, *4* (9), 3381-3394.
29. Levy, D. E.; Fügedi, P., *The Organic Chemistry of Sugars*. CRC Press: 2005.
30. Yang, F.; Wang, Q.; Yu, B., *Tetrahedron Letters* **2012**, *53* (39), 5231-5234.
31. Adhikari, S.; Li, X.; Zhu, J., *Journal of Carbohydrate Chemistry* **2013**, *32* (5-6), 336-359.
32. (a) Crich, D.; Smith, M., *Journal of the American Chemical Society* **2001**, *123* (37), 9015-9020; (b) Walvoort, M. T. C.; van der Marel, G. A.; Overkleeft, H. S.; Codee, J. D. C., *Chemical Science* **2013**, *4* (3), 897-906; (c) Fascione, M. A.; Brabham, R.; Turnbull, W. B., *Chemistry – A European Journal* **2016**, *22* (12), 3916-3928.
33. Takeo, K.; Nakagen, M.; Teramoto, Y.; Nitta, Y., *Carbohydrate Research* **1990**, *201* (2), 261-275.

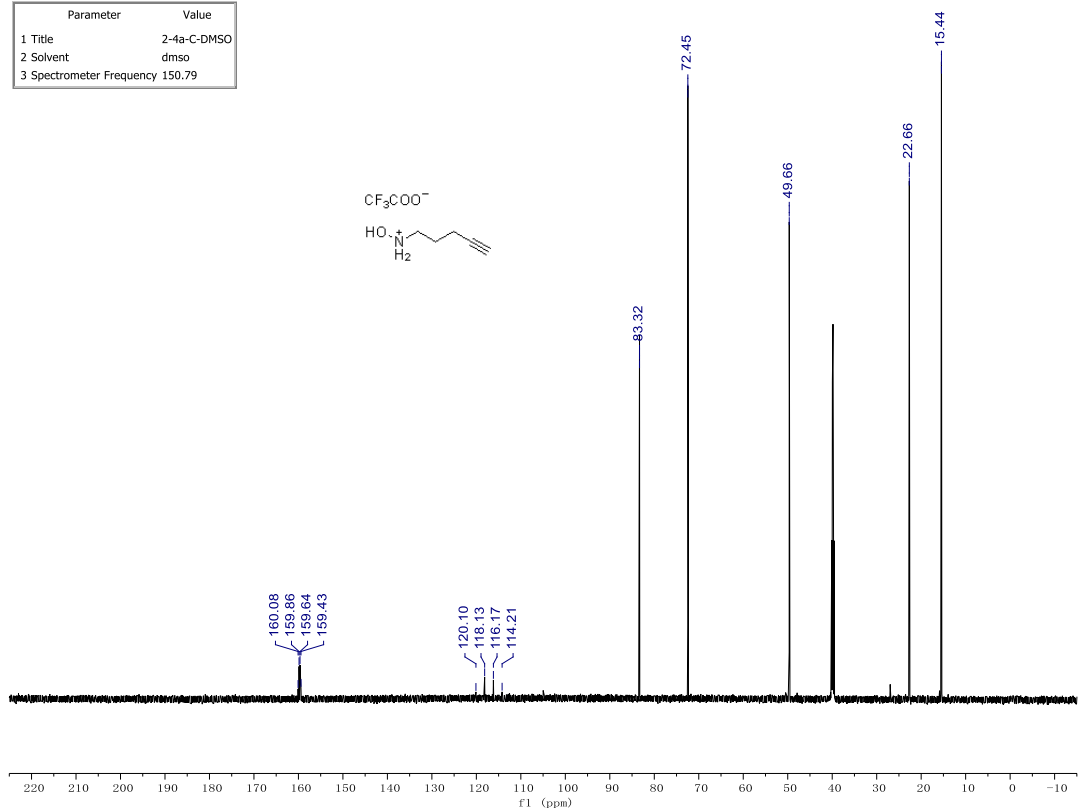
Appendix: NMR Spectra for Selected Compounds

NMR Spectra for Compounds in Chapter 2

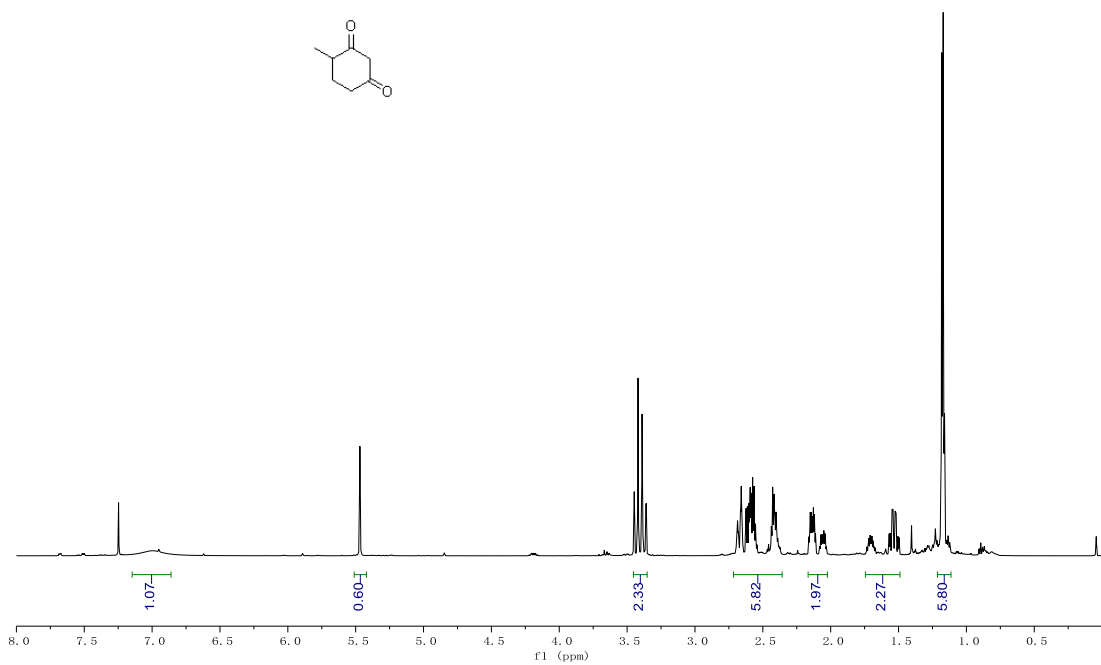
Parameter	Value
1 Title	2-4a-H-DMSO
2 Solvent	dmsd
3 Spectrometer Frequency	599.64



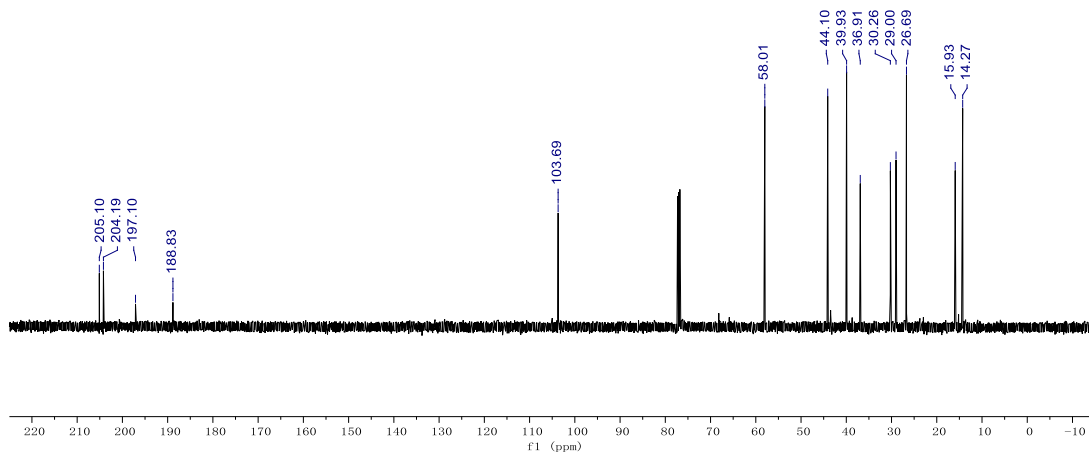
Parameter	Value
1 Title	2-4a-C-DMSO
2 Solvent	dmsO
3 Spectrometer Frequency	150.79



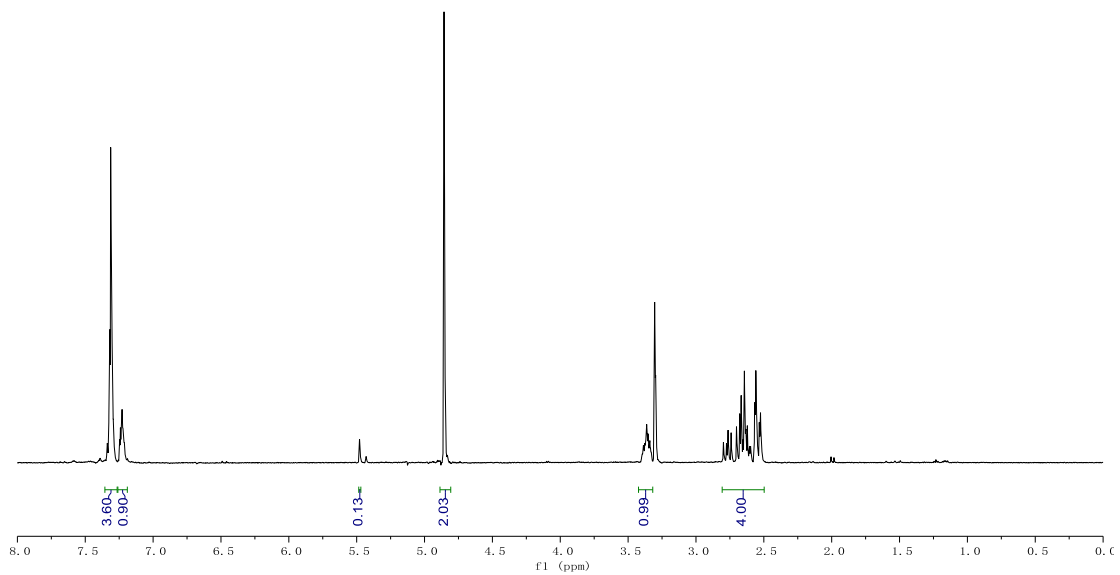
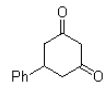
Parameter	Value
1 Title	2-3c-H
2 Solvent	cdcl3
3 Spectrometer Frequency	599.64



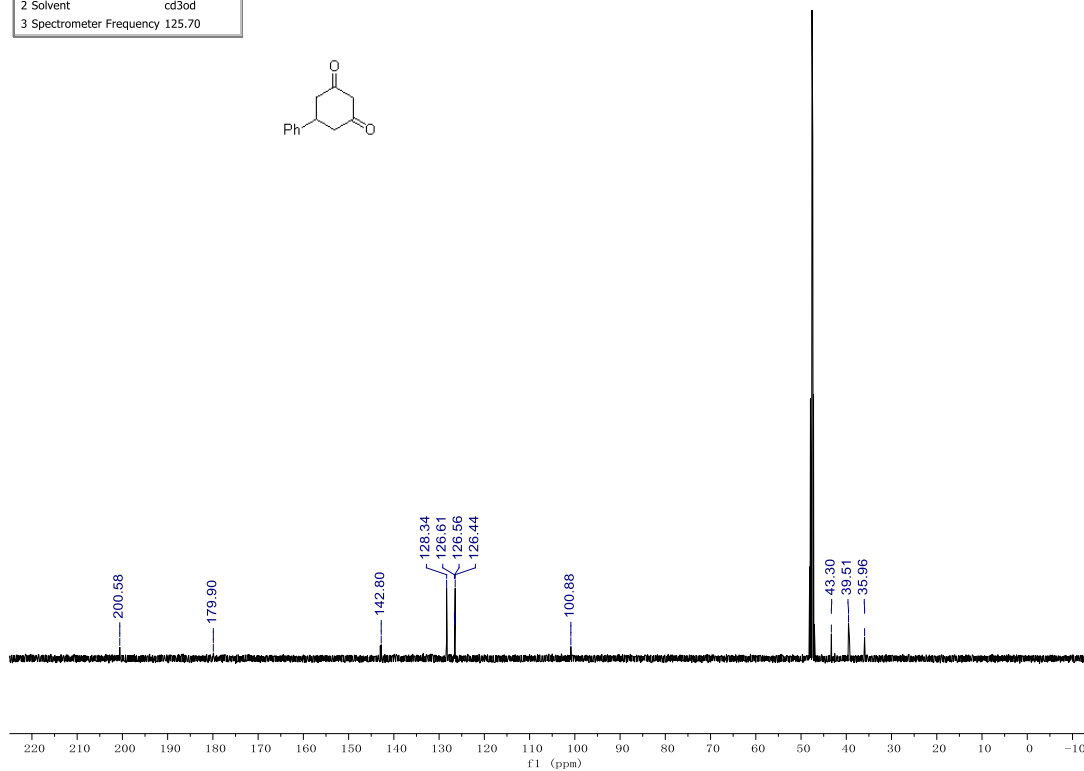
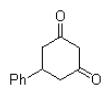
Parameter	Value
1 Title	2-3c-C
2 Solvent	CDCl3
3 Spectrometer Frequency	125.70



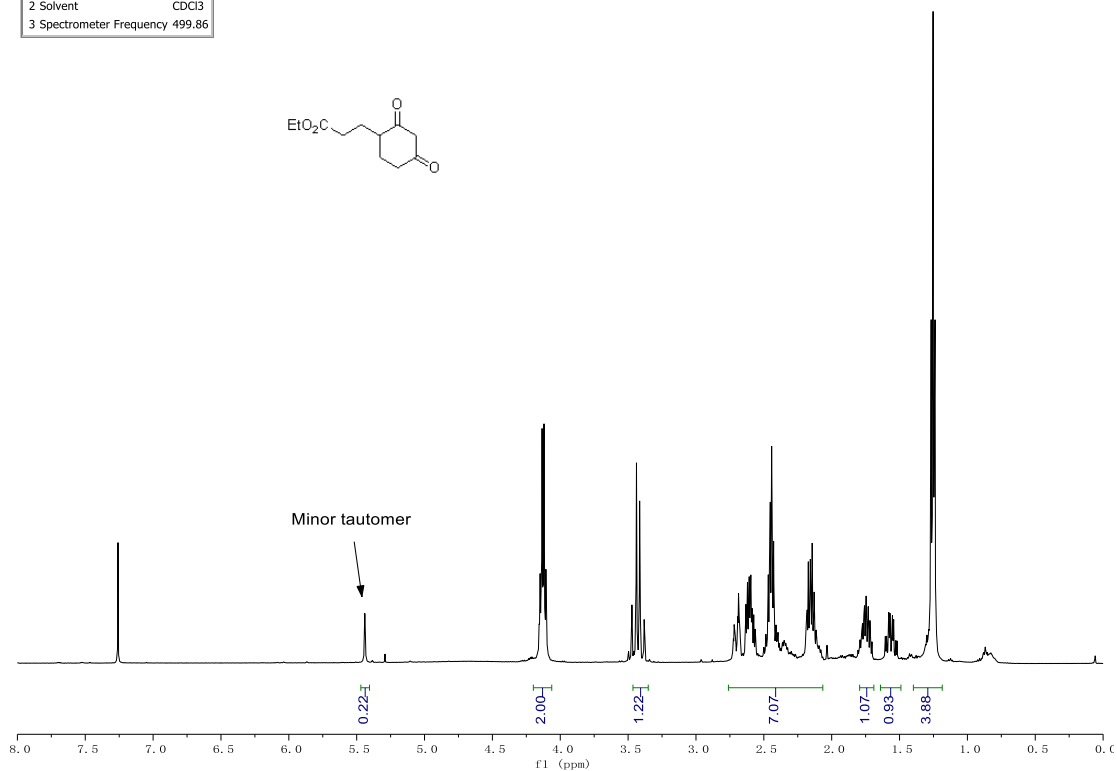
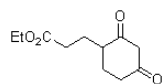
Parameter	Value
1 Title	2-3e-H_MeOH
2 Solvent	cd3od
3 Spectrometer Frequency	499.86



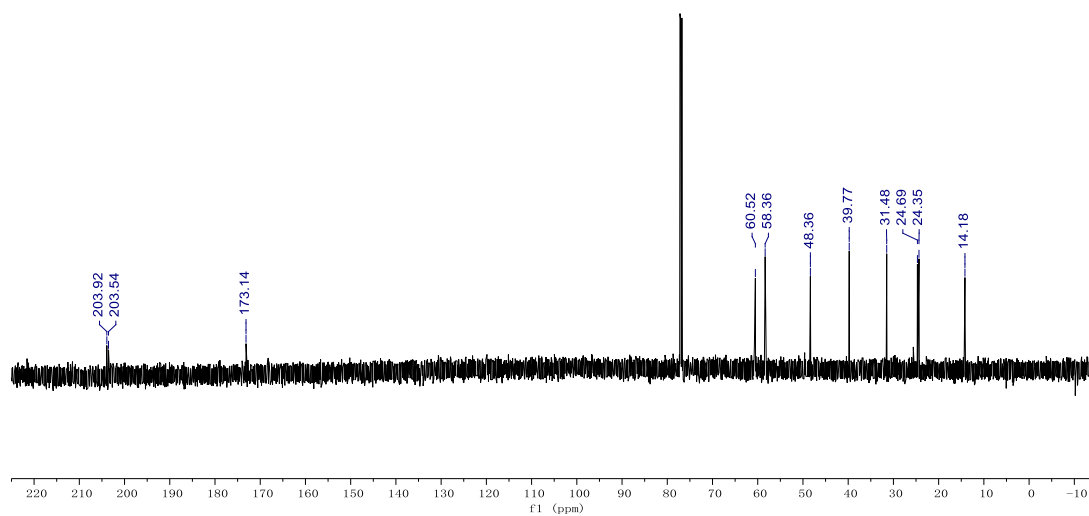
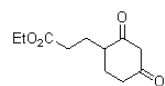
Parameter	Value
1 Title	2-3e-C ₂ MeOH
2 Solvent	cd3od
3 Spectrometer Frequency	125.70



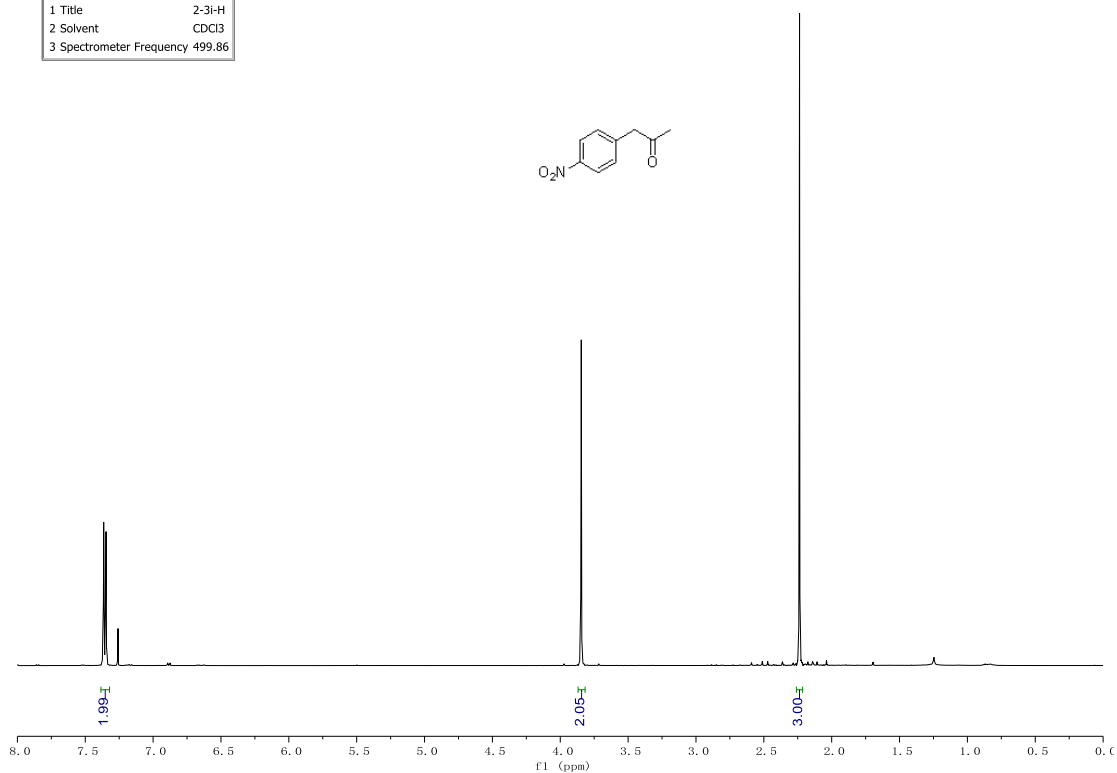
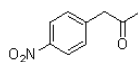
Parameter	Value
1 Title	2-3f-H
2 Solvent	CDCl ₃
3 Spectrometer Frequency	499.86



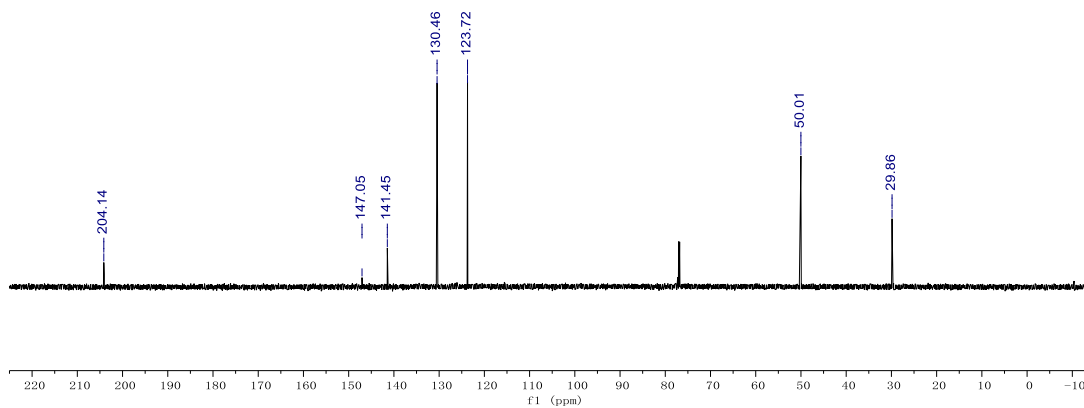
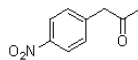
Parameter	Value
1 Title	2-3f-C
2 Solvent	cdcl3
3 Spectrometer Frequency	150.79



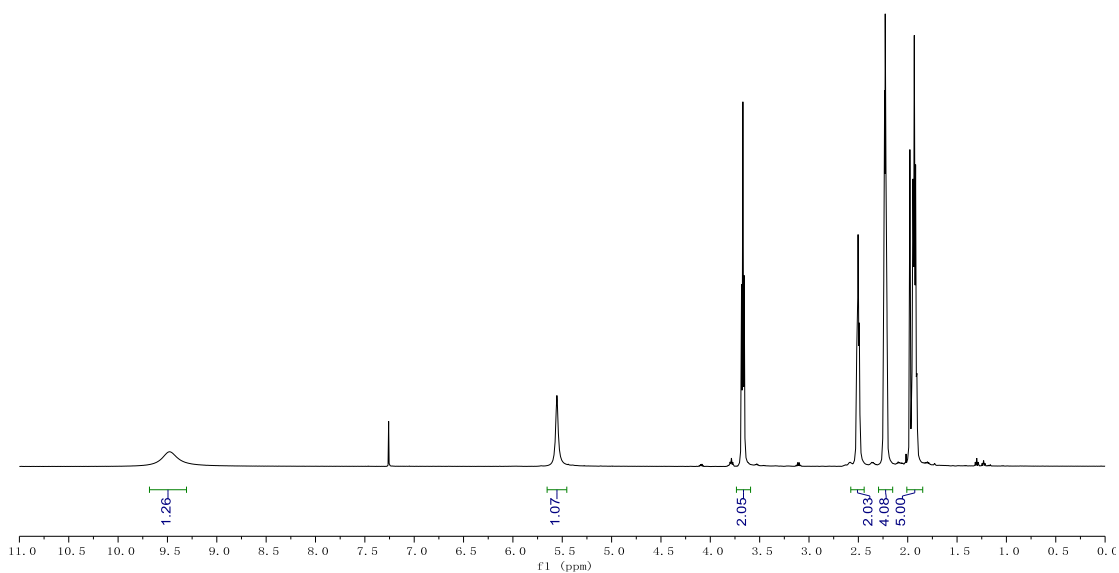
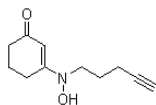
Parameter	Value
1 Title	2-3f-H
2 Solvent	CDCl3
3 Spectrometer Frequency	499.86



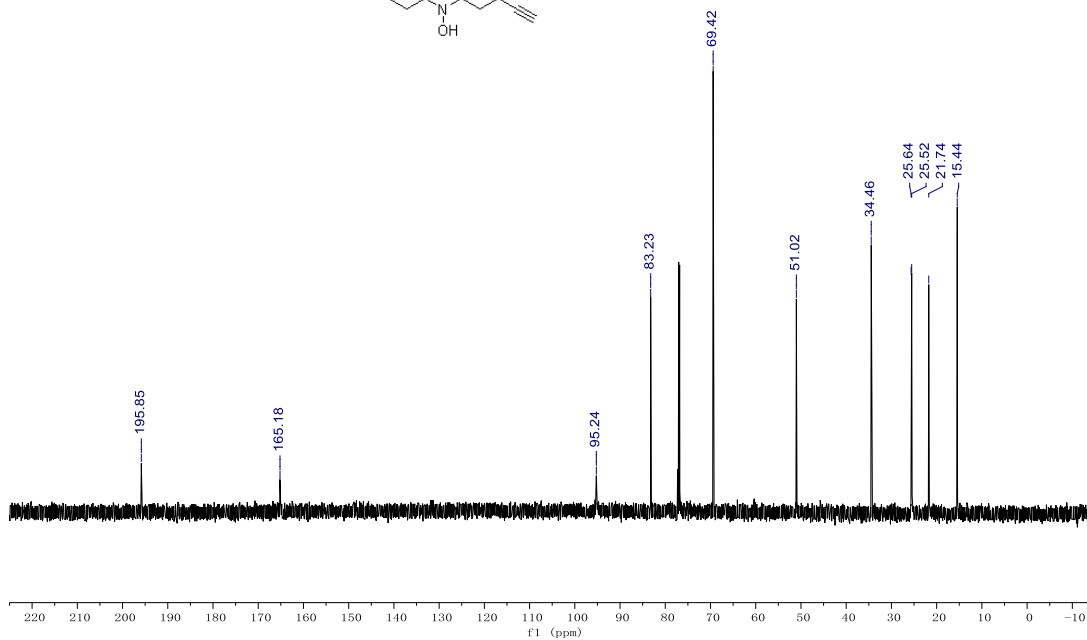
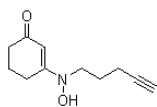
Parameter	Value
1 Title	2-3i-C
2 Solvent	cdcl3
3 Spectrometer Frequency	150.79



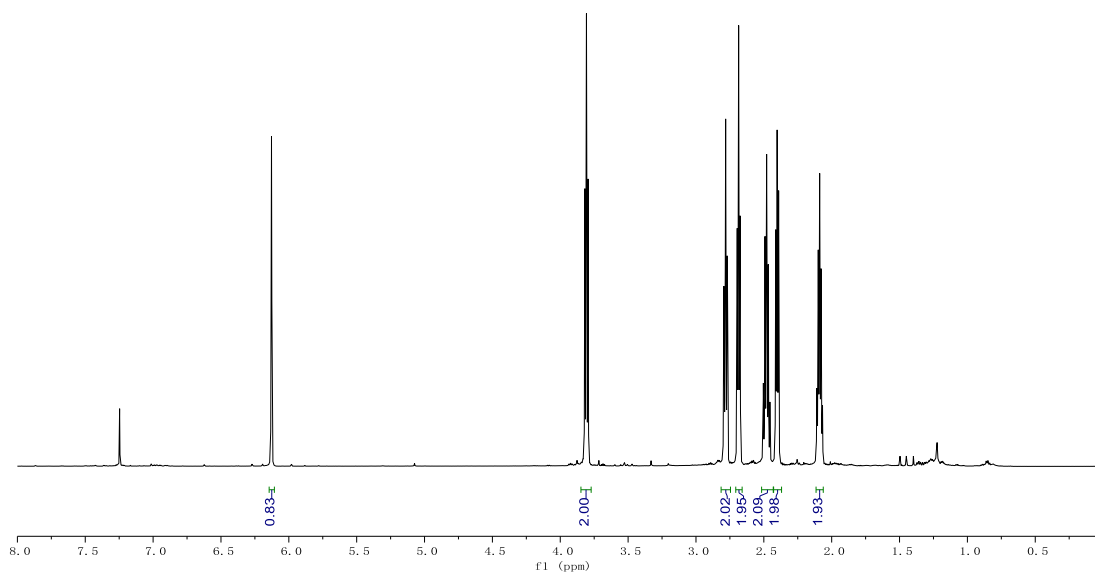
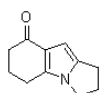
Parameter	Value
1 Title	2-5a-H
2 Solvent	CDCl3
3 Spectrometer Frequency	499.86



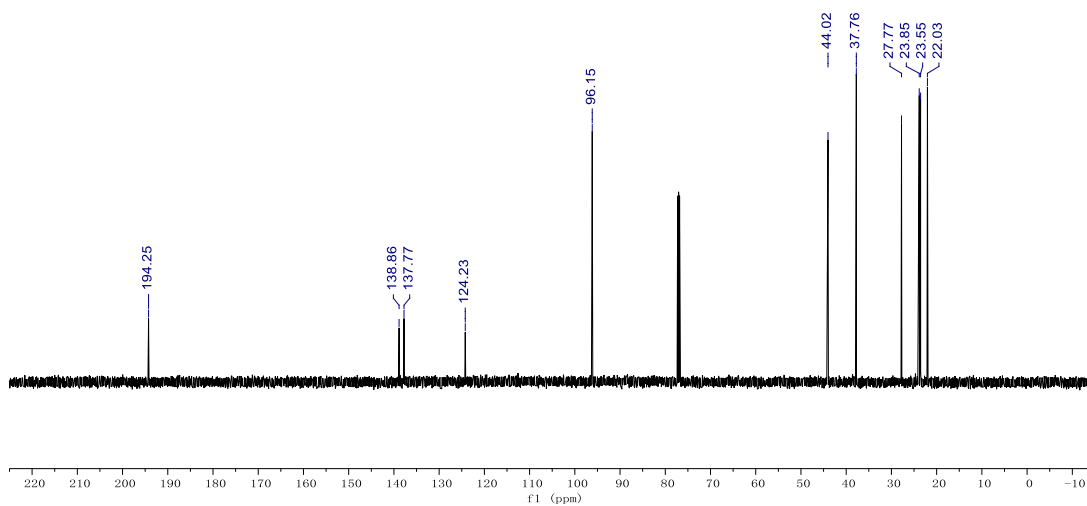
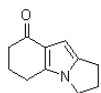
Parameter	Value
1 Title	2-5a-C
2 Solvent	cdcl3
3 Spectrometer Frequency	150.79



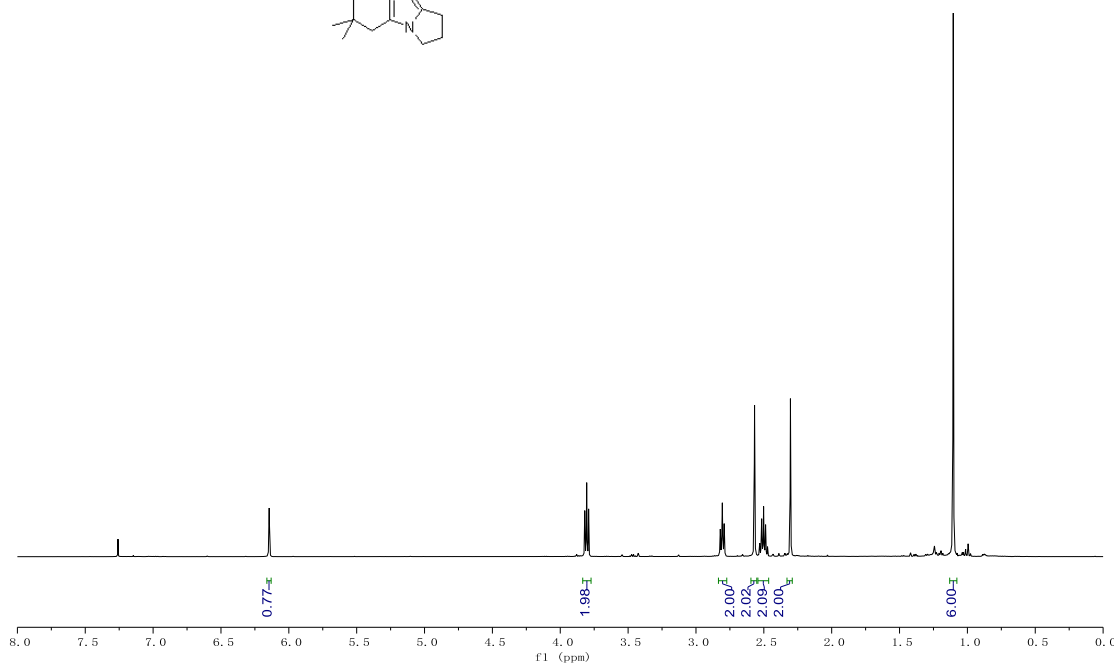
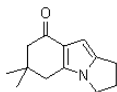
Parameter	Value
1 Title	2-9a-H
2 Solvent	cdcl3
3 Spectrometer Frequency	599.64



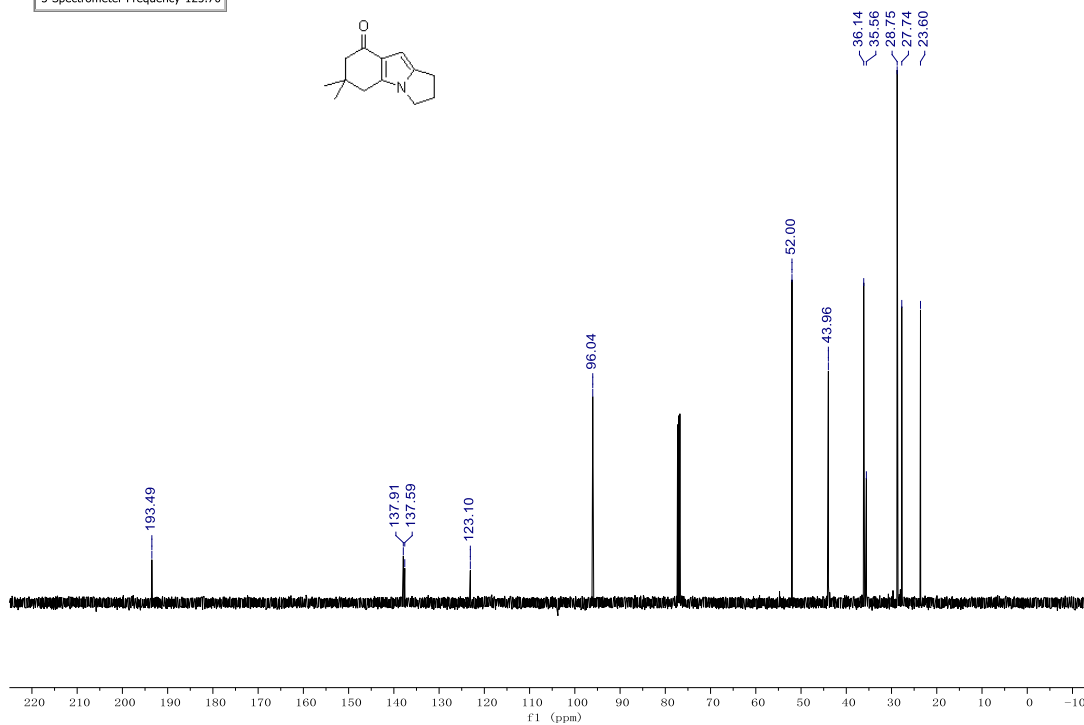
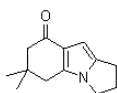
Parameter	Value
1 Title	2-9a-C
2 Solvent	cdcl3
3 Spectrometer Frequency	150.79



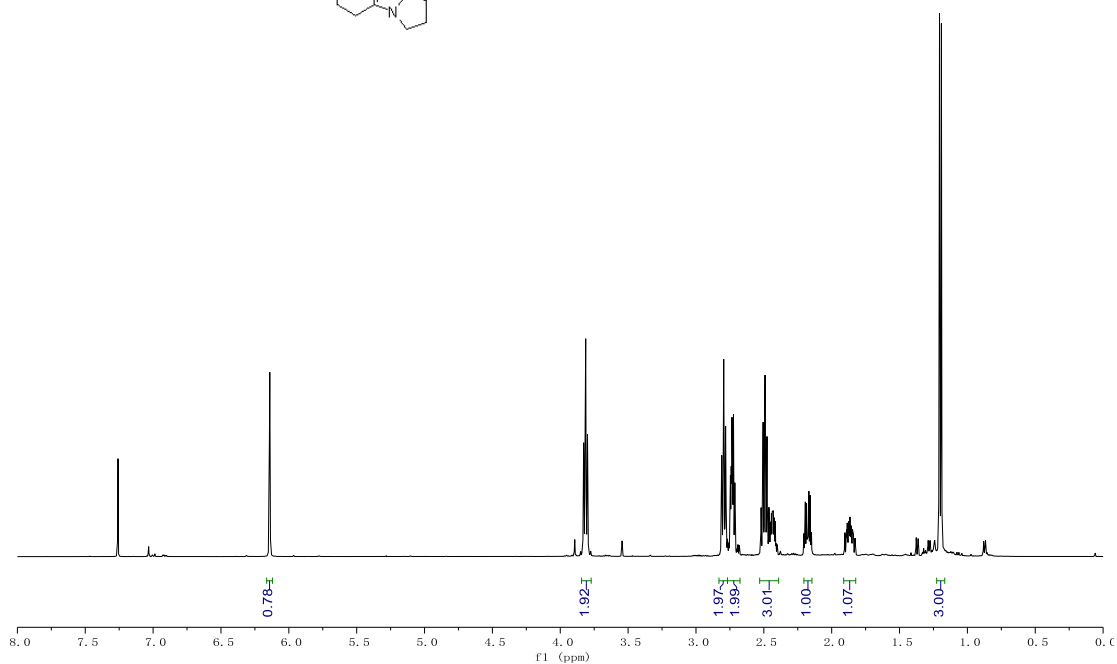
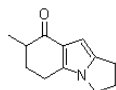
Parameter	Value
1 Title	2-9b-H
2 Solvent	CDCl3
3 Spectrometer Frequency	499.86



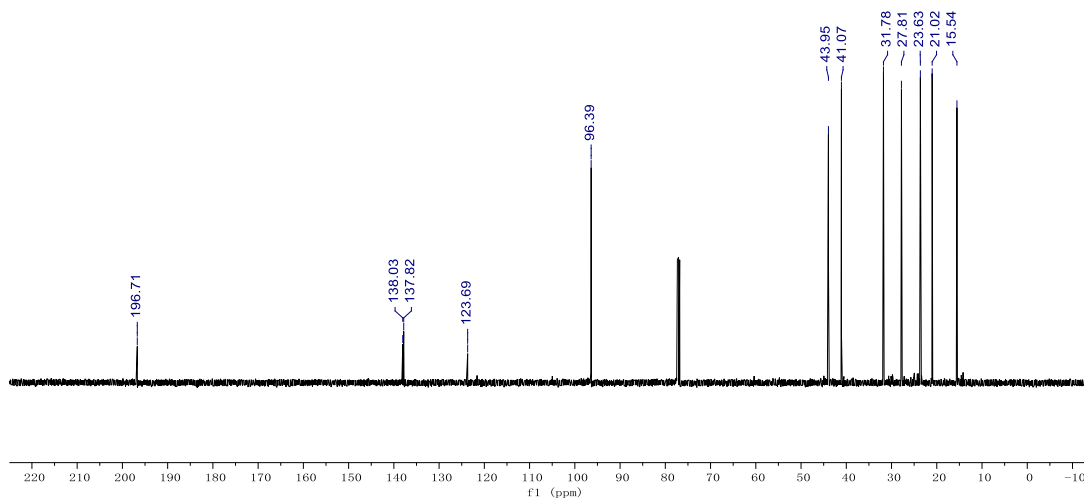
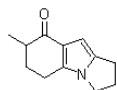
Parameter	Value
1 Title	2-9b-C
2 Solvent	CDCl3
3 Spectrometer Frequency	125.70



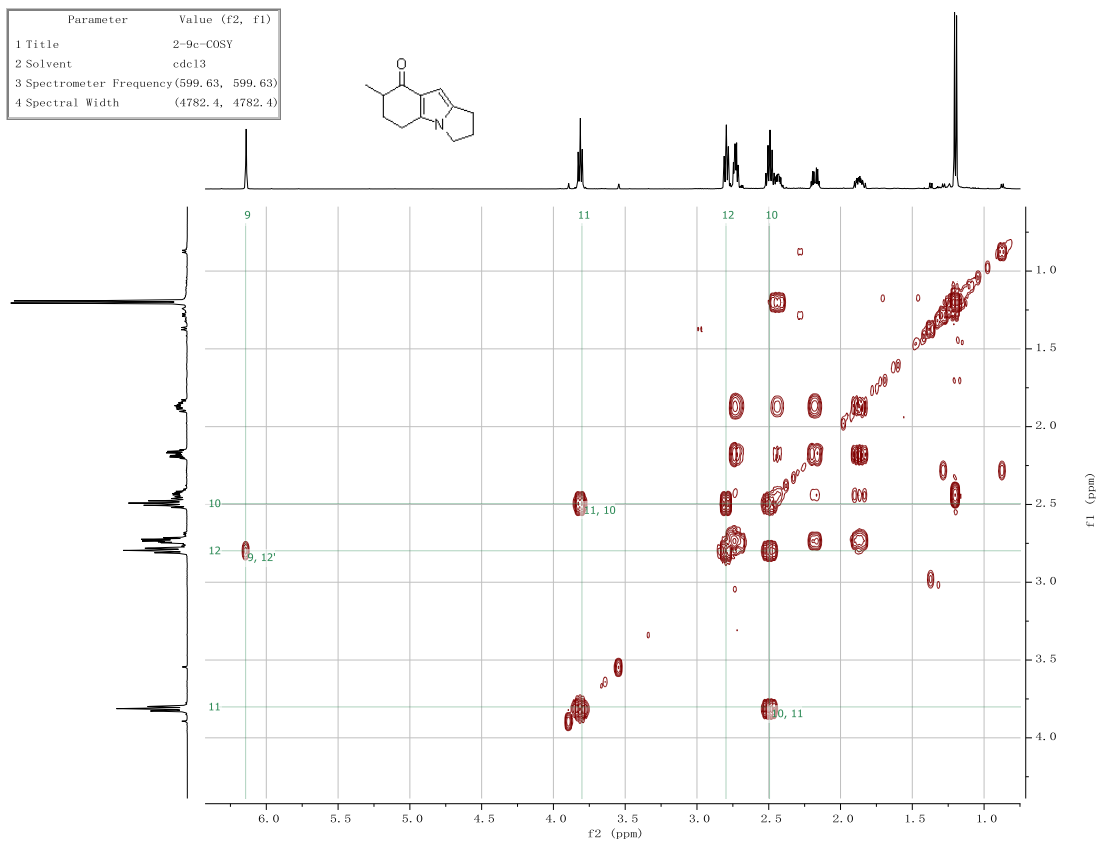
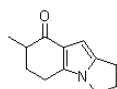
Parameter	Value
1 Title	2-9c-H
2 Solvent	CDCl3
3 Spectrometer Frequency	499.86



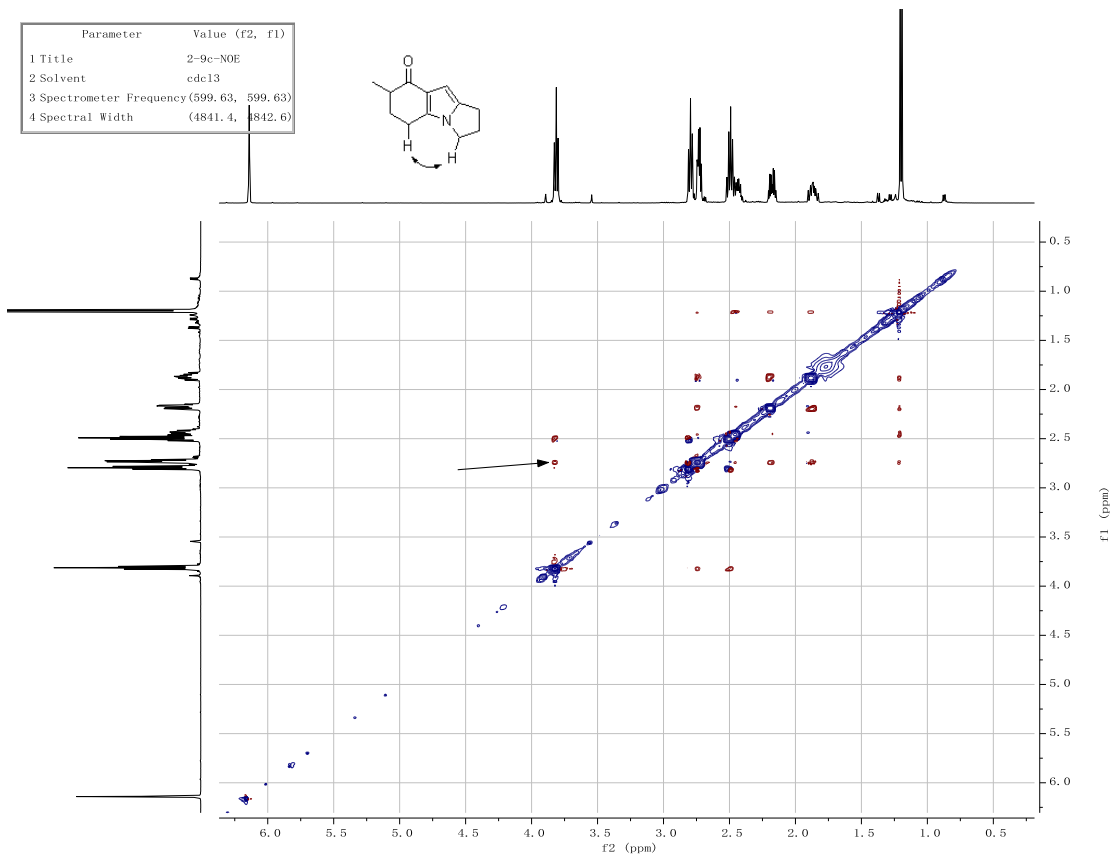
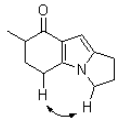
Parameter	Value
1 Title	2-9c-C
2 Solvent	CDCl3
3 Spectrometer Frequency	125.70



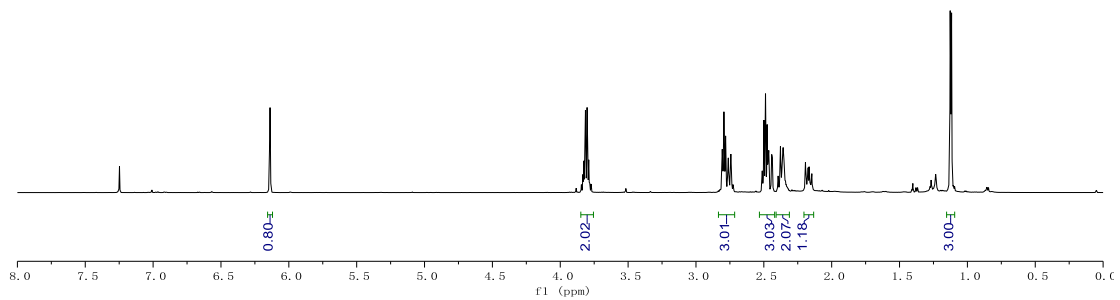
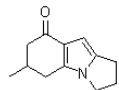
Parameter	Value (f2, f1)
1 Title	2-9c-COSY
2 Solvent	cdc13
3 Spectrometer Frequency (599.63, 599.63)	
4 Spectral Width (4782.4, 4782.4)	



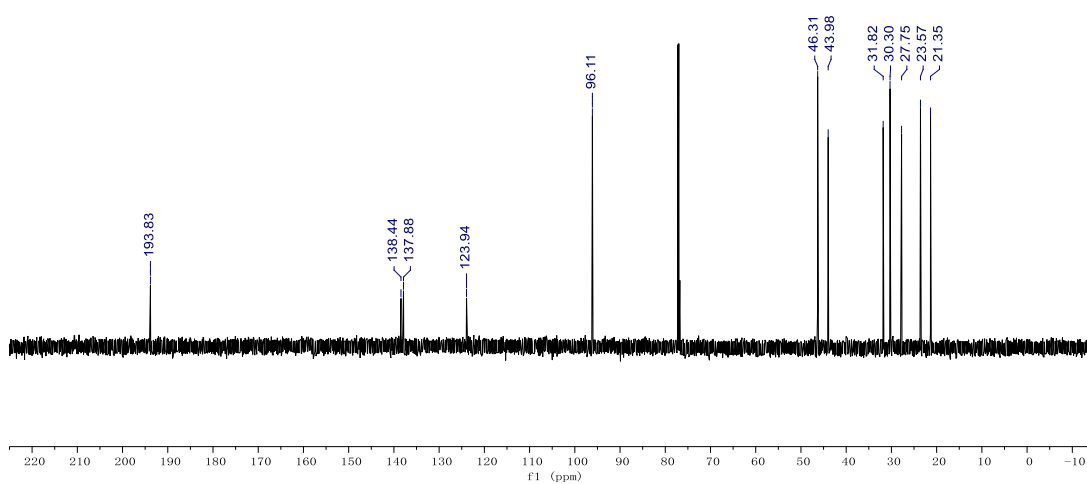
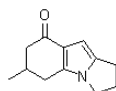
Parameter	Value (f2, f1)
1 Title	2-9e-NOE
2 Solvent	cdcl3
3 Spectrometer Frequency	(599.63, 599.63)
4 Spectral Width	(4841.4, 842.6)



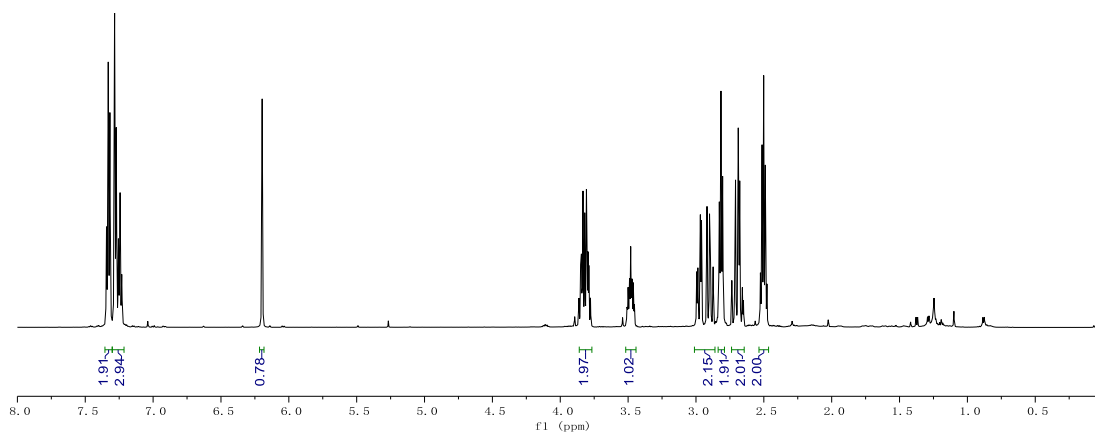
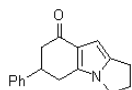
Parameter	Value
1 Title	2-9d-H
2 Solvent	cdcl3
3 Spectrometer Frequency	599.63



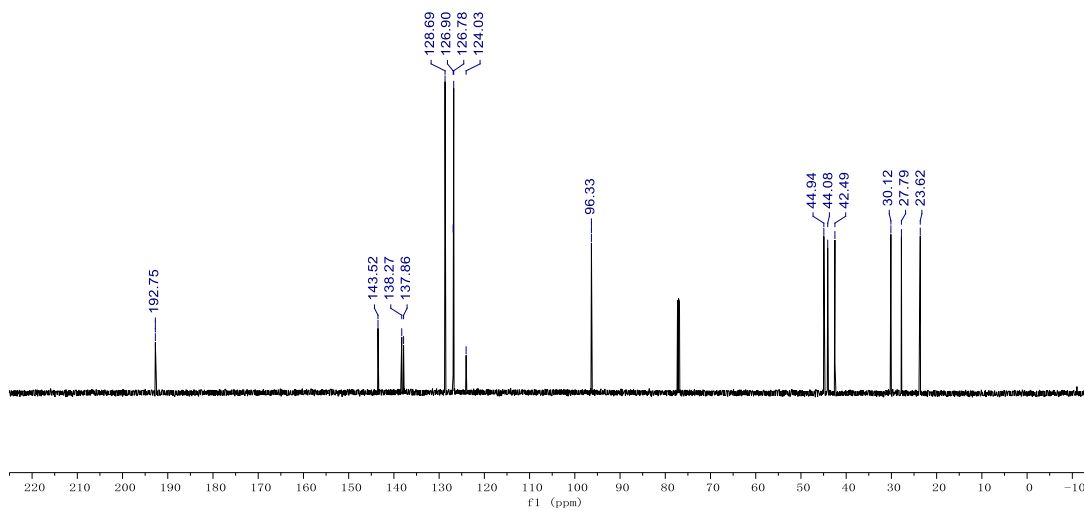
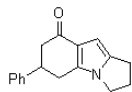
Parameter	Value
1 Title	2-9d-C
2 Solvent	cdcl3
3 Spectrometer Frequency	150.79



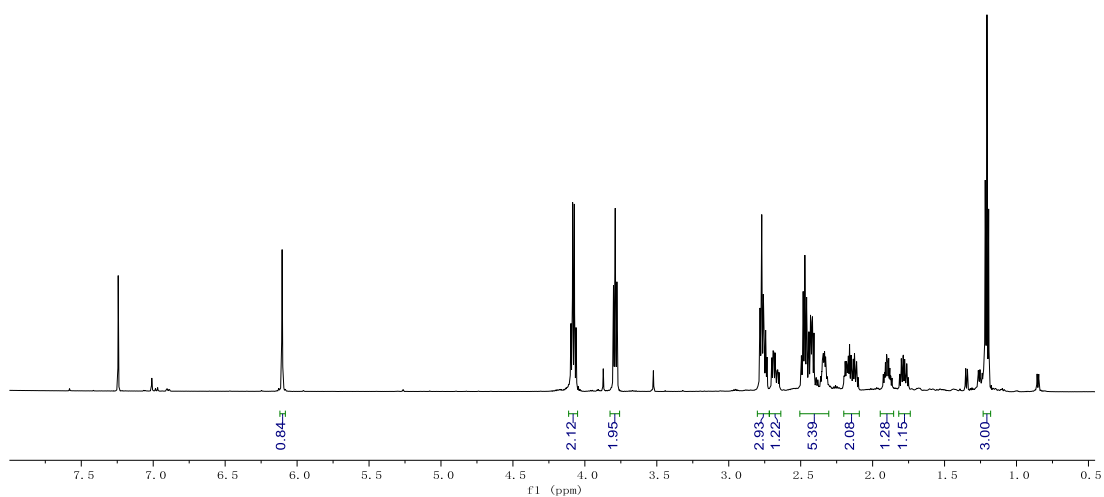
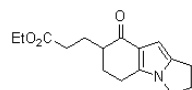
Parameter	Value
1 Title	2-9e-H
2 Solvent	cdcl3
3 Spectrometer Frequency	599.64



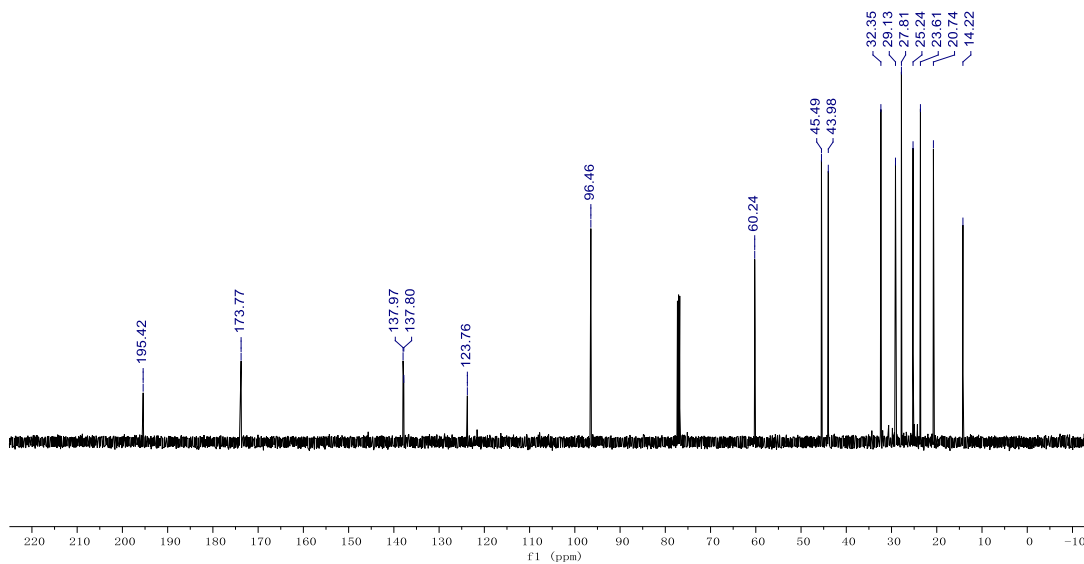
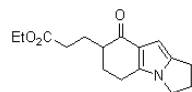
Parameter	Value
1 Title	2-9e-C
2 Solvent	cdcl3
3 Spectrometer Frequency	150.79



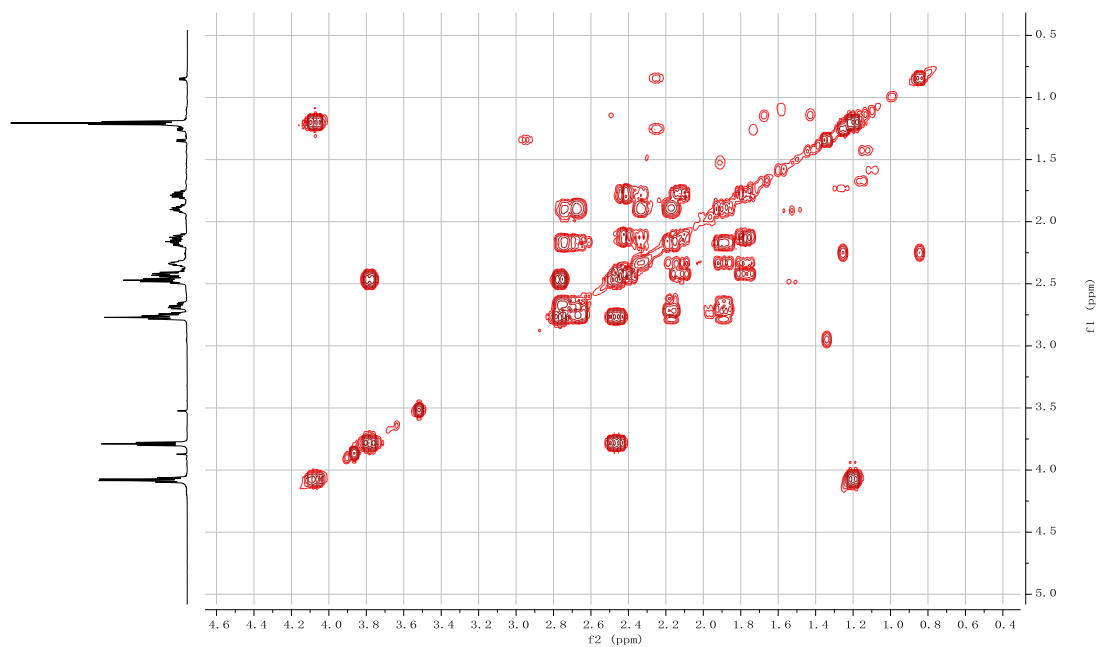
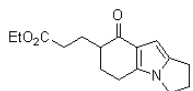
Parameter	Value
1 Title	2-9f-H
2 Solvent	cdcl3
3 Spectrometer Frequency	599.63



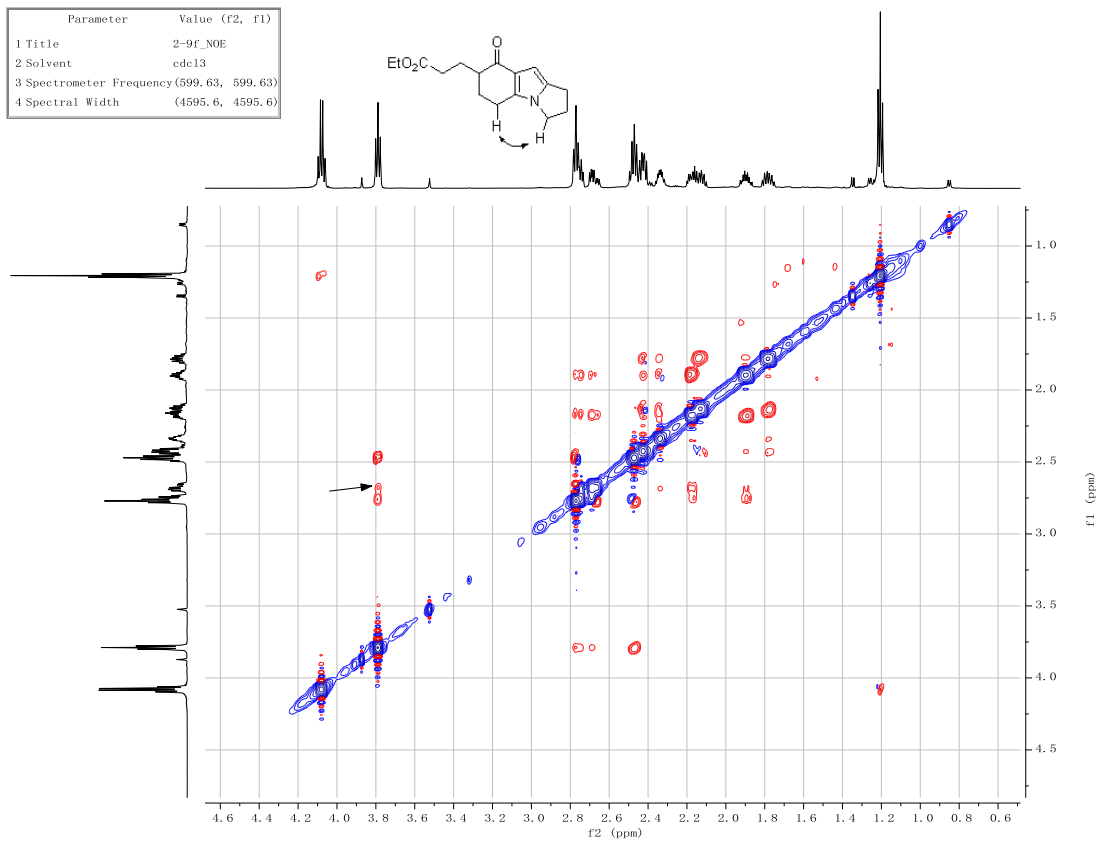
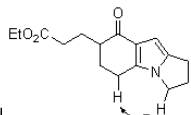
Parameter	Value
1 Title	2-9f-C
2 Solvent	CDCl3
3 Spectrometer Frequency	125.70



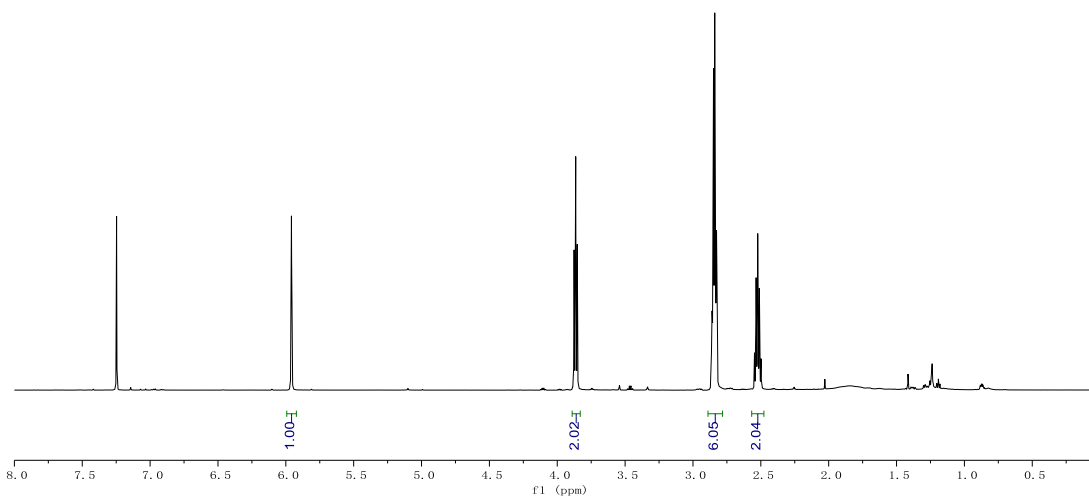
Parameter	Value (f2, f1)
1 Title	2-9f_COSY
2 Solvent	cdc13
3 Spectrometer Frequency	(599.63, 599.63)
4 Spectral Width	(4595.6, 4595.6)



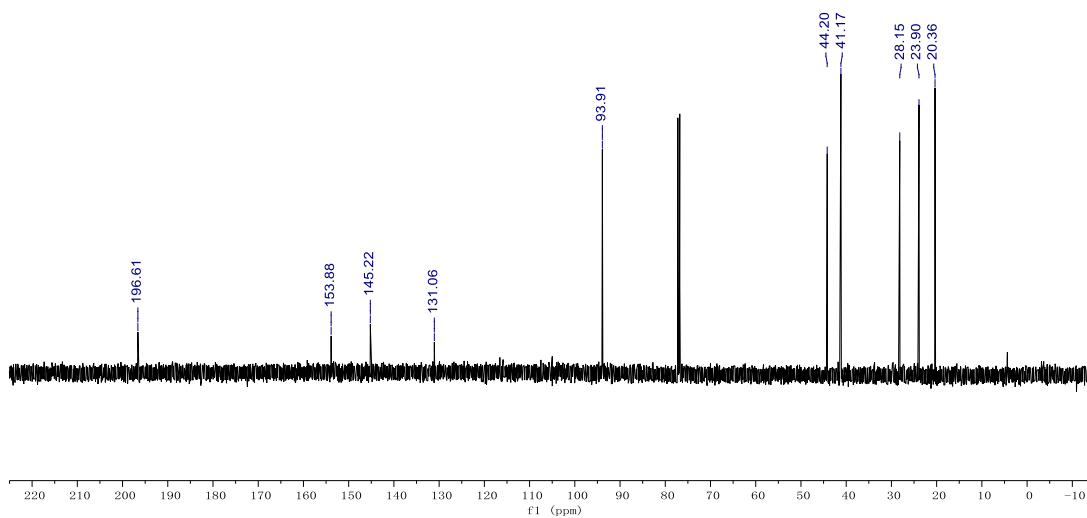
Parameter	Value (f2, f1)
1 Title	2-9f_NOE
2 Solvent	cdcl3
3 Spectrometer Frequency	(599.63, 599.63)
4 Spectral Width	(4595.6, 4595.6)



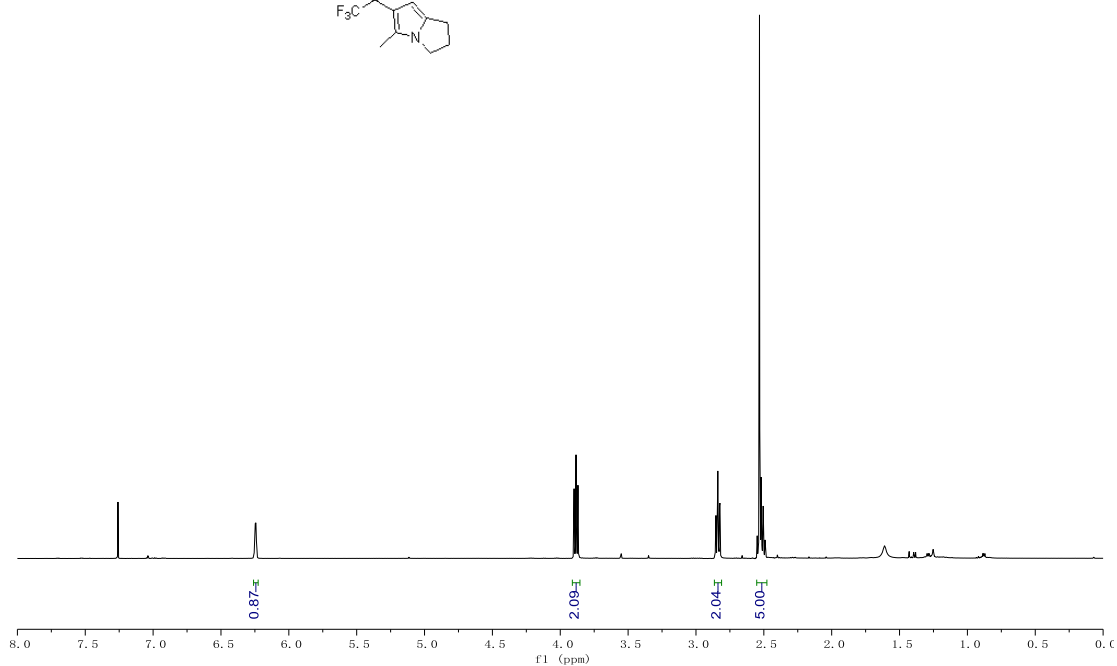
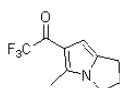
Parameter	Value
1 Title	2-9g-H
2 Solvent	cdcl3
3 Spectrometer Frequency	599.64



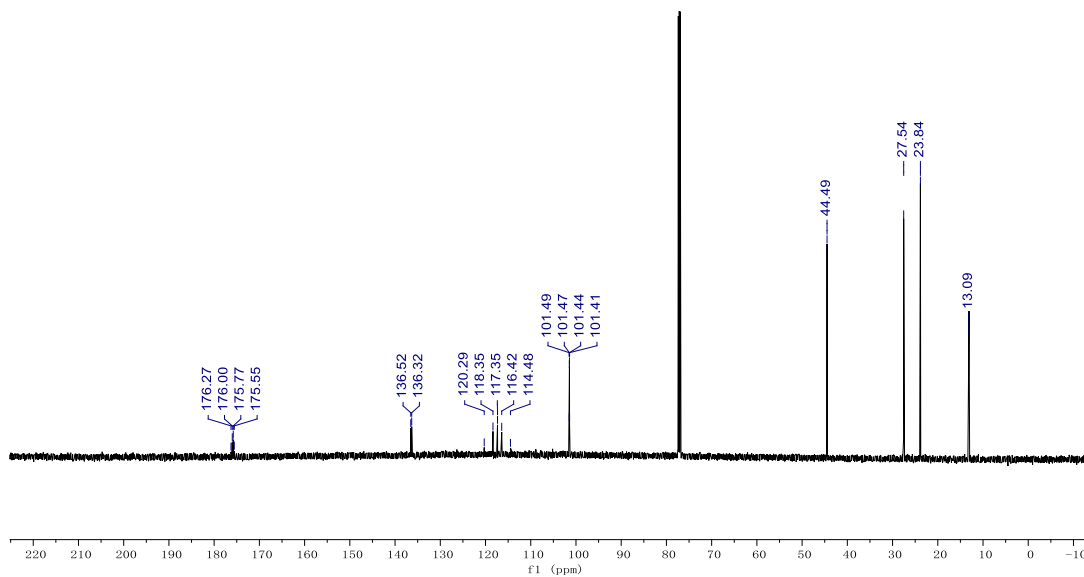
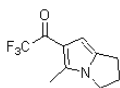
Parameter	Value
1 Title	2-9g-C
2 Solvent	cdcl3
3 Spectrometer Frequency	150.79



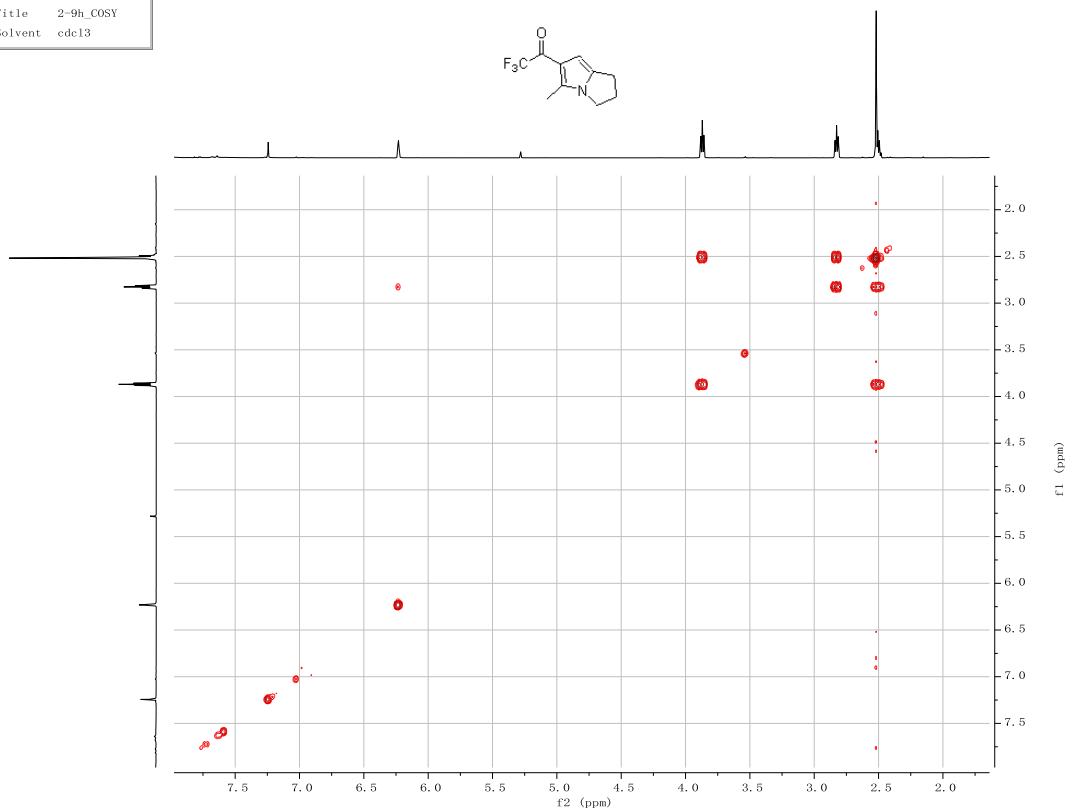
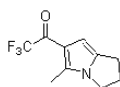
Parameter	Value
1 Title	2-9h-H
2 Solvent	CDCl3
3 Spectrometer Frequency	499.86



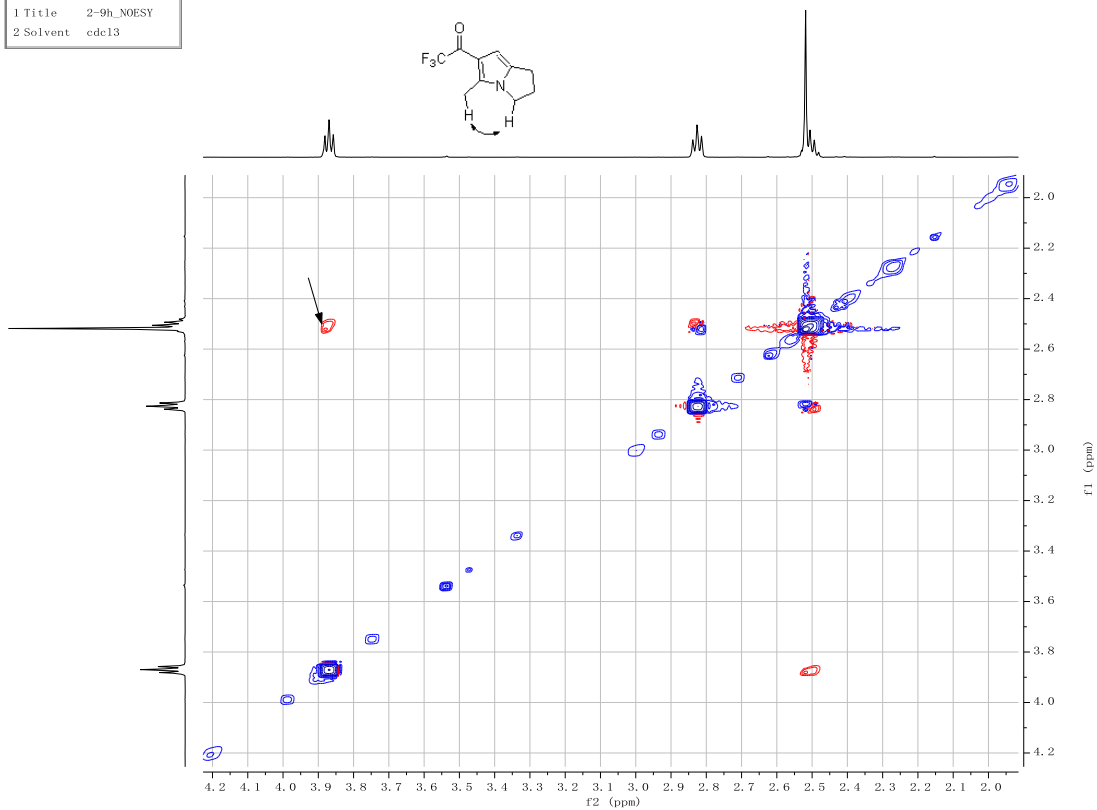
Parameter	Value
1 Title	2-9h-C
2 Solvent	cdcl3
3 Spectrometer Frequency	150.79



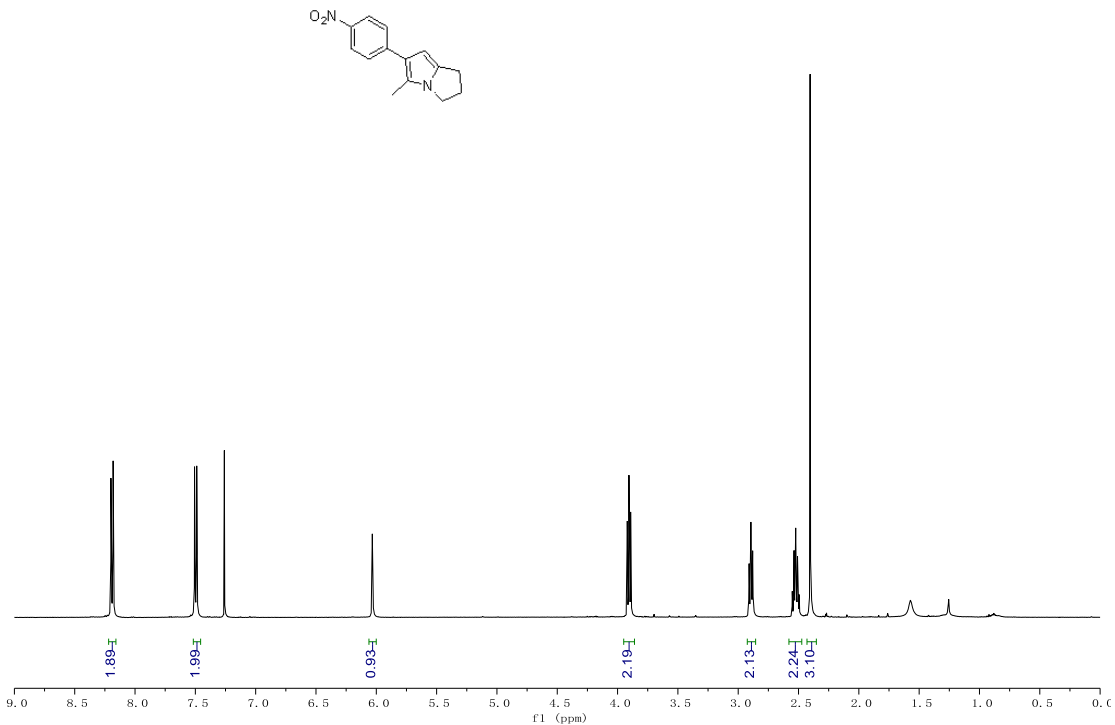
Parameter	Value (f2, f1)
1 Title	2-9h_COSY
2 Solvent	cdcl3



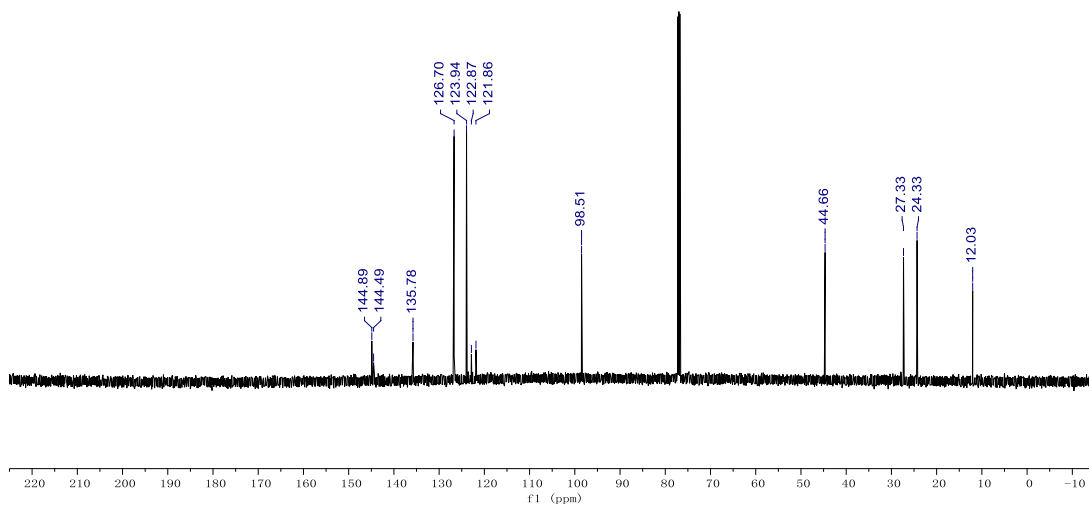
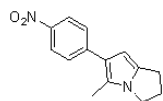
Parameter	Value (f2, f1)
1 Title	2-9h_NOESY
2 Solvent	cdcl3



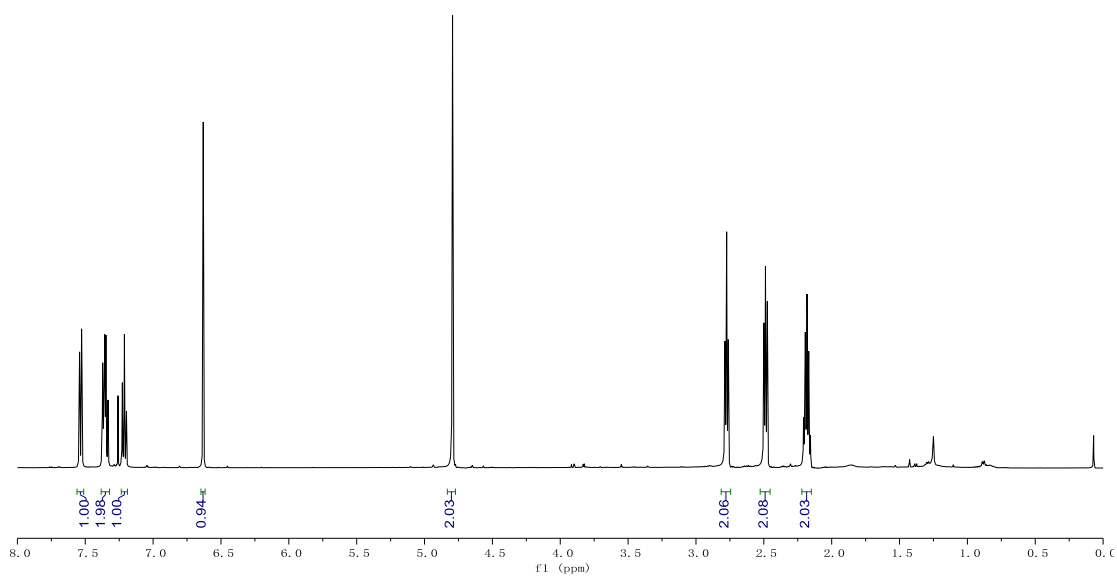
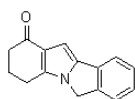
Parameter	Value
1 Title	2-9i-H
2 Solvent	CDCl3
3 Spectrometer Frequency	499.86



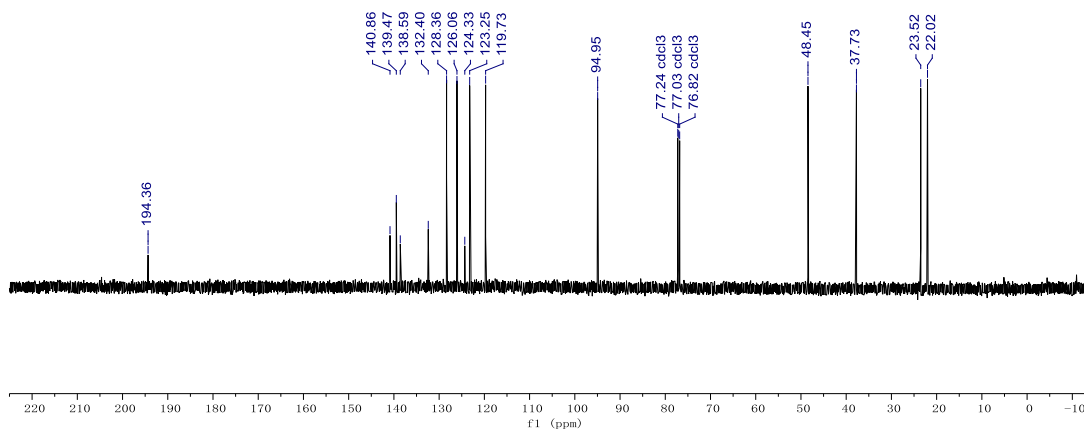
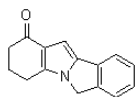
Parameter	Value
1 Title	2-9i-C
2 Solvent	cdcl3
3 Spectrometer Frequency	150.79



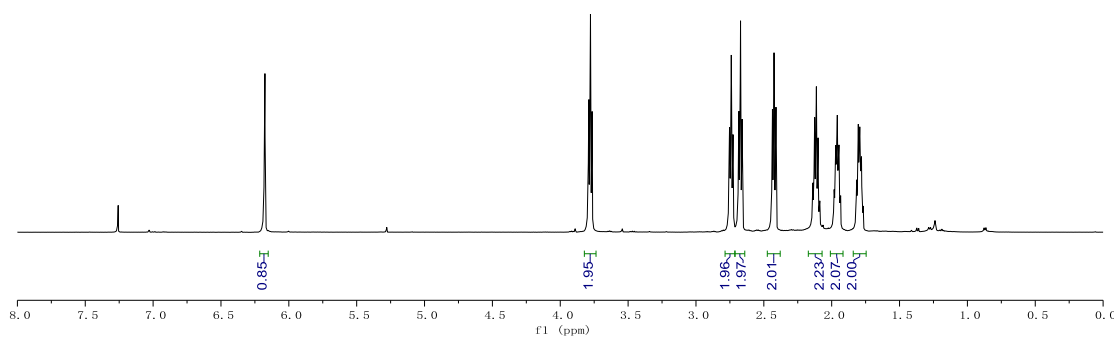
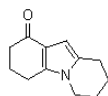
Parameter	Value
1 Title	2-9j-H
2 Solvent	CDCl3
3 Spectrometer Frequency	499.86



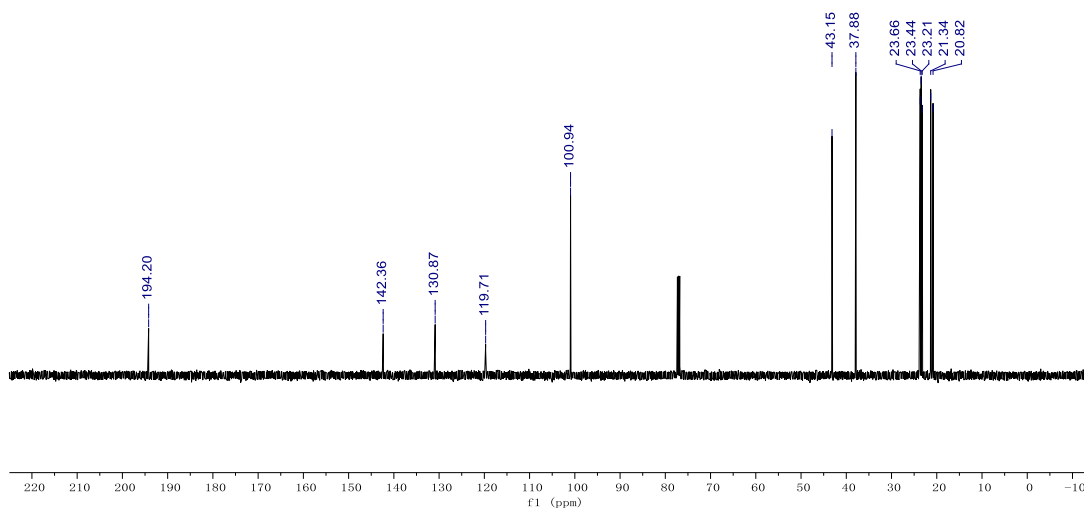
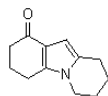
Parameter	Value
1 Title	2-9j-C
2 Solvent	cdcl3
3 Spectrometer Frequency	150.79



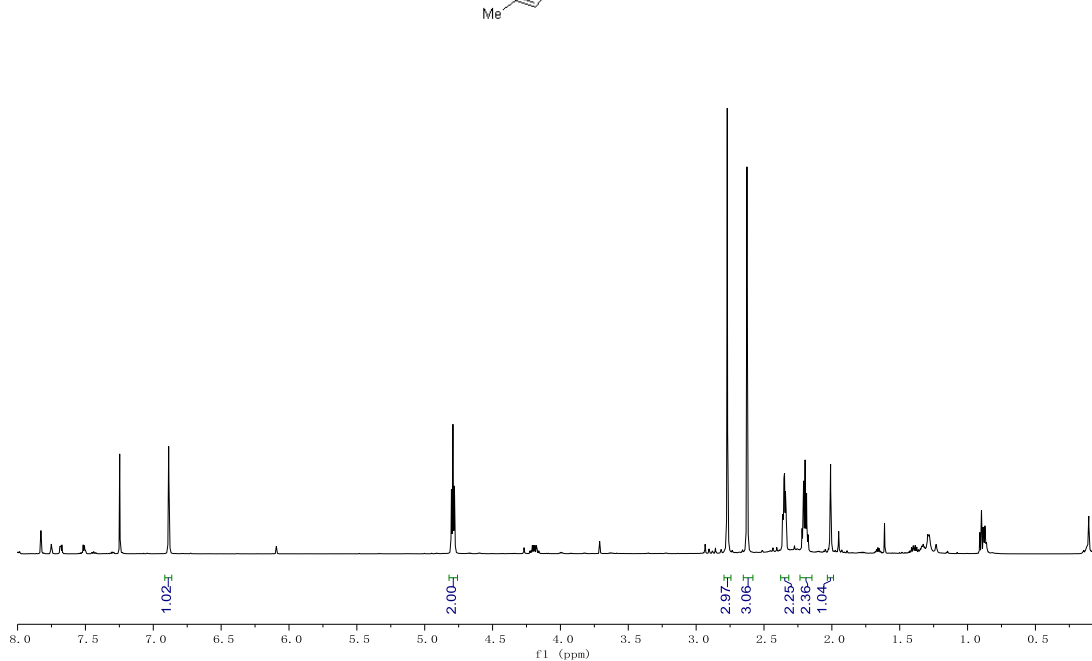
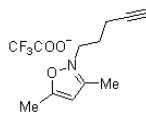
Parameter	Value
1 Title	2-9k-H
2 Solvent	CDCl3
3 Spectrometer Frequency	499.86



Parameter	Value
1 Title	2-9k-C
2 Solvent	CDCl3
3 Spectrometer Frequency	125.70

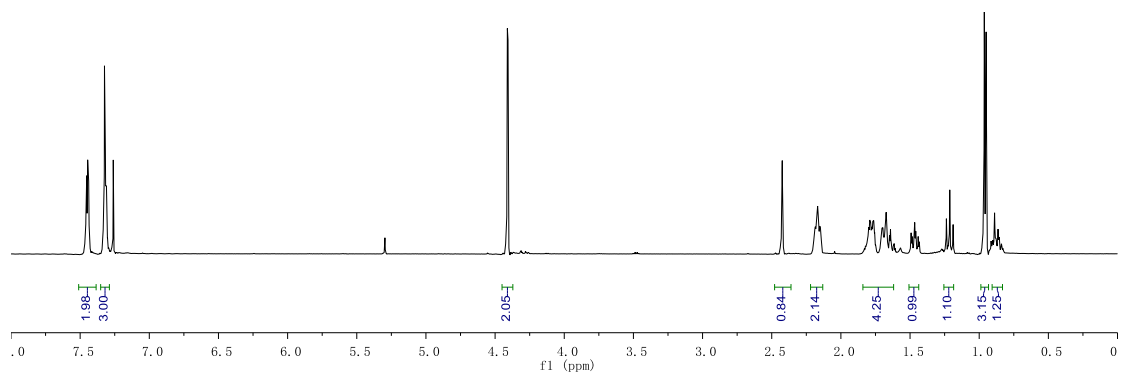
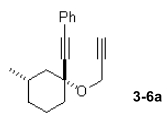


Parameter	Value
1 Title	2-11-H-crude
2 Solvent	cdcl3
3 Spectrometer Frequency	599.64

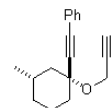


NMR Spectra for Compounds in Chapter 3

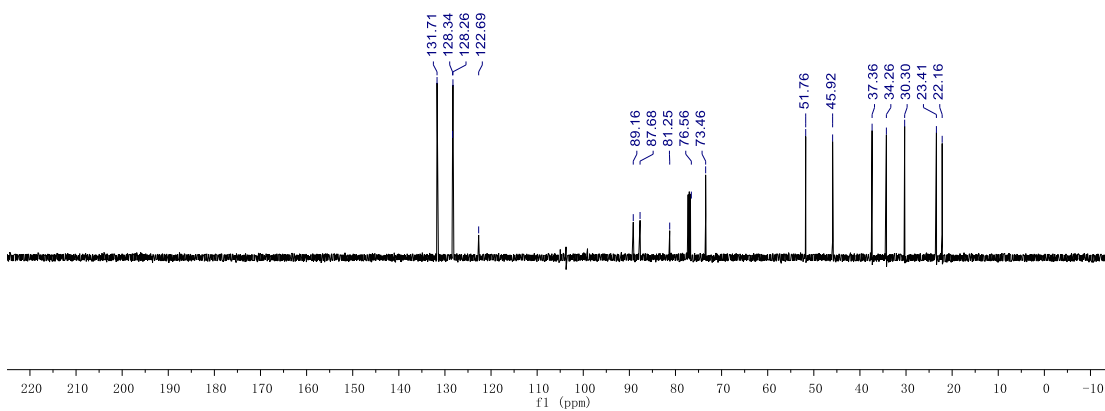
Parameter	Value
1 Title	zzt-5-2-3-SM-H
2 Solvent	CDCl ₃
3 Relaxation Delay	4.8000
4 Spectrometer Frequency	499.86



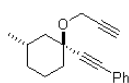
Parameter	Value
1 Title	zzt-5-2-3-SM-C
2 Solvent	CDCl3
3 Relaxation Delay	1.0000
4 Spectrometer Frequency	125.70



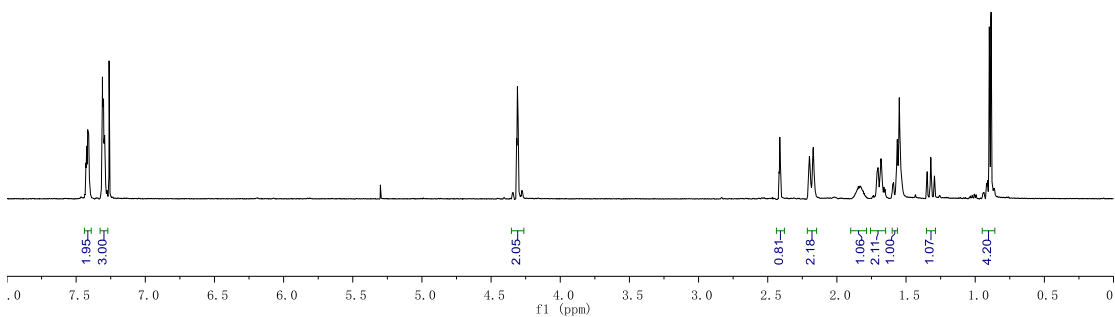
3-6a



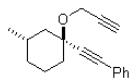
Parameter	Value
1 Title	zzt-4-145
2 Solvent	CDCl3
3 Relaxation Delay	4.8000
4 Spectrometer Frequency	499.86



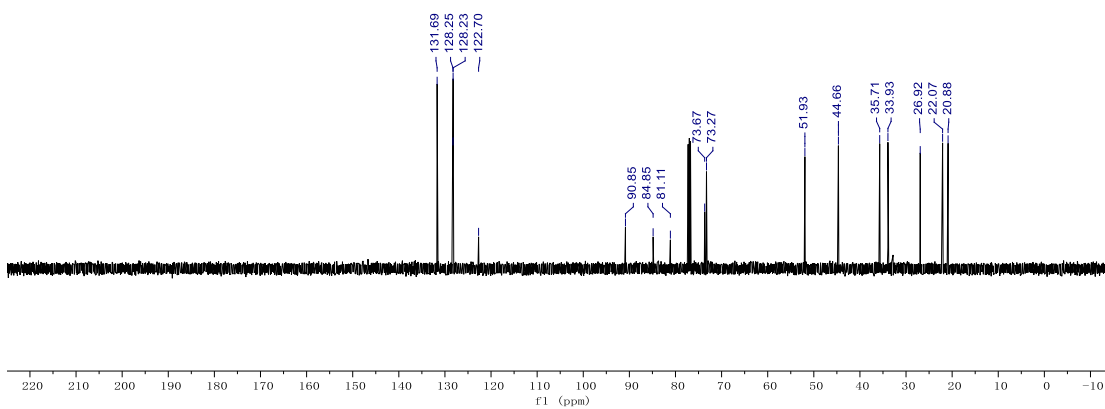
3-6a'



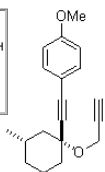
Parameter	Value
1 Title	zzt-4-145-C
2 Solvent	CDCl3
3 Spectrometer Frequency	125.70
4 Nucleus	13C



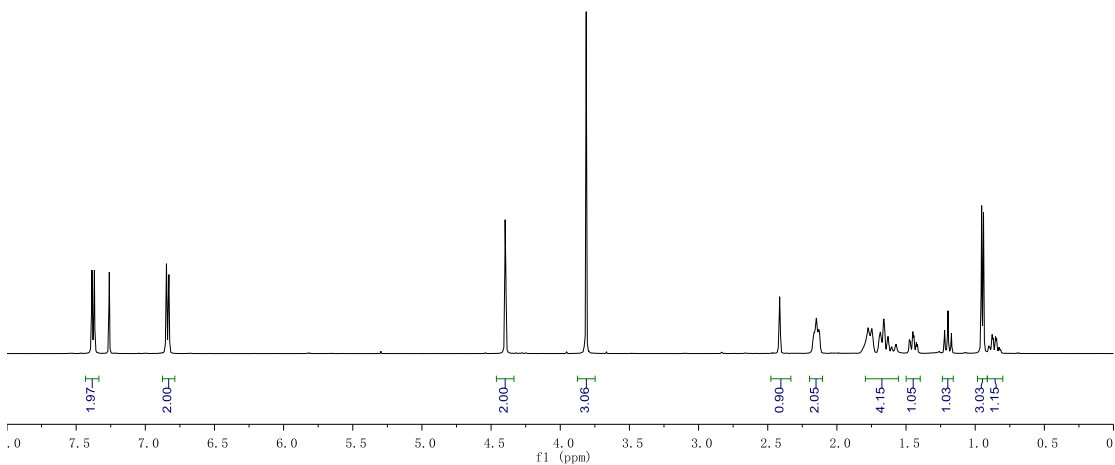
3-6a'



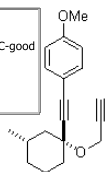
Parameter	Value
1 Title	zzt-4-151-1-SM-H
2 Solvent	CDCl3
3 Relaxation Delay	4.8000
4 Spectrometer Frequency	499.86



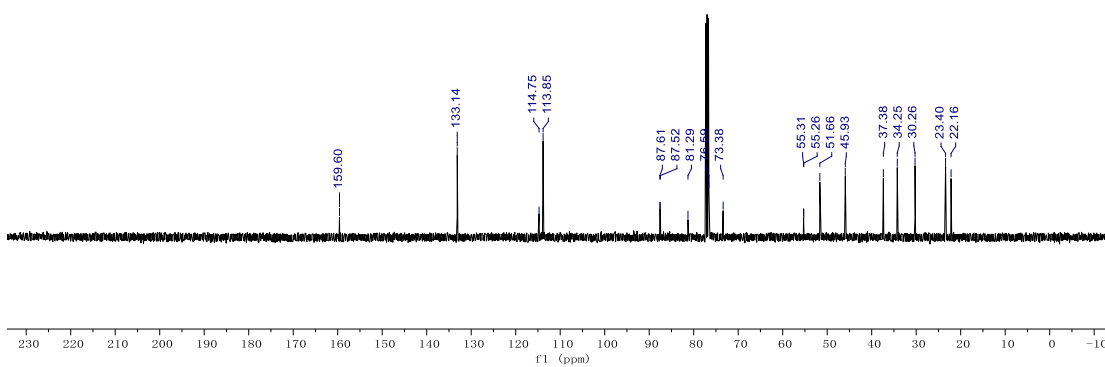
3-6b



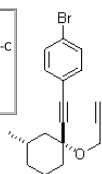
Parameter	Value
1 Title	zzt-4-151-1-SM-C-good
2 Solvent	cdcl3
3 Spectrometer Frequency	100.53
4 Nucleus	13C



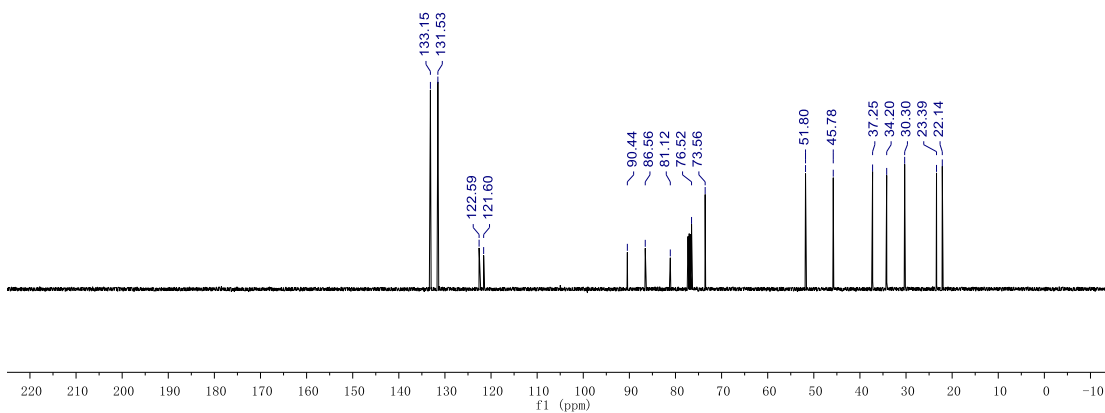
3-6b



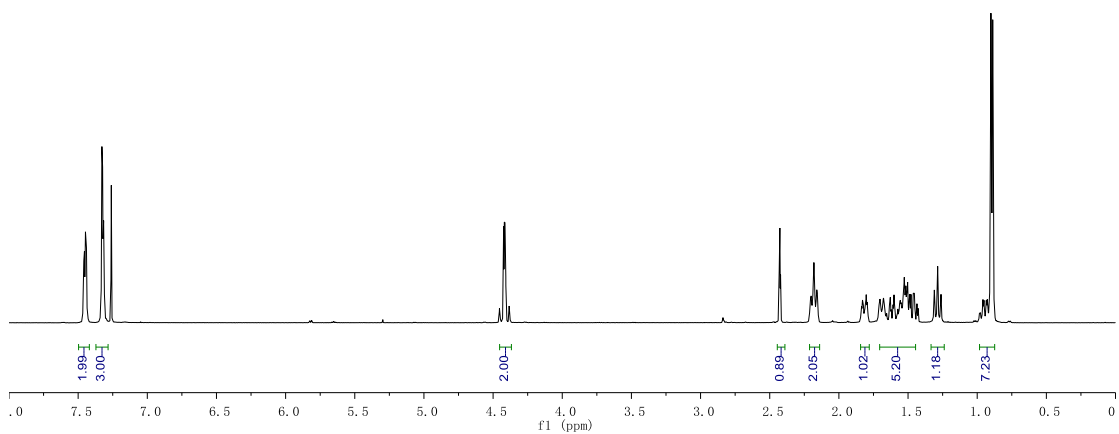
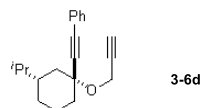
Parameter	Value
1 Title	zzt-5-26-5-SM-C
2 Solvent	CDCl3
3 Relaxation Delay	1.0000
4 Spectrometer Frequency	125.70



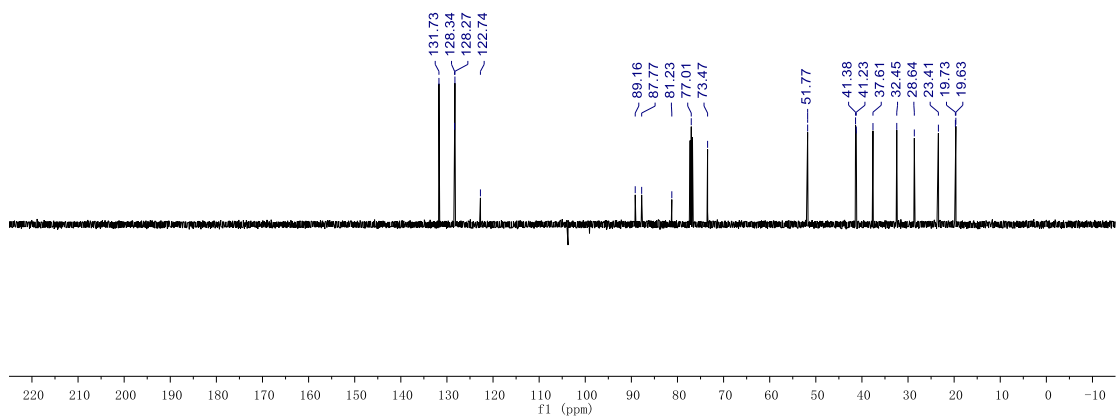
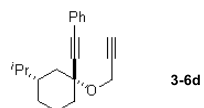
3-6c



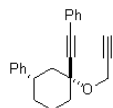
Parameter	Value
1 Title	zzt-5-18-1-SM-H
2 Solvent	CDCl3
3 Relaxation Delay	4.8000
4 Spectrometer Frequency	499.86



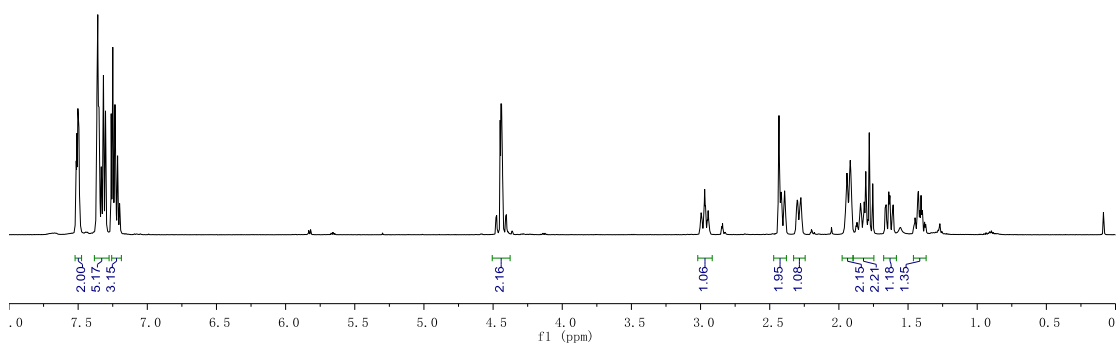
Parameter	Value
1 Title	zzt-5-18-1-SM-C
2 Solvent	CDCl3
3 Relaxation Delay	1.0000
4 Spectrometer Frequency	125.70



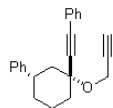
Parameter	Value
1 Title	zzt-4-280-2-H
2 Solvent	CDCl3
3 Relaxation Delay	4.8000
4 Spectrometer Frequency	499.86



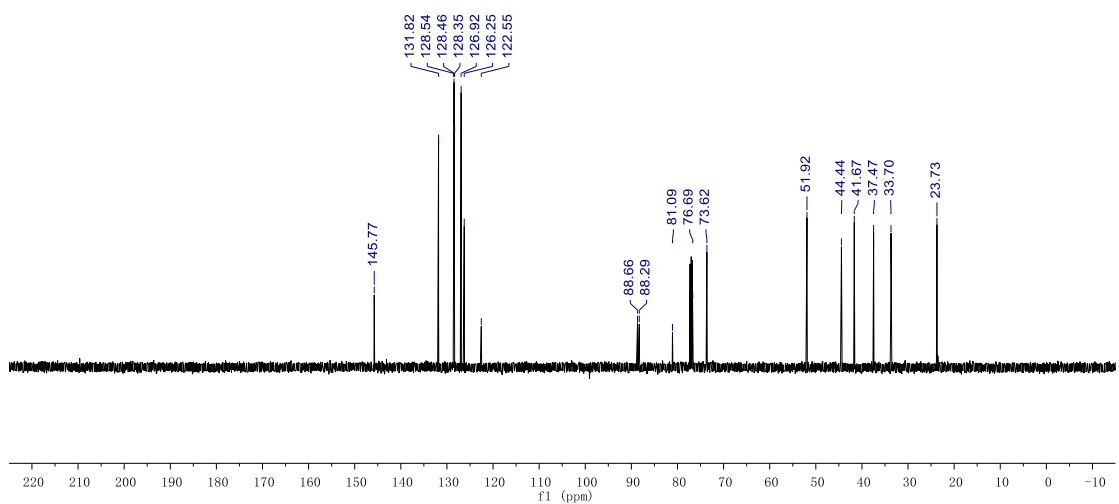
3-6e



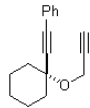
Parameter	Value
1 Title	zzt-4-280-2-C
2 Solvent	CDCl3
3 Relaxation Delay	1.0000
4 Spectrometer Frequency	125.70



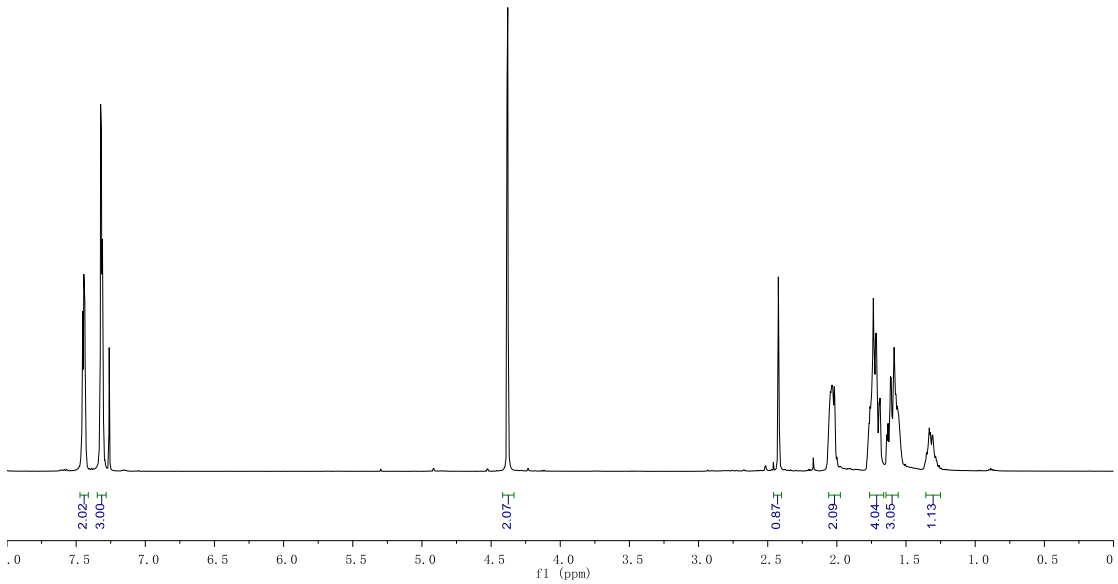
3-6e



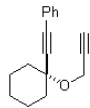
Parameter	Value
1 Title	zzt-5-26-3-SM-H
2 Solvent	CDCl3
3 Relaxation Delay	4.8000
4 Spectrometer Frequency	499.86



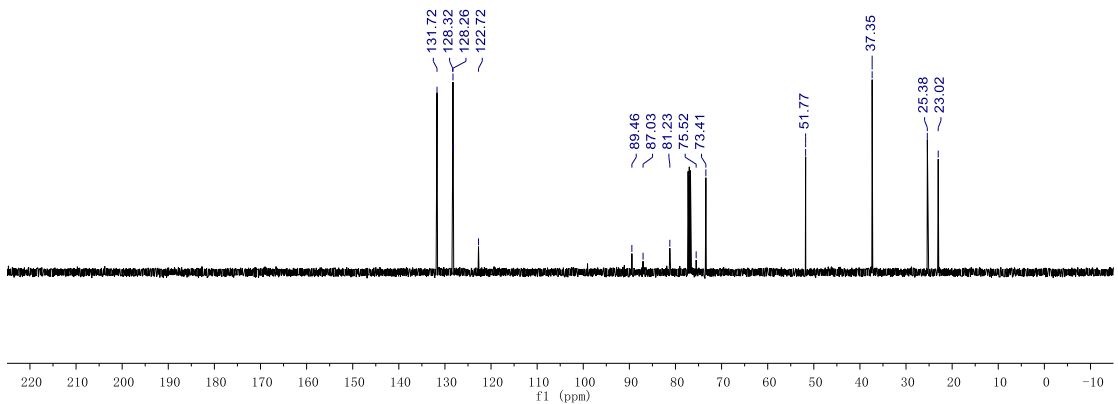
3-6f



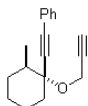
Parameter	Value
1 Title	zzt-5-26-3-SM-C
2 Solvent	CDCl3
3 Relaxation Delay	1.0000
4 Spectrometer Frequency	125.70



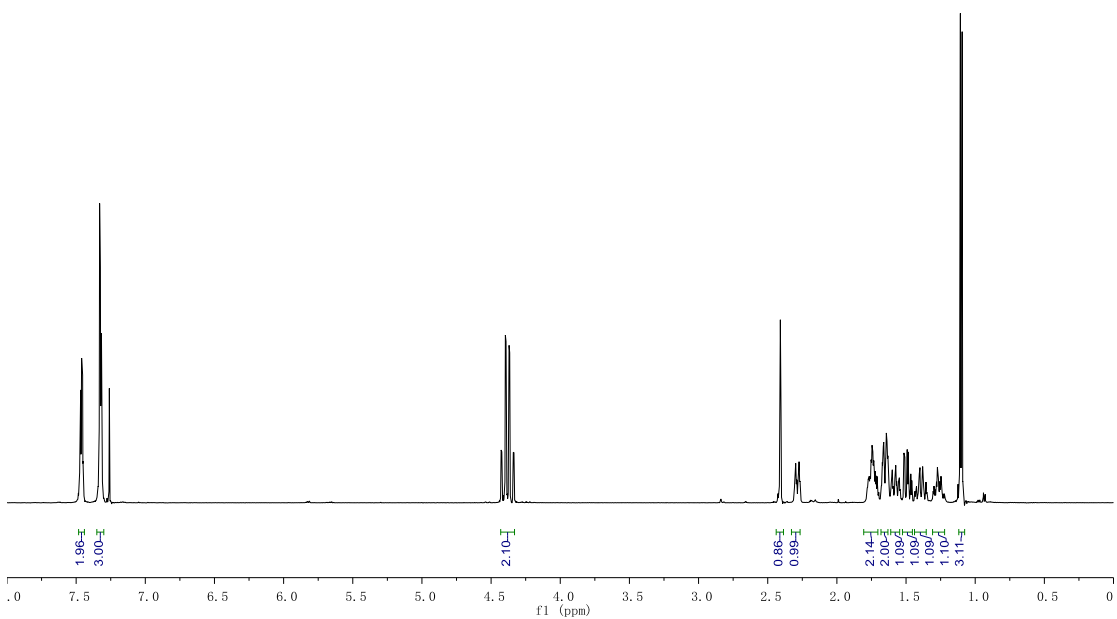
3-6f



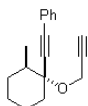
Parameter	Value
1 Title	zzt-4-170-1-SM-H
2 Solvent	CDCl3
3 Relaxation Delay	4.8000
4 Spectrometer Frequency	499.86



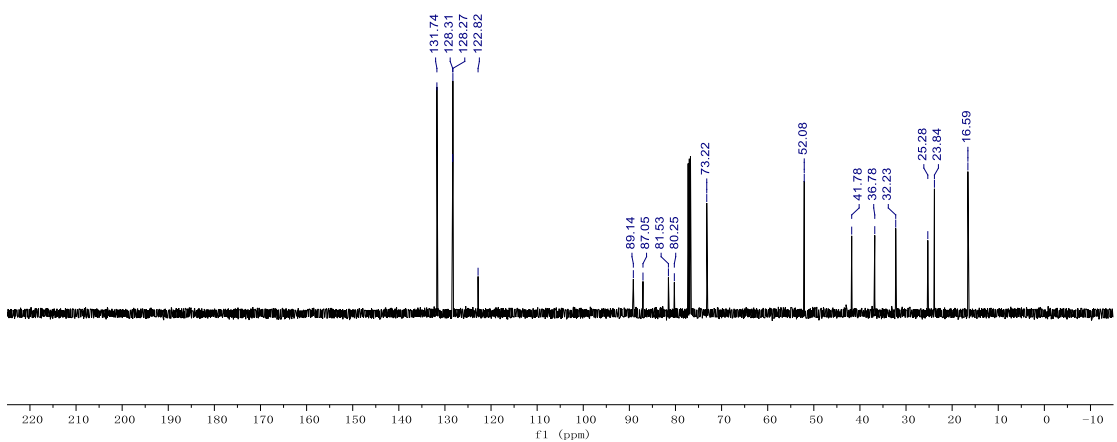
3-6g



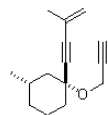
Parameter	Value
1 Title	zzt-4-170-1-SM-C-new
2 Solvent	CDCl3
3 Spectrometer Frequency	125.70
4 Nucleus	13C



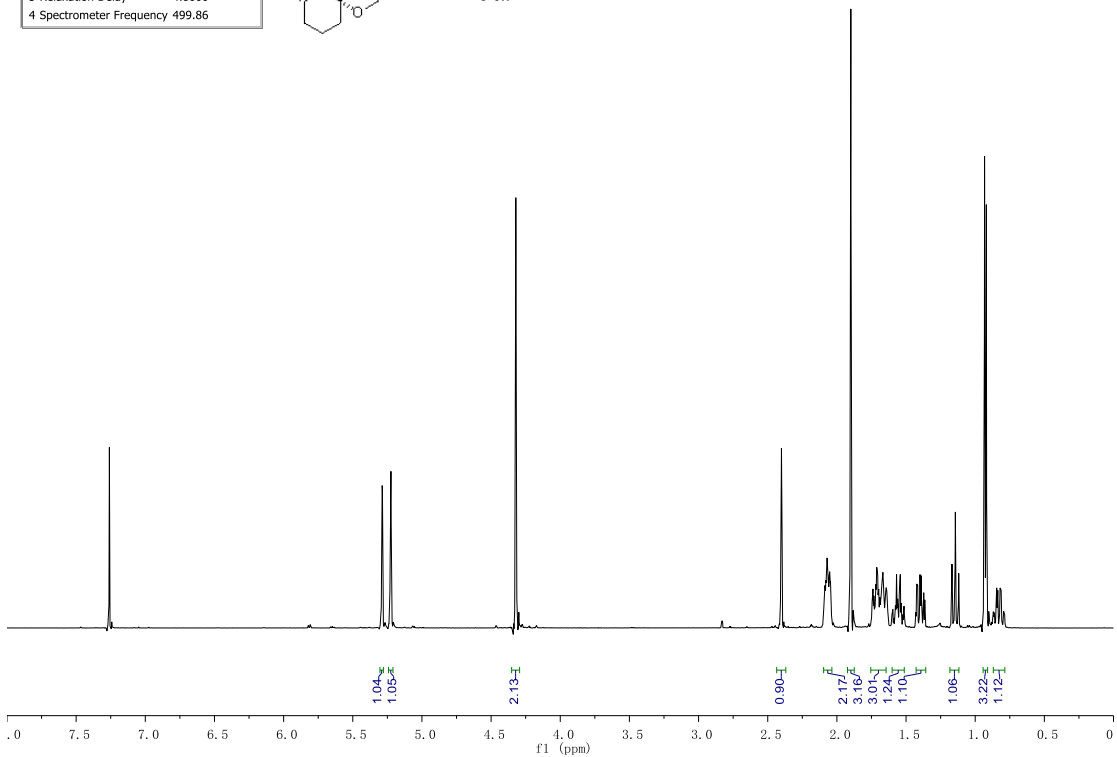
3-6g



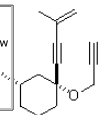
Parameter	Value
1 Title	zzt-5-26-2-SM-H
2 Solvent	CDCl3
3 Relaxation Delay	4.8000
4 Spectrometer Frequency	499.86



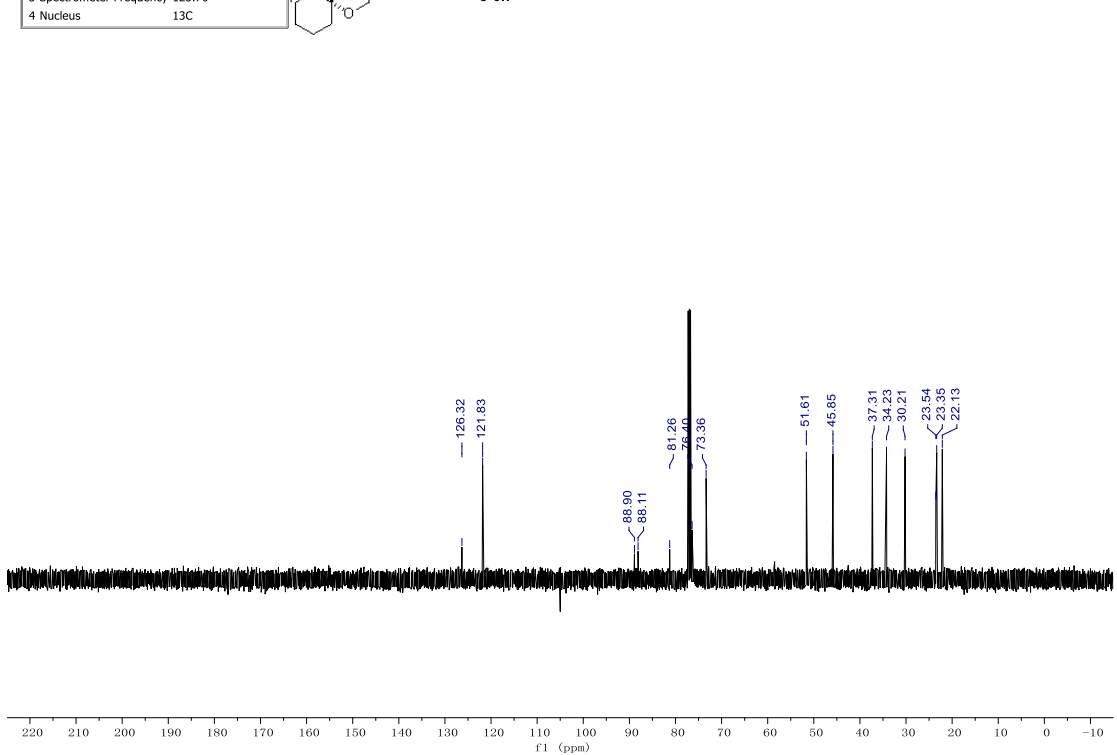
3-6h



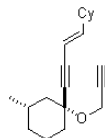
Parameter	Value
1 Title	zzt-5-26-2-SM-C-new
2 Solvent	CDCl3
3 Spectrometer Frequency	125.70
4 Nucleus	13C



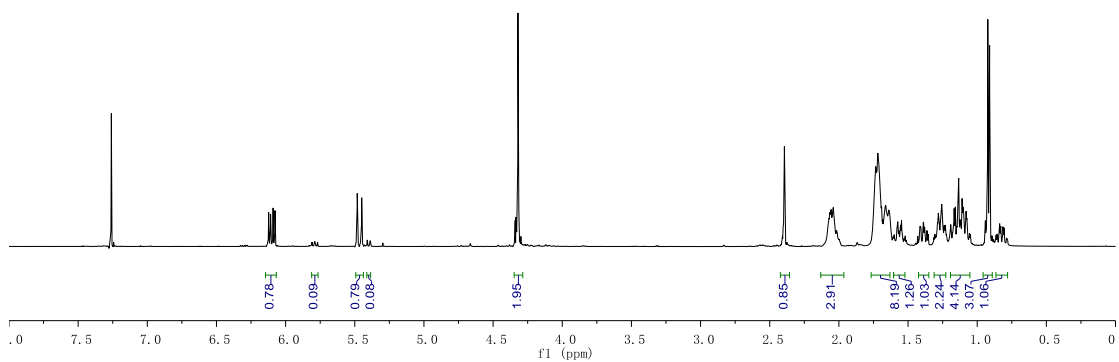
3-6h



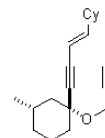
Parameter	Value
1 Title	zzt-5-26-1-SM-H
2 Solvent	CDCl3
3 Relaxation Delay	4.8000
4 Spectrometer Frequency	499.86



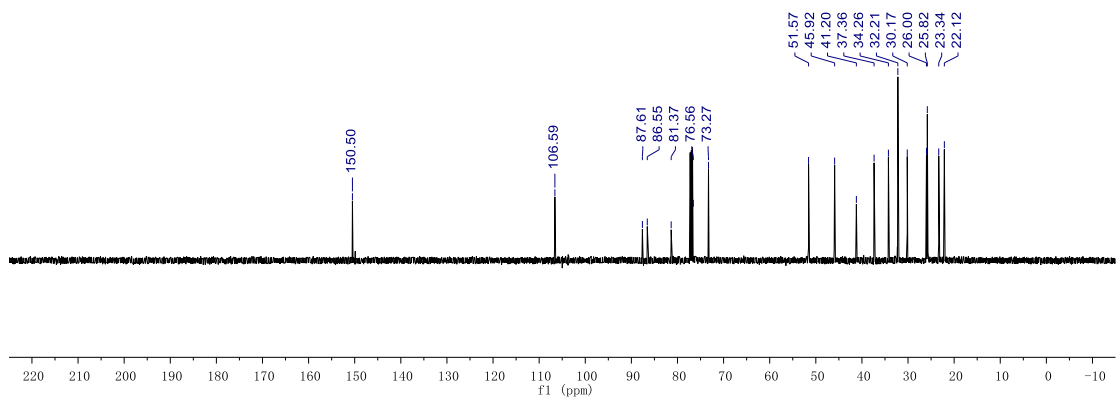
3-6i
cis : trans = 10:1



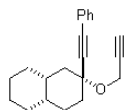
Parameter	Value
1 Title	zzt-5-26-1-SM-C
2 Solvent	CDCl3
3 Relaxation Delay	1.0000
4 Spectrometer Frequency	125.70



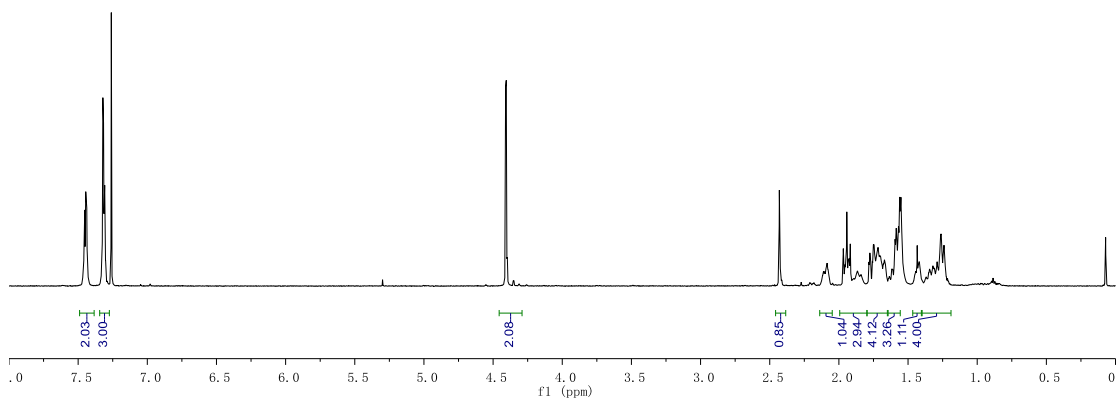
3-6i



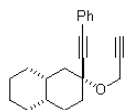
Parameter	Value
1 Title	zzt-4-298-1-H
2 Solvent	CDCl3
3 Relaxation Delay	4.8000
4 Spectrometer Frequency	499.86



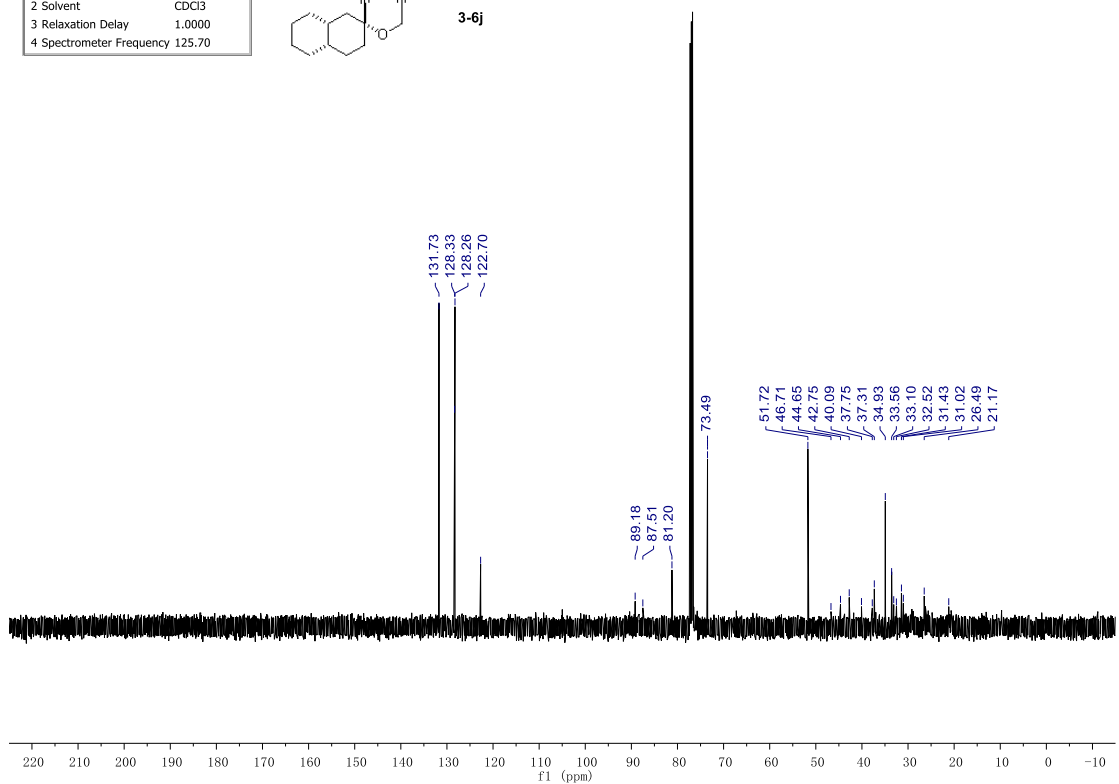
3-6j



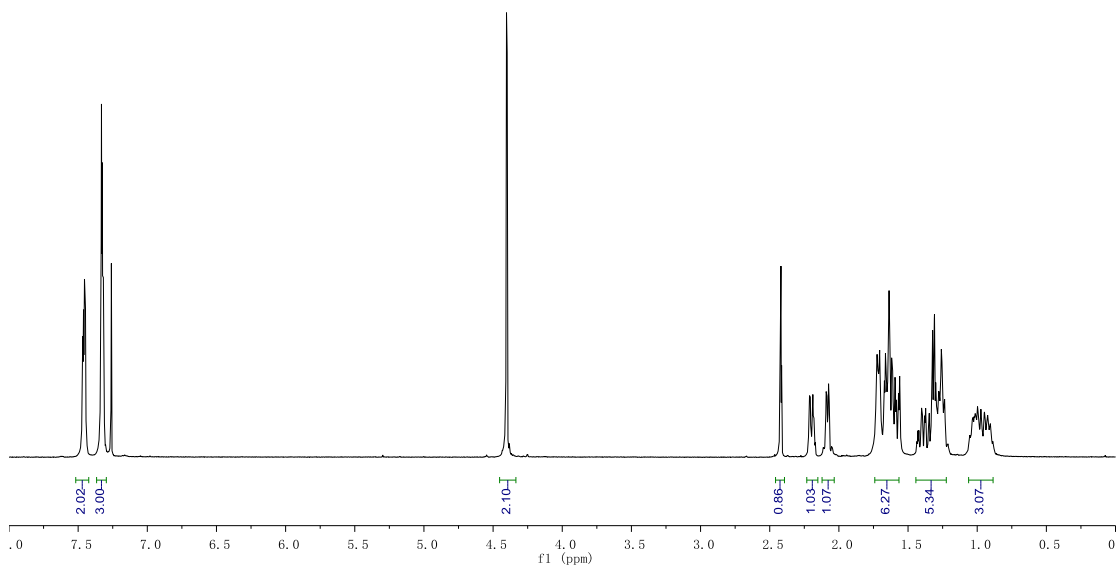
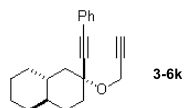
Parameter	Value
1 Title	zzt-4-298-1-C
2 Solvent	CDCl3
3 Relaxation Delay	1.0000
4 Spectrometer Frequency	125.70



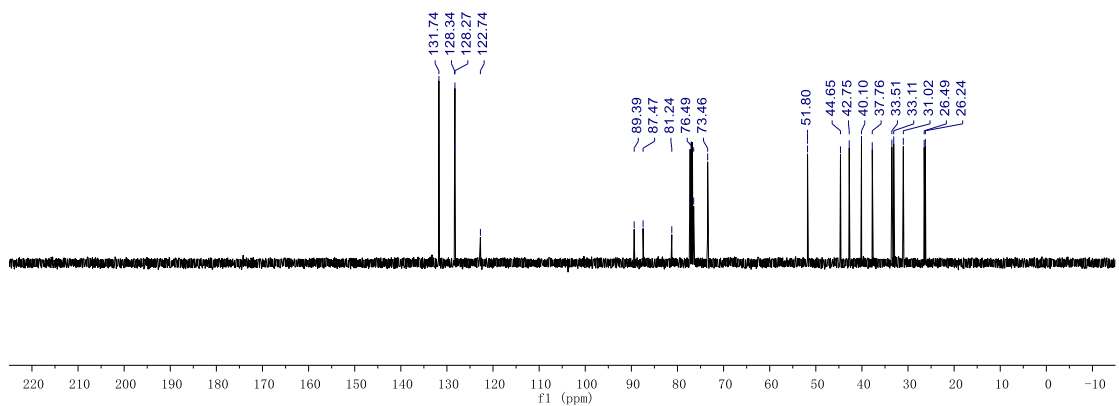
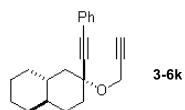
3-6j



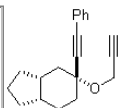
Parameter	Value
1 Title	zzt-5-18-3-SM-H
2 Solvent	CDCl3
3 Relaxation Delay	4.8000
4 Spectrometer Frequency	499.86



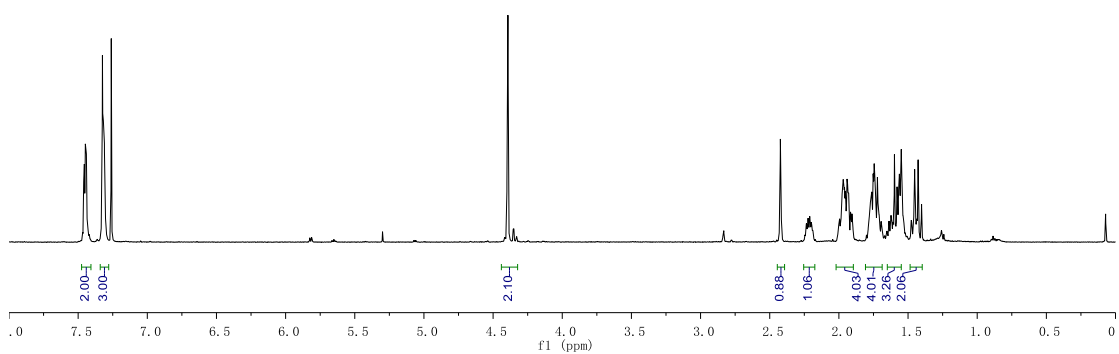
Parameter	Value
1 Title	zzt-5-18-3-SM-C
2 Solvent	CDCl3
3 Relaxation Delay	1.0000
4 Spectrometer Frequency	125.70



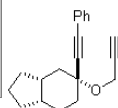
Parameter	Value
1 Title	zzt-4-302-3-H
2 Solvent	CDCl3
3 Relaxation Delay	4.8000
4 Spectrometer Frequency	499.86



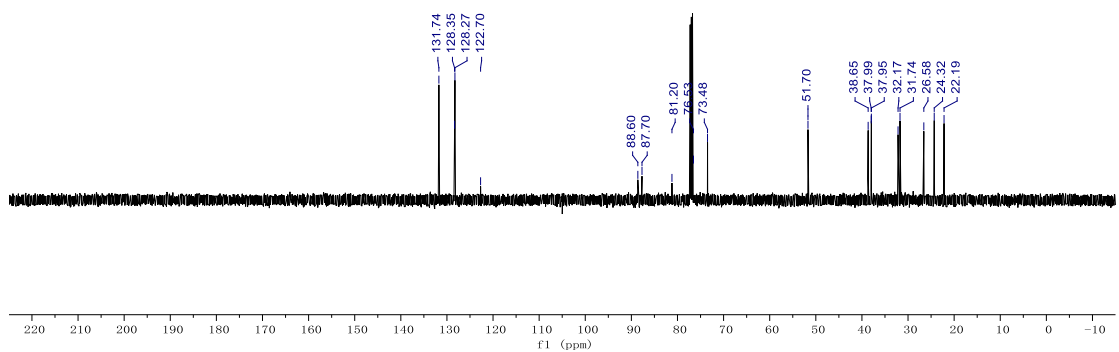
3-61



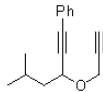
Parameter	Value
1 Title	zzt-4-302-3-C-new
2 Solvent	CDCl3
3 Spectrometer Frequency	125.70
4 Nucleus	13C



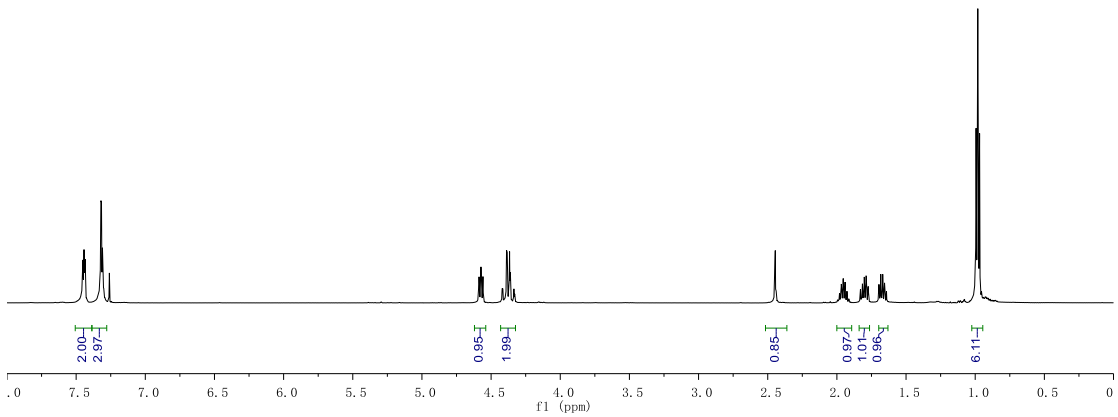
3-61



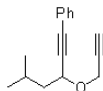
Parameter	Value
1 Title	zzt-4-151-2-SM-H
2 Solvent	CDCl3
3 Relaxation Delay	4.8000
4 Spectrometer Frequency	499.86



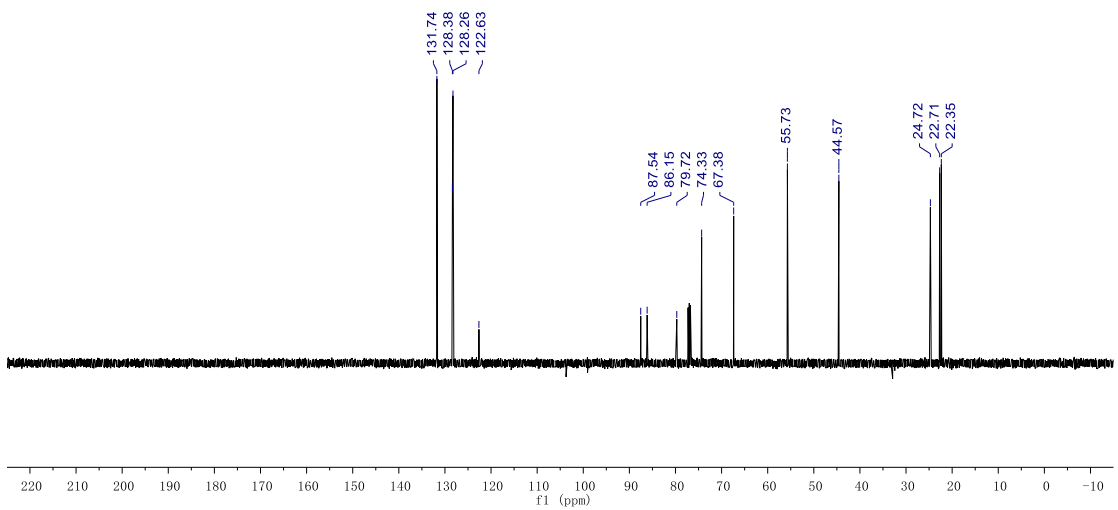
3-6m



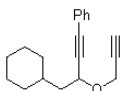
Parameter	Value
1 Title	zzt-4-151-2-SM-C
2 Solvent	CDCl3
3 Relaxation Delay	1.0000
4 Spectrometer Frequency	125.70



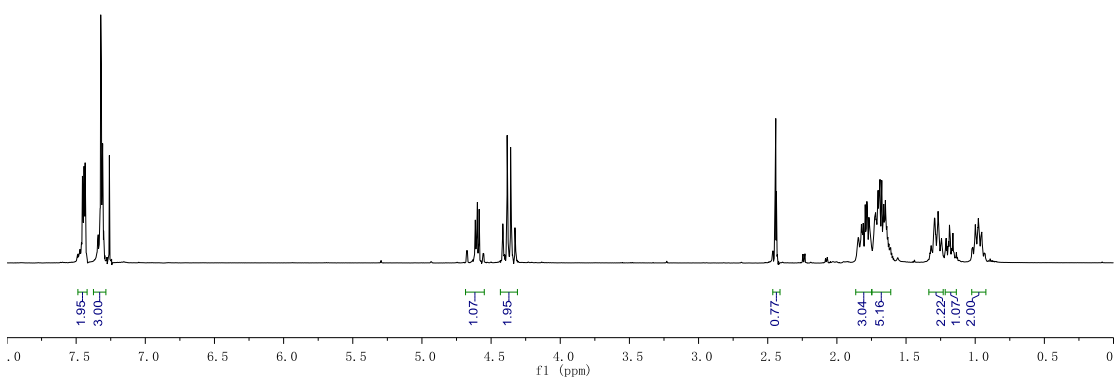
3-6m



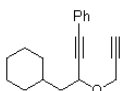
Parameter	Value
1 Title	zzt-5-9-2-SM-H
2 Solvent	CDCl3
3 Relaxation Delay	4.8000
4 Spectrometer Frequency	499.86



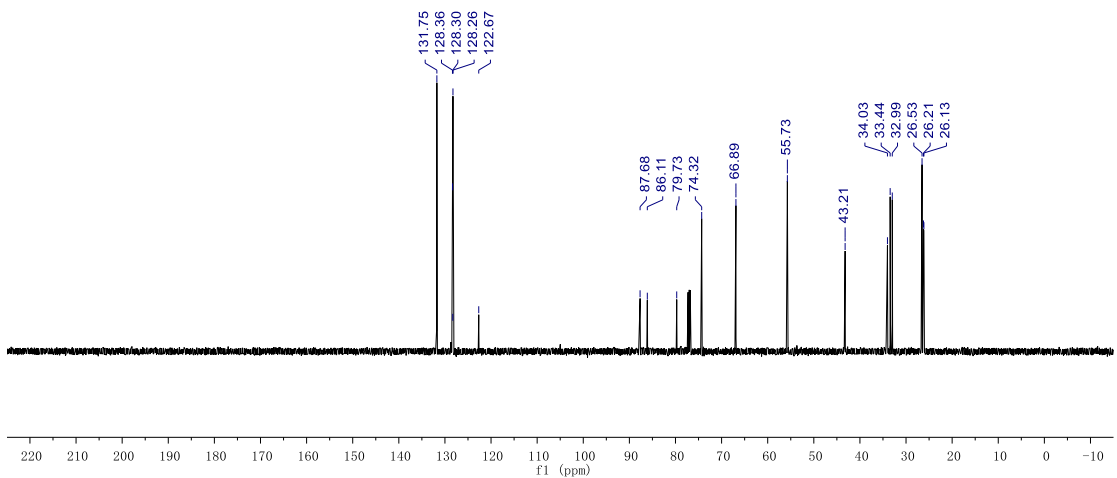
3-6n



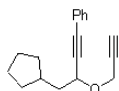
Parameter	Value
1 Title	zzt-5-9-2-SM-C
2 Solvent	CDCl3
3 Relaxation Delay	1.0000
4 Spectrometer Frequency	125.70



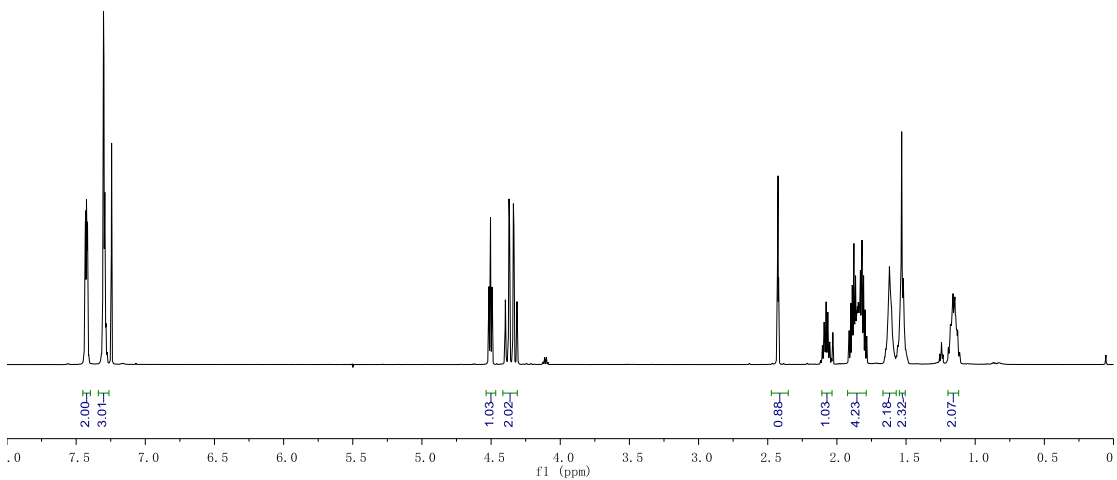
3-6n



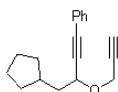
Parameter	Value
1 Title	zzt-5-9-3-SM-H-new
2 Solvent	cdcl3
3 Relaxation Delay	4.8000
4 Spectrometer Frequency	599.64



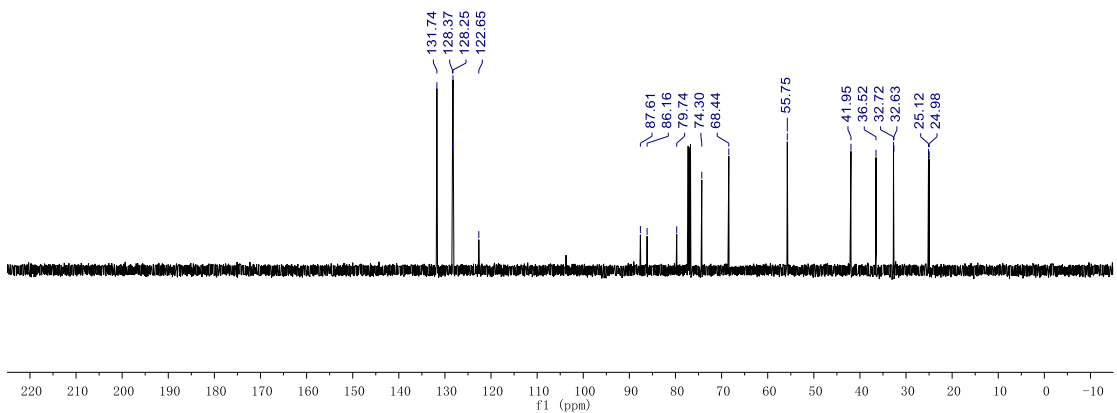
3-6o



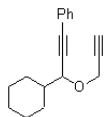
Parameter	Value
1 Title	zzt-5-9-3-SM-C
2 Solvent	CDCl3
3 Relaxation Delay	1.0000
4 Spectrometer Frequency	125.70



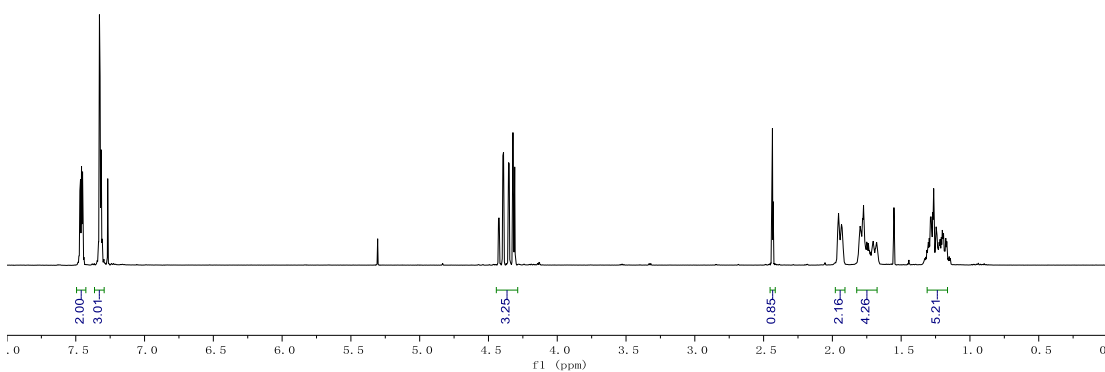
3-6o



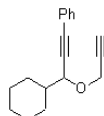
Parameter	Value
1 Title	zzt-18-4-SM-H
2 Solvent	CDCl3
3 Spectrometer Frequency	499.86
4 Nucleus	1H



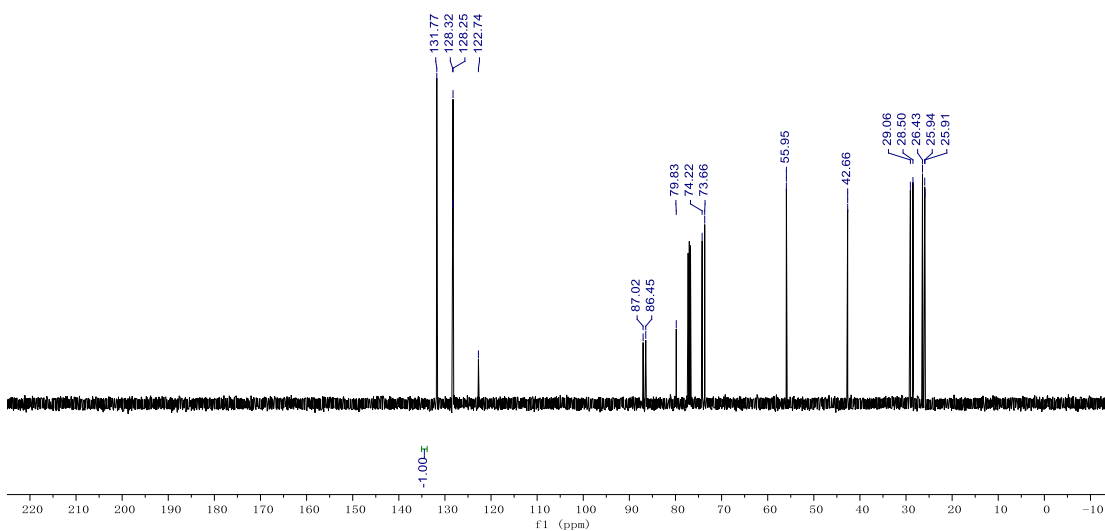
3-6p



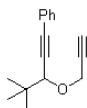
Parameter	Value
1 Title	zzt-18-4-SM-C
2 Solvent	CDCl3
3 Spectrometer Frequency	125.70
4 Nucleus	13C



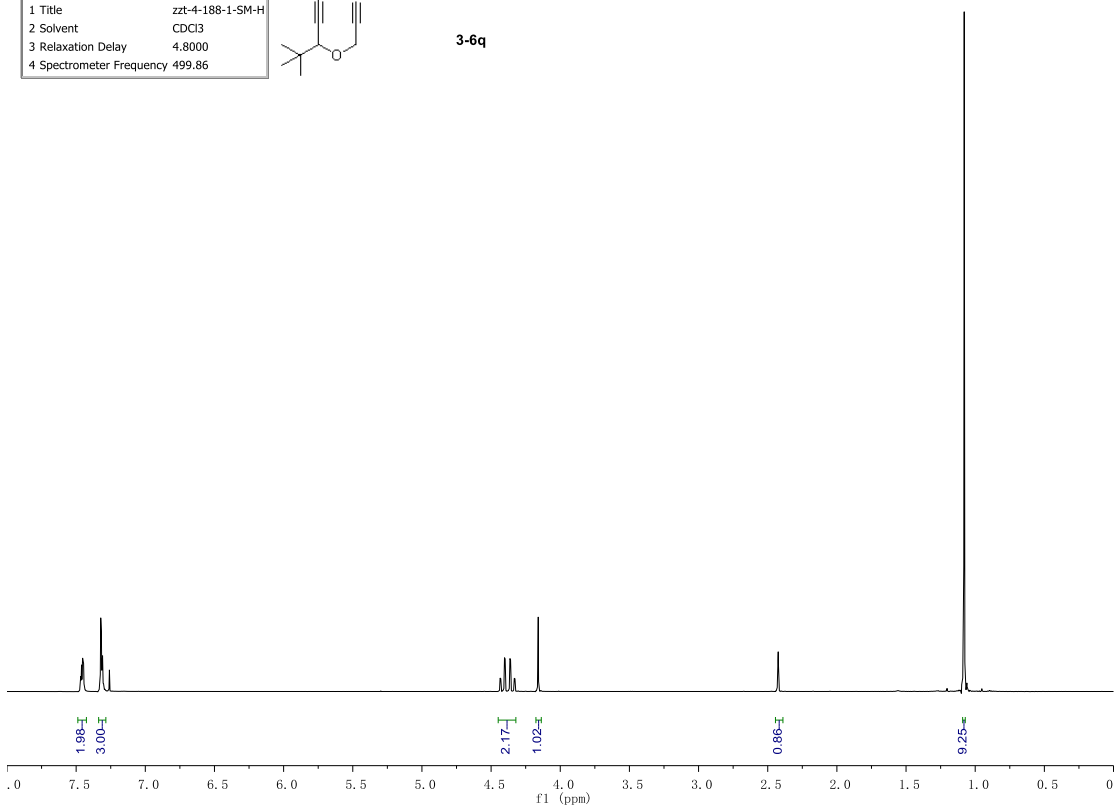
3-6p



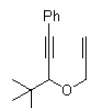
Parameter	Value
1 Title	zzt-4-188-1-SM-H
2 Solvent	CDCl3
3 Relaxation Delay	4.8000
4 Spectrometer Frequency	499.86



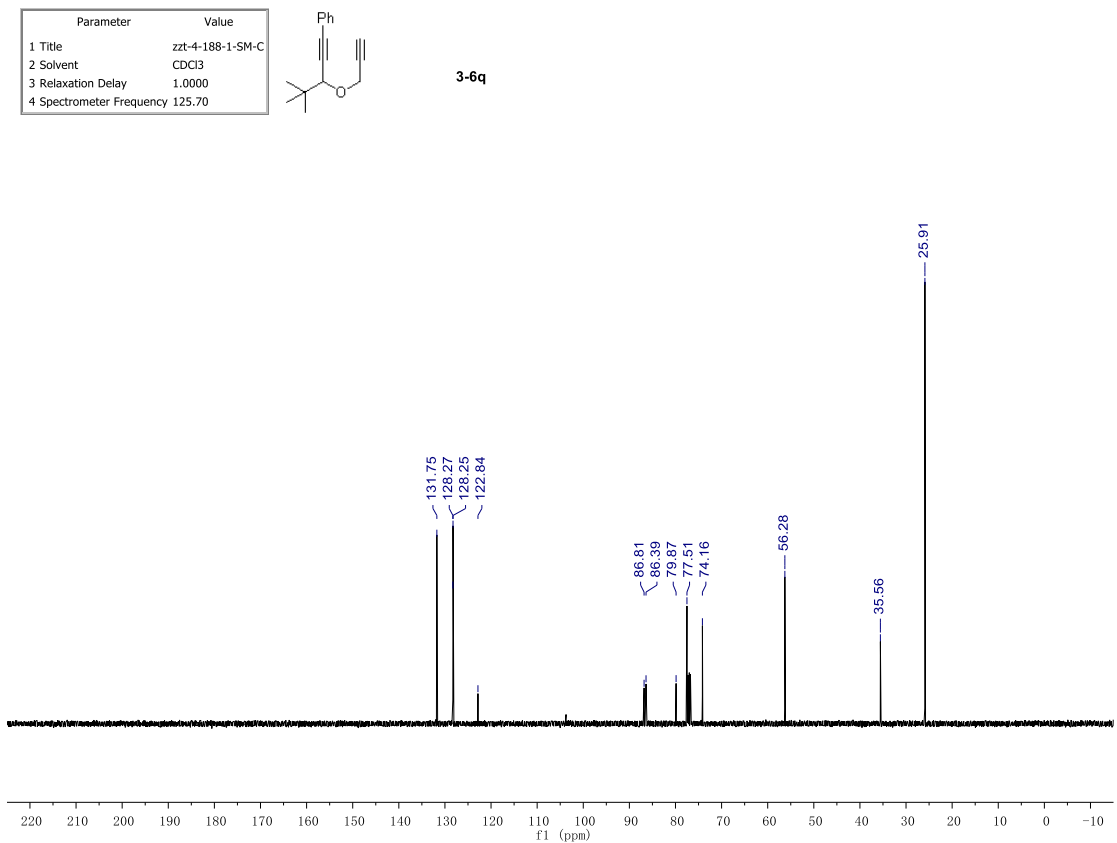
3-6q



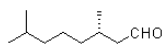
Parameter	Value
1 Title	zzt-4-188-1-SM-C
2 Solvent	CDCl3
3 Relaxation Delay	1.0000
4 Spectrometer Frequency	125.70



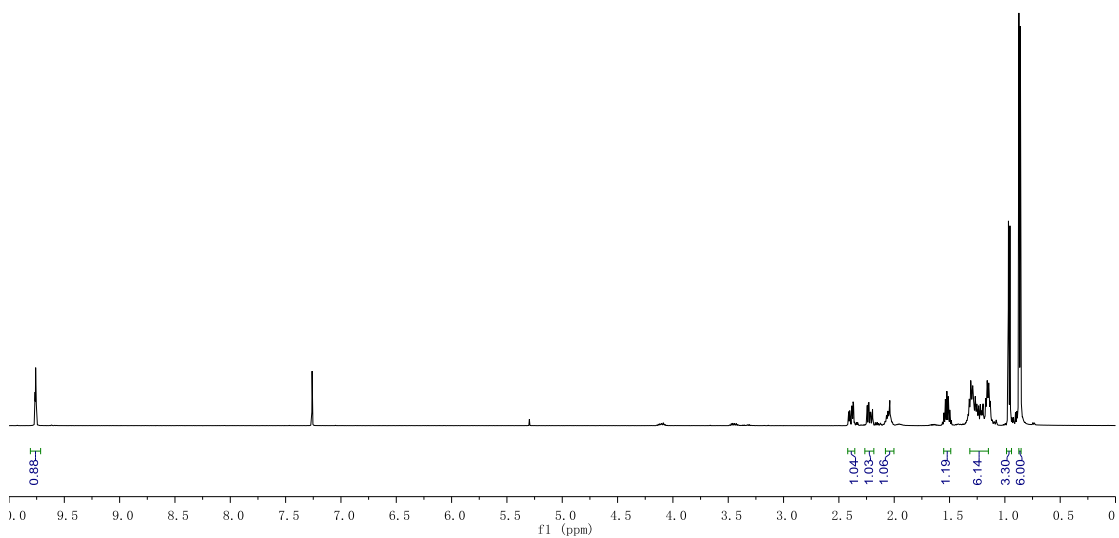
3-6q



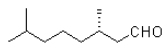
Parameter	Value
1 Title	zzt-5-8-2-H
2 Solvent	CDCl3
3 Relaxation Delay	4.8000
4 Spectrometer Frequency	499.86



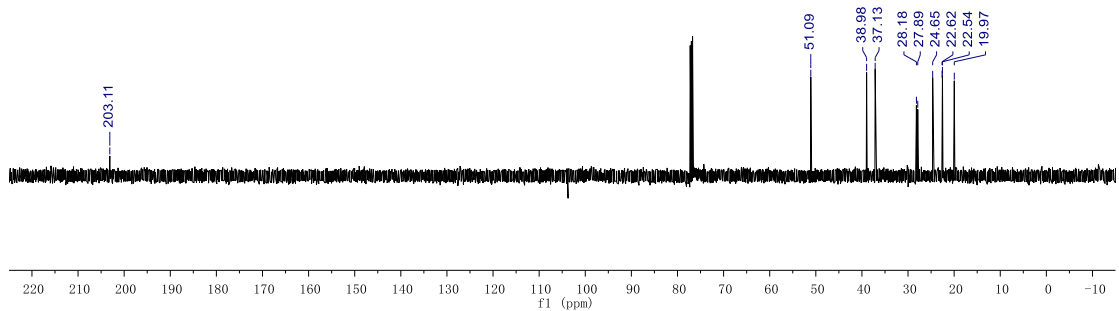
3-A



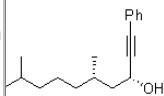
Parameter	Value
1 Title	zzt-5-8-2-C
2 Solvent	CDCl3
3 Relaxation Delay	1.0000
4 Spectrometer Frequency	125.70



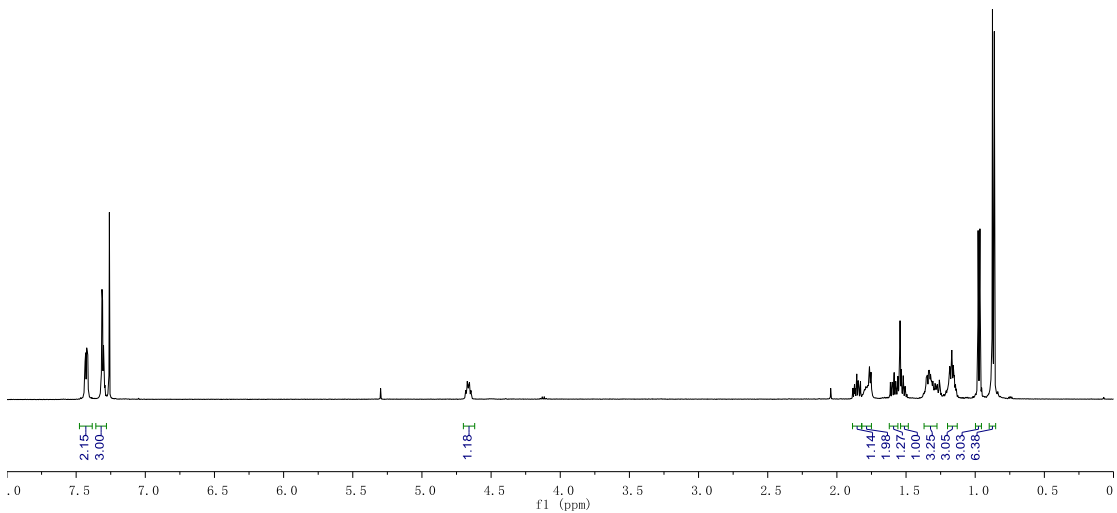
3-A



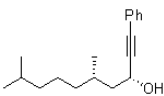
Parameter	Value
1 Title	zzt-5-8-3-H-good
2 Solvent	CDCl3
3 Relaxation Delay	4.8000
4 Spectrometer Frequency	499.86



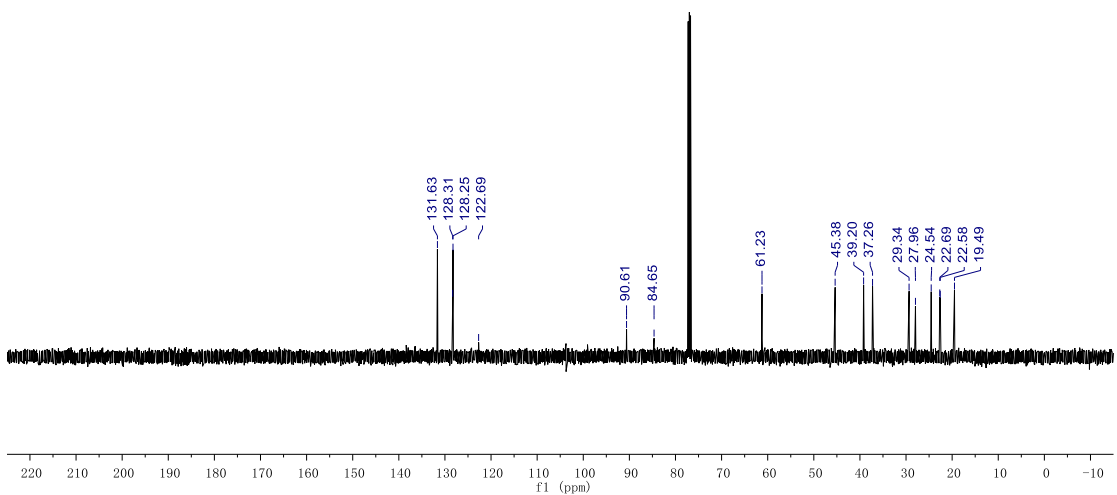
3-B



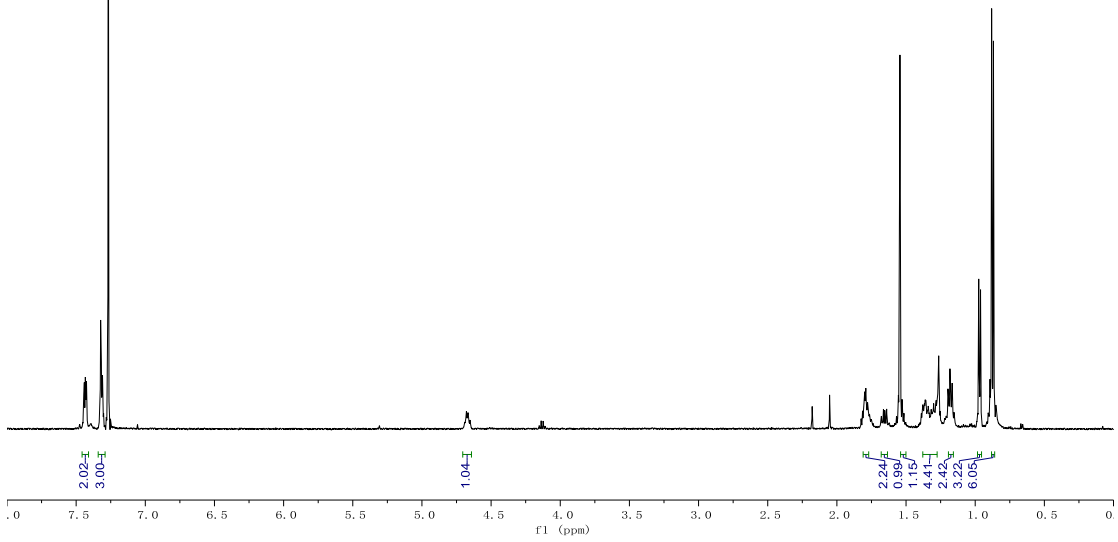
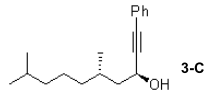
Parameter	Value
1 Title	zzt-5-8-3-C
2 Solvent	CDCl3
3 Relaxation Delay	1.0000
4 Spectrometer Frequency	125.70



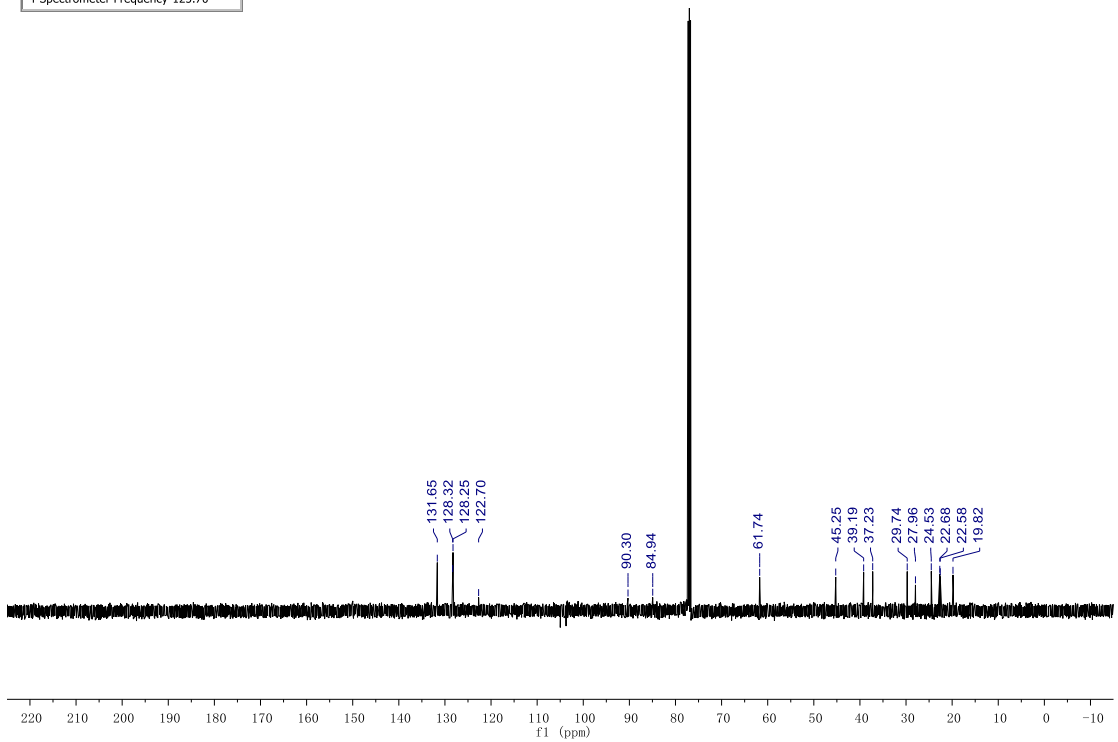
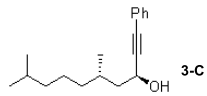
3-B



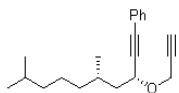
Parameter	Value
1 Title	zzt-5-12-2-H-new
2 Solvent	CDCl3
3 Spectrometer Frequency	499.86
4 Nucleus	1H



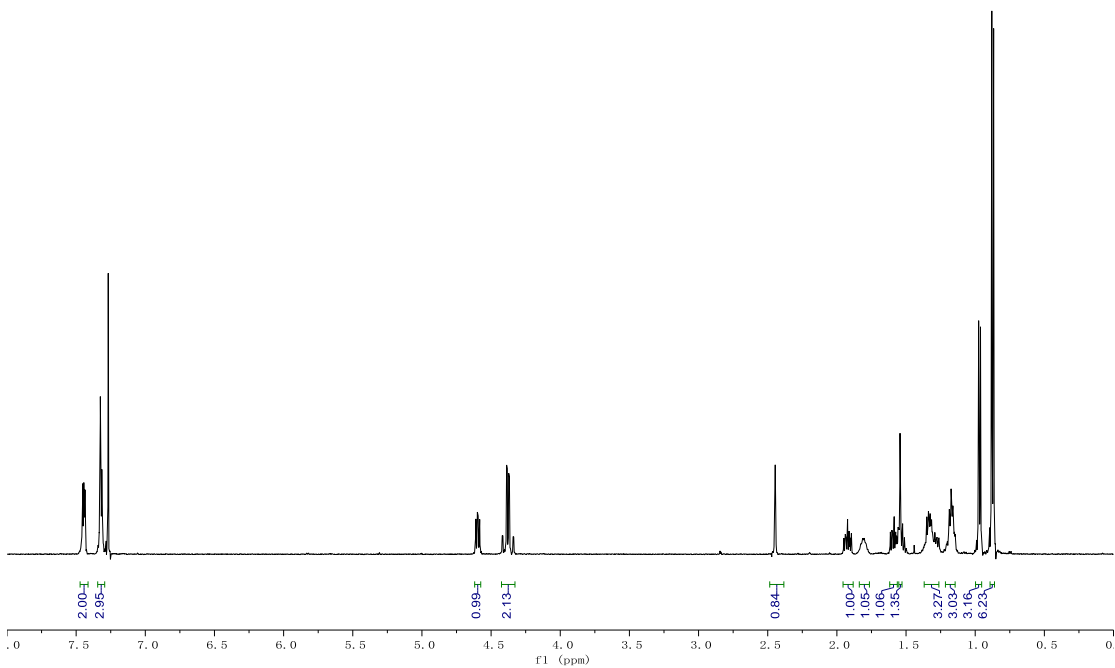
Parameter	Value
1 Title	zzt-5-12-2-C
2 Solvent	CDCl3
3 Relaxation Delay	1.0000
4 Spectrometer Frequency	125.70



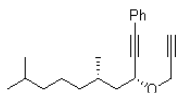
Parameter	Value
1 Title	zzt-5-10-2-H-new
2 Solvent	CDCl3
3 Spectrometer Frequency	499.86
4 Nucleus	1H



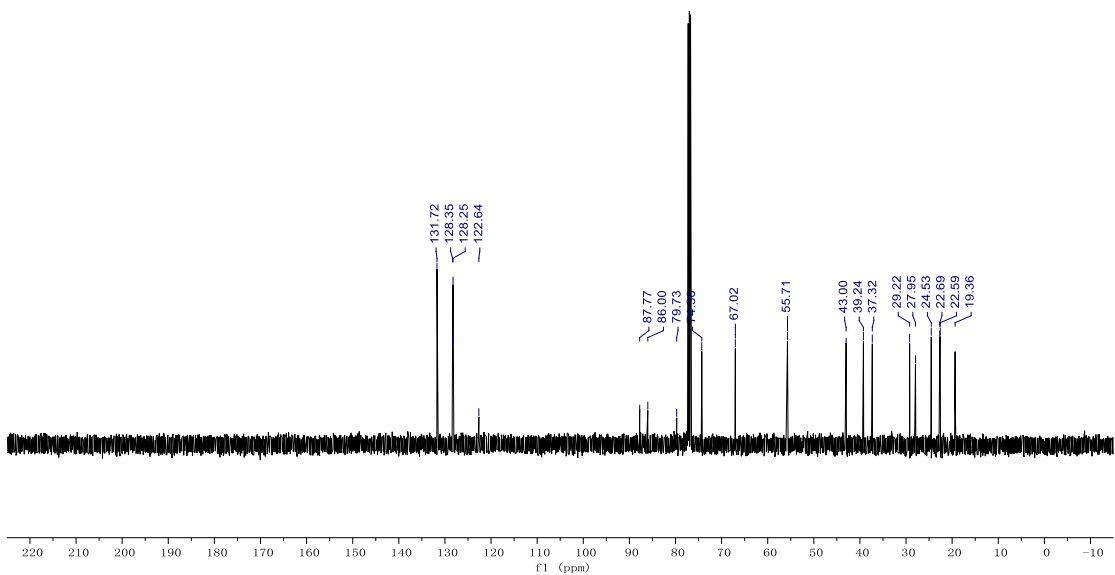
(3R, 5S)-3-6r



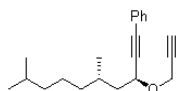
Parameter	Value
1 Title	zzt-5-10-2-C-new
2 Solvent	CDCl3
3 Spectrometer Frequency	125.70
4 Nucleus	13C



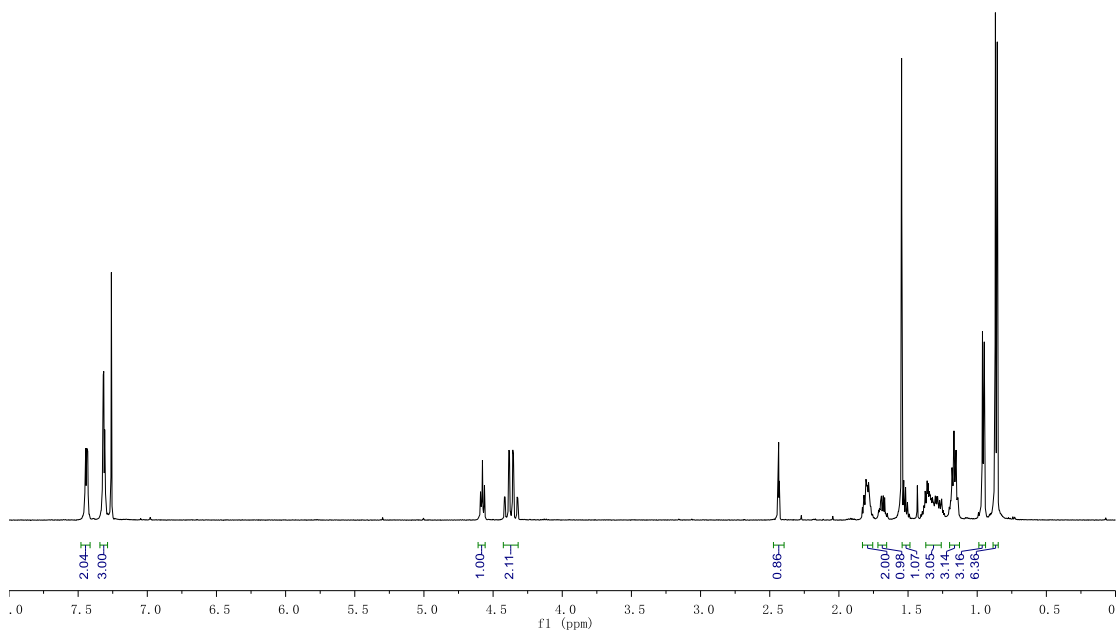
(3R, 5S)-3-6r



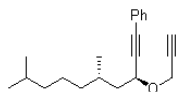
Parameter	Value
1 Title	zzt-5-12-3-H
2 Solvent	CDCl3
3 Relaxation Delay	4.8000
4 Spectrometer Frequency	499.86



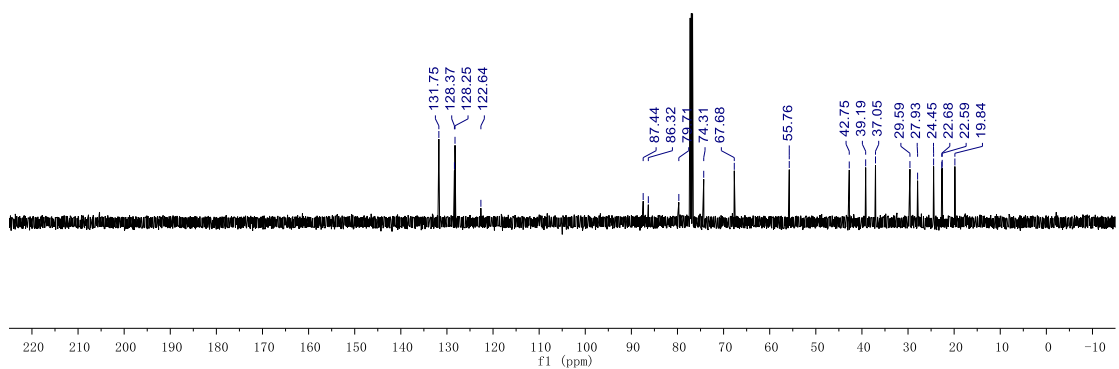
(3S, 5S)-3-6r



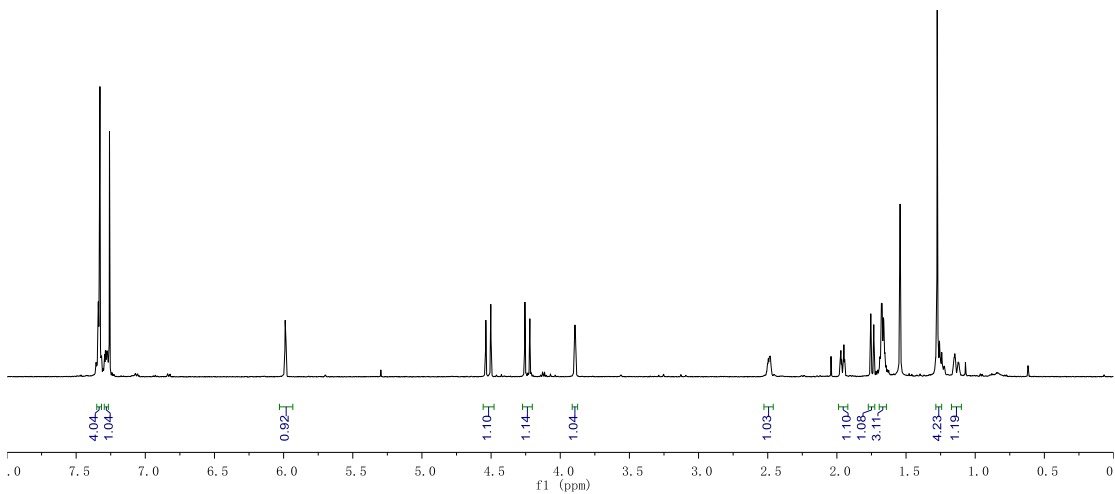
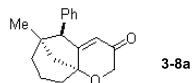
Parameter	Value
1 Title	zzt-5-12-3-C
2 Solvent	CDCl3
3 Relaxation Delay	1.0000
4 Spectrometer Frequency	125.70



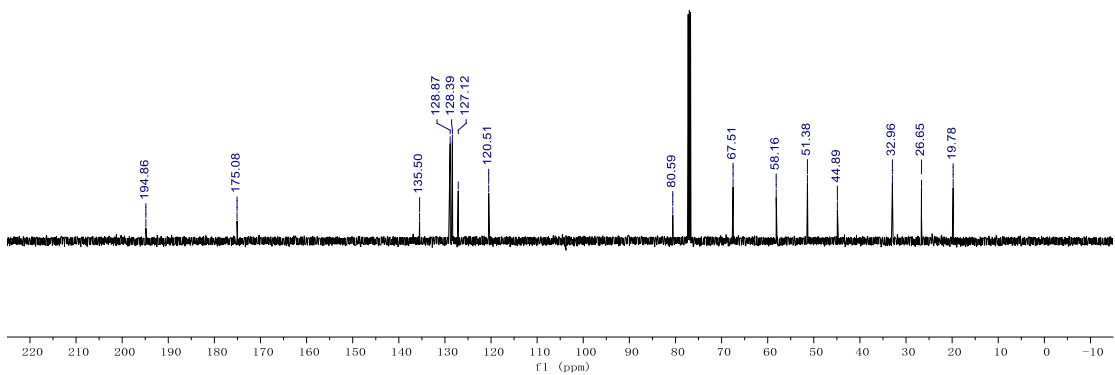
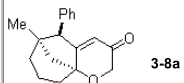
(3S, 5S)-3-6r

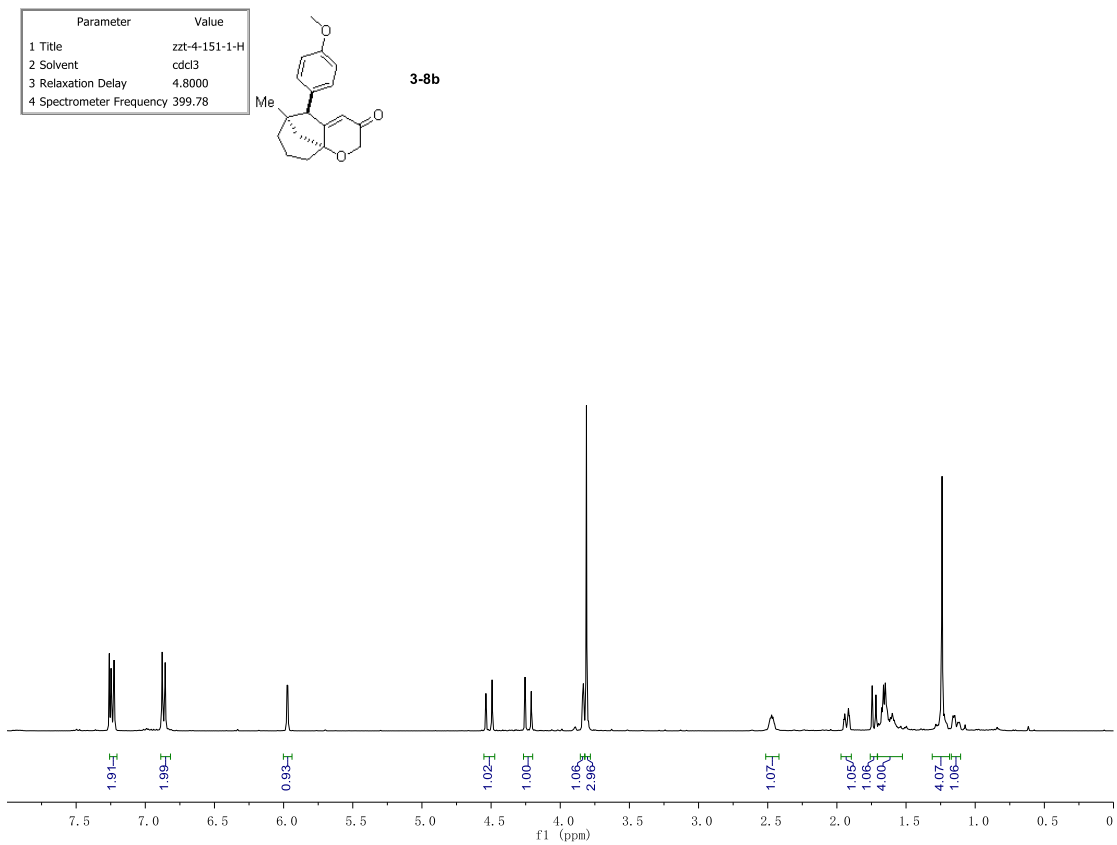
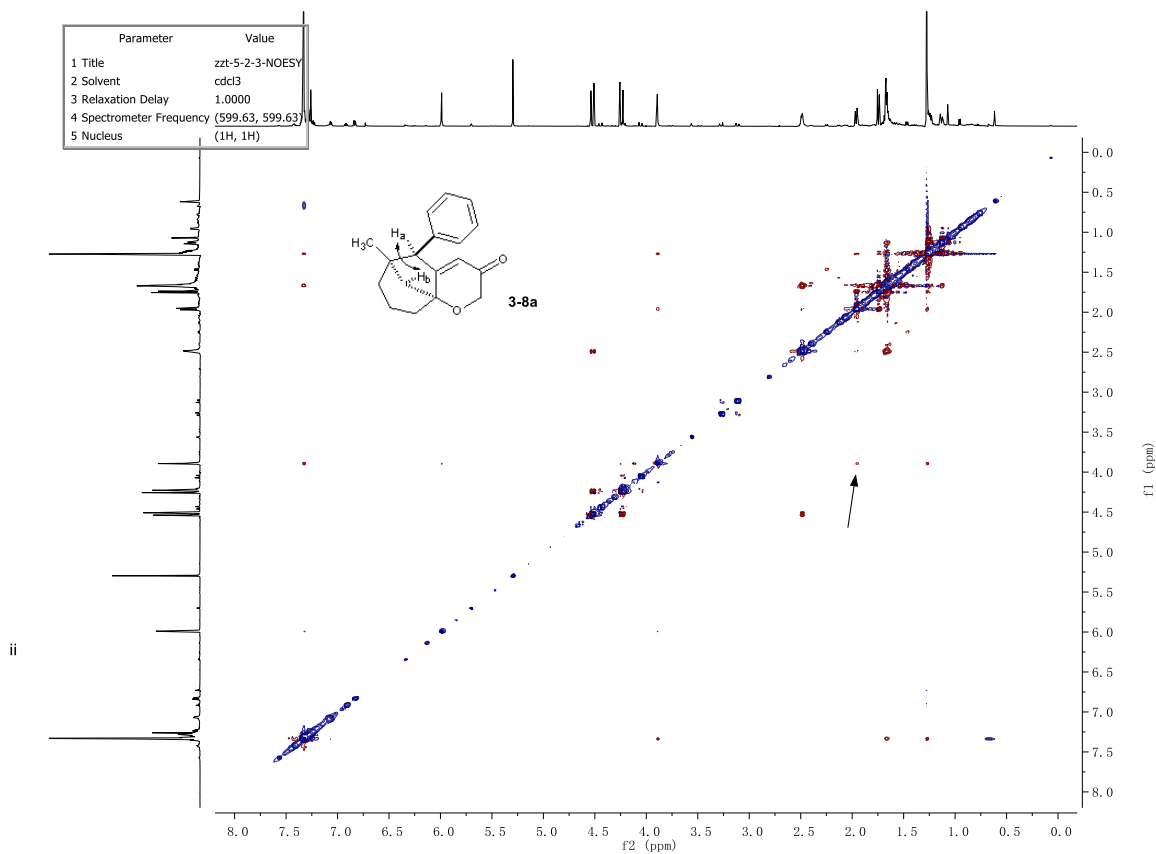


Parameter	Value
1 Title	zzt-5-2-3-pure-H
2 Solvent	CDCl3
3 Relaxation Delay	4.8000
4 Spectrometer Frequency	499.86

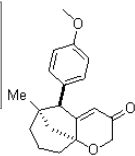


Parameter	Value
1 Title	zzt-5-2-3-C-new
2 Solvent	CDCl3
3 Spectrometer Frequency	125.70
4 Nucleus	13C

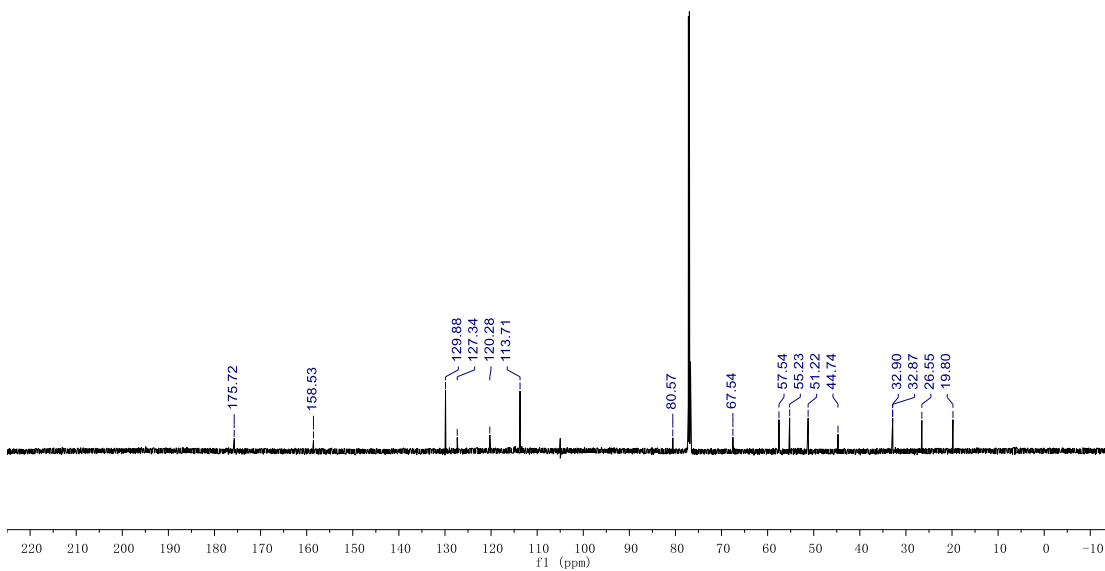




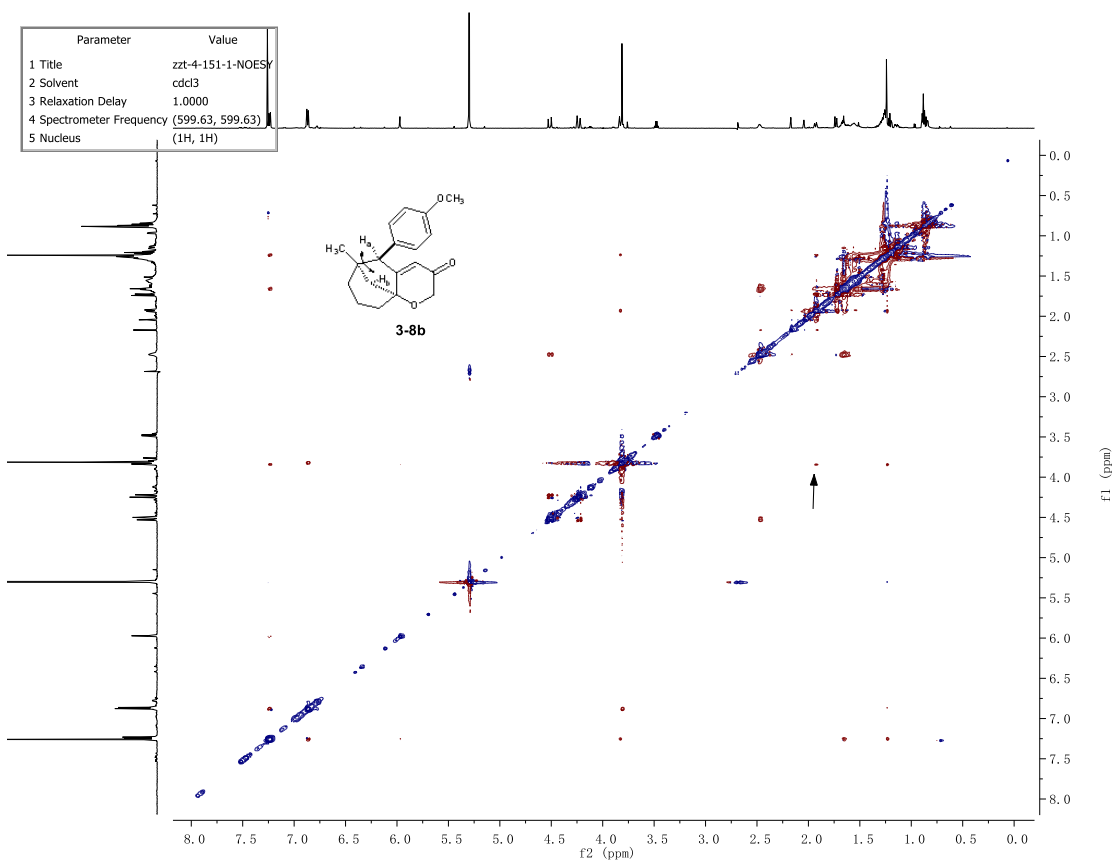
Parameter	Value
1 Title	zzt-4-151-1-C
2 Solvent	cdcl3
3 Relaxation Delay	1.0000
4 Spectrometer Frequency	150.79

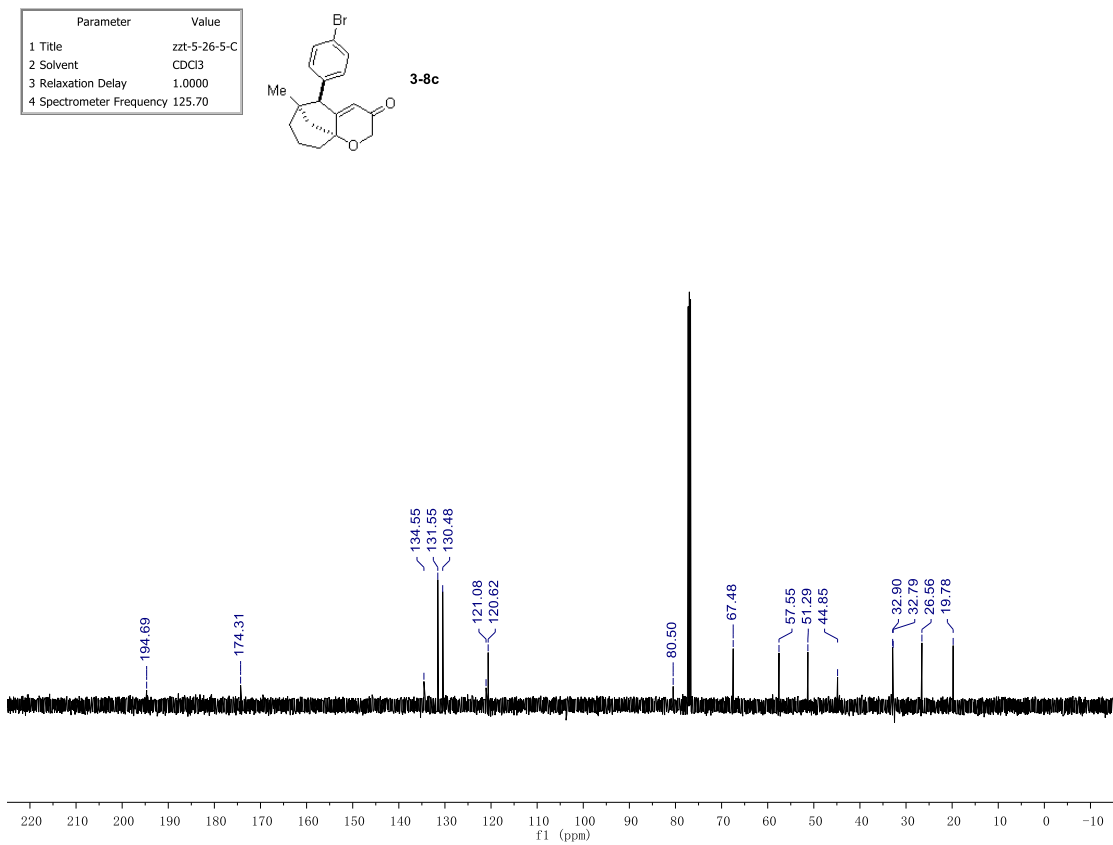
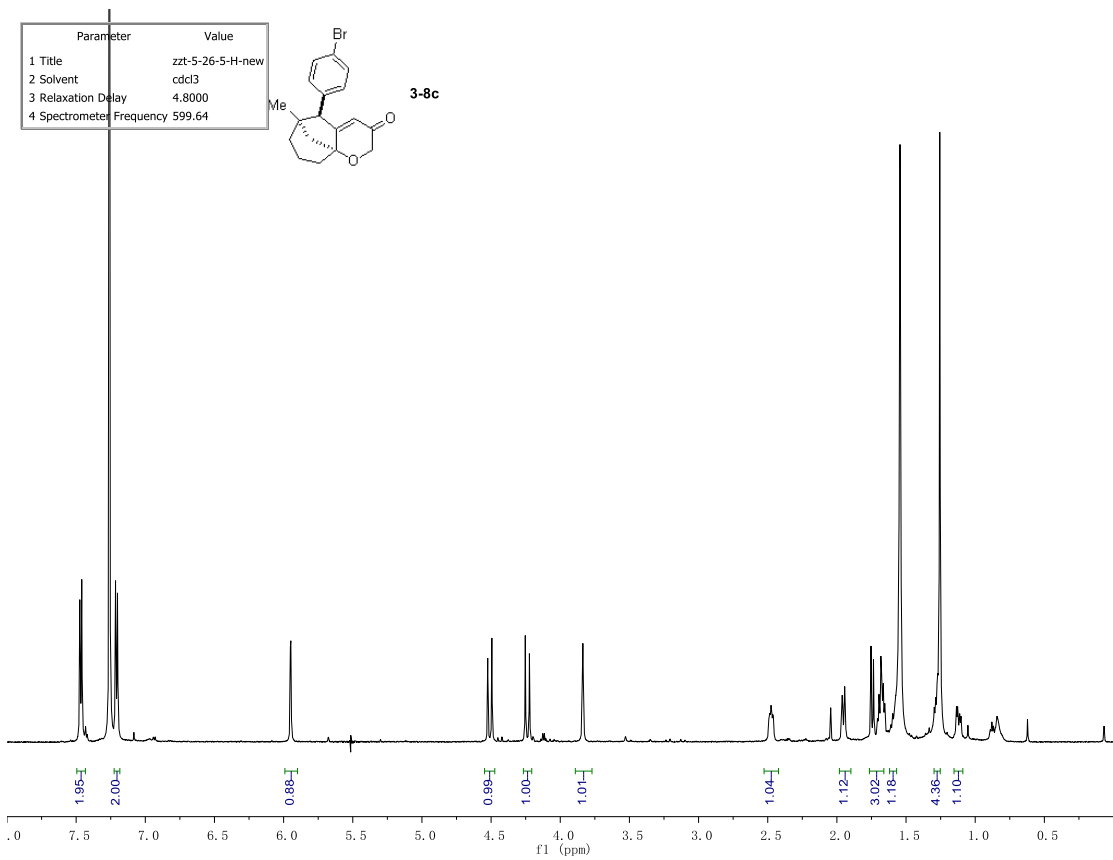


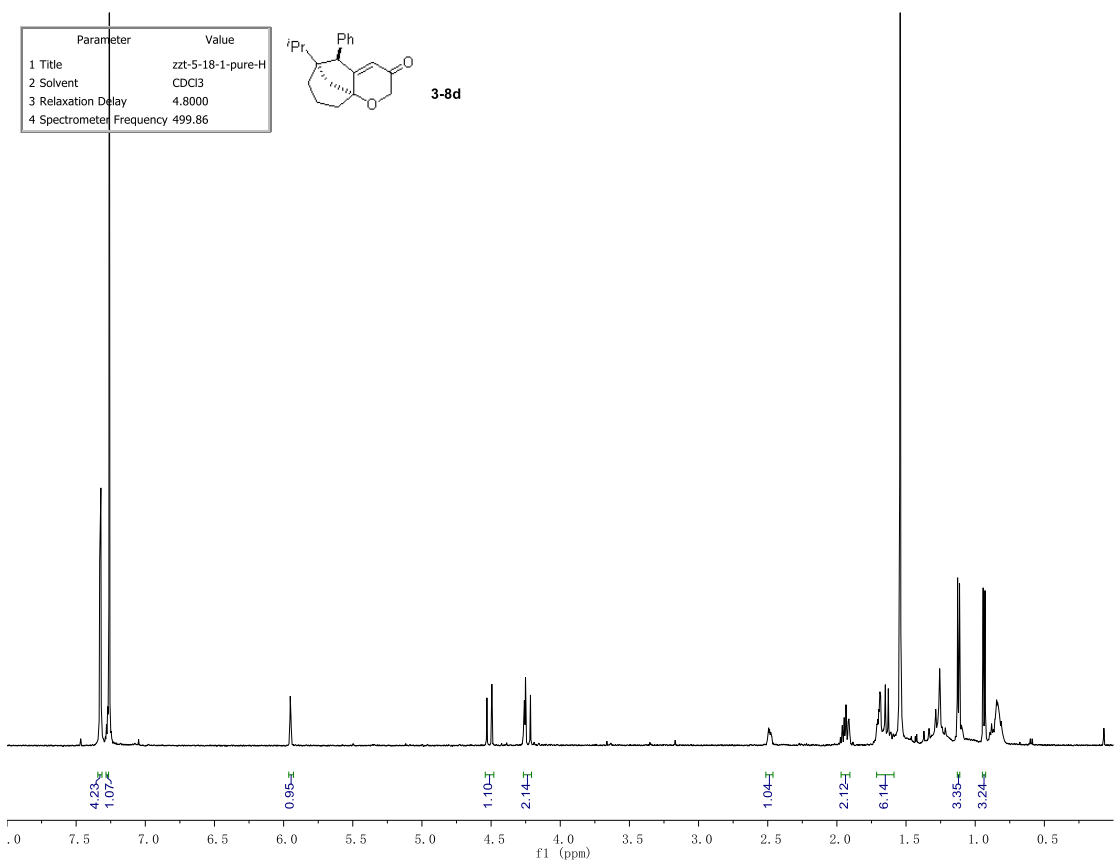
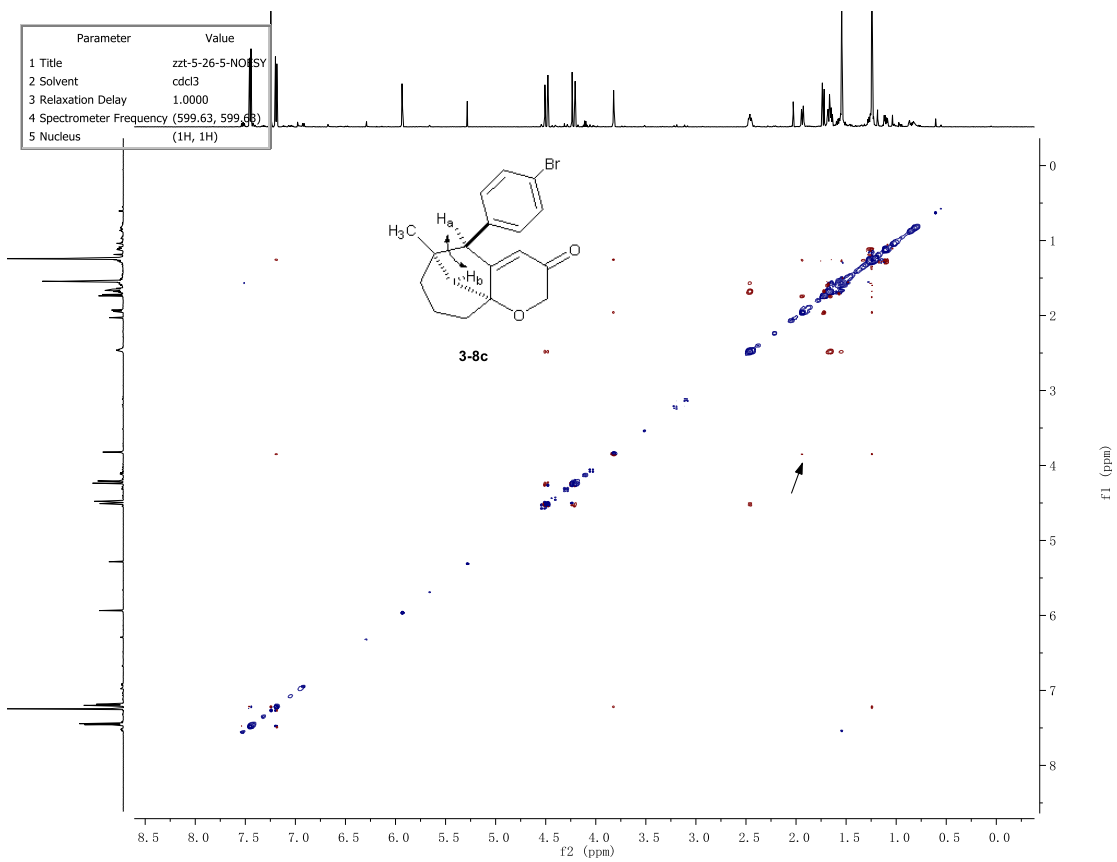
3-8b



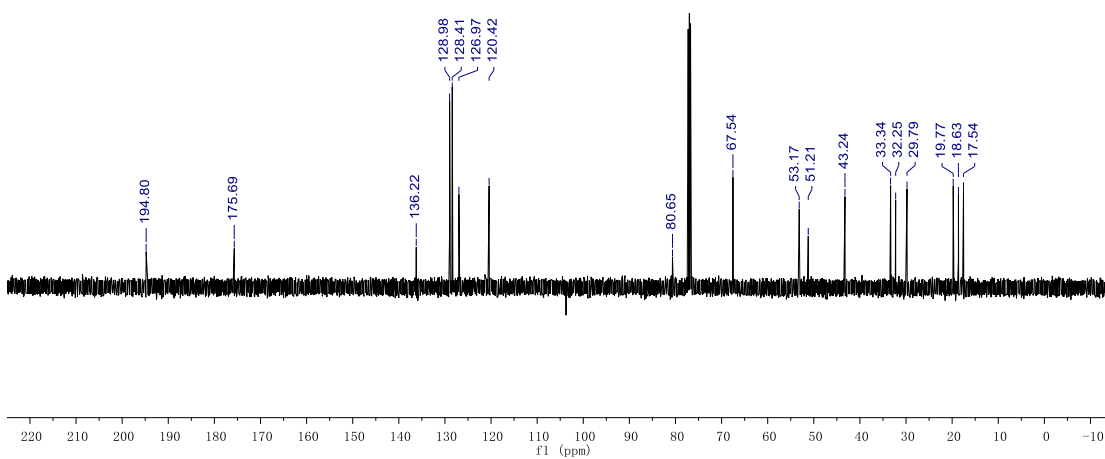
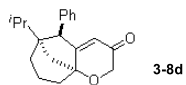
Parameter	Value
1 Title	zzt-4-151-1-NOESY
2 Solvent	cdcl3
3 Relaxation Delay	1.0000
4 Spectrometer Frequency	(599.63, 599.63)
5 Nucleus	(1H, 1H)



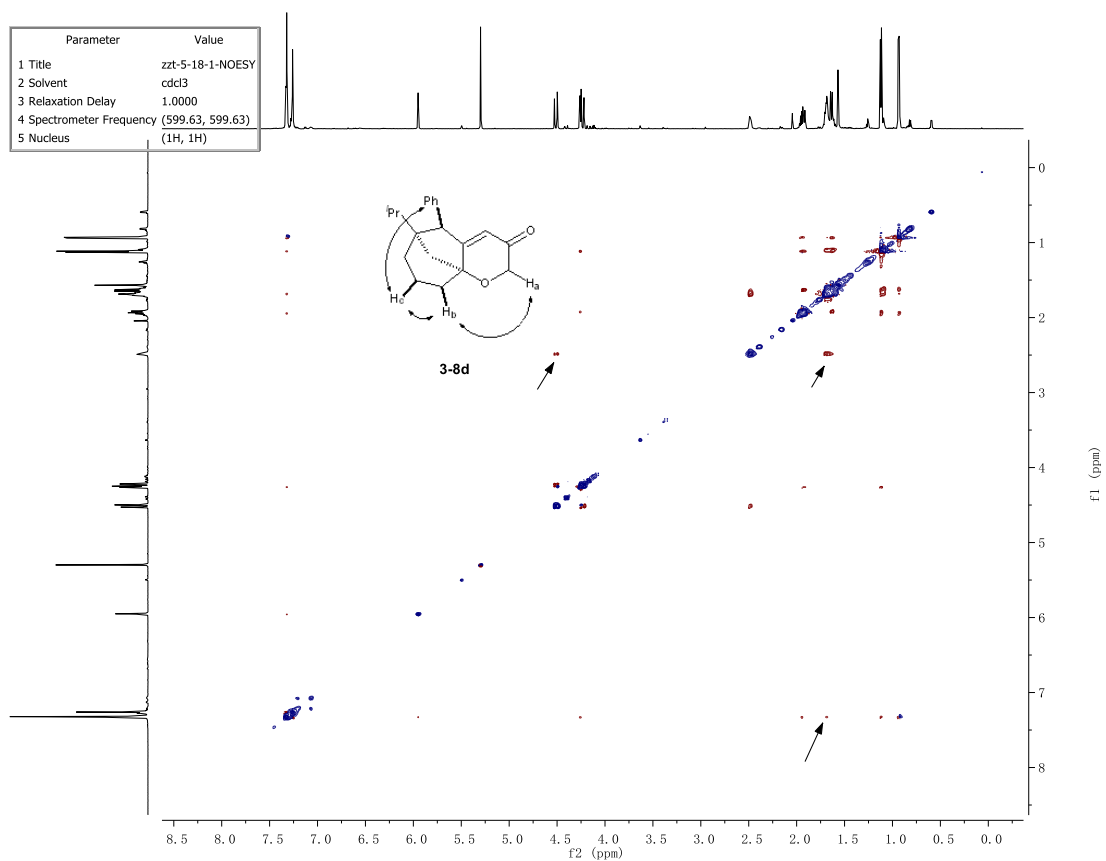


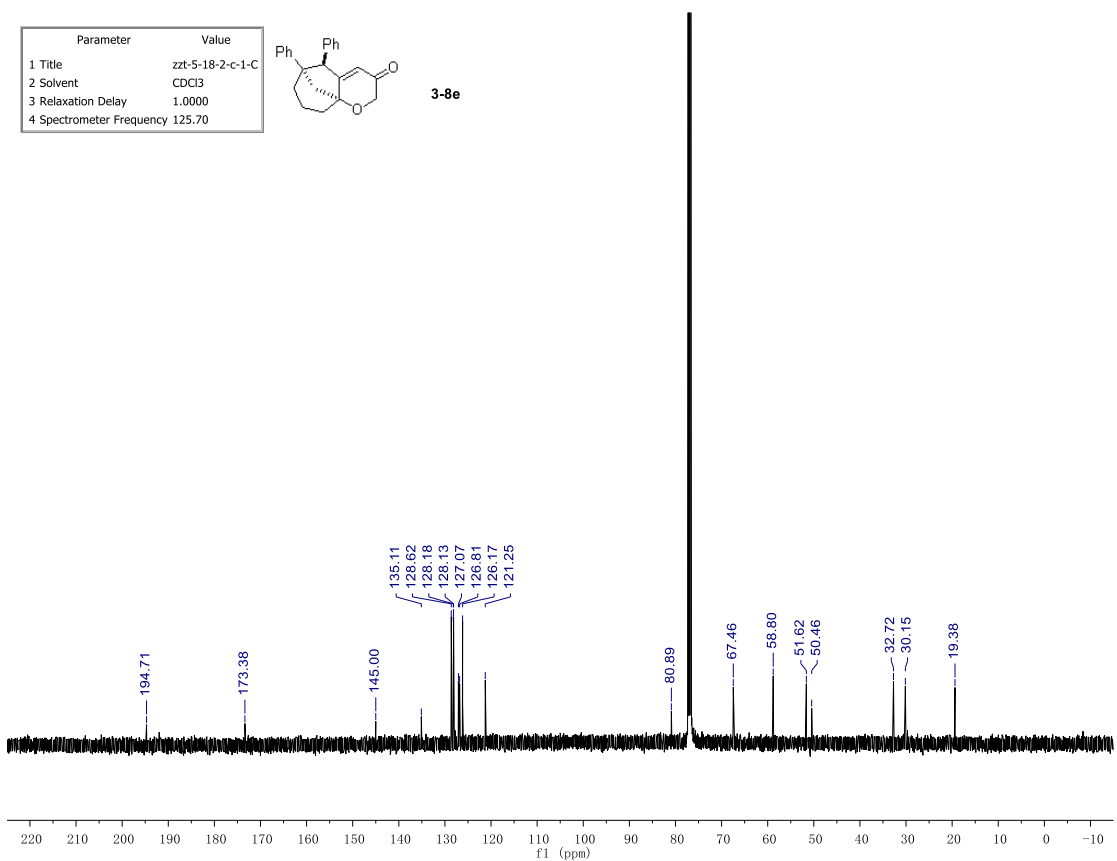
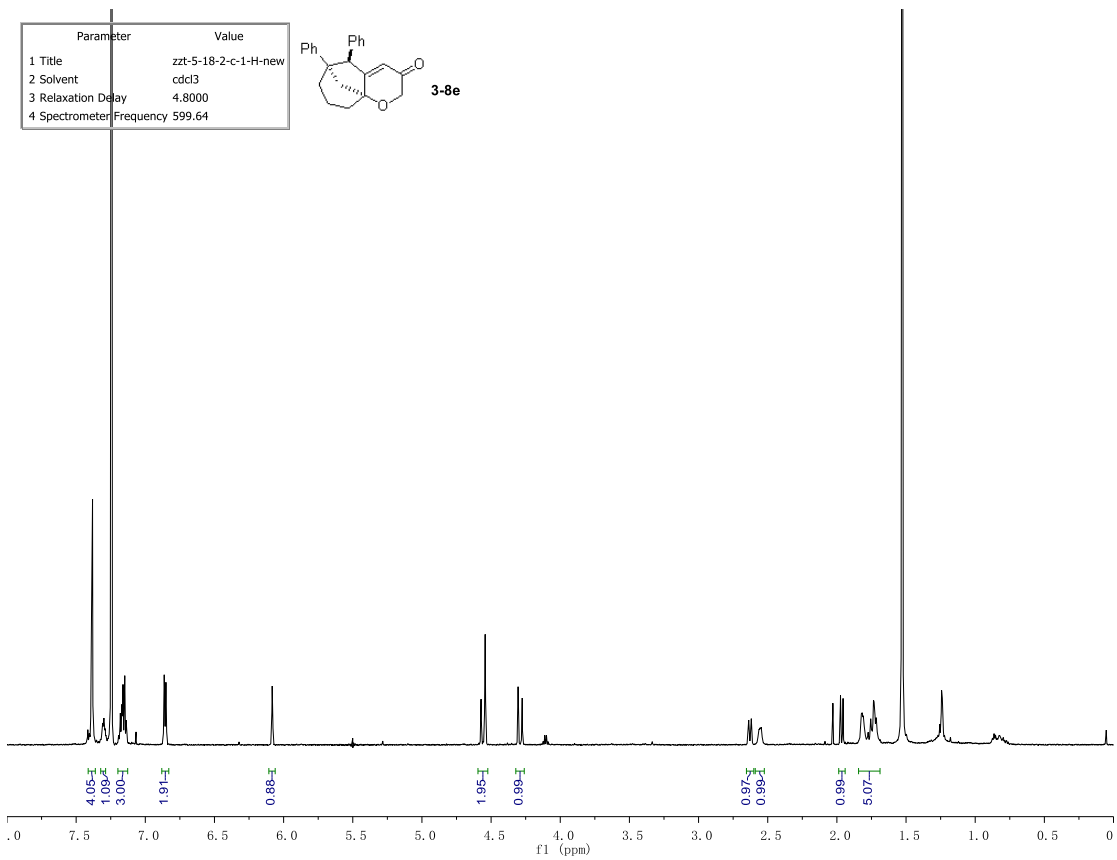


Parameter	Value
1 Title	zzt-5-18-1-C
2 Solvent	CDCl3
3 Relaxation Delay	1.0000
4 Spectrometer Frequency	125.70

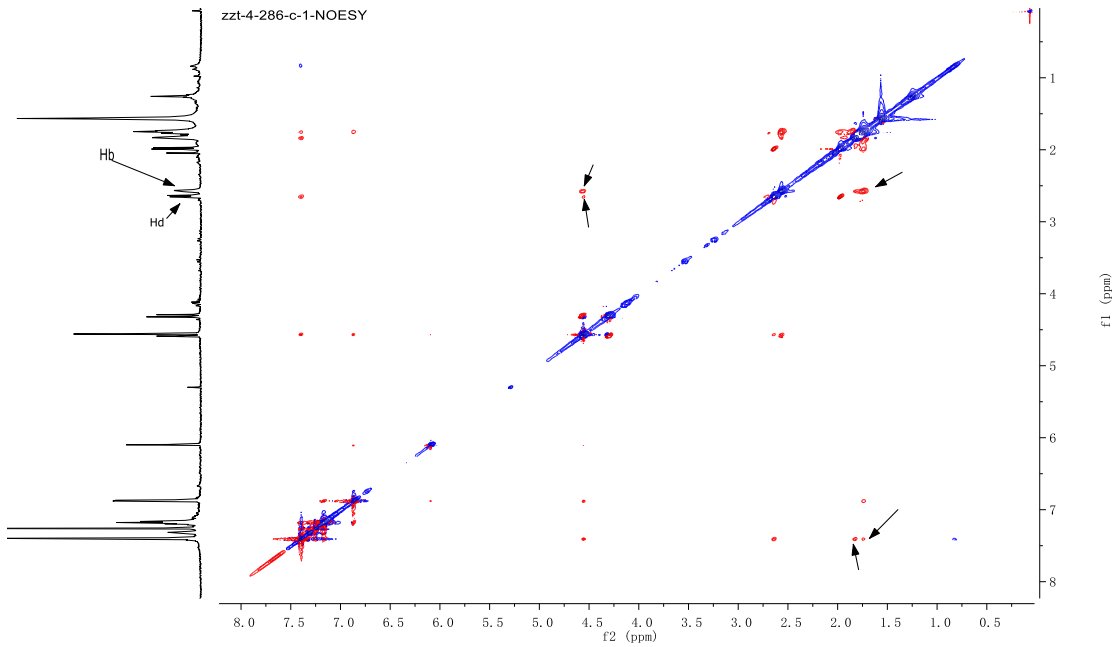
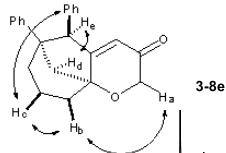


Parameter	Value
1 Title	zzt-5-18-1-NOESY
2 Solvent	cdcl3
3 Relaxation Delay	1.0000
4 Spectrometer Frequency	(599.63, 599.63)
5 Nucleus	(1H, 1H)

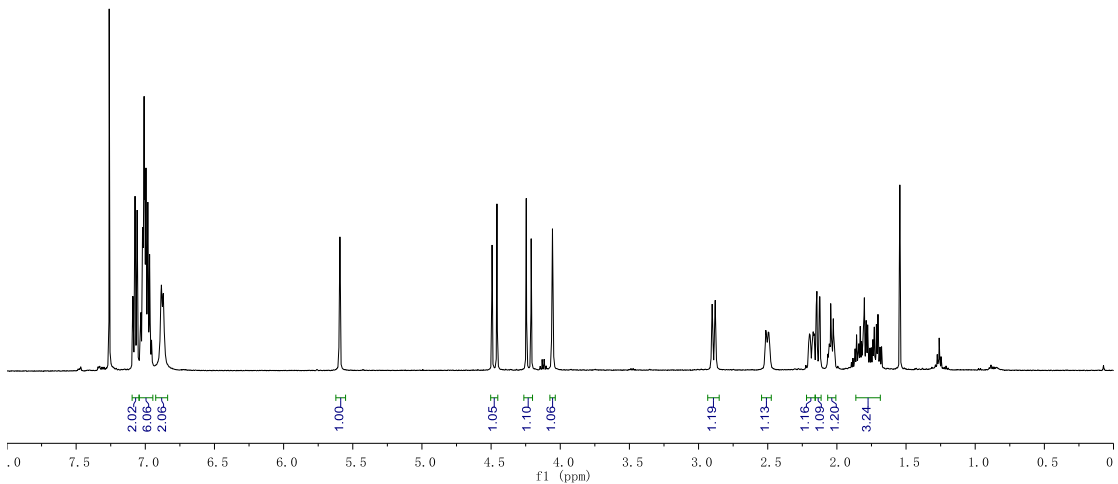
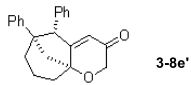




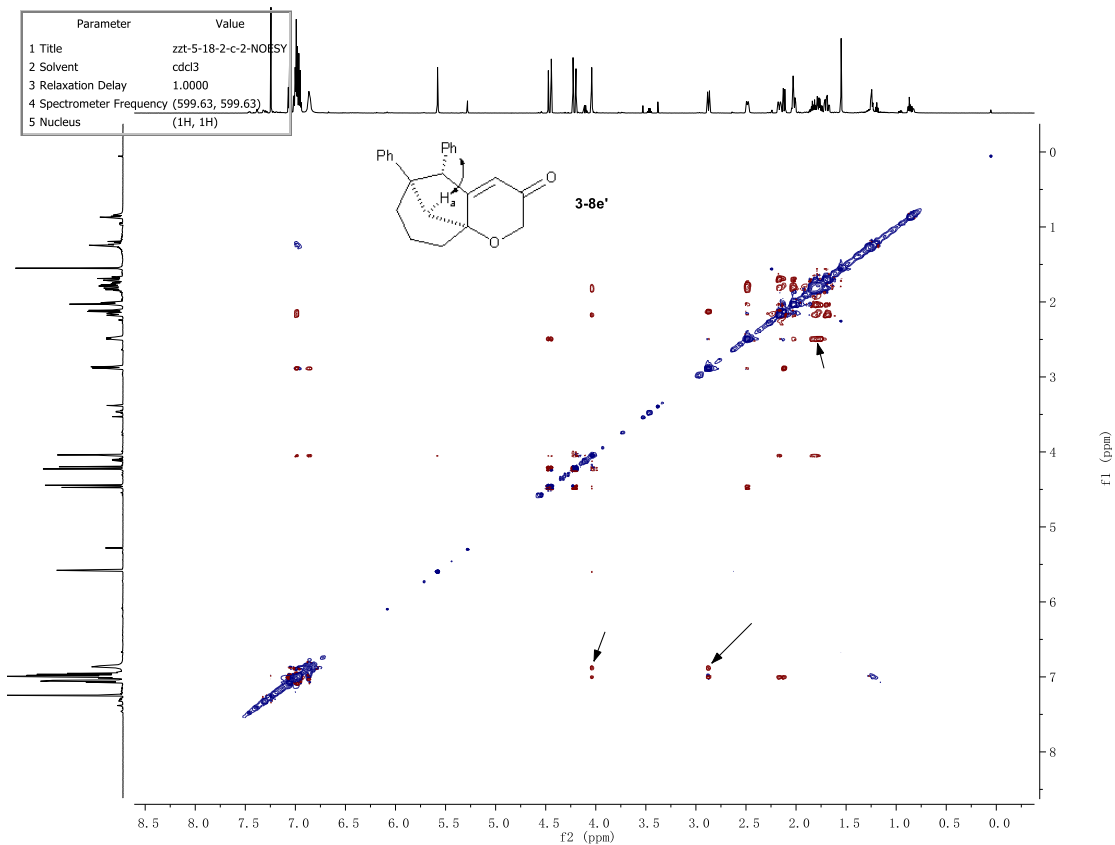
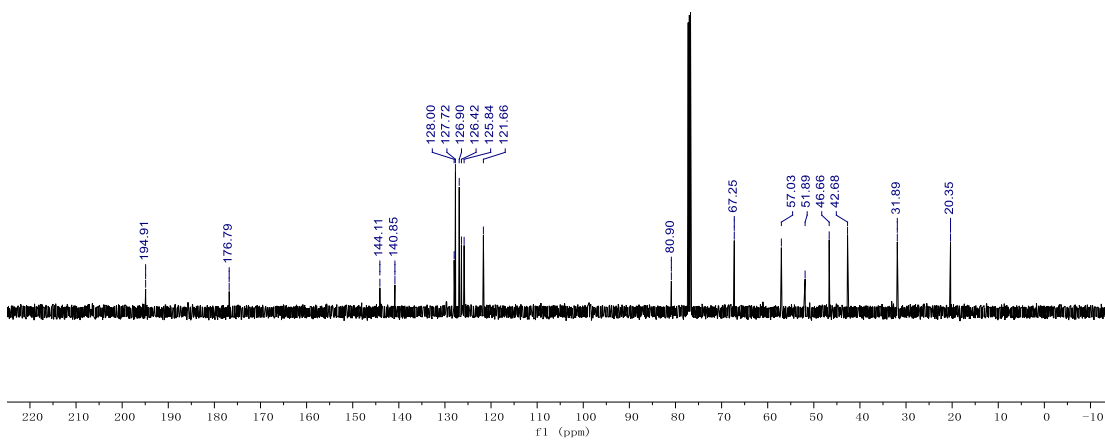
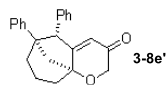
Parameter	Value
1 Title	zzt-4-286-c-1-NOESY
2 Solvent	cdcl3
3 Relaxation Delay	1.0000
4 Spectrometer Frequency (599.63, 599.63)	
5 Nucleus	(1H, 1H)



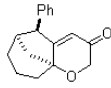
Parameter	Value
1 Title	zzt-4-18-2-c-2-H
2 Solvent	CDCl3
3 Relaxation Delay	4.8000
4 Spectrometer Frequency 499.86	



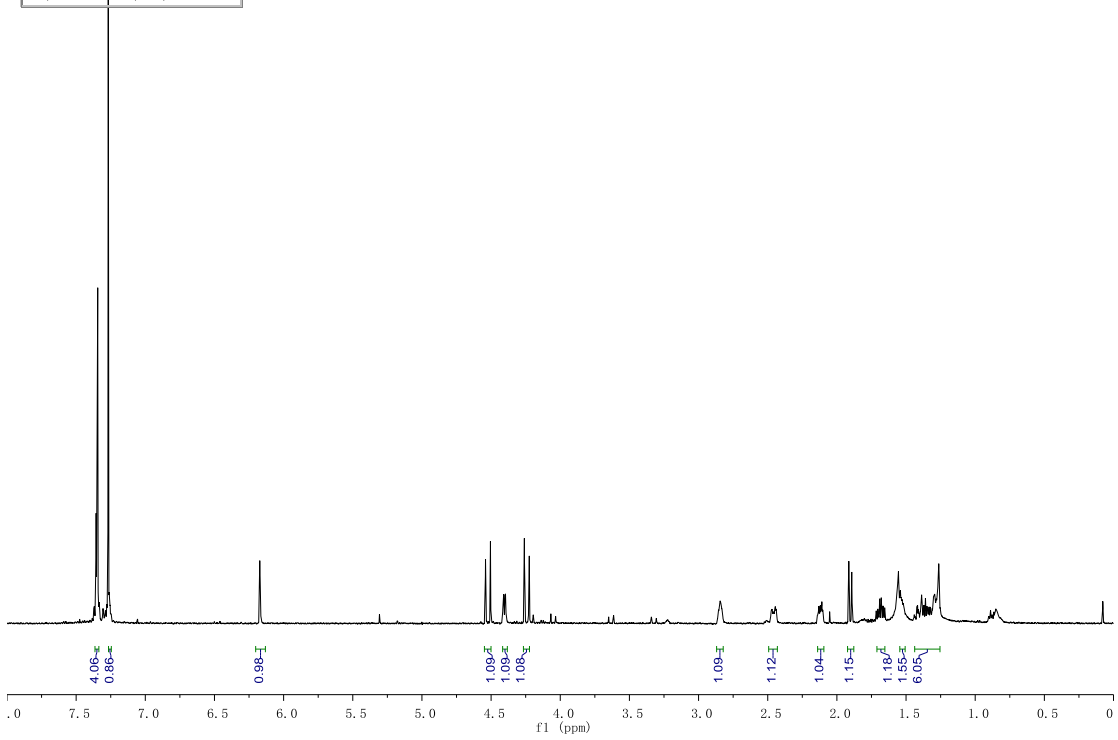
Parameter	Value
1 Title	zzt-5-18-2-c-2-Cnew
2 Solvent	CDCl3
3 Spectrometer Frequency	125.70
4 Nucleus	13C



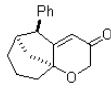
Parameter	Value
1 Title	zzt-5-26-3-H
2 Solvent	CDCl3
3 Relaxation Delay	4.8000
4 Spectrometer Frequency	499.86



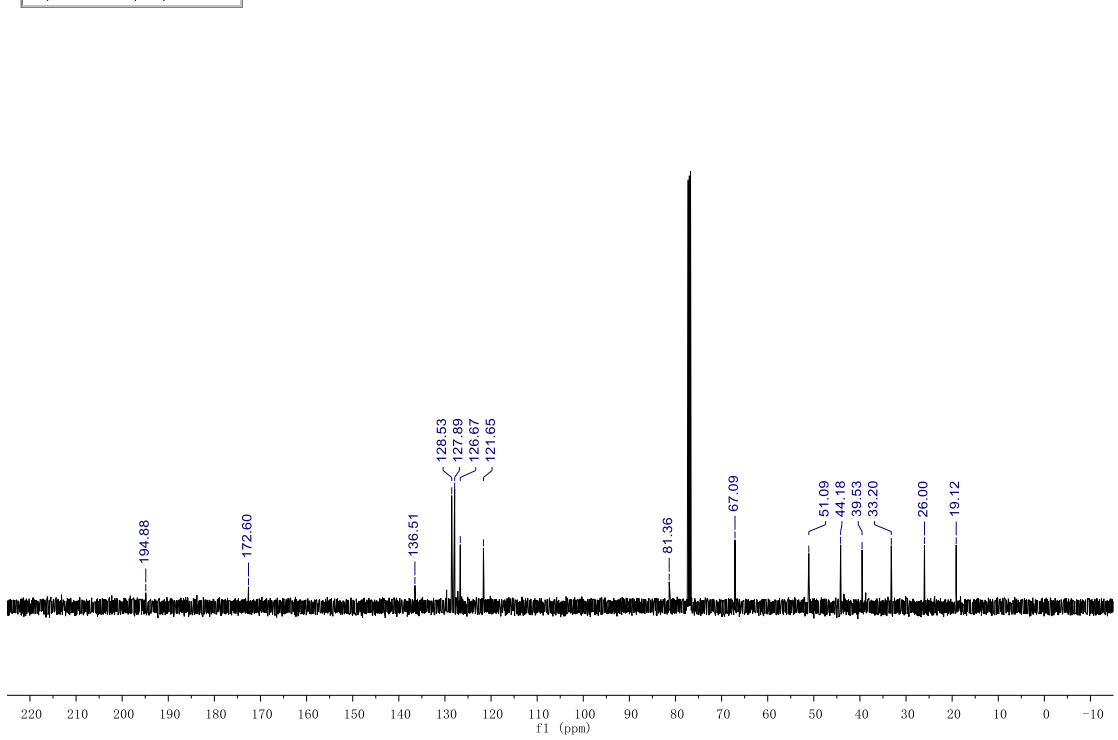
3-8f

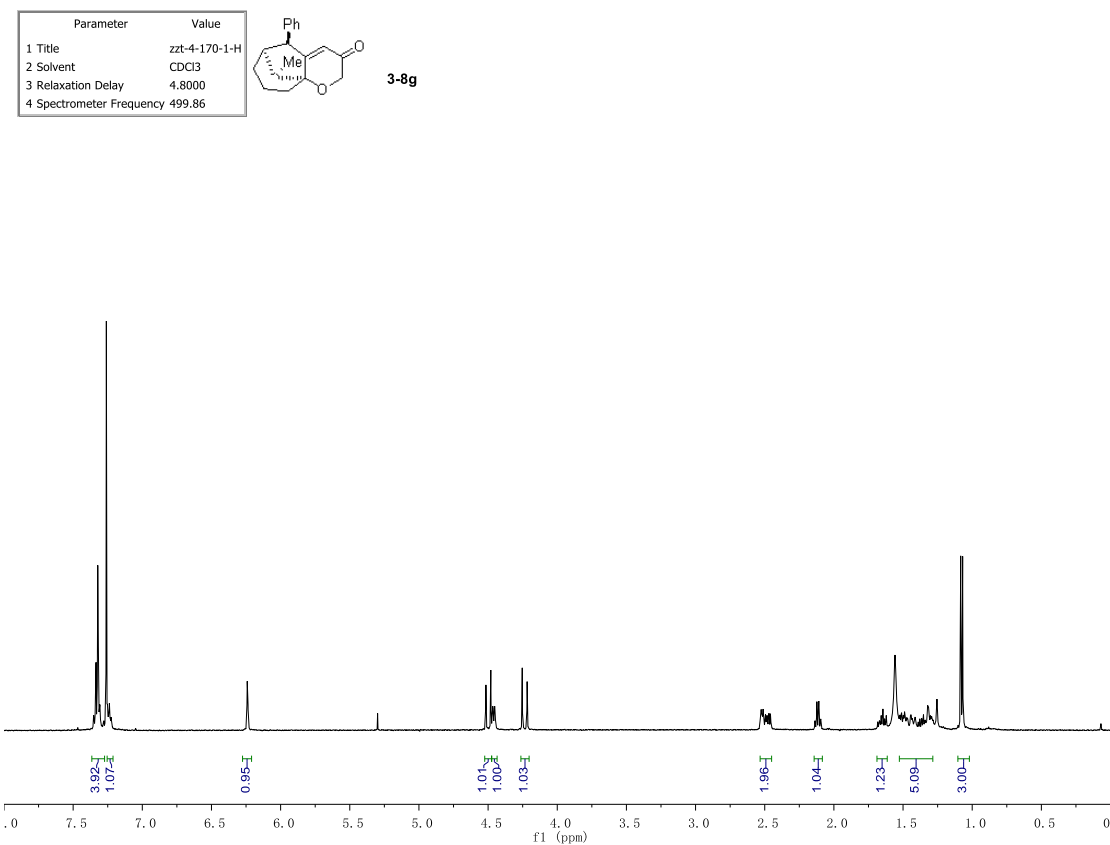
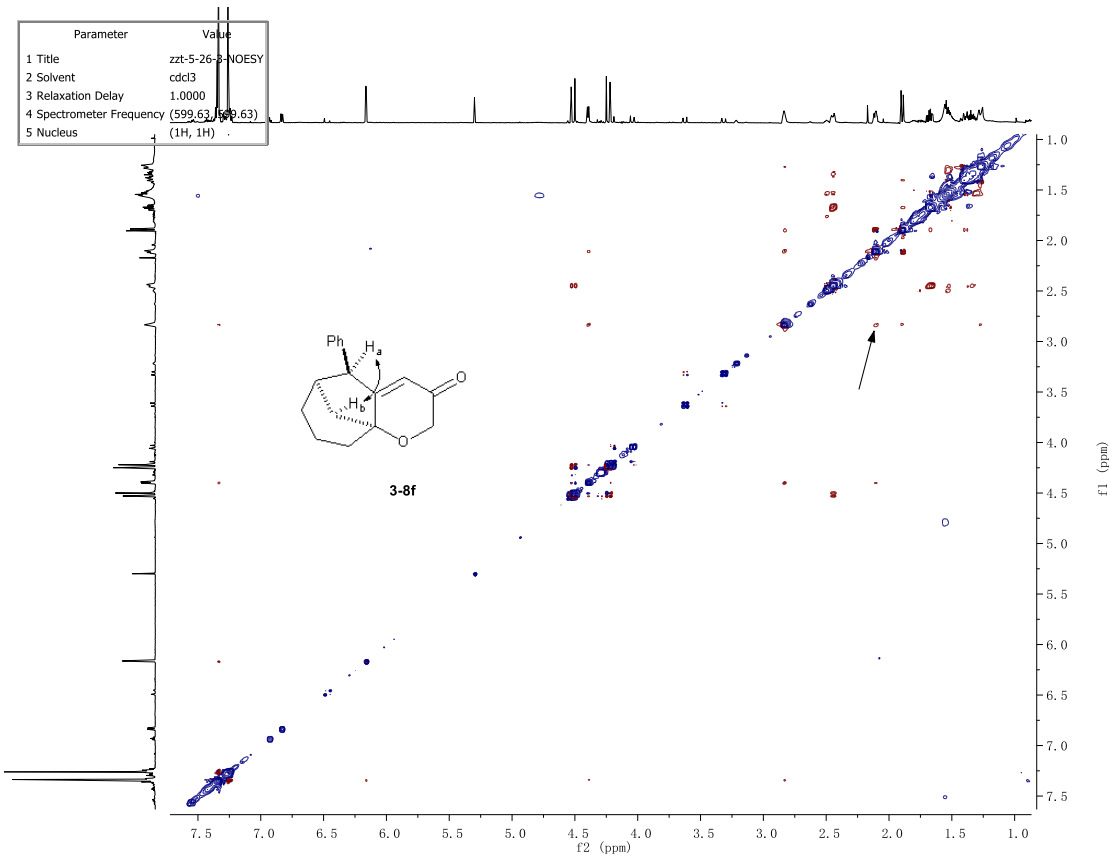


Parameter	Value
1 Title	zzt-5-26-3-C
2 Solvent	CDCl3
3 Relaxation Delay	1.0000
4 Spectrometer Frequency	125.70

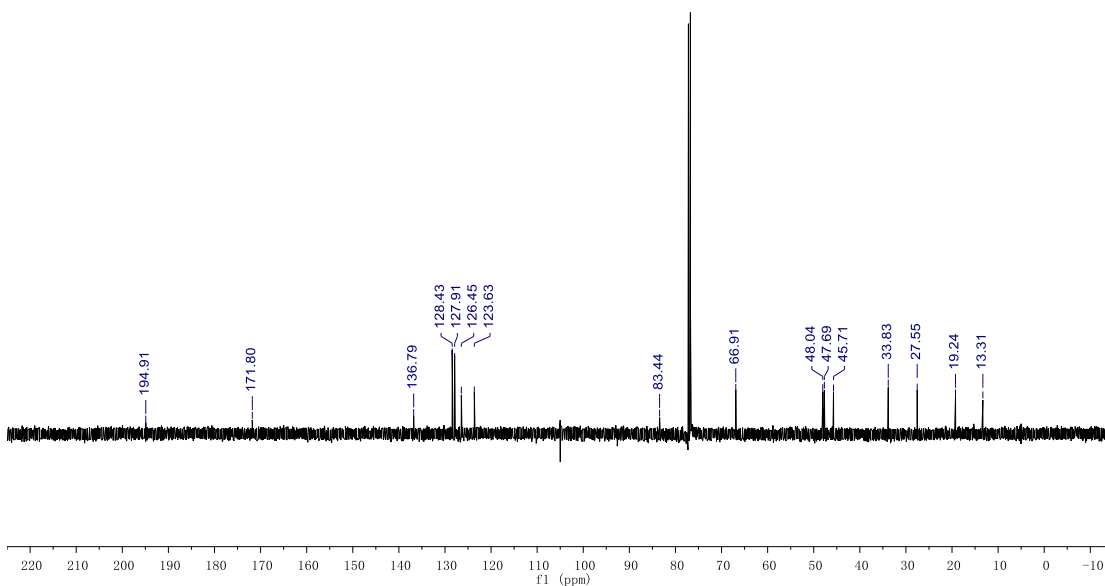
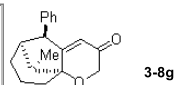


3-8f

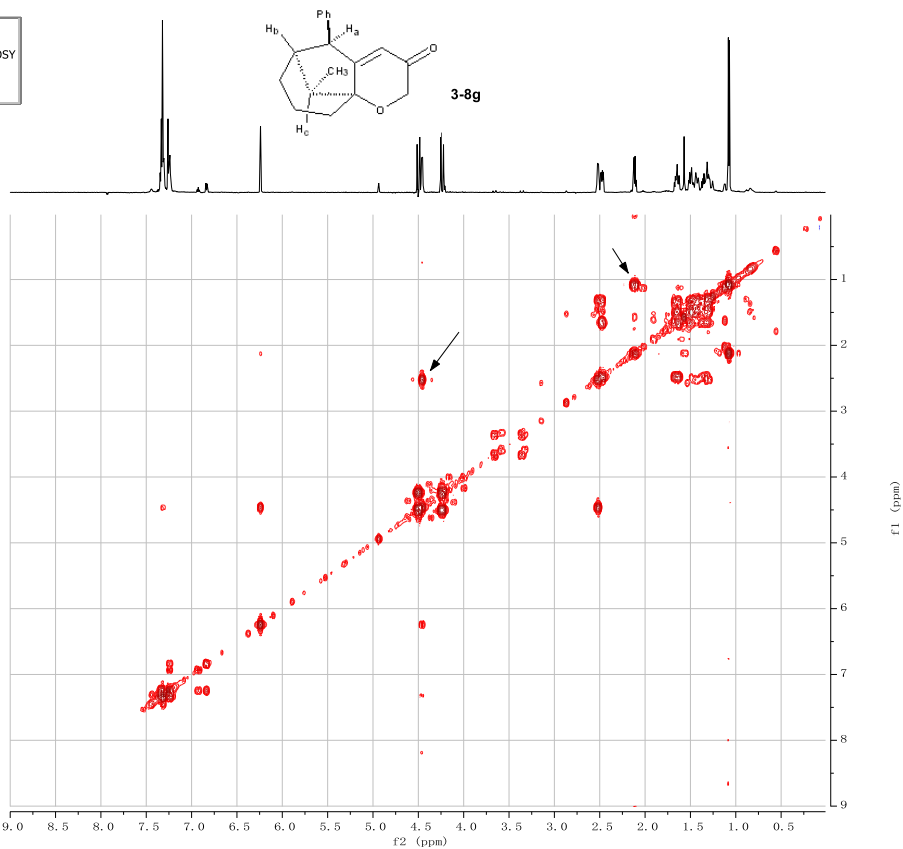




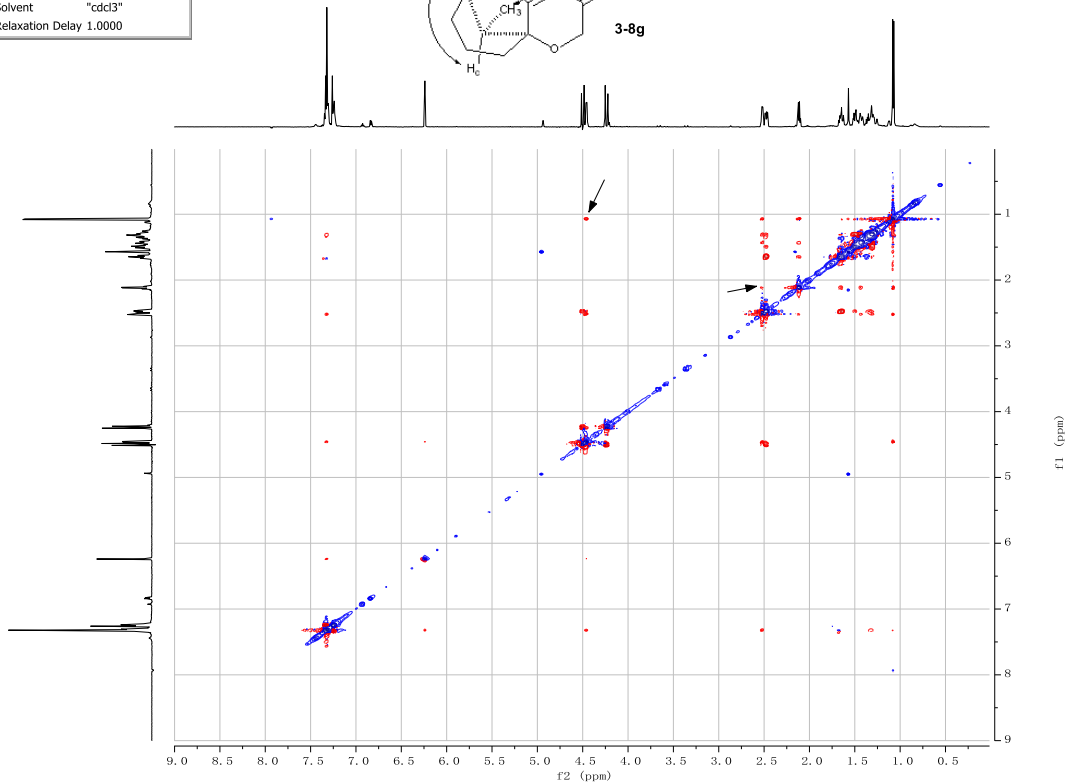
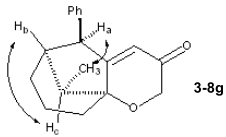
Parameter	Value
1 Title	zzt-4-170-1-C
2 Solvent	cdcl3
3 Relaxation Delay	1.0000
4 Spectrometer Frequency	150.79



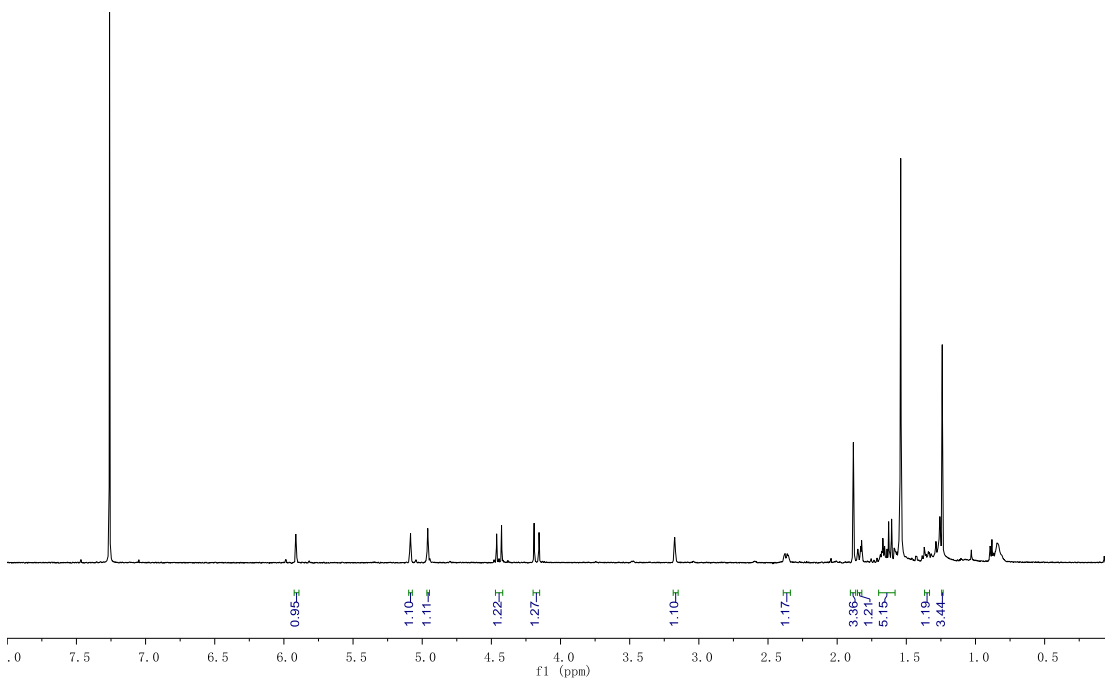
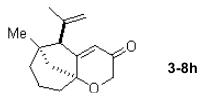
Parameter	Value
1 Title	zzt-4-170-1-COSY
2 Solvent	"cdcl3"
3 Relaxation Delay	1.0000



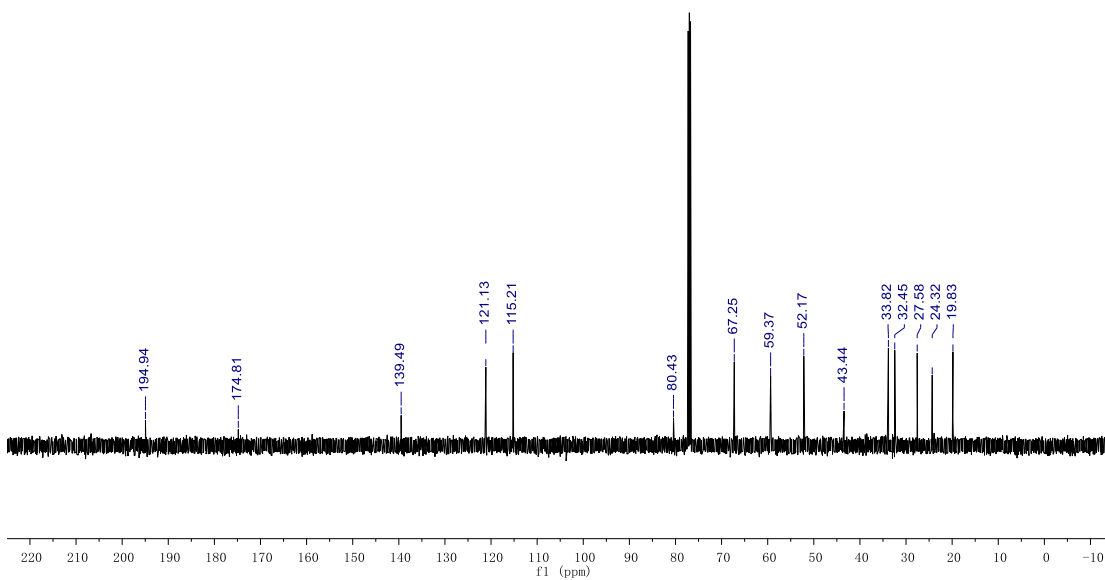
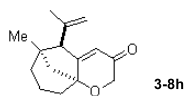
Parameter	Value
1 Title	zzt-4-170-1-NOESY
2 Solvent	"cdcl3"
3 Relaxation Delay	1.0000



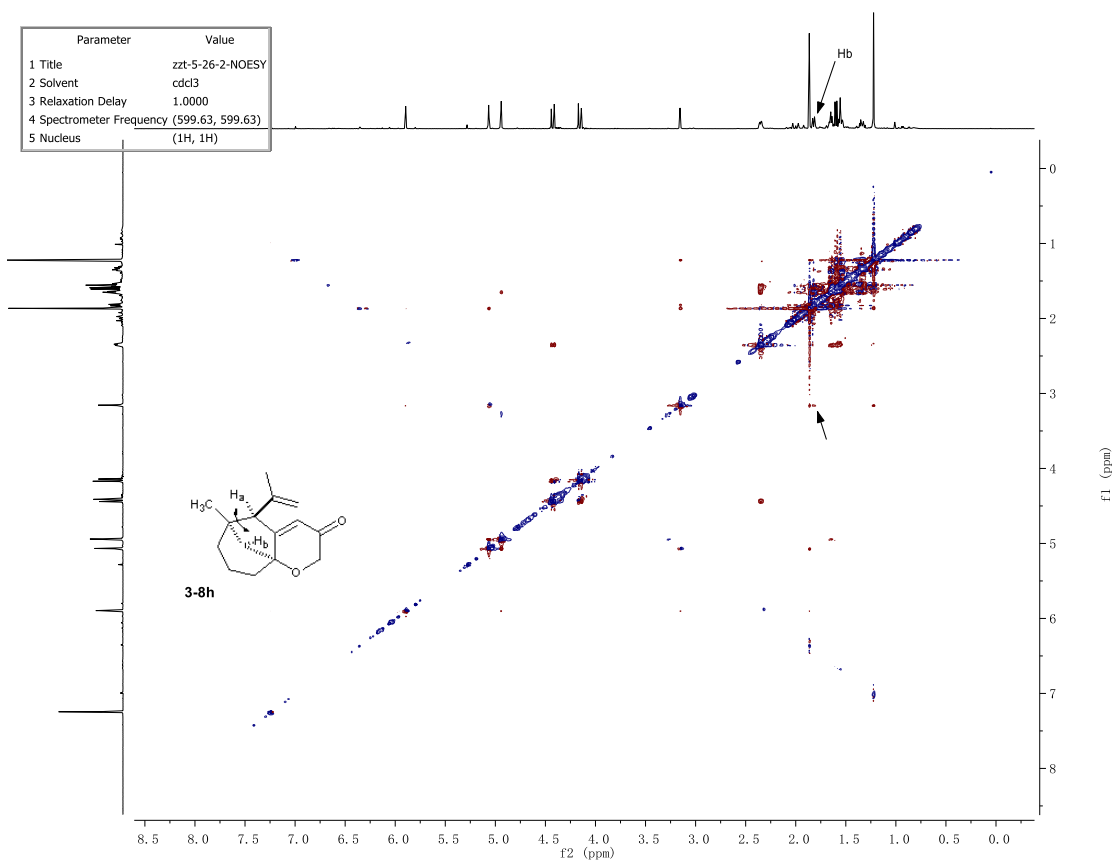
Parameter	Value
1 Title	zzt-5-26-2-pure-H
2 Solvent	CDCl3
3 Relaxation Delay	4.8000
4 Spectrometer Frequency	499.86



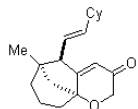
Parameter	Value
1 Title	zzt-5-26-2-C
2 Solvent	CDCl3
3 Relaxation Delay	1.0000
4 Spectrometer Frequency	125.70



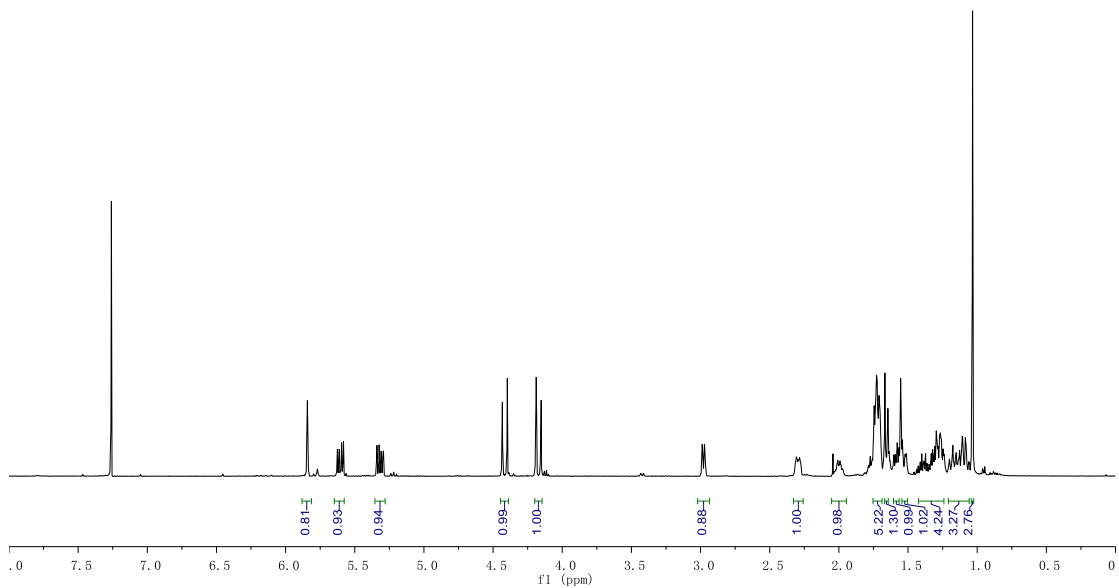
Parameter	Value
1 Title	zzt-5-26-2-NOESY
2 Solvent	cdcl3
3 Relaxation Delay	1.0000
4 Spectrometer Frequency	(599.63, 599.63)
5 Nucleus	(1H, 1H)



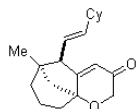
Parameter	Value
1 Title	zzt-5-26-1-H
2 Solvent	CDCl3
3 Relaxation Delay	4.8000
4 Spectrometer Frequency	499.86



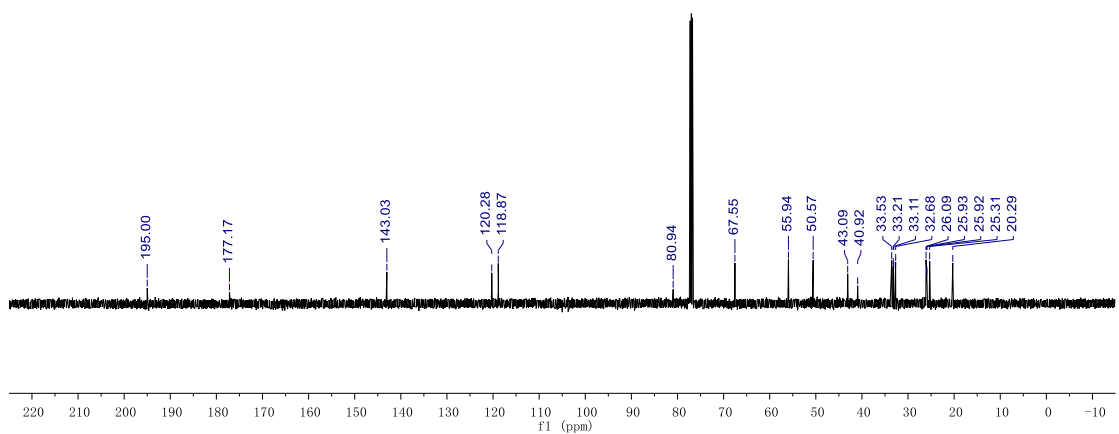
3-8i

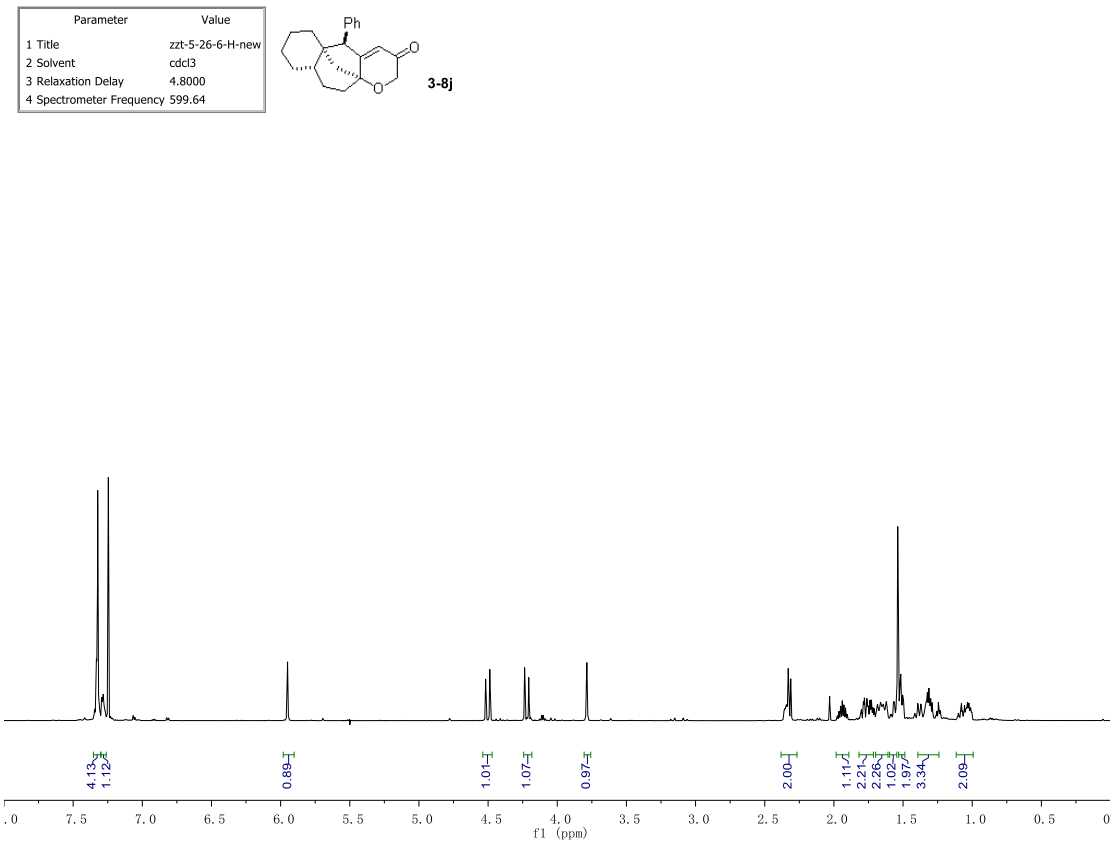
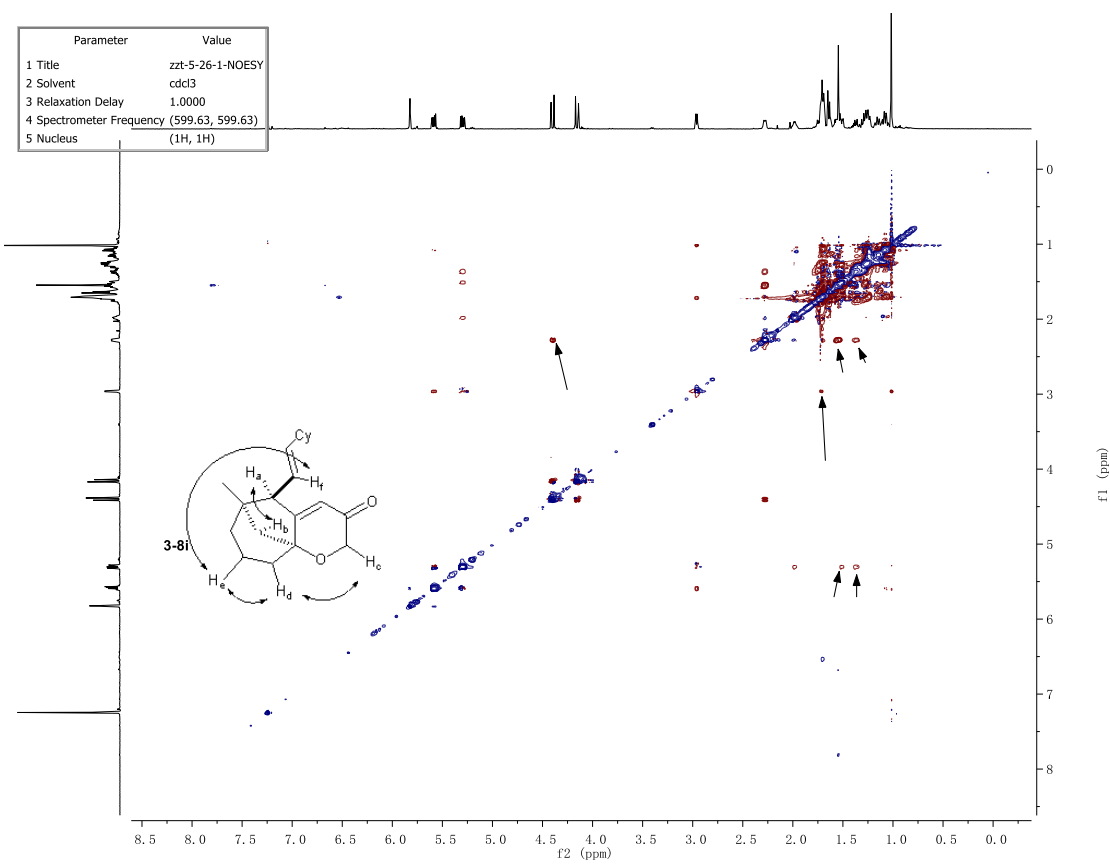


Parameter	Value
1 Title	zzt-5-26-1-C
2 Solvent	CDCl3
3 Relaxation Delay	1.0000
4 Spectrometer Frequency	125.70

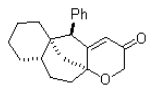


3-8i

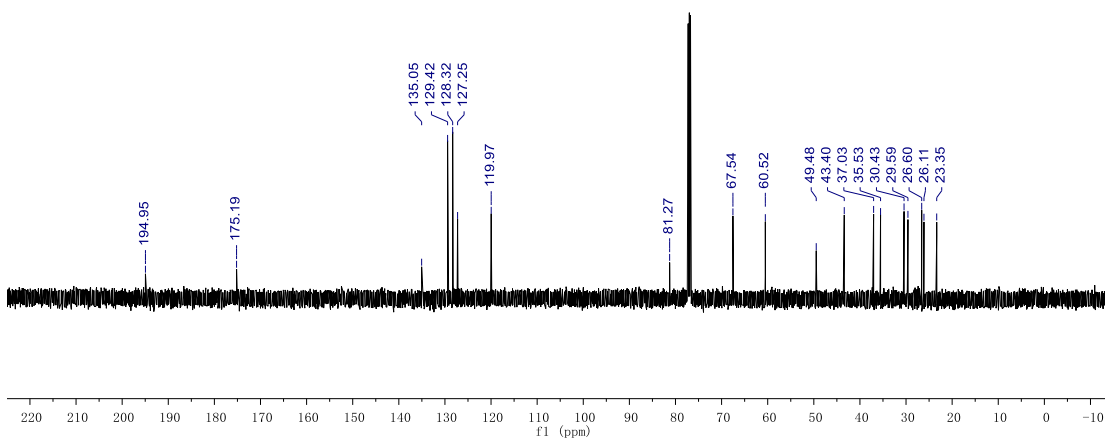




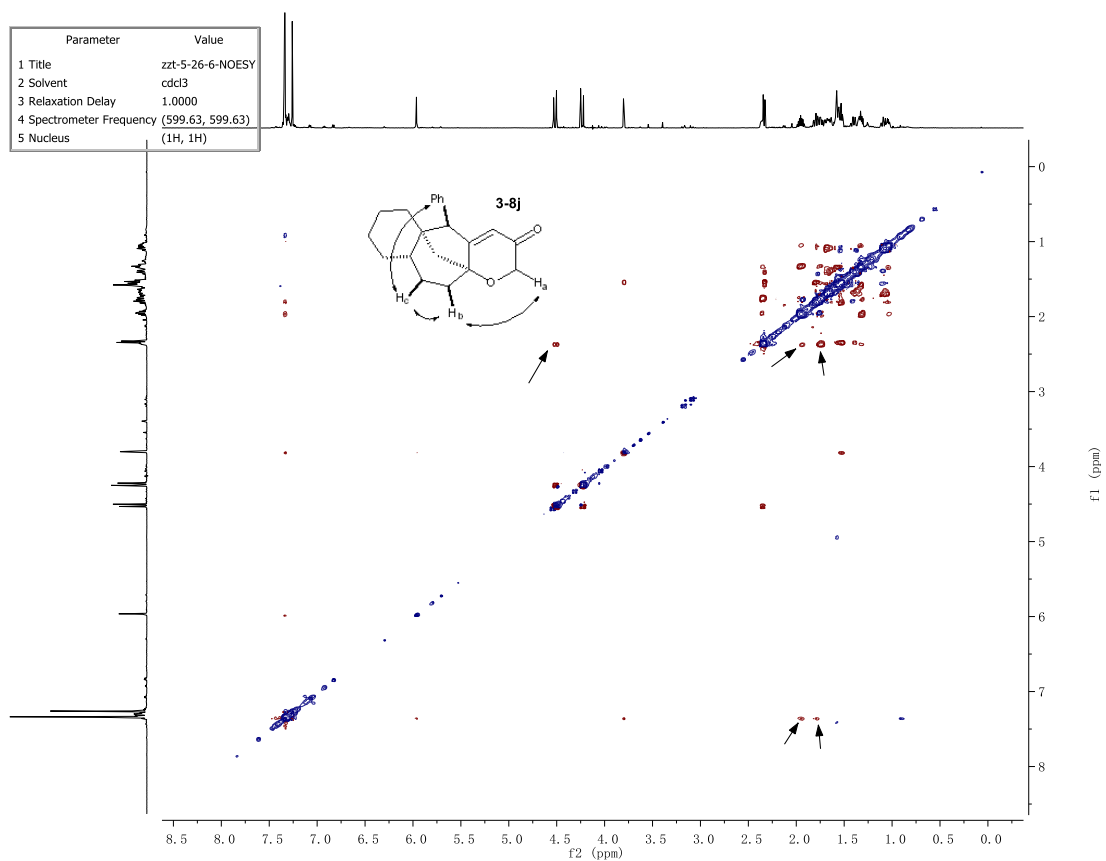
Parameter	Value
1 Title	zzt-5-26-6-C
2 Solvent	CDCl3
3 Relaxation Delay	1.0000
4 Spectrometer Frequency	125.70



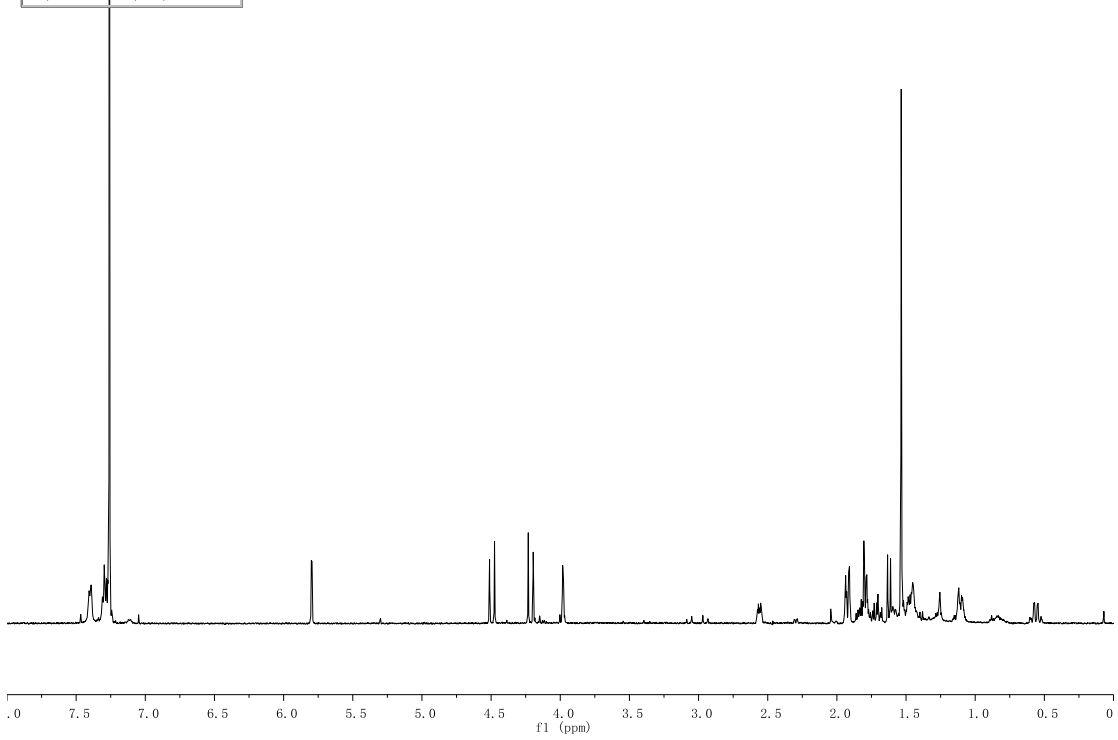
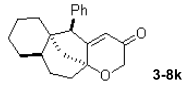
3-8j



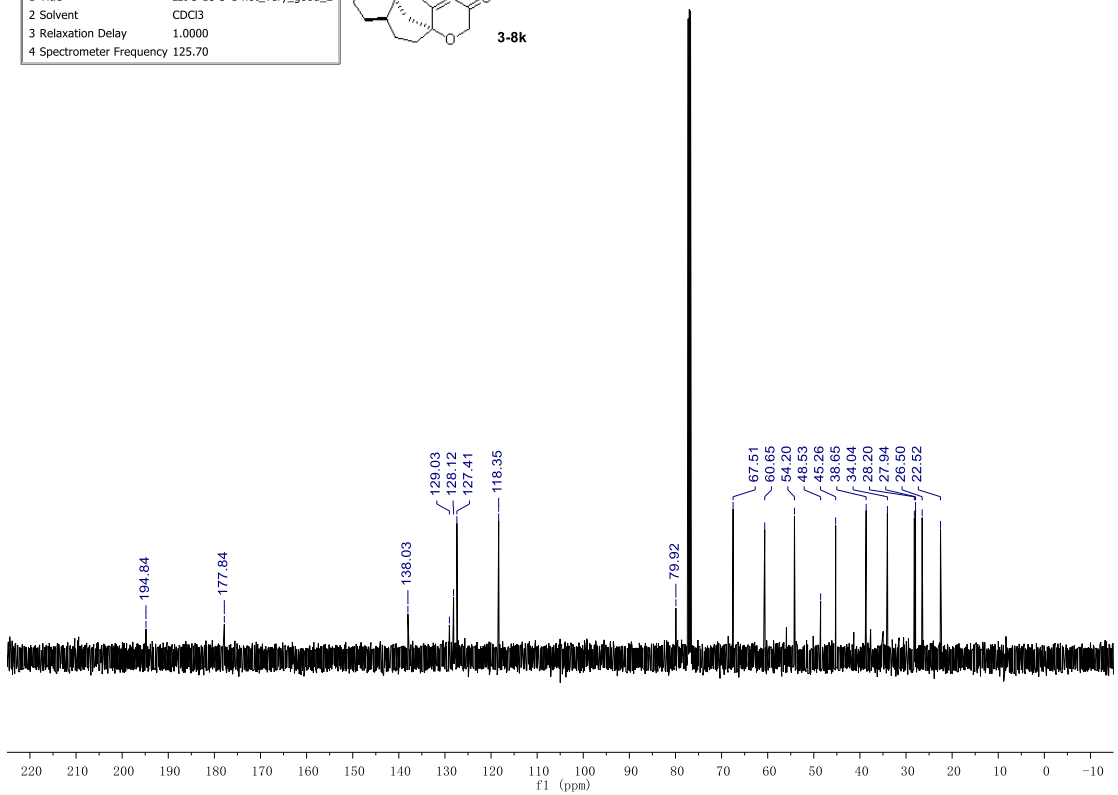
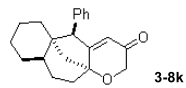
Parameter	Value
1 Title	zzt-5-26-6-NOESY
2 Solvent	cdcl3
3 Relaxation Delay	1.0000
4 Spectrometer Frequency	(599.63, 599.63)
5 Nucleus	(1H, 1H)



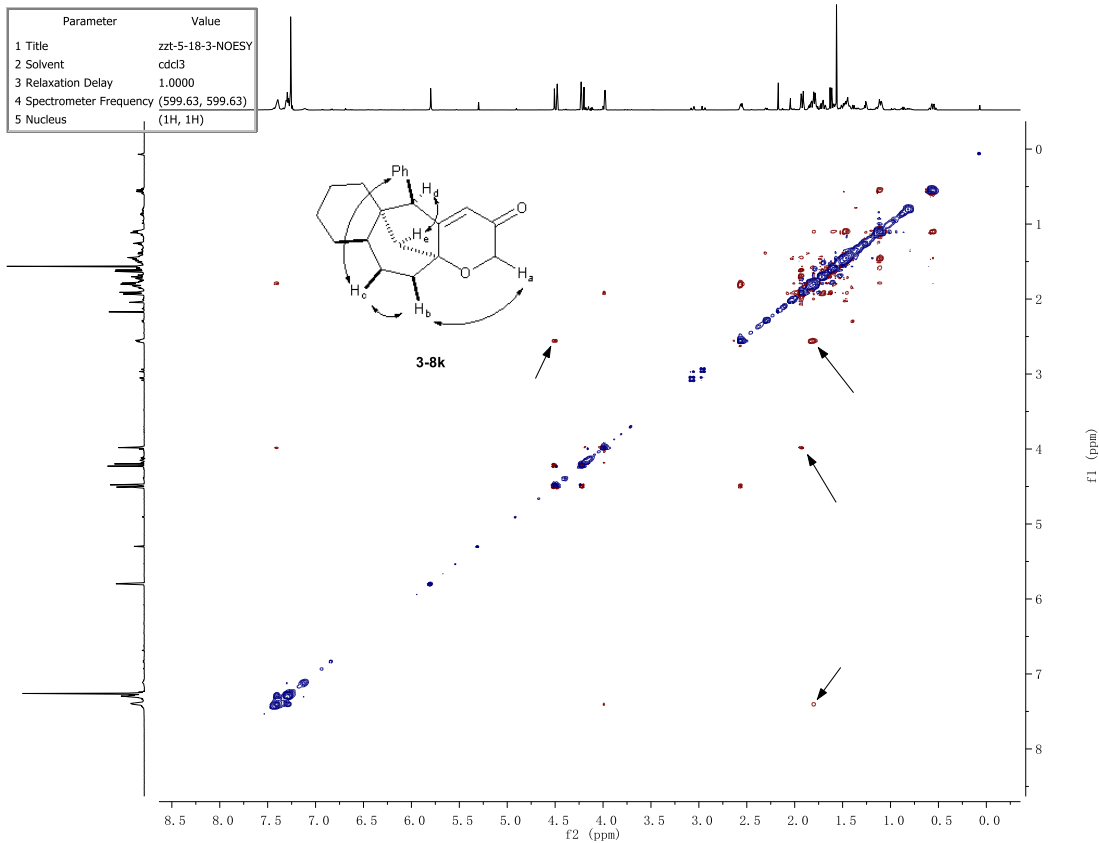
Parameter	Value
1 Title	zzt-5-18-3-H
2 Solvent	CDCl3
3 Relaxation Delay	4.8000
4 Spectrometer Frequency	499.86



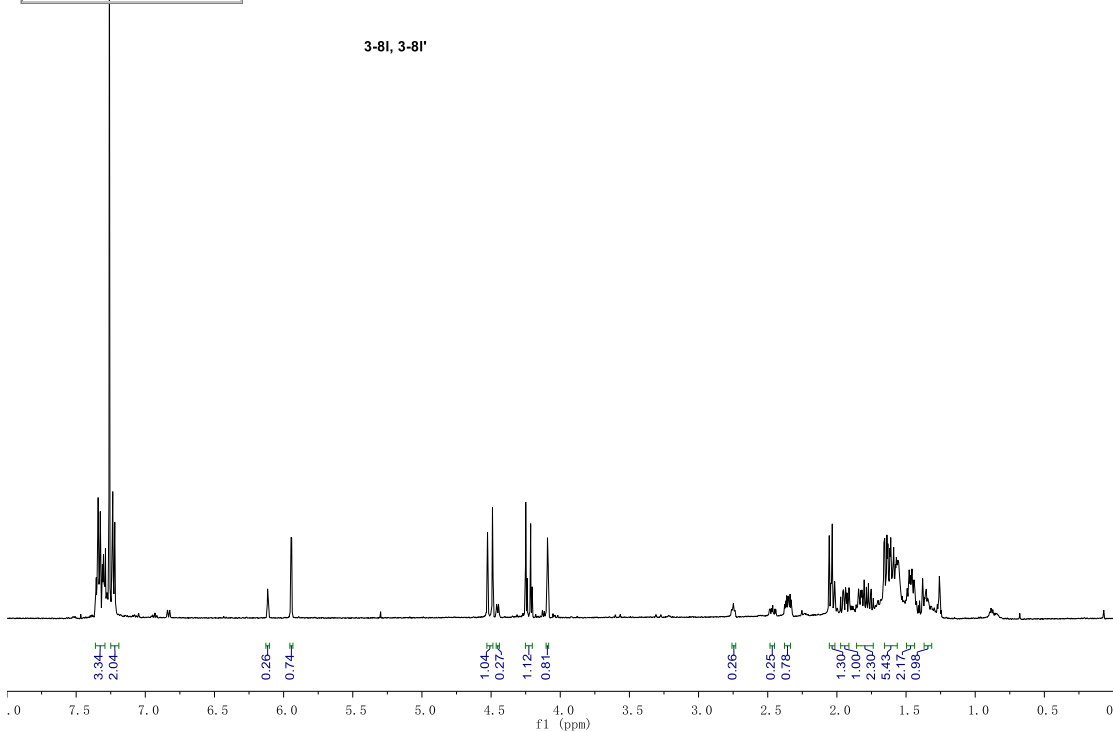
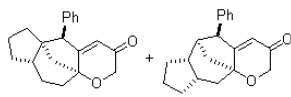
Parameter	Value
1 Title	zzt-5-18-3-C-not_very_good_2
2 Solvent	CDCl3
3 Relaxation Delay	1.0000
4 Spectrometer Frequency	125.70



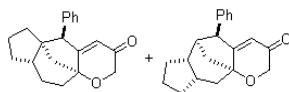
Parameter	Value
1 Title	zzt-5-18-3-NOESY
2 Solvent	cdcl3
3 Relaxation Delay	1.0000
4 Spectrometer Frequency	(599.63, 599.63)
5 Nucleus	(1H, 1H)



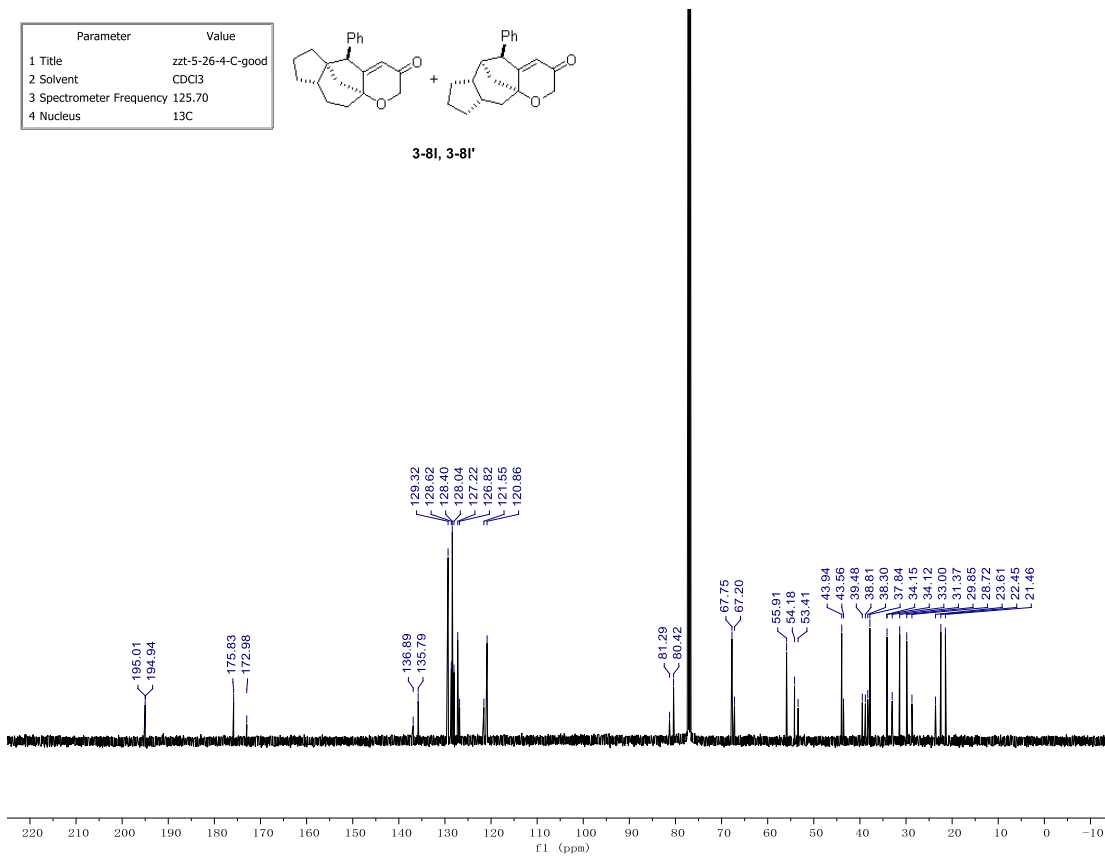
Parameter	Value
1 Title	zzt-5-26-4-H
2 Solvent	CDCl3
3 Relaxation Delay	4.8000
4 Spectrometer Frequency	499.86



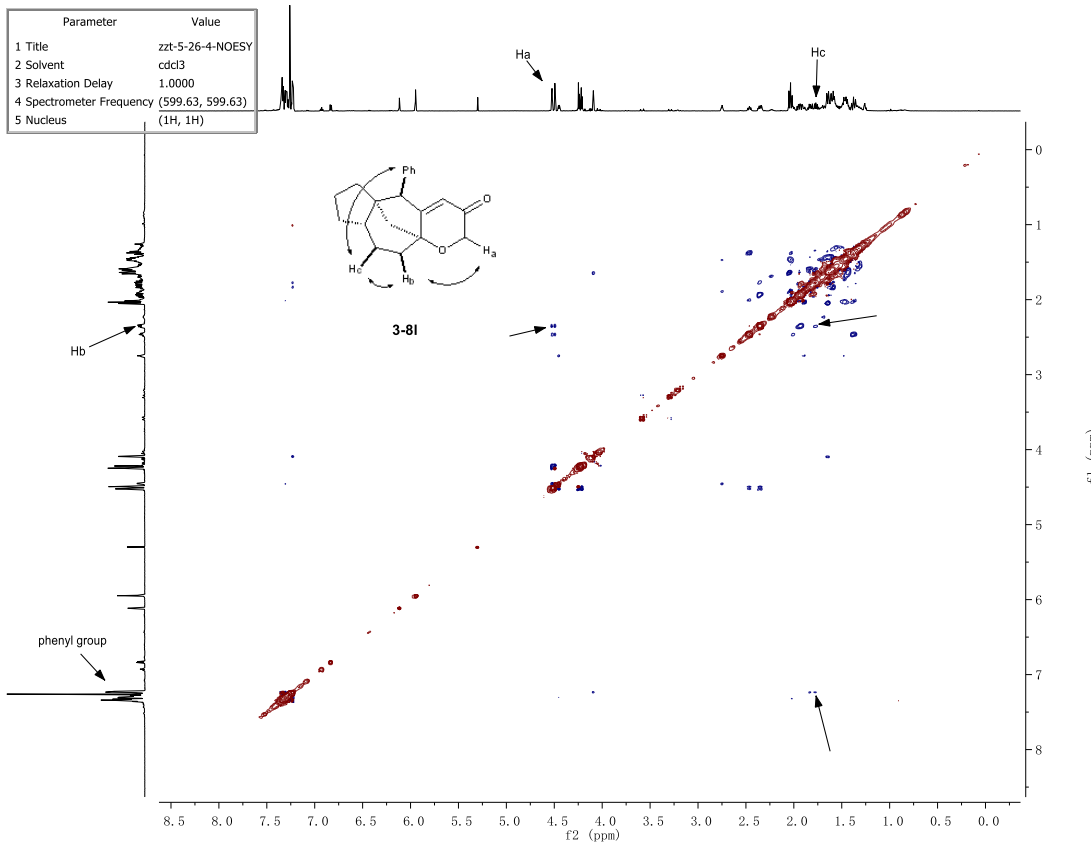
Parameter	Value
1 Title	zzt-5-26-4-C-good
2 Solvent	CDCl3
3 Spectrometer Frequency	125.70
4 Nucleus	13C



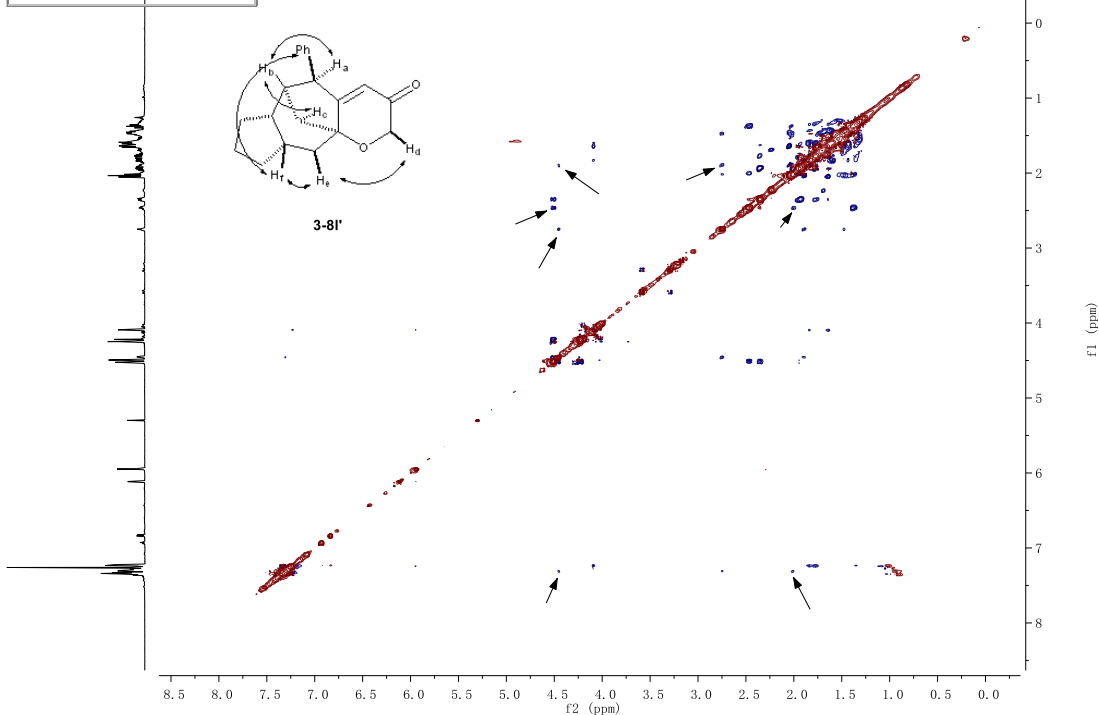
3-8I, 3-8I'



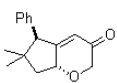
Parameter	Value
1 Title	zzt-5-26-4-NOESY
2 Solvent	cdcl3
3 Relaxation Delay	1.0000
4 Spectrometer Frequency	(599.63, 599.63)
5 Nucleus	(1H, 1H)



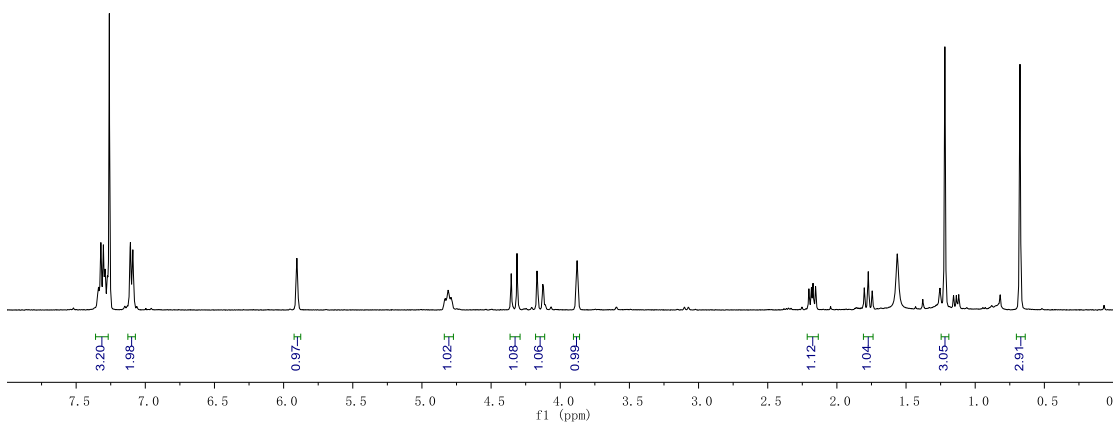
Parameter	Value
1 Title	zzt-5-26-4-NOESY
2 Solvent	cdcl3
3 Relaxation Delay	1.0000
4 Spectrometer Frequency	(599.63, 599.63)
5 Nucleus	(1H, 1H)



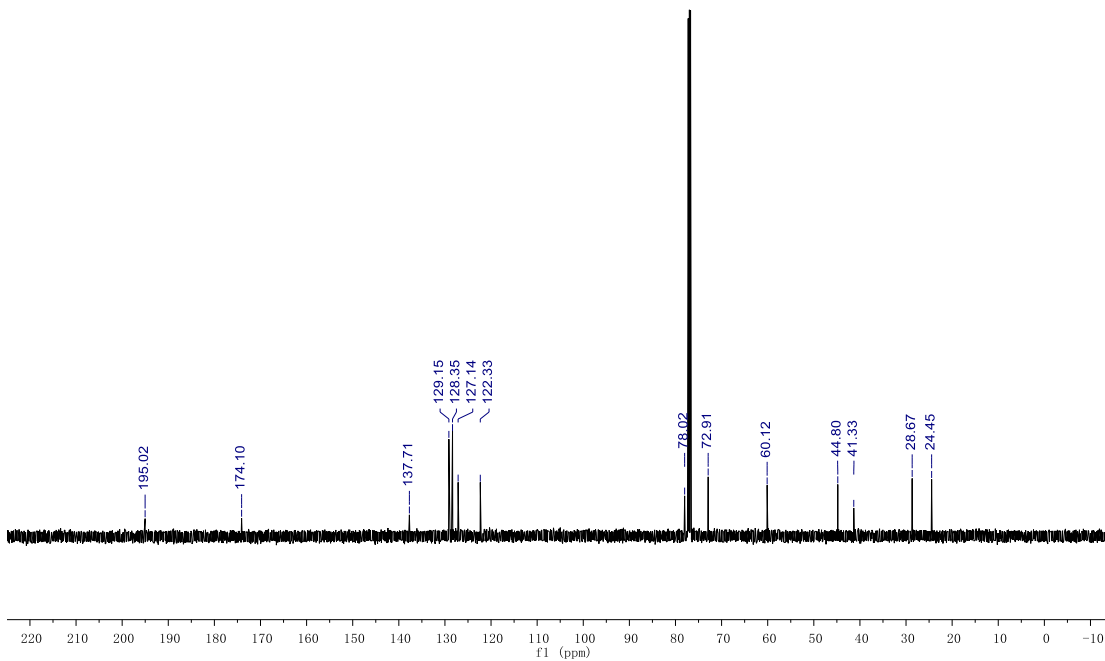
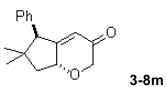
Parameter	Value
1 Title	zzt-4-151-2-F-H
2 Solvent	cdcl3
3 Relaxation Delay	4.8000
4 Spectrometer Frequency	399.78



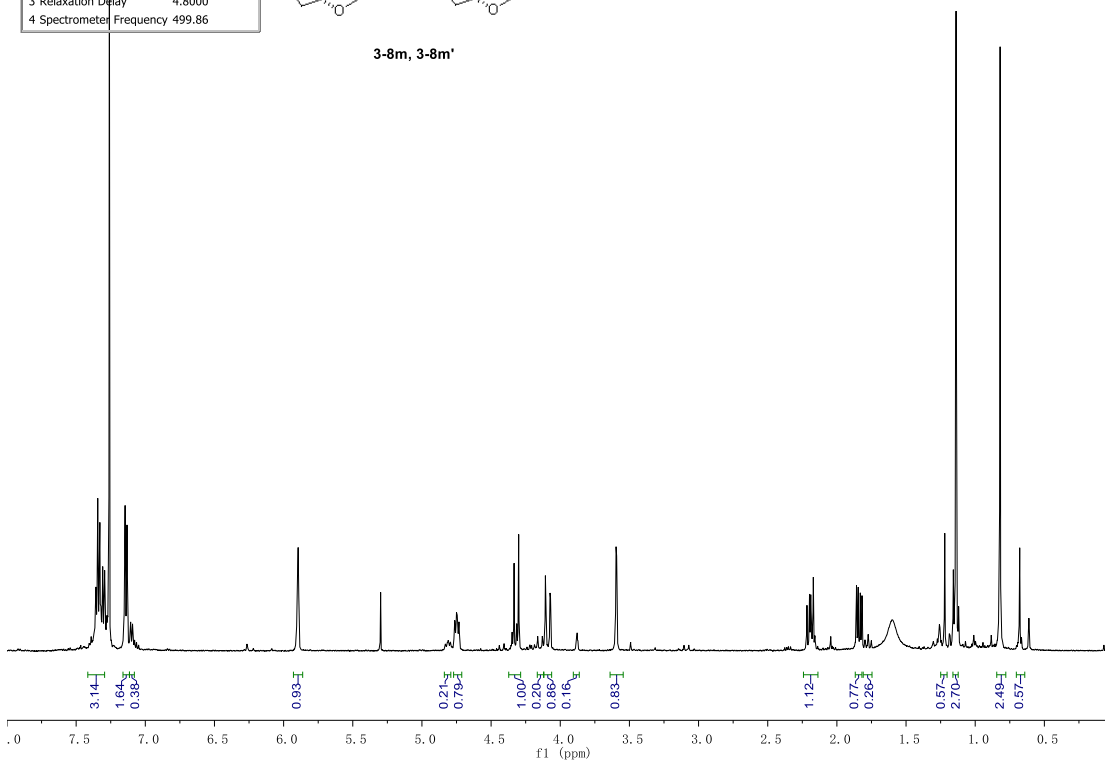
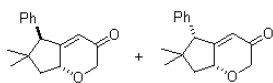
3-8m



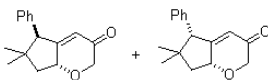
Parameter	Value
1 Title	zzt-4-151-2-F-C
2 Solvent	CDCl3
3 Relaxation Delay	1.0000
4 Spectrometer Frequency	125.70



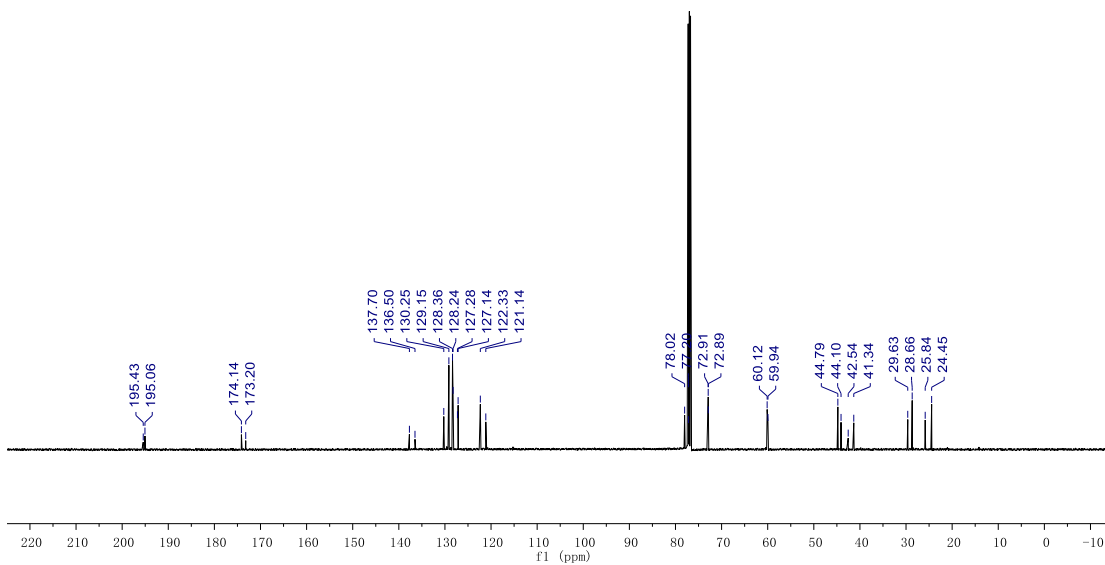
Parameter	Value
1 Title	zzt-4-151-2-B-H
2 Solvent	CDCl3
3 Relaxation Delay	4.8000
4 Spectrometer Frequency	499.86



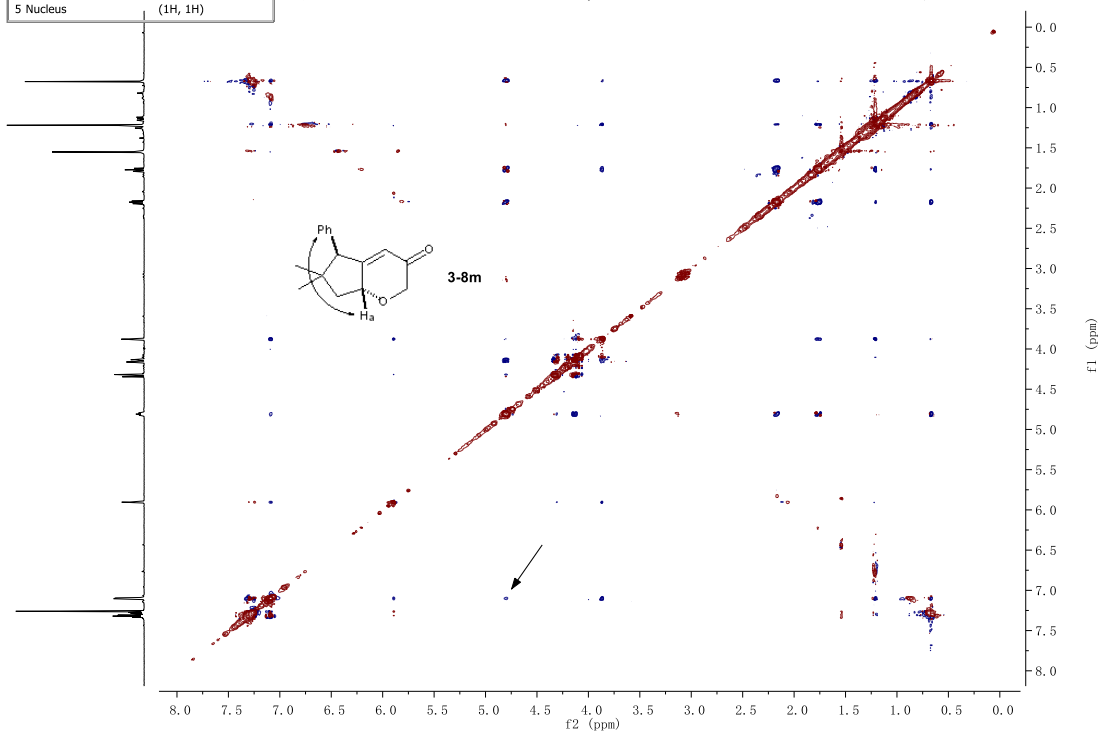
Parameter	Value
1 Title	zzt-4-151-2-B-C-with_diastereomer
2 Solvent	CDCl3
3 Relaxation Delay	1.0000
4 Spectrometer Frequency	125.70

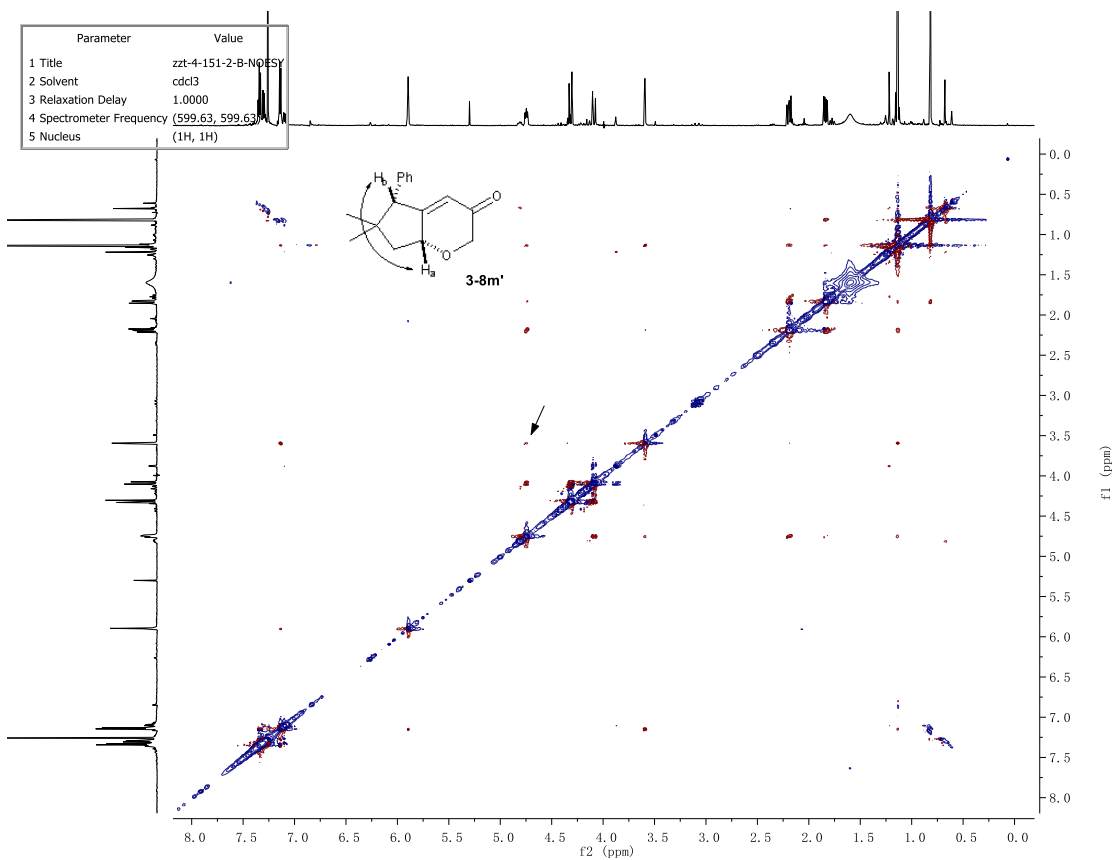


3-8m, 3-8m'

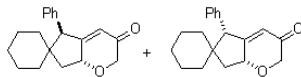


Parameter	Value
1 Title	zzt-4-151-2-F-NOESY
2 Solvent	cdcl3
3 Relaxation Delay	1.0000
4 Spectrometer Frequency	(599.63, 599.63)
5 Nucleus	(1H, 1H)

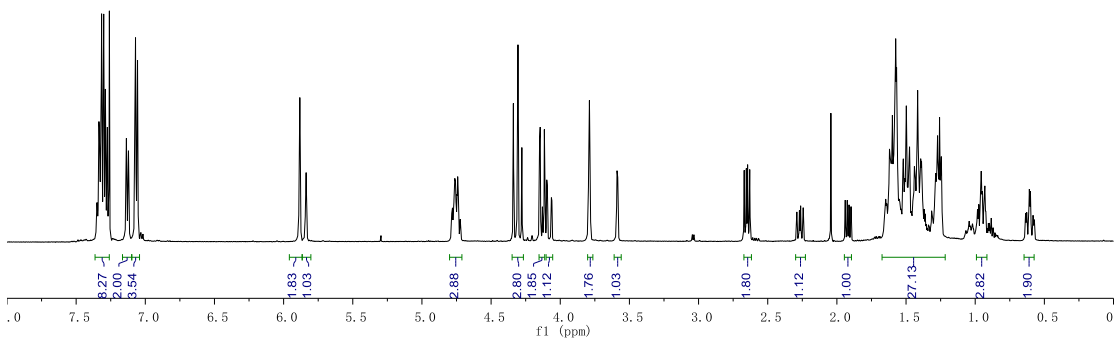




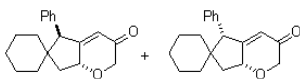
Parameter	Value
1 Title	zzt-5-9-2-H
2 Solvent	CDCl3
3 Relaxation Delay	4.8000
4 Spectrometer Frequency	499.86



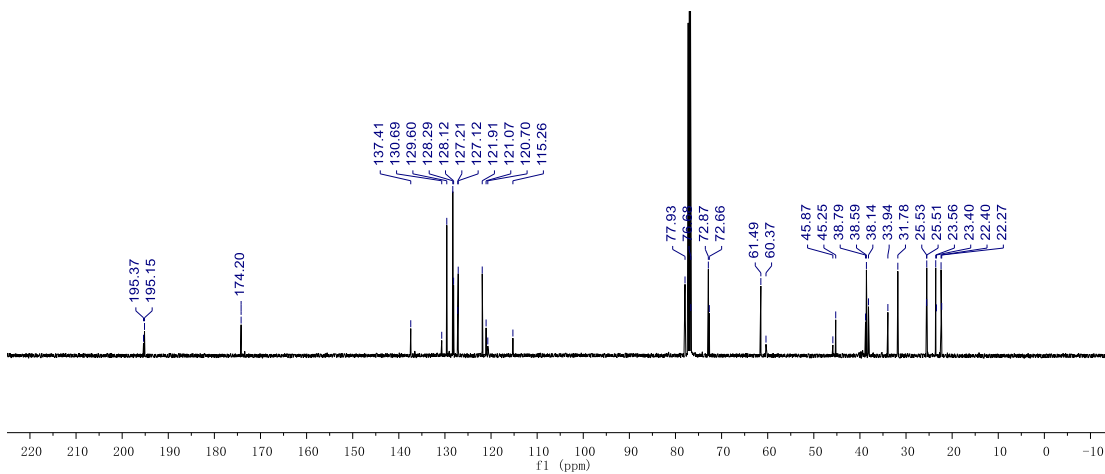
3-8n, 3-8n'



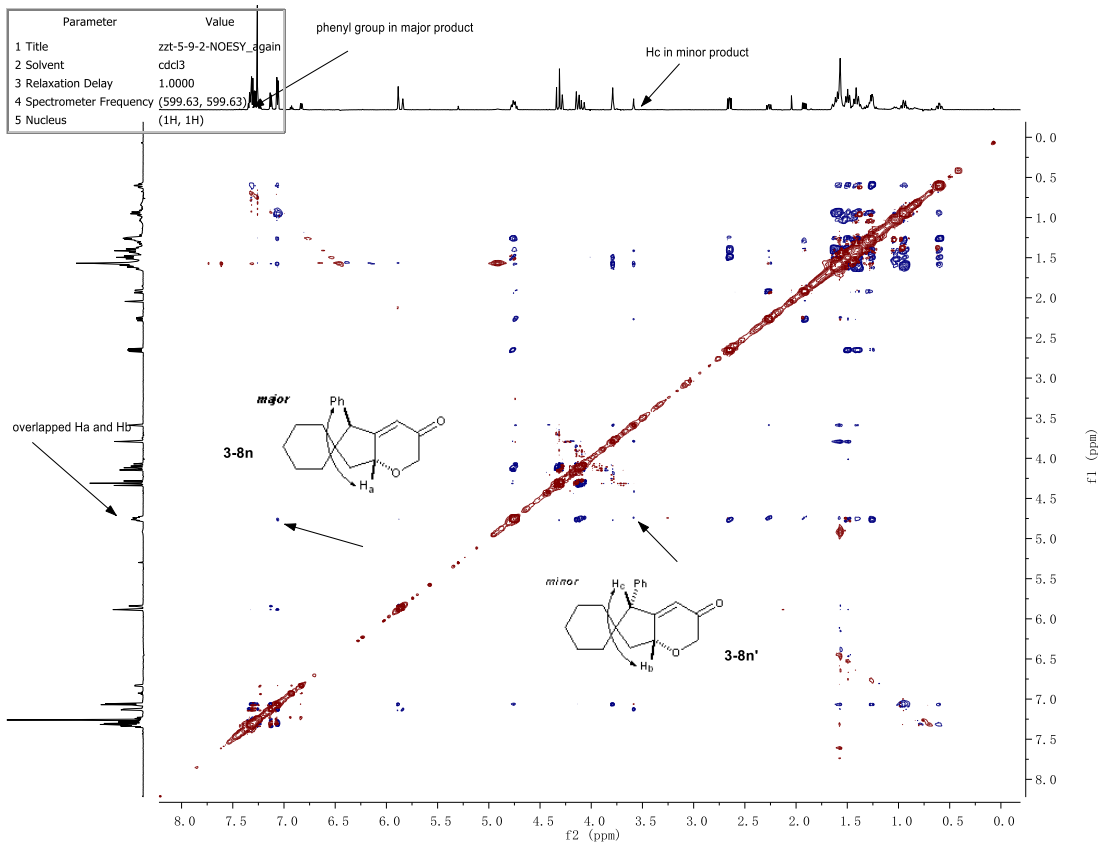
Parameter	Value
1 Title	zzt-5-9-2-C-final
2 Solvent	CDCl3
3 Relaxation Delay	1.0000
4 Spectrometer Frequency	125.70



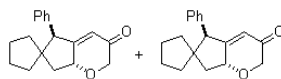
3-8n, 3-8n'



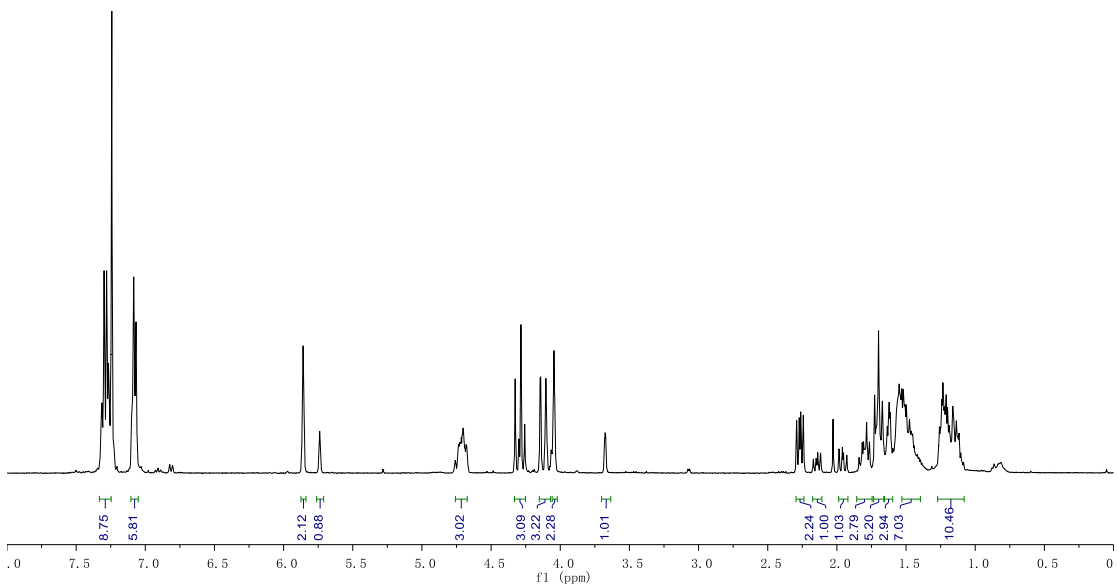
Parameter	Value
1 Title	zzt-5-9-2-NOESY_again
2 Solvent	cdcl3
3 Relaxation Delay	1.0000
4 Spectrometer Frequency	(599.63, 599.63)
5 Nucleus	(1H, 1H)



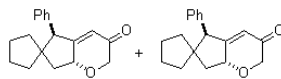
Parameter	Value
1 Title	zzt-5-9-3-H_good
2 Solvent	cdcl3
3 Relaxation Delay	4.8000
4 Spectrometer Frequency	399.78



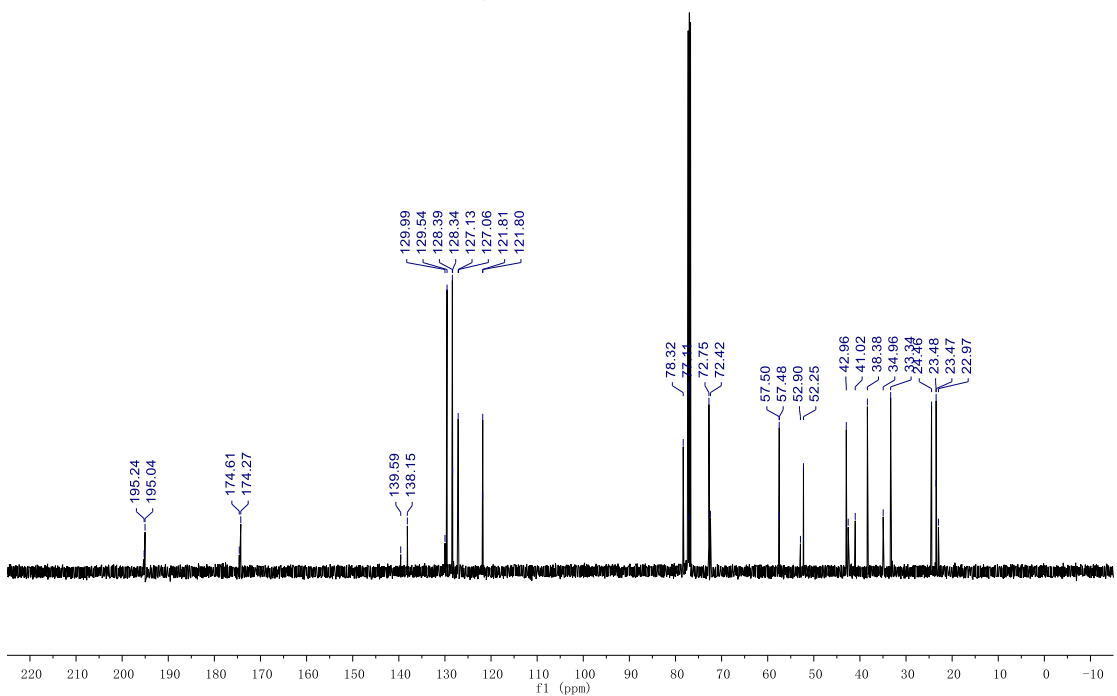
3-8o, 3-8o'

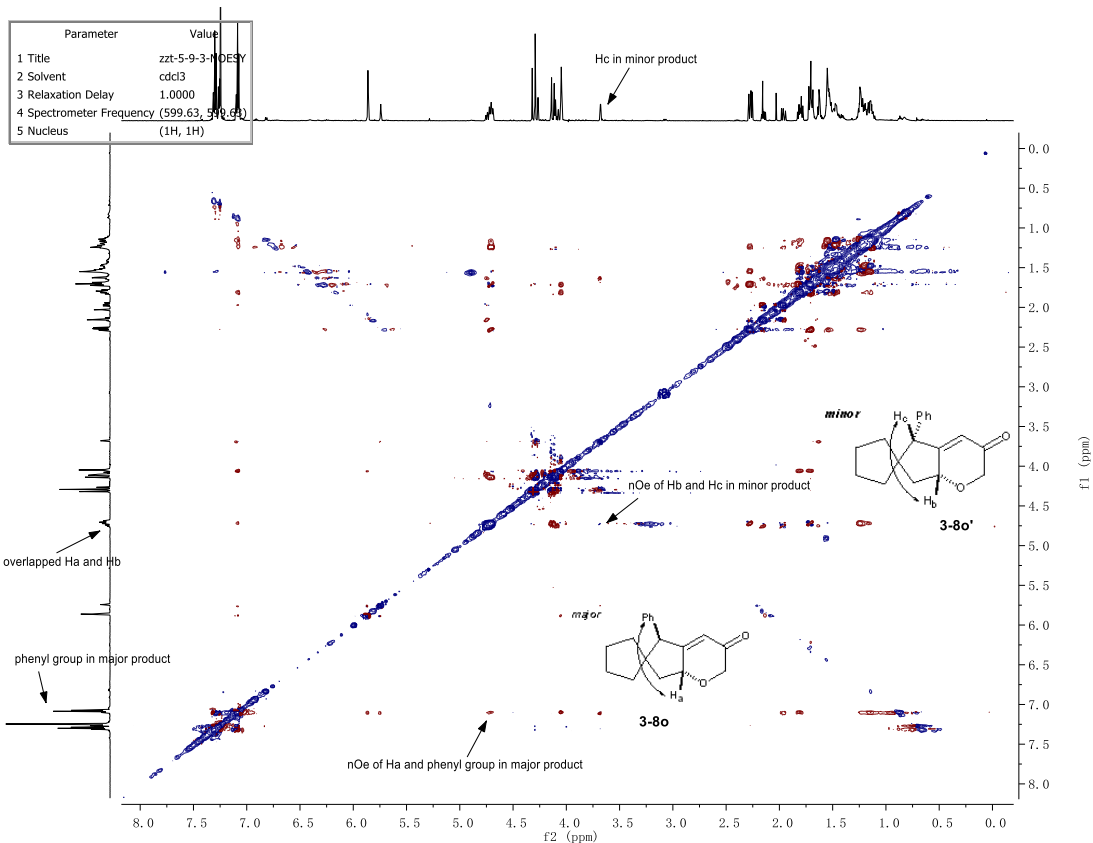


Parameter	Value
1 Title	zzt-5-9-3-C
2 Solvent	CDCl3
3 Relaxation Delay	1.0000
4 Spectrometer Frequency	125.70

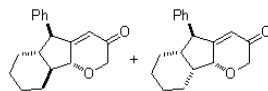


3-8o, 3-8o'

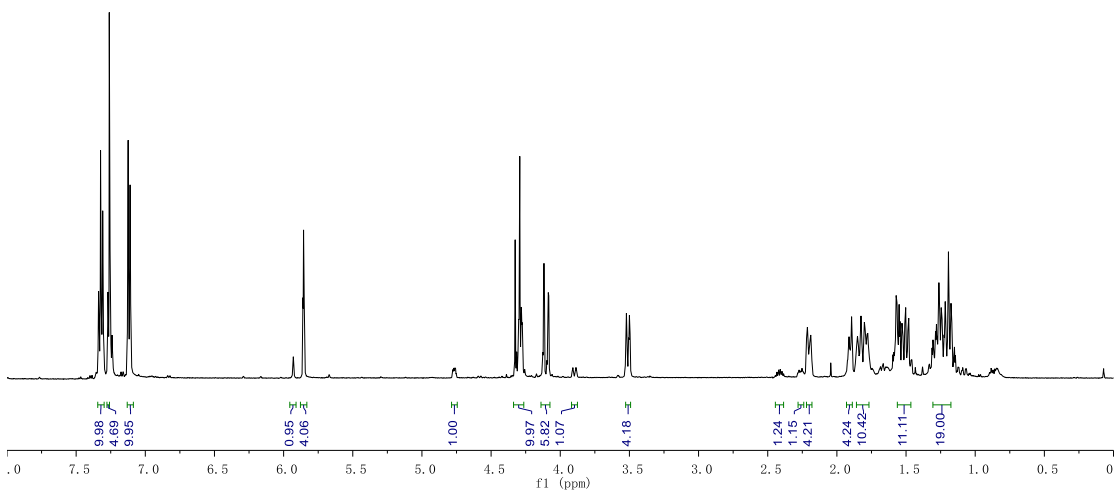




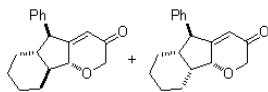
Parameter	Value
1 Title	zzt-5-18-4-H
2 Solvent	CDCl3
3 Relaxation Delay	4.8000
4 Spectrometer Frequency	499.86



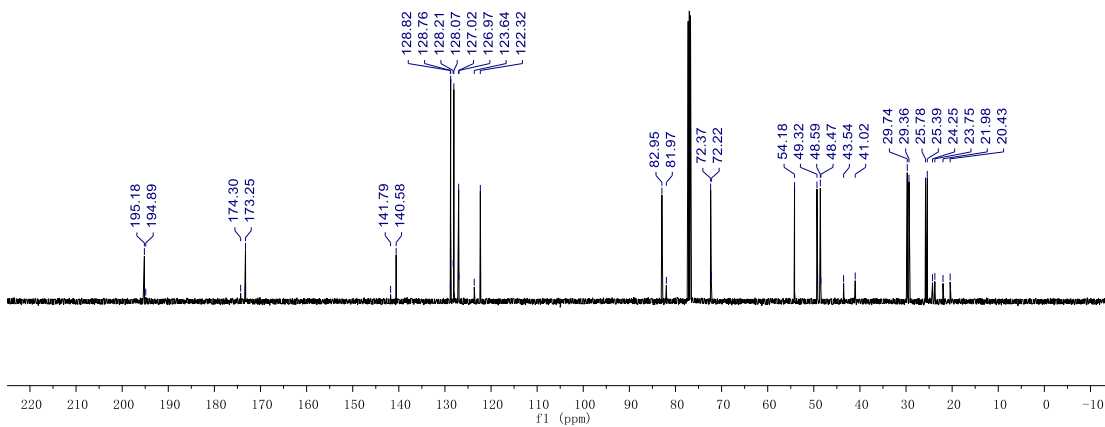
3-8p, 3-8p'



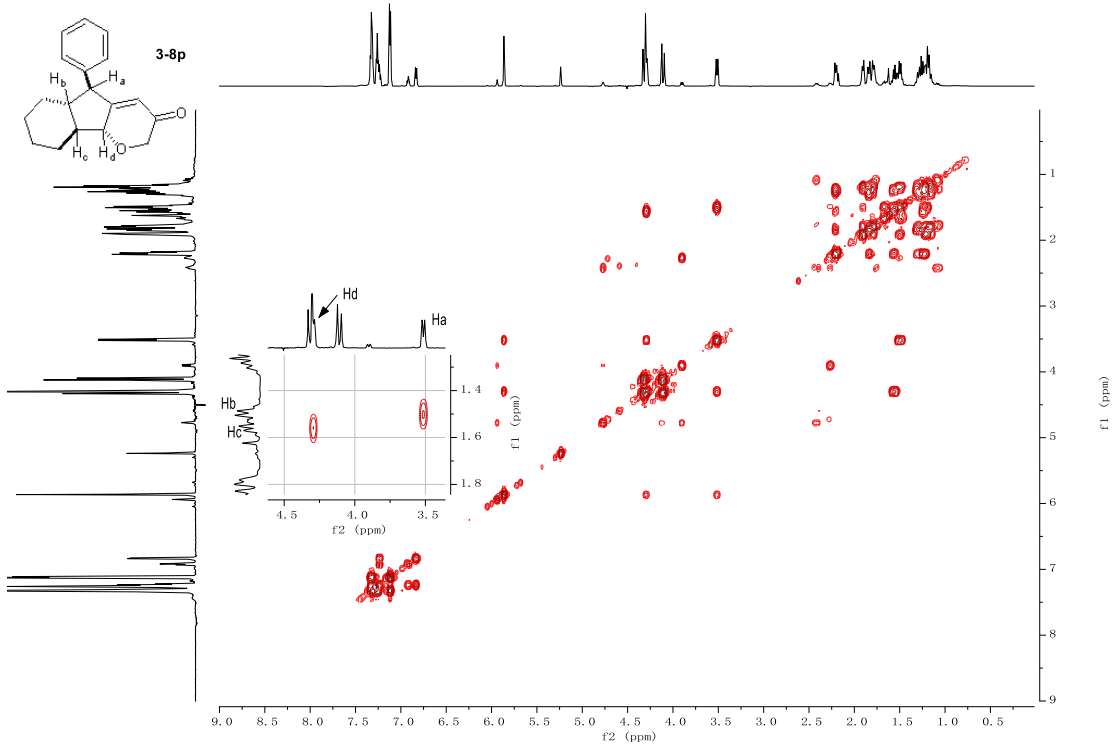
Parameter	Value
1 Title	zzt-5-18-4-C
2 Solvent	CDCl3
3 Relaxation Delay	1.0000
4 Spectrometer Frequency	125.70



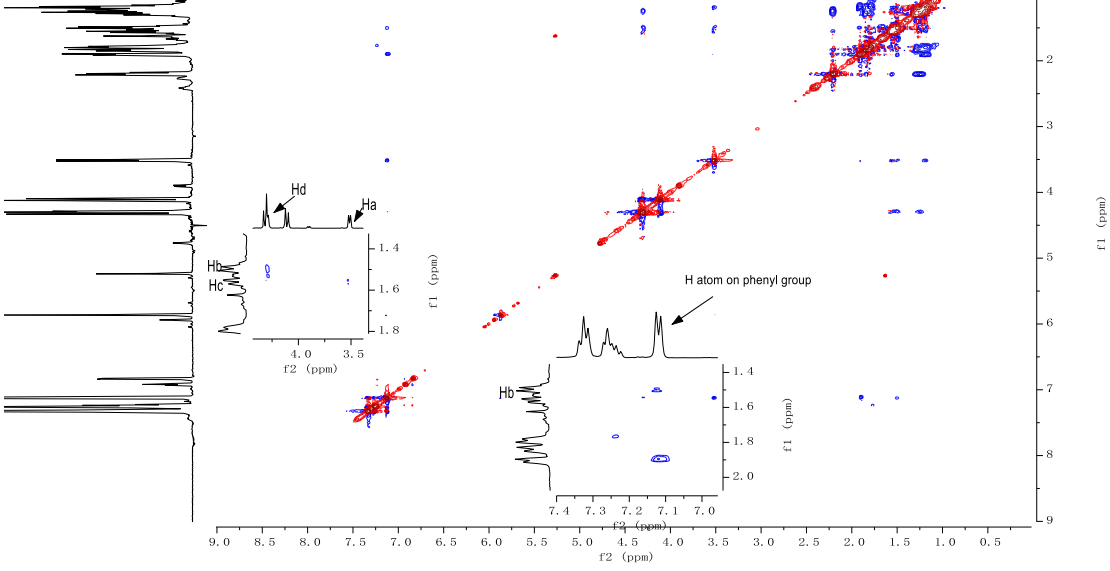
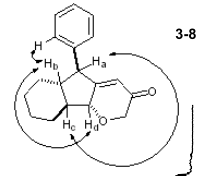
3-8p, 3-8p'



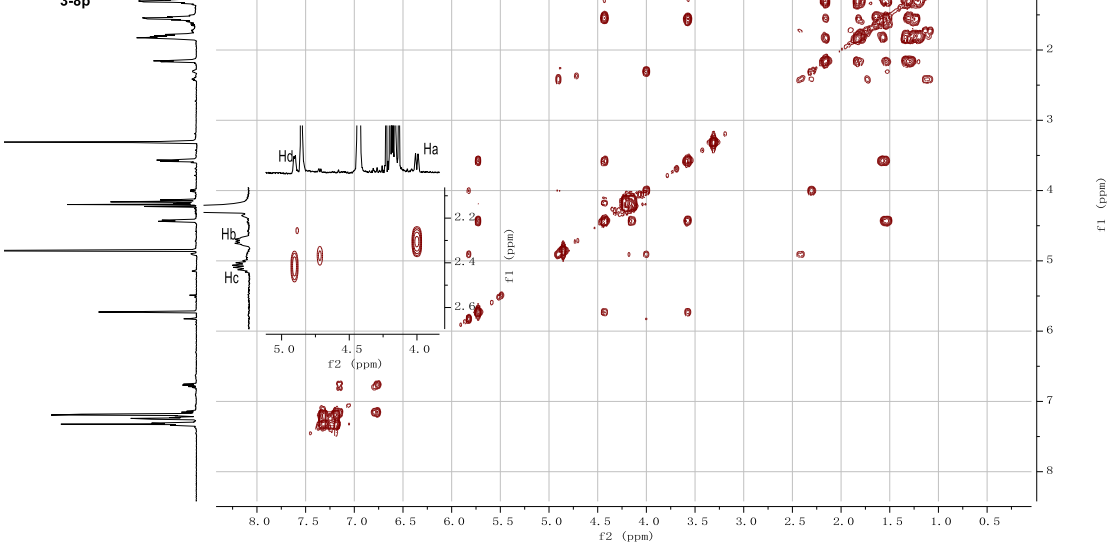
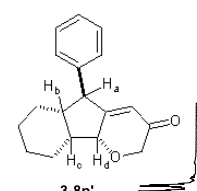
Parameter	Value
1 Title	zzt-4-170-2-COSY
2 Solvent	"cdcl3"
3 Relaxation Delay	1.0000

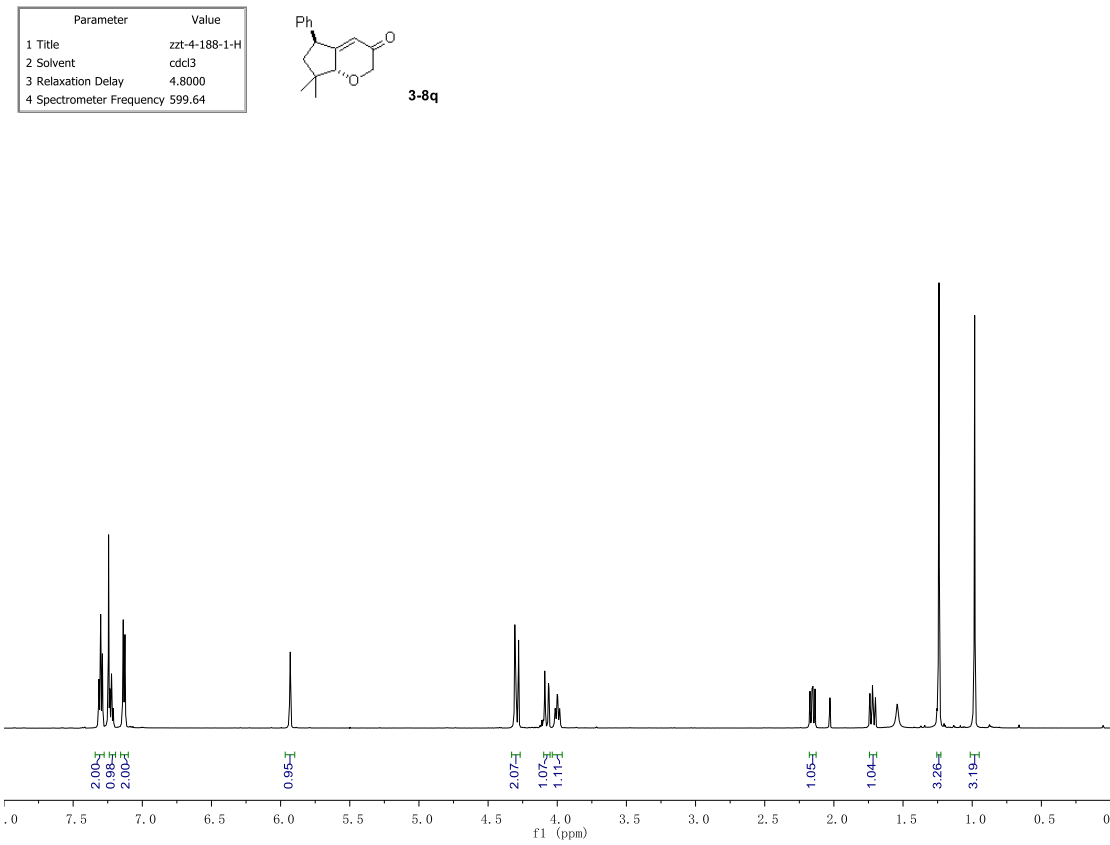
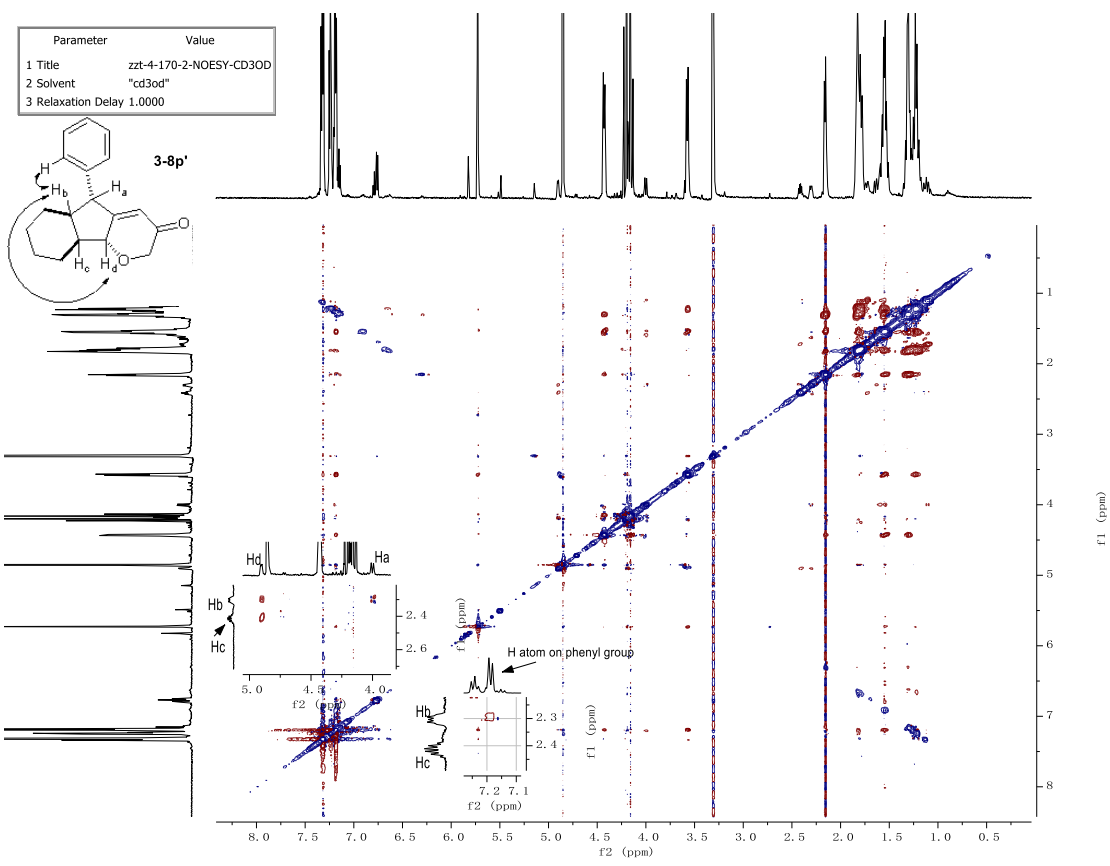


Parameter	Value
1 Title	zzt-4-170-2-NOESY
2 Solvent	"cdcl3"
3 Relaxation Delay	1.0000

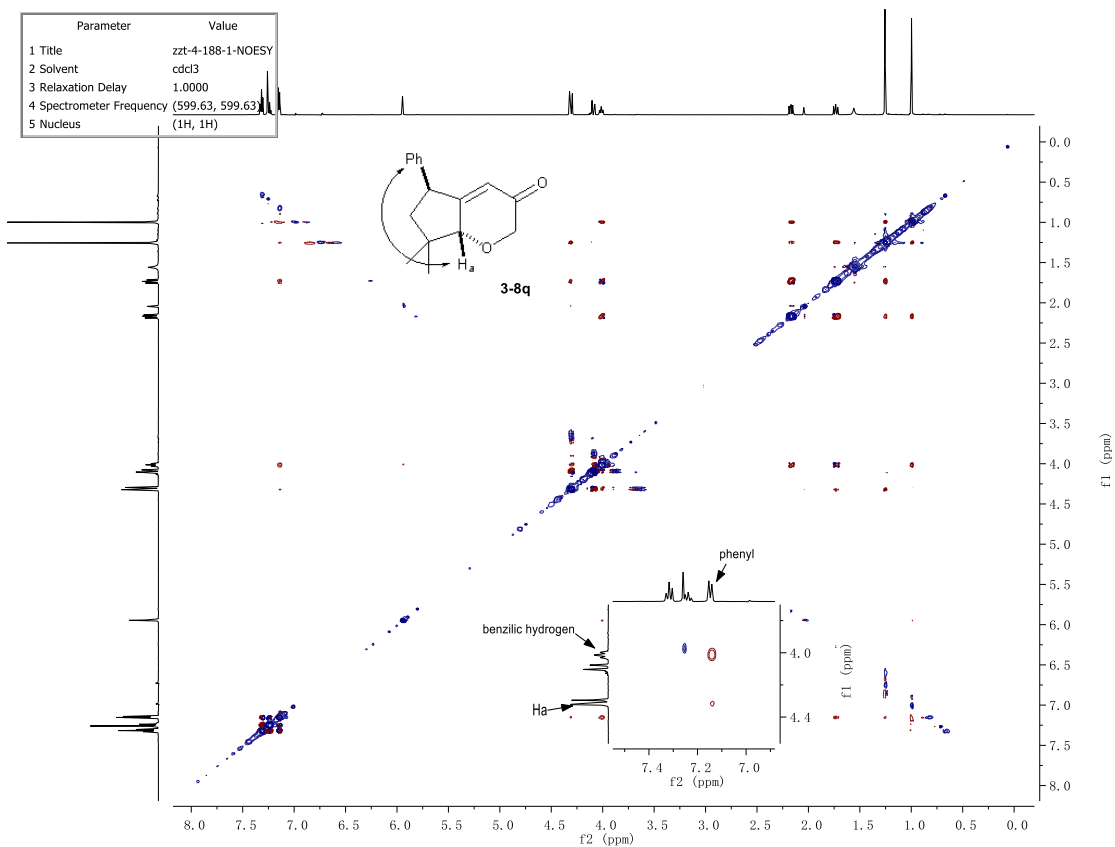
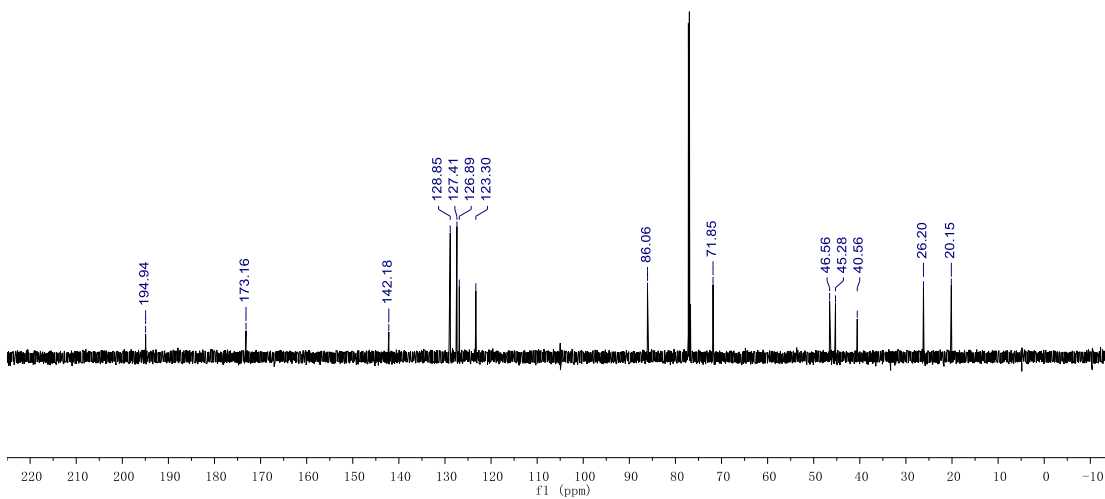
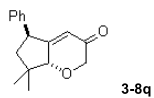


Parameter	Value
1 Title	zzt-4-170-2-COSY-CD3OD
2 Solvent	"cd3od"
3 Relaxation Delay	1.0000

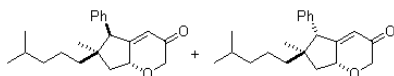




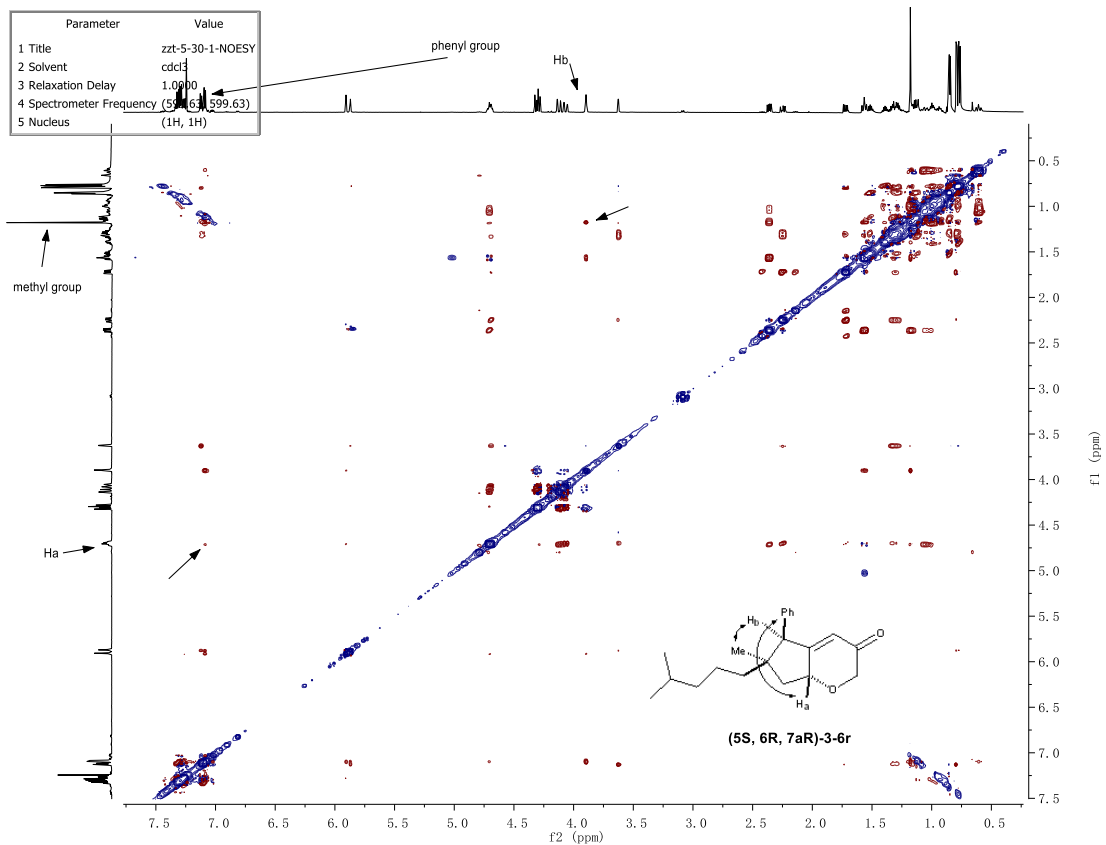
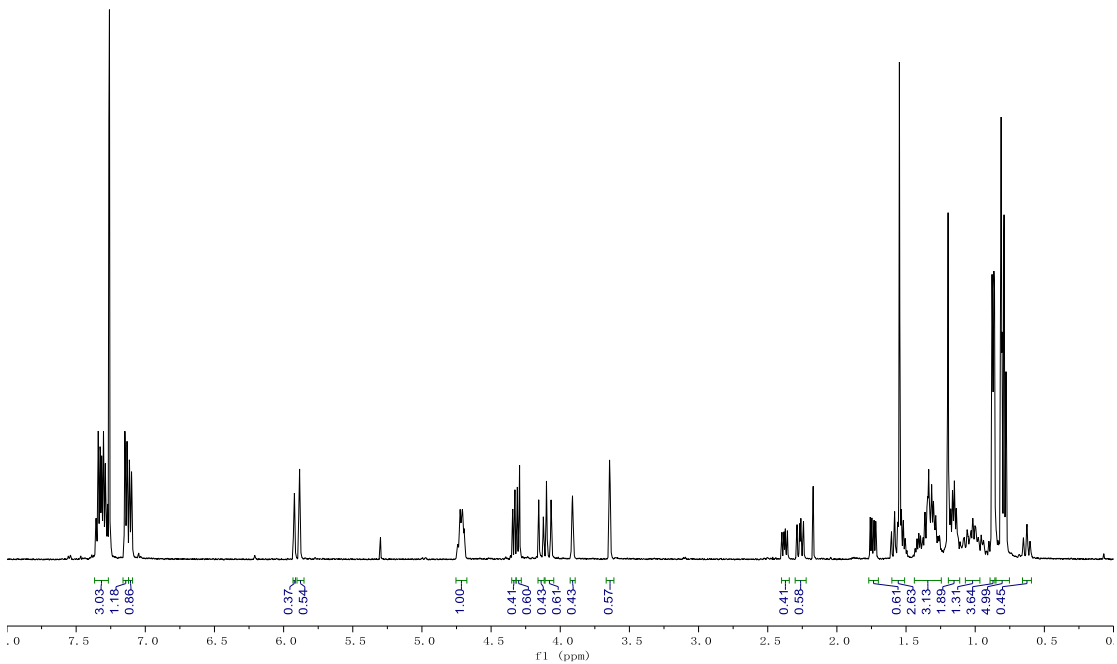
Parameter	Value
1 Title	zzt-4-188-1-C
2 Solvent	cdcl3
3 Relaxation Delay	1.0000
4 Spectrometer Frequency	150.79

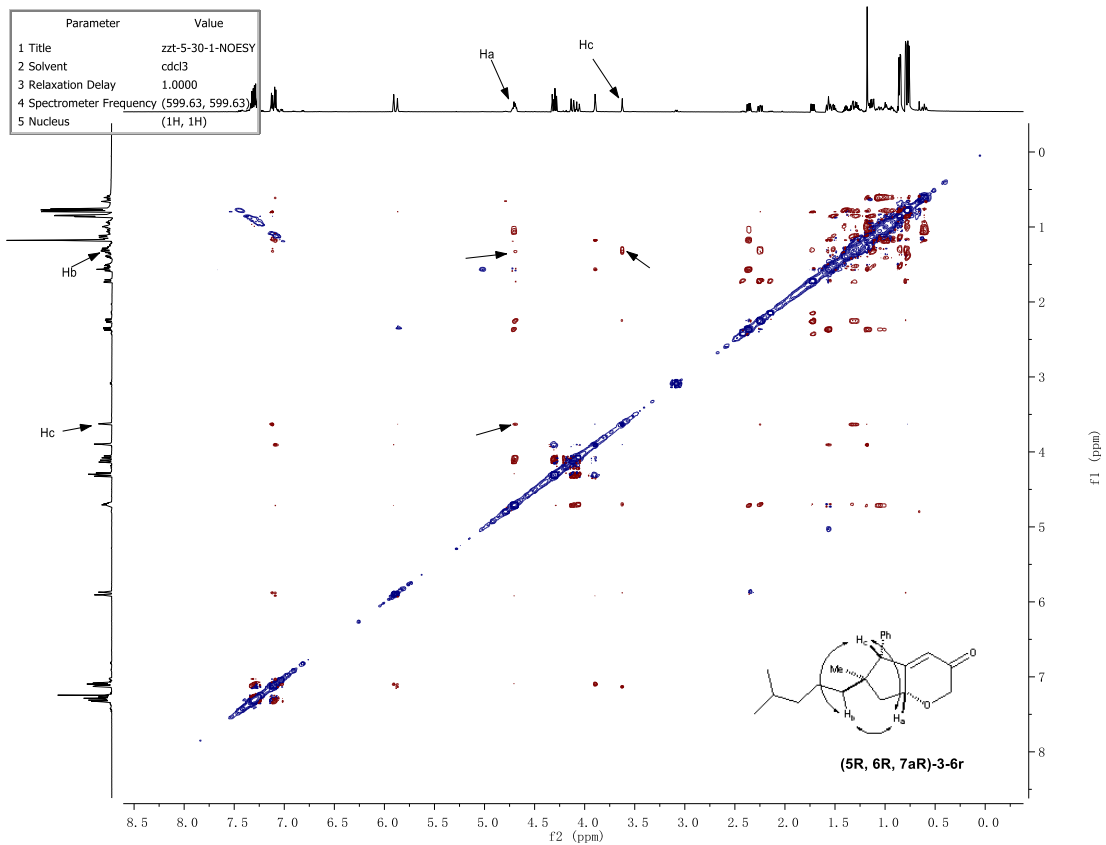


Parameter	Value
1 Title	zzt-5-30-1-H-again
2 Solvent	CDCl3
3 Spectrometer Frequency	499.86
4 Nucleus	1H

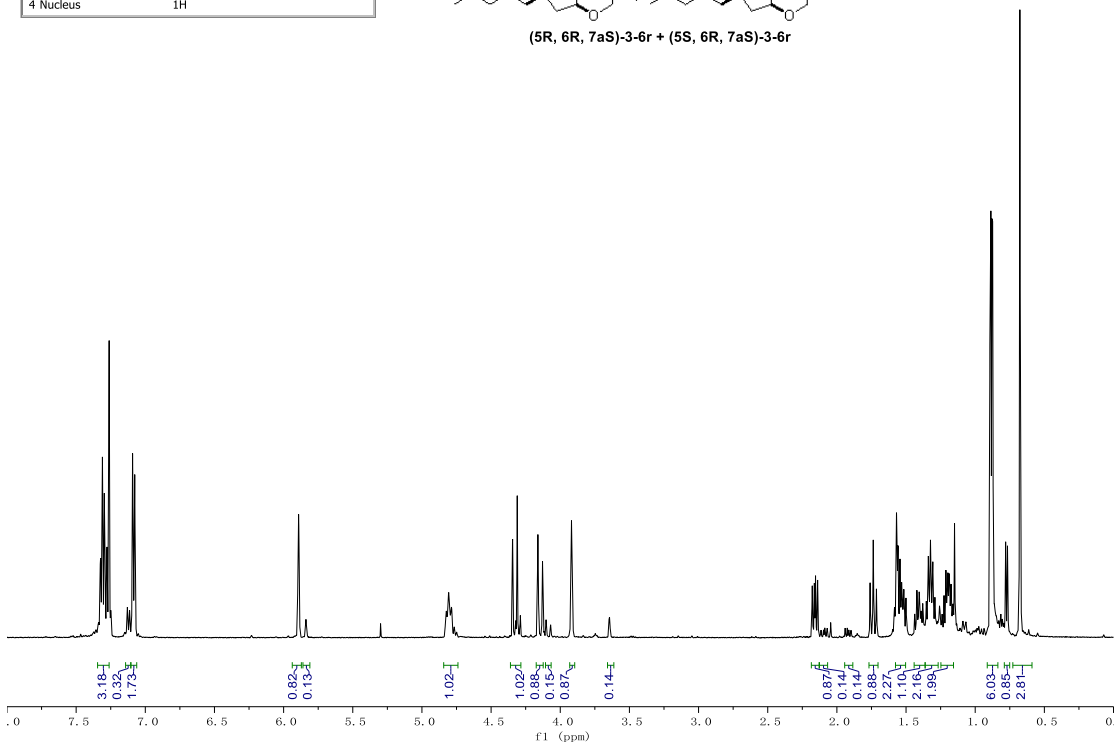
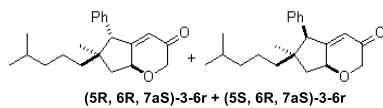


(5S, 6R, 7aR)-3-8r, (5R, 6R, 7aR)-3-8r

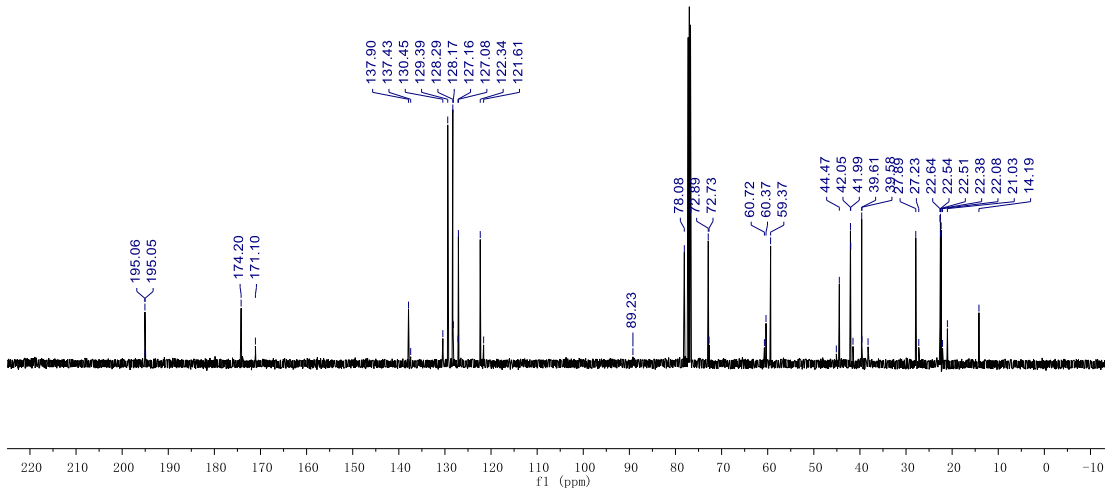
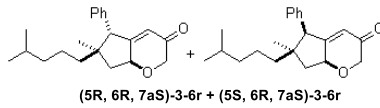




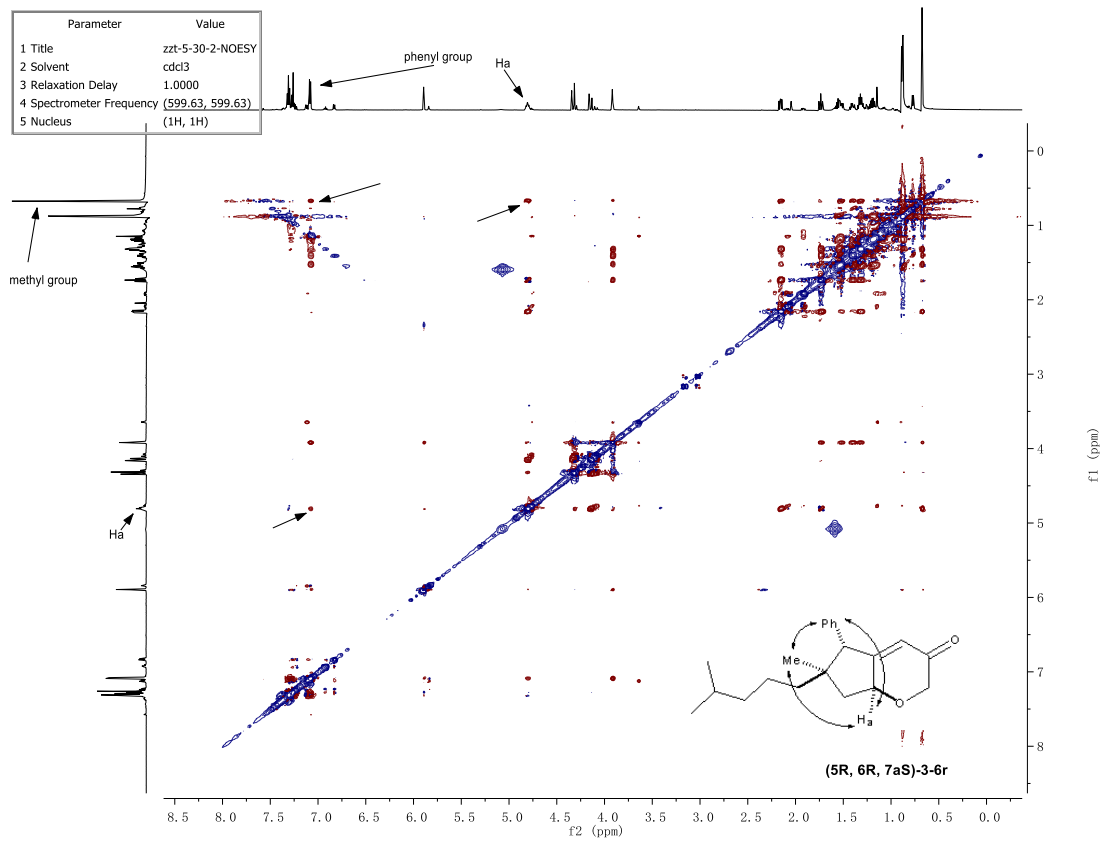
Parameter	Value
1 Title	(5R, 6R, 7aS)-3r + (5S, 6R, 7aS)-3r-H
2 Solvent	CDCl3
3 Spectrometer Frequency	499.86
4 Nucleus	1H

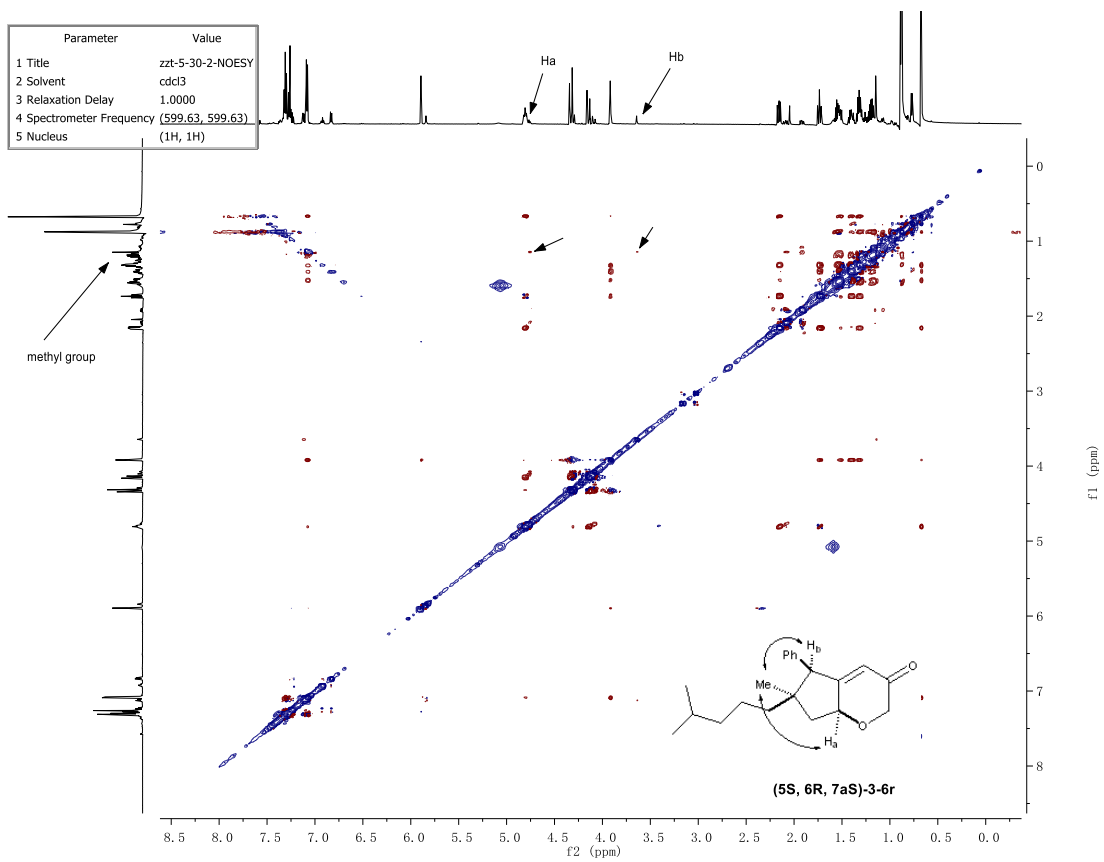


Parameter	Value
1 Title	zzt-5-30-2-C-maybe_overlapped
2 Solvent	CDCl3
3 Relaxation Delay	1.0000
4 Spectrometer Frequency	125.70

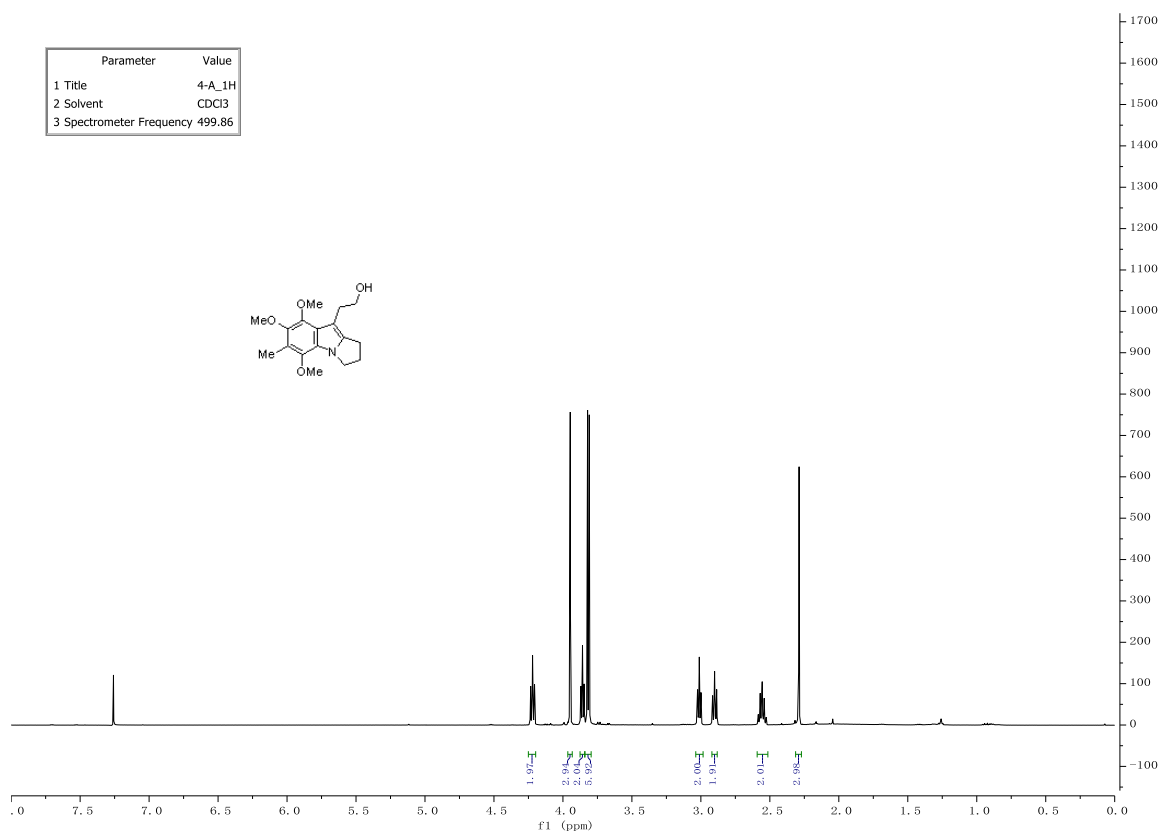


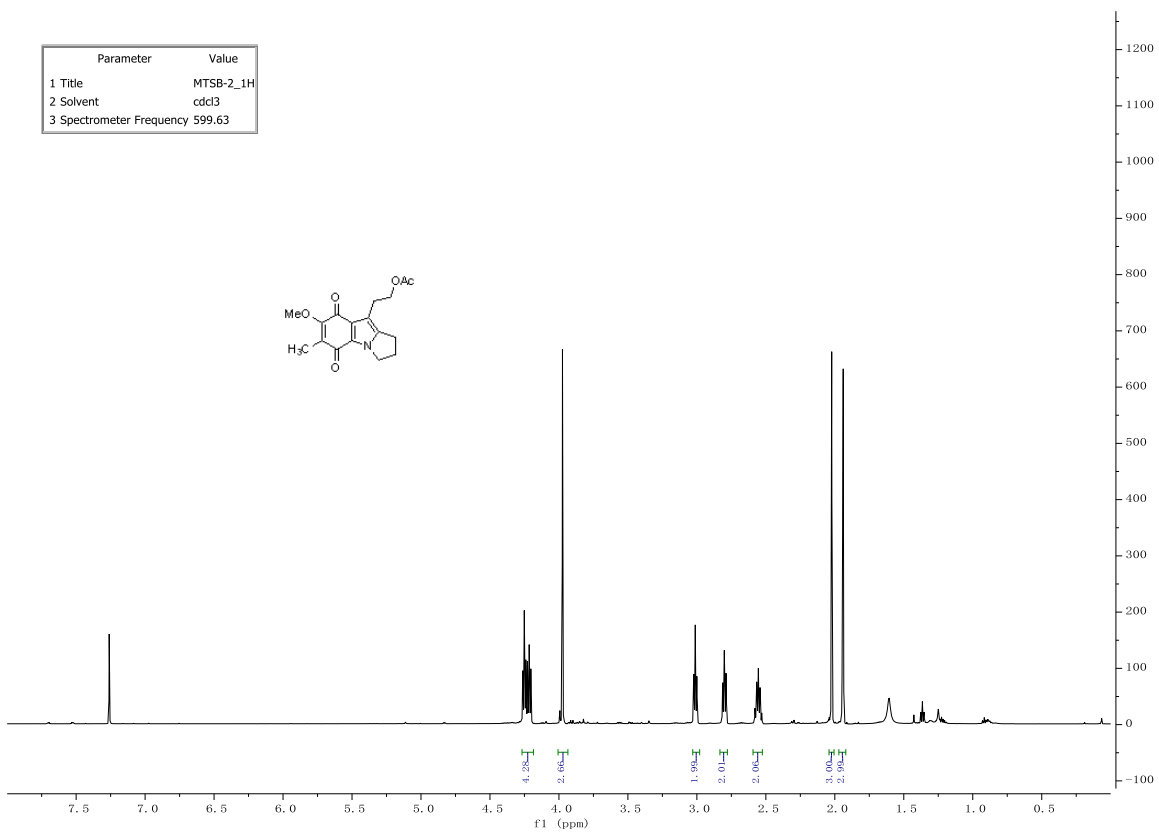
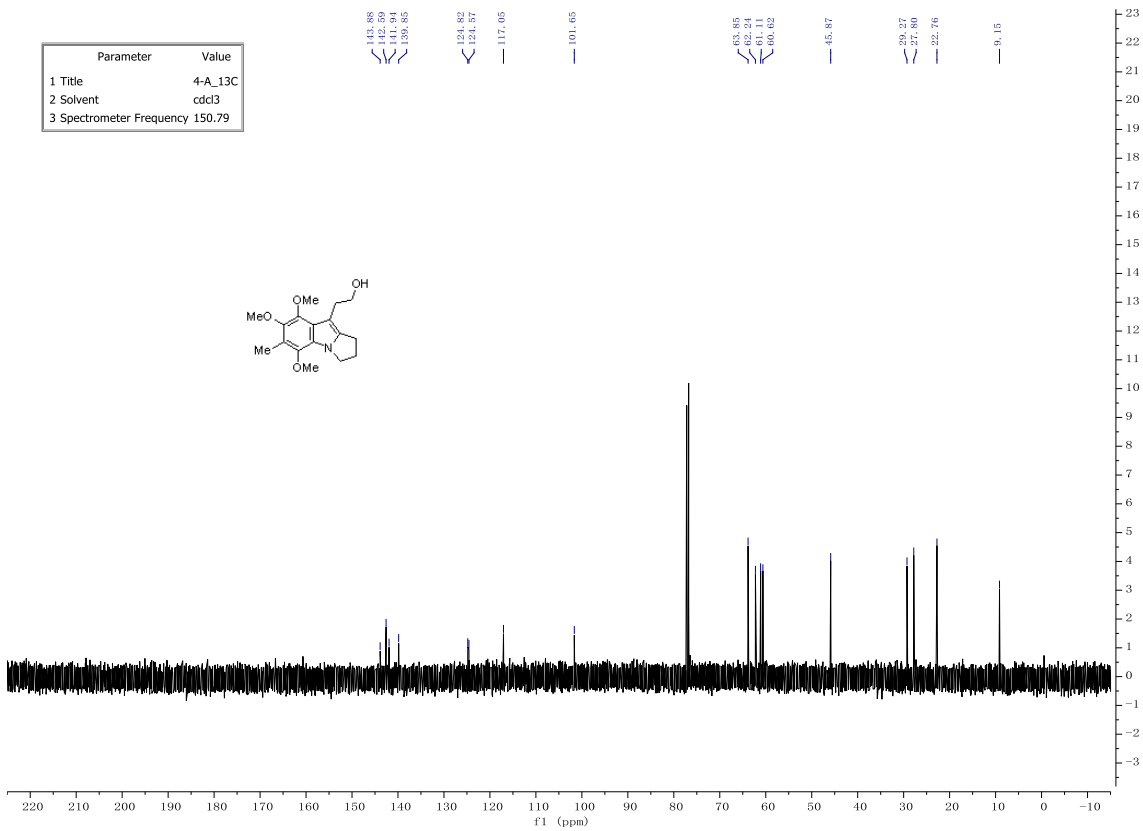
Parameter	Value
1 Title	zzt-5-30-2-NOESY
2 Solvent	cdcl3
3 Relaxation Delay	1.0000
4 Spectrometer Frequency	(599.63, 599.63)
5 Nucleus	(1H, 1H)

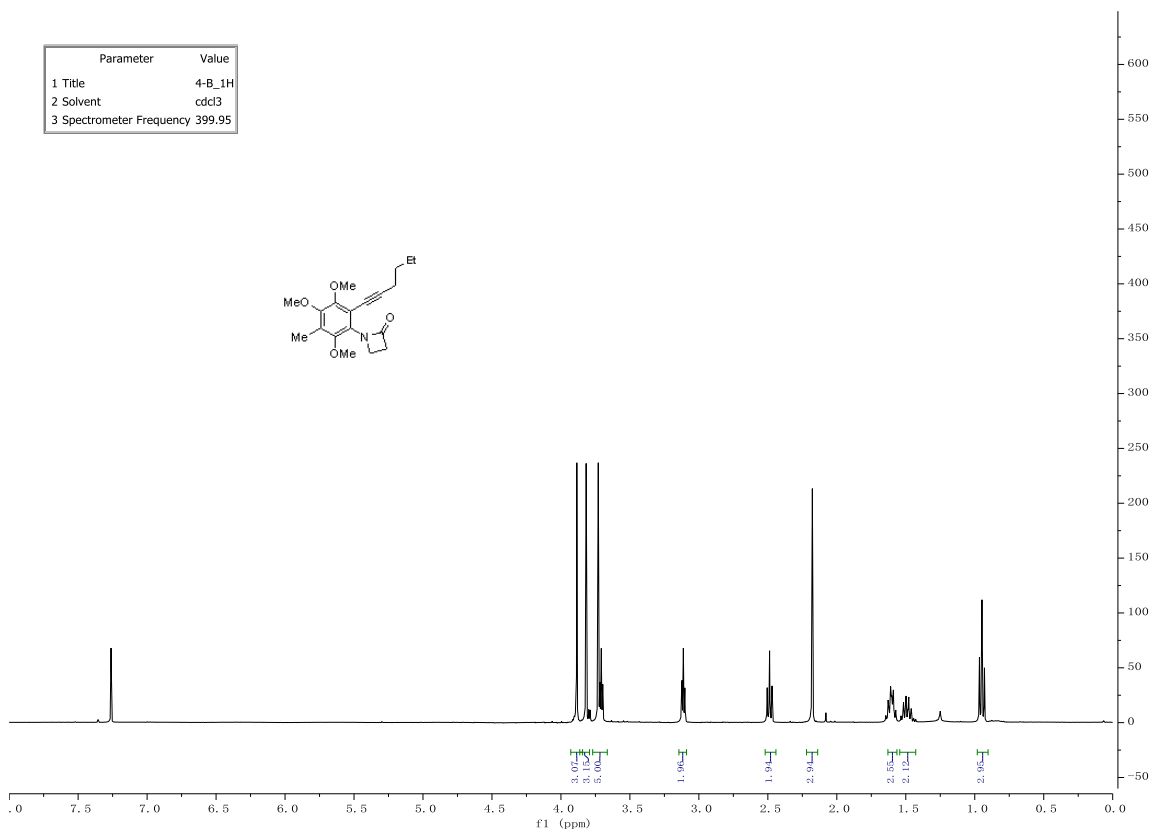
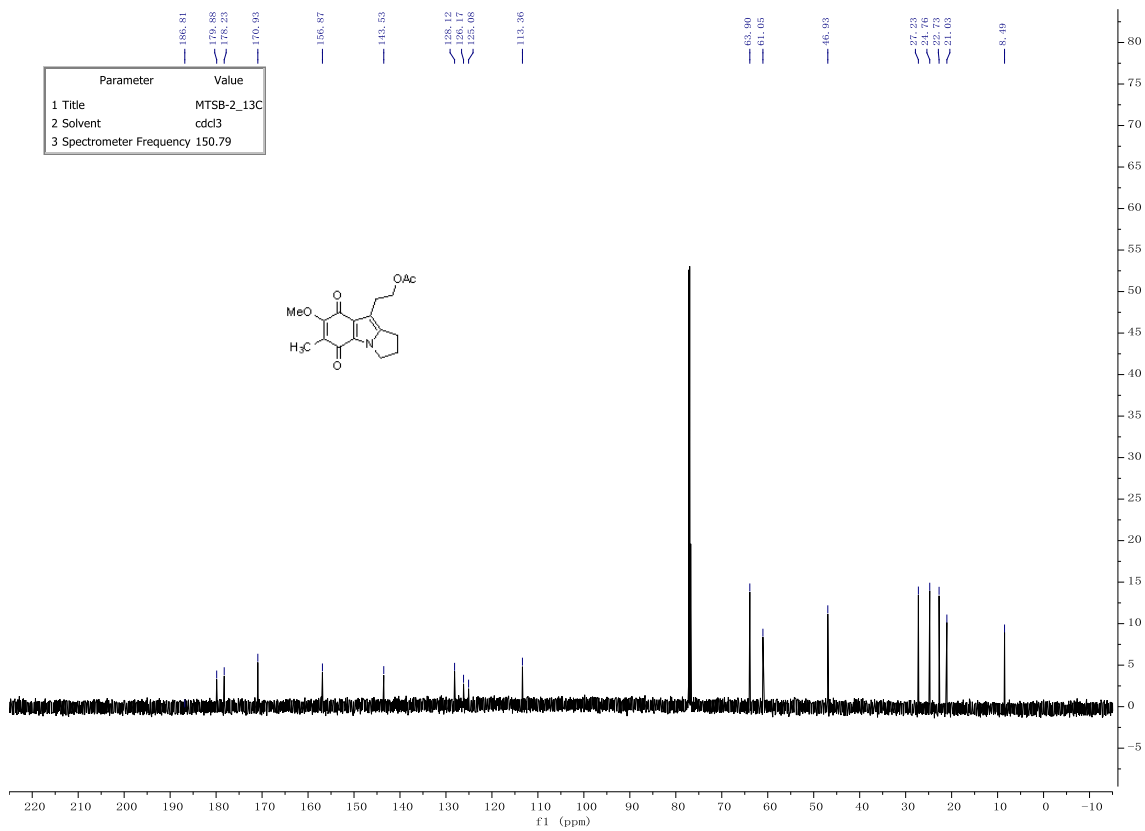


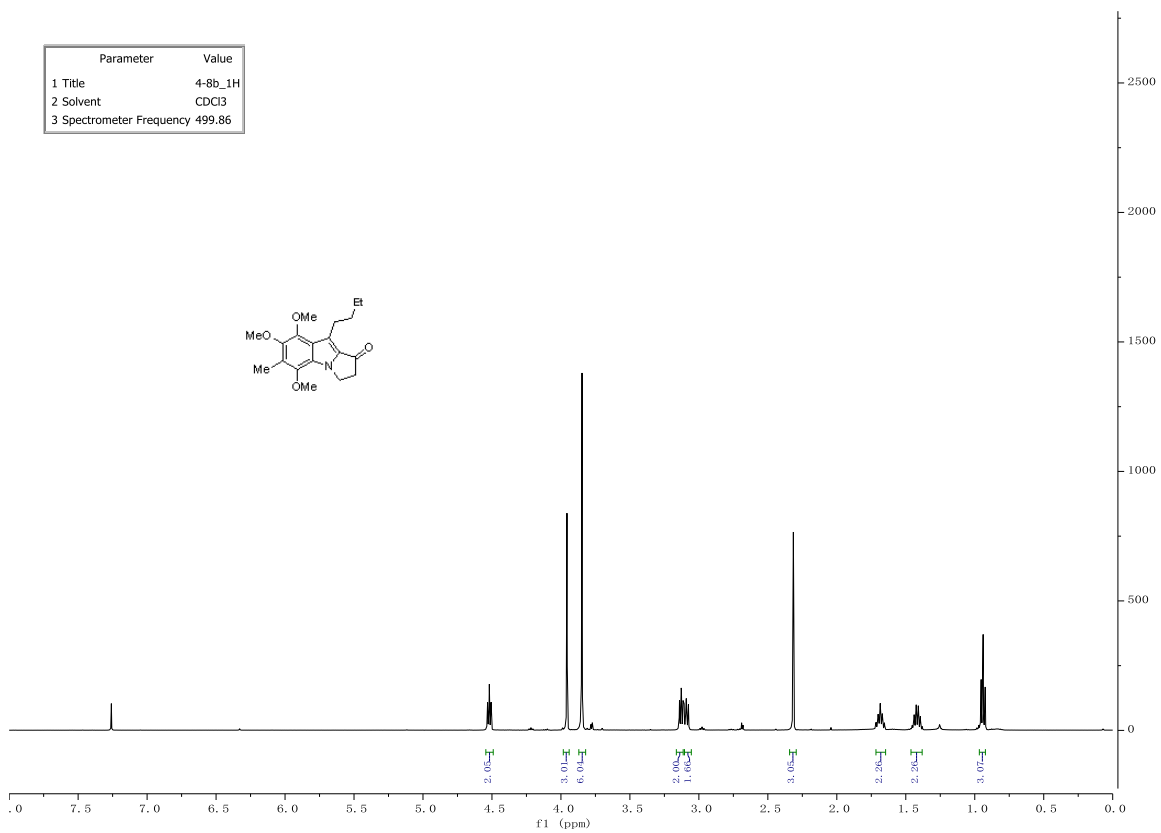
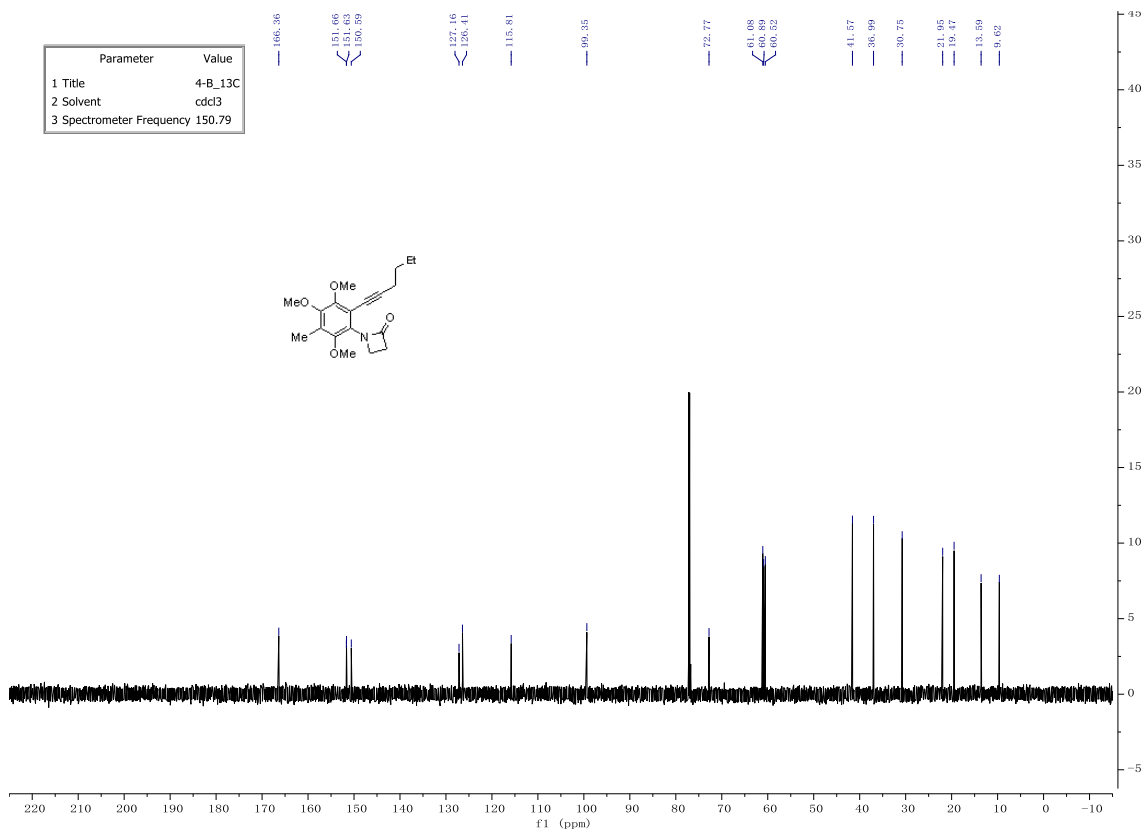


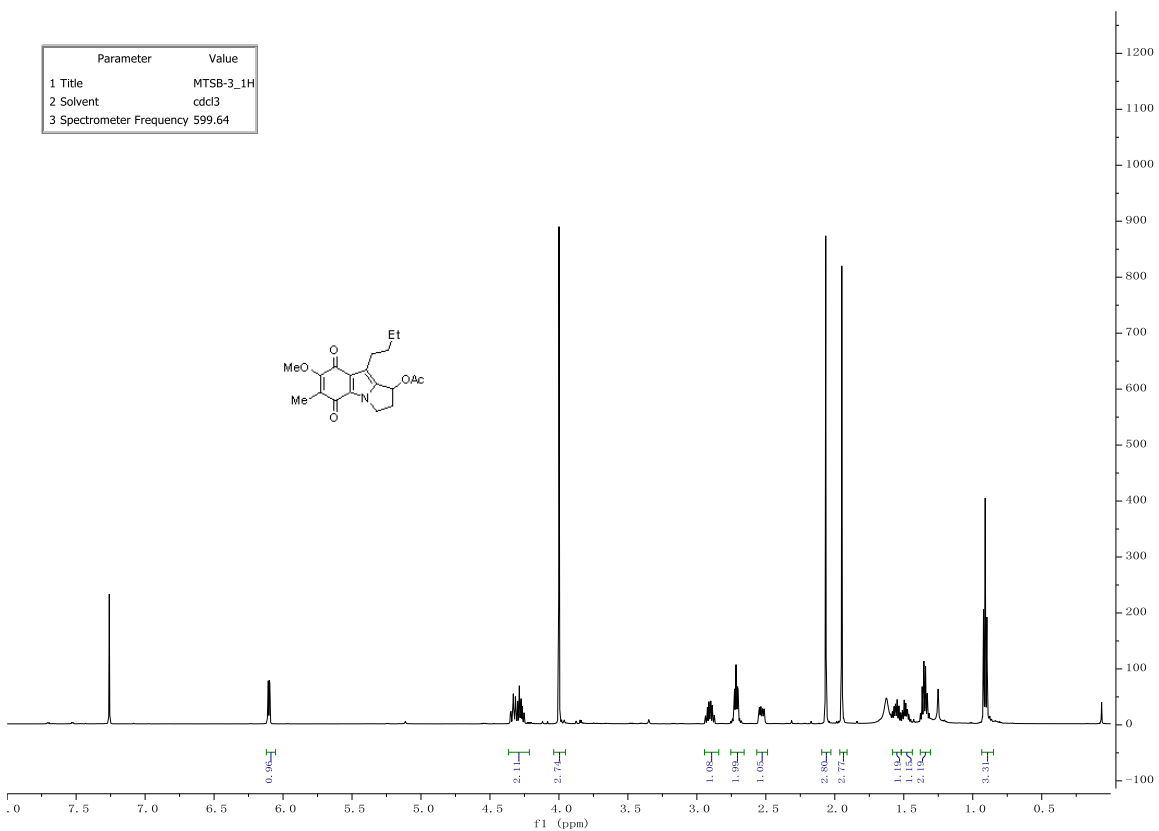
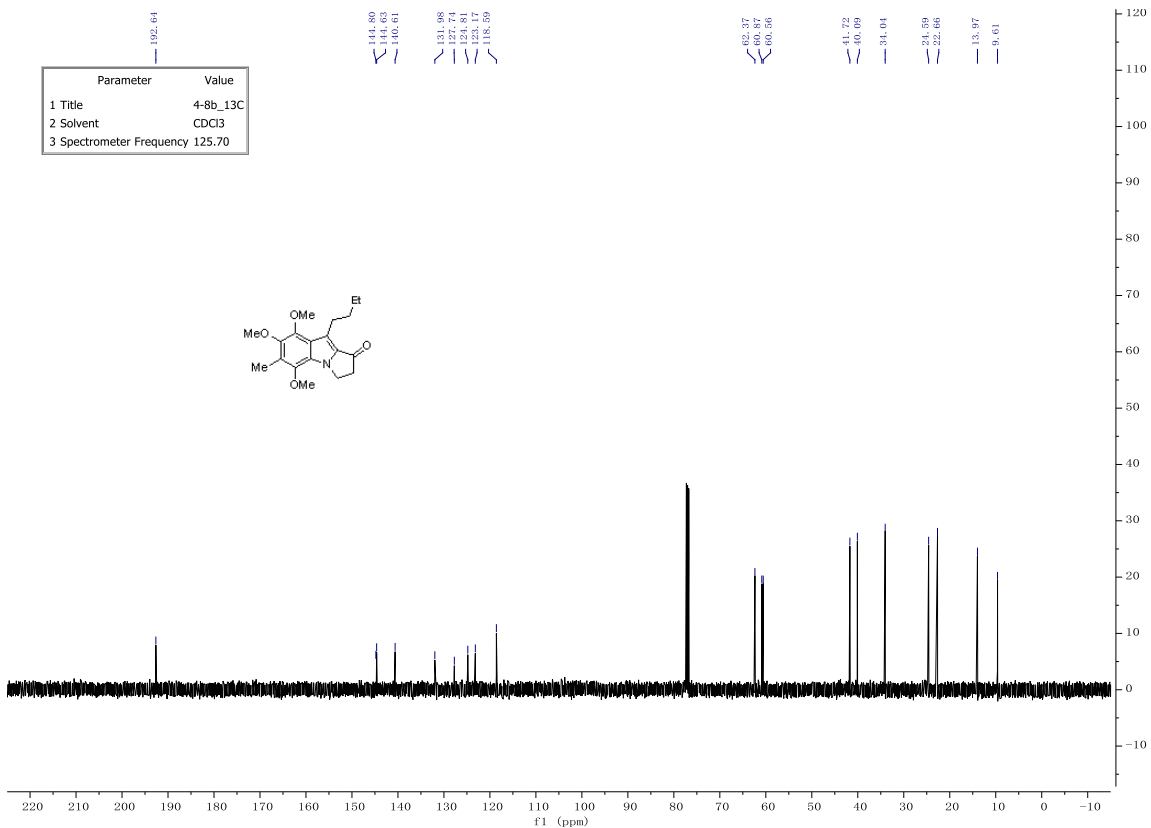
NMR Spectra for Compounds in Chapter 4

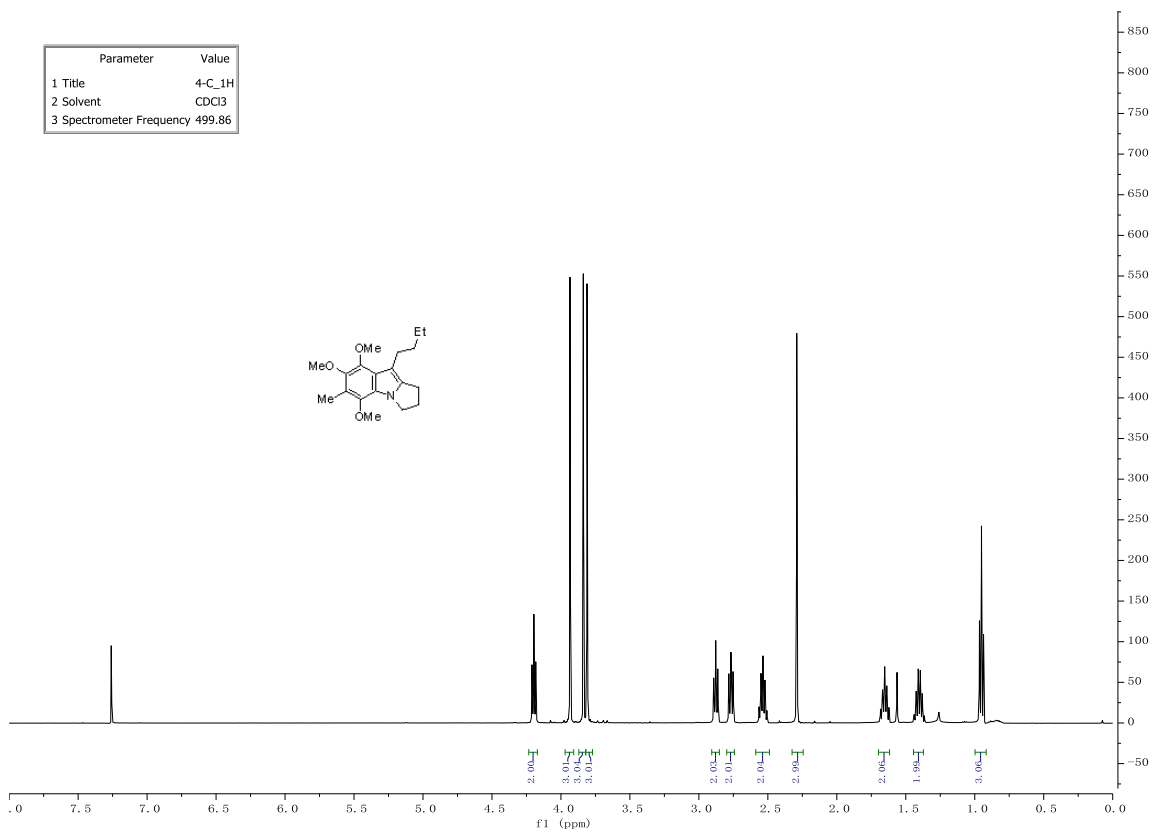
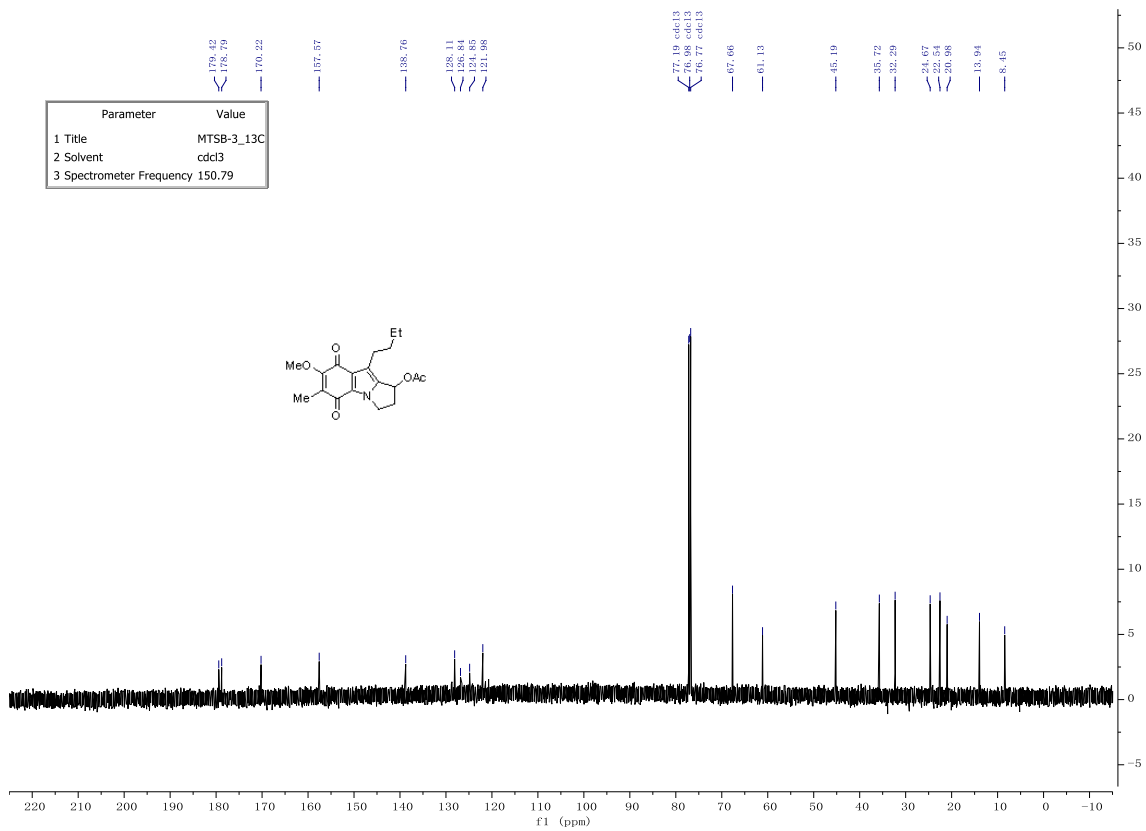


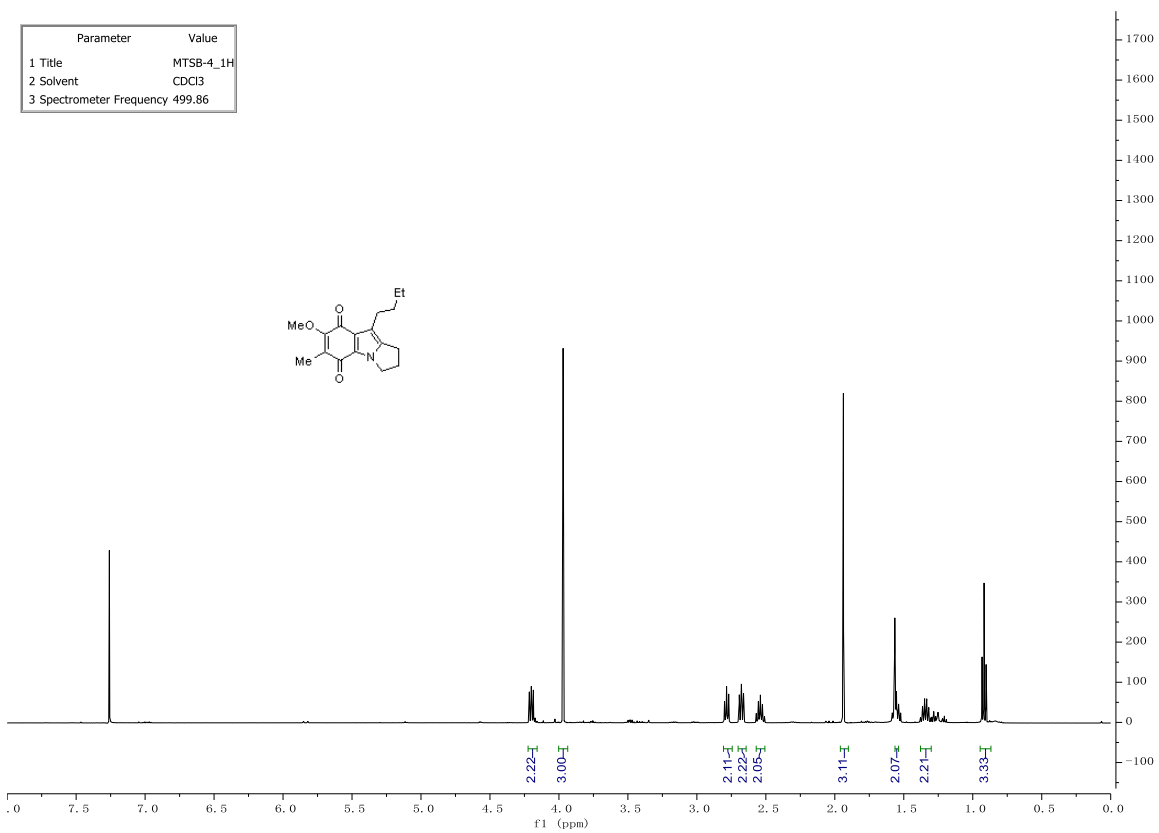
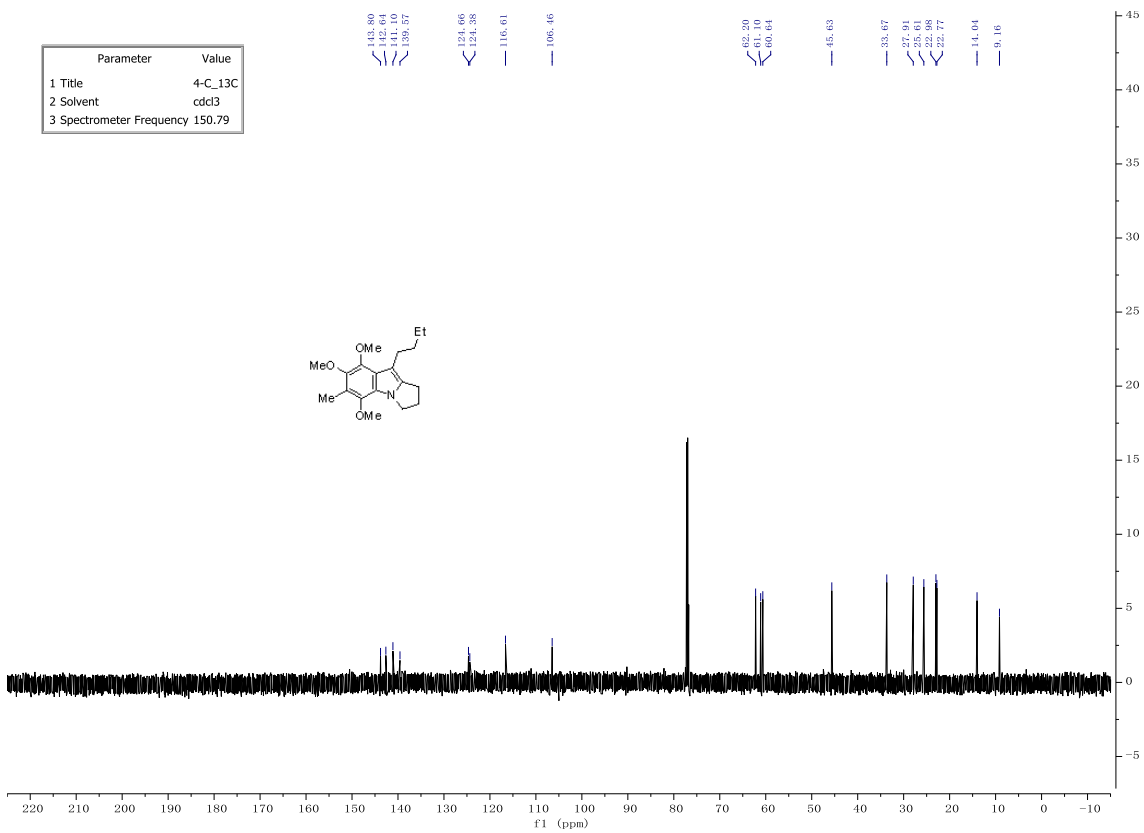


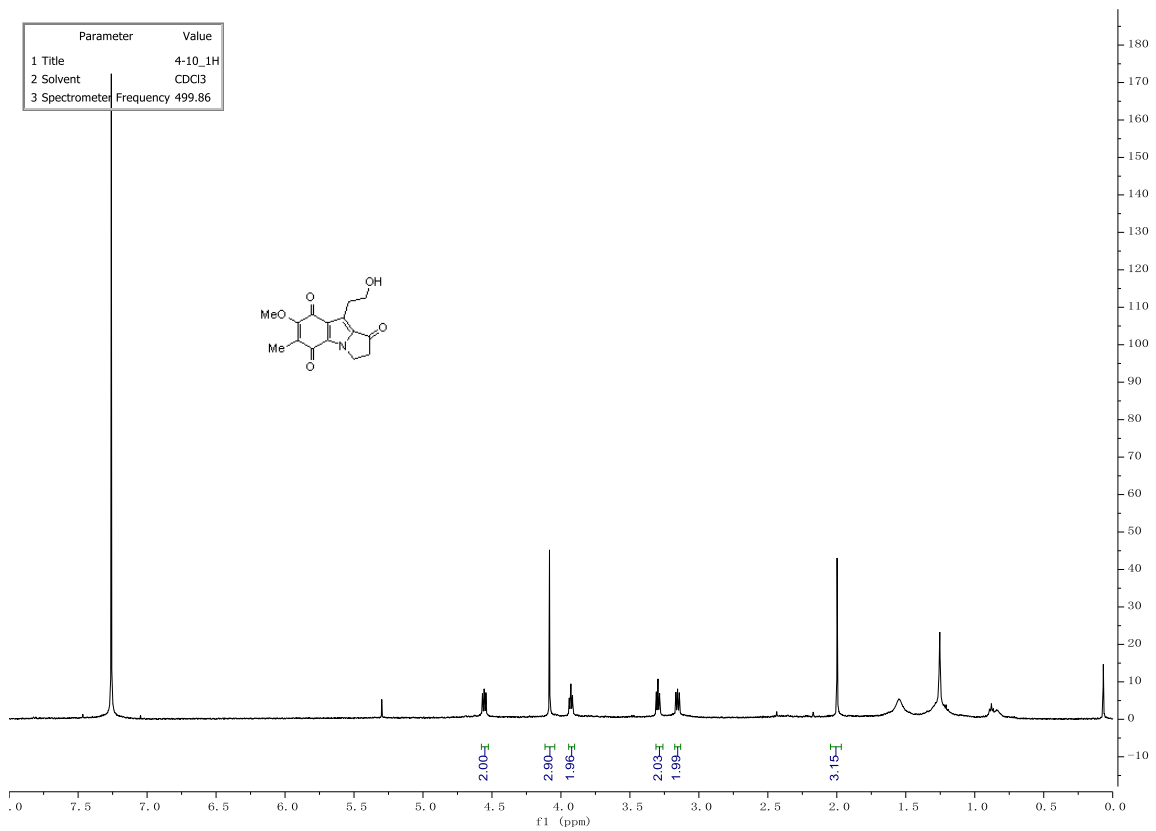
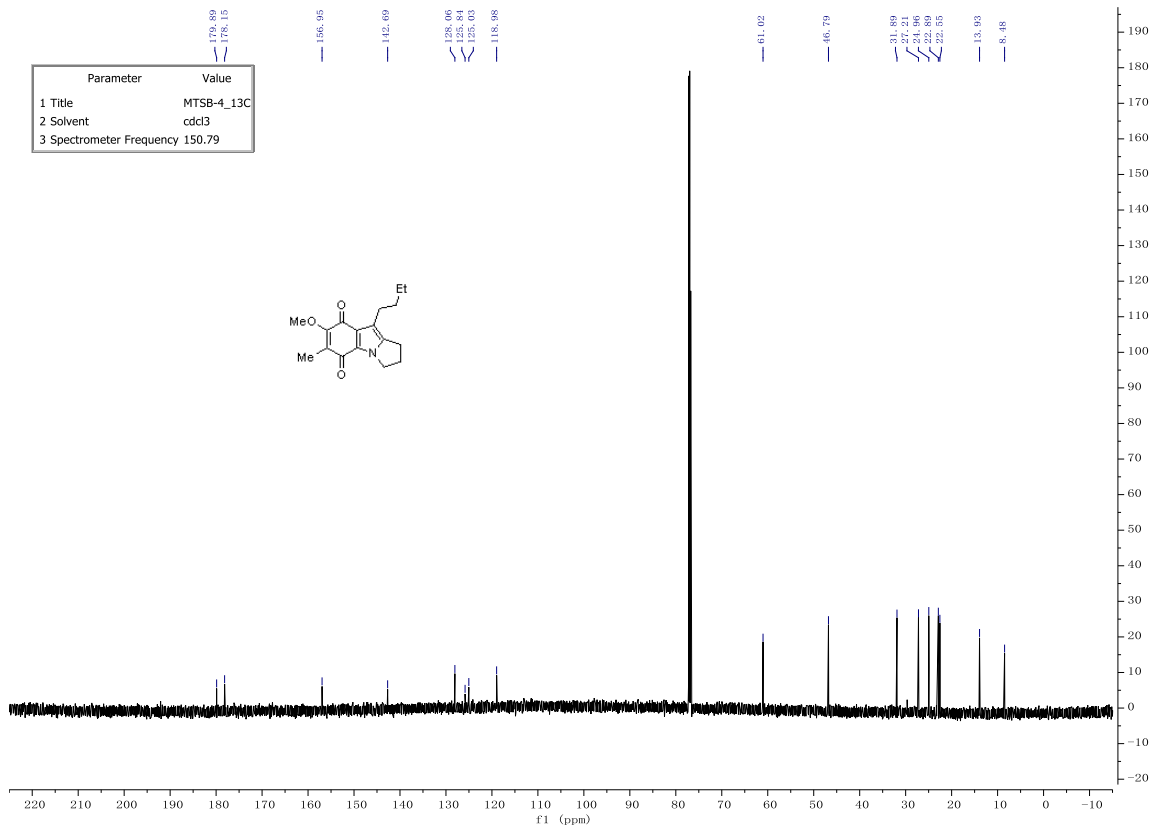


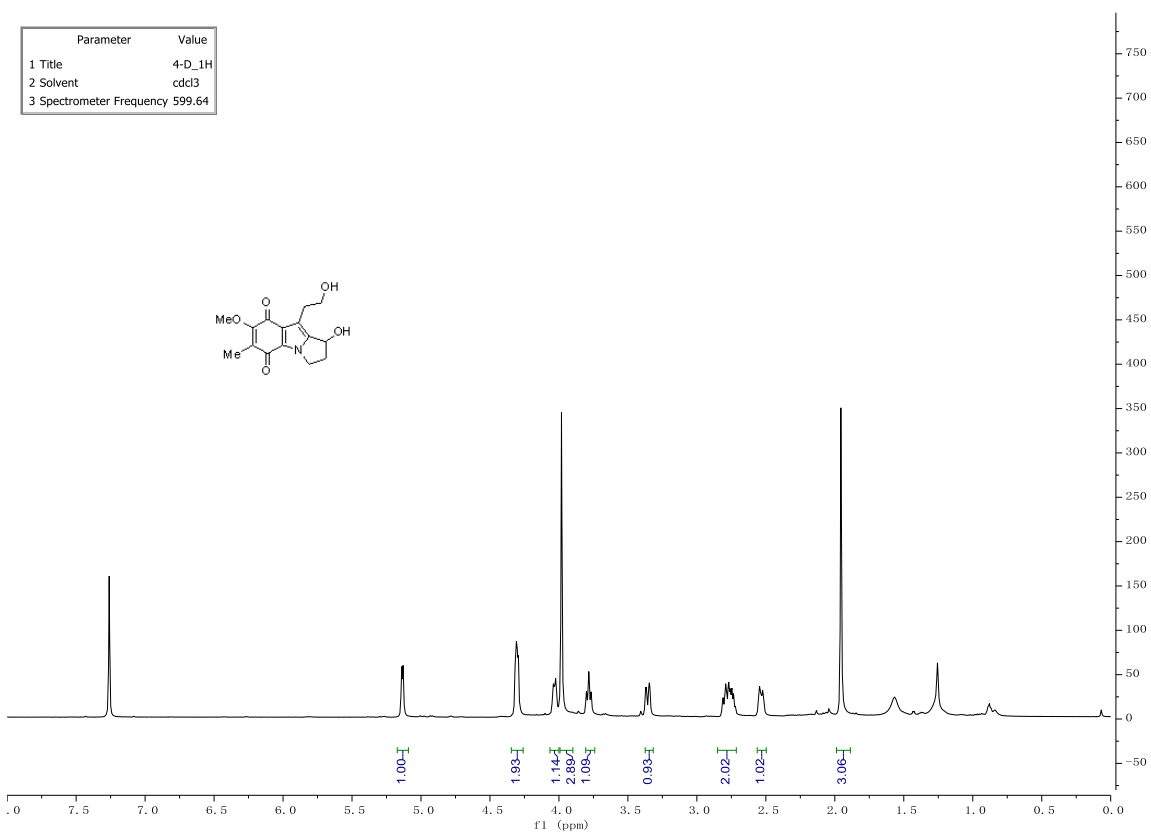
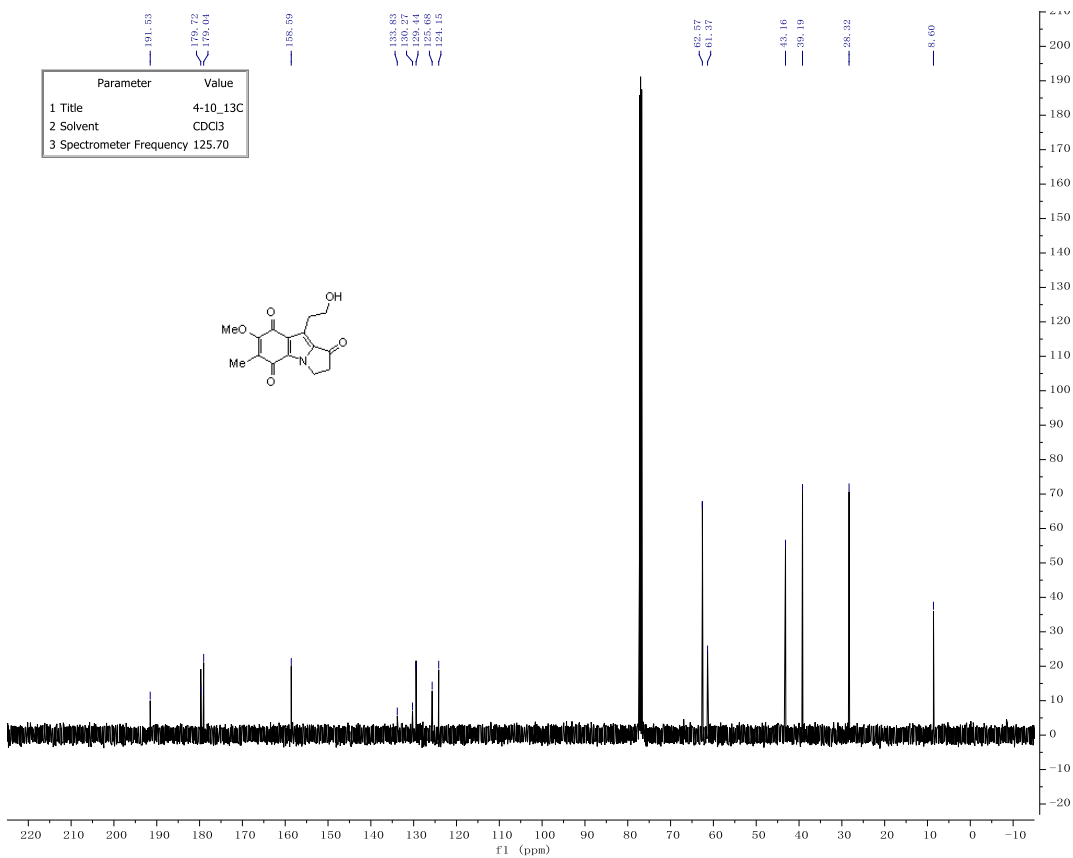


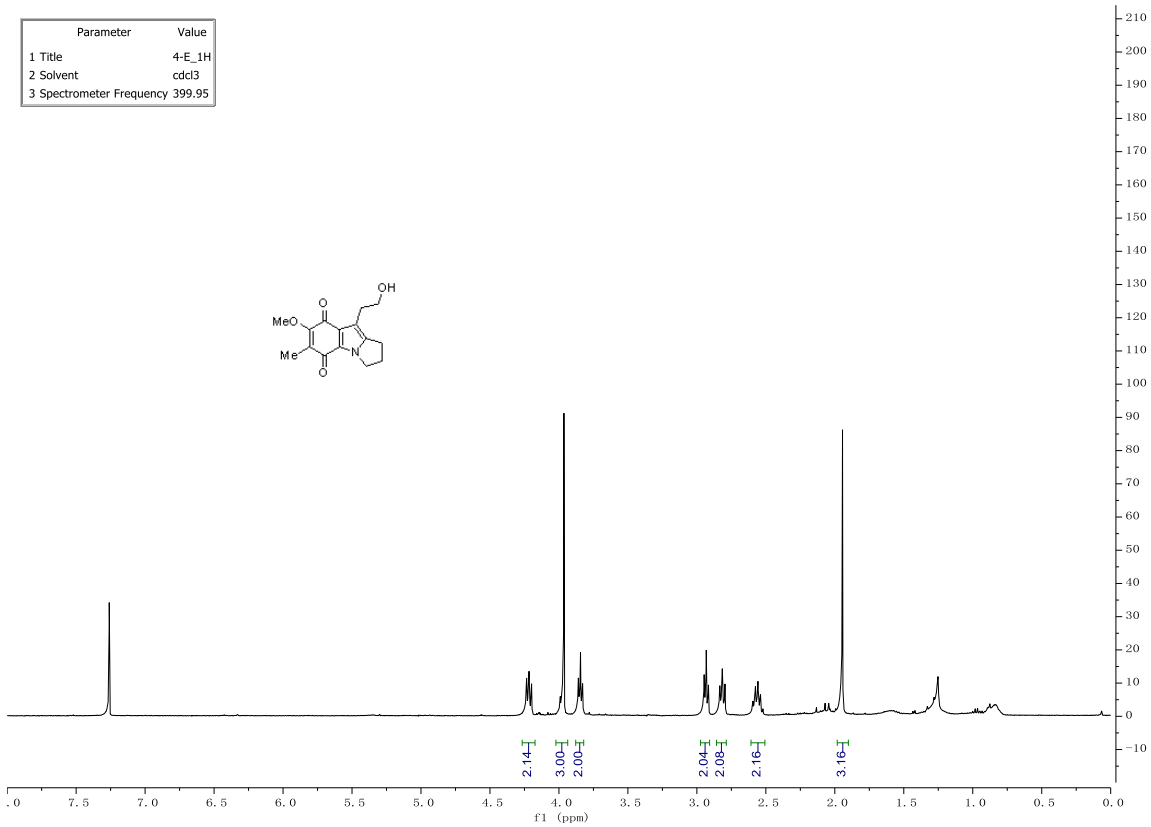
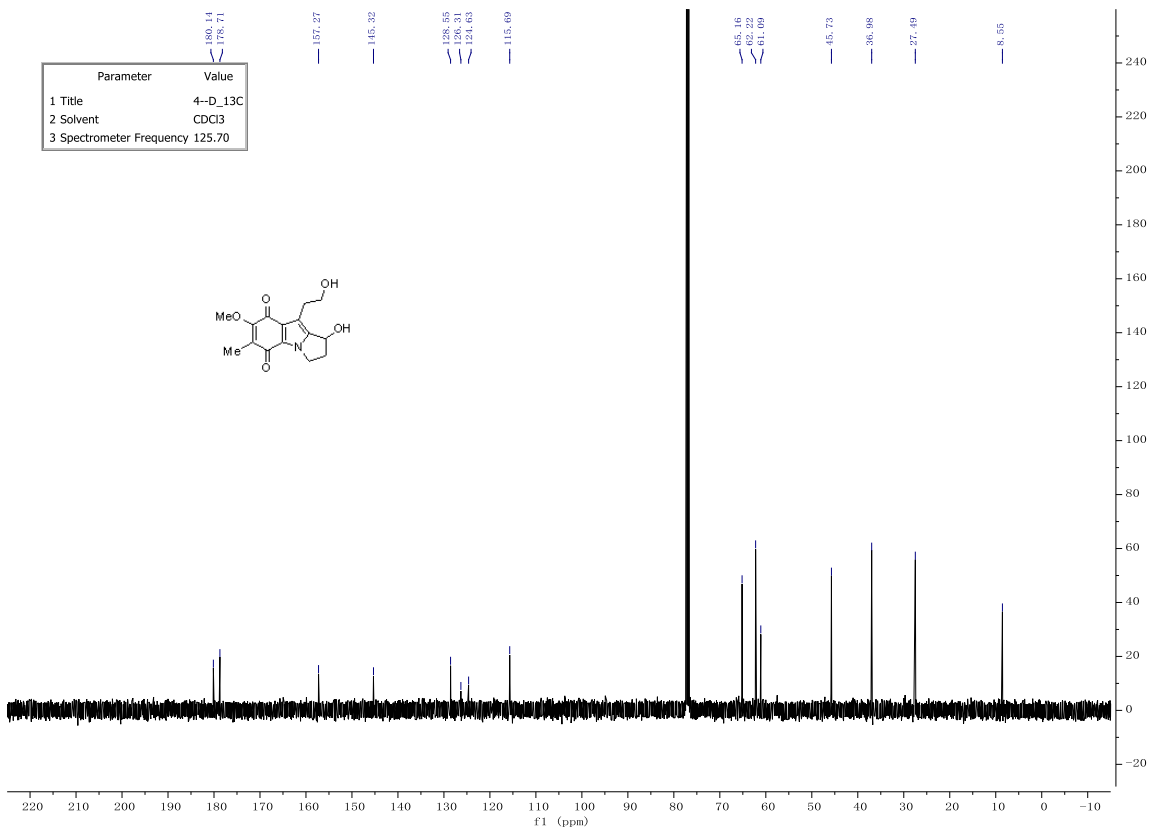


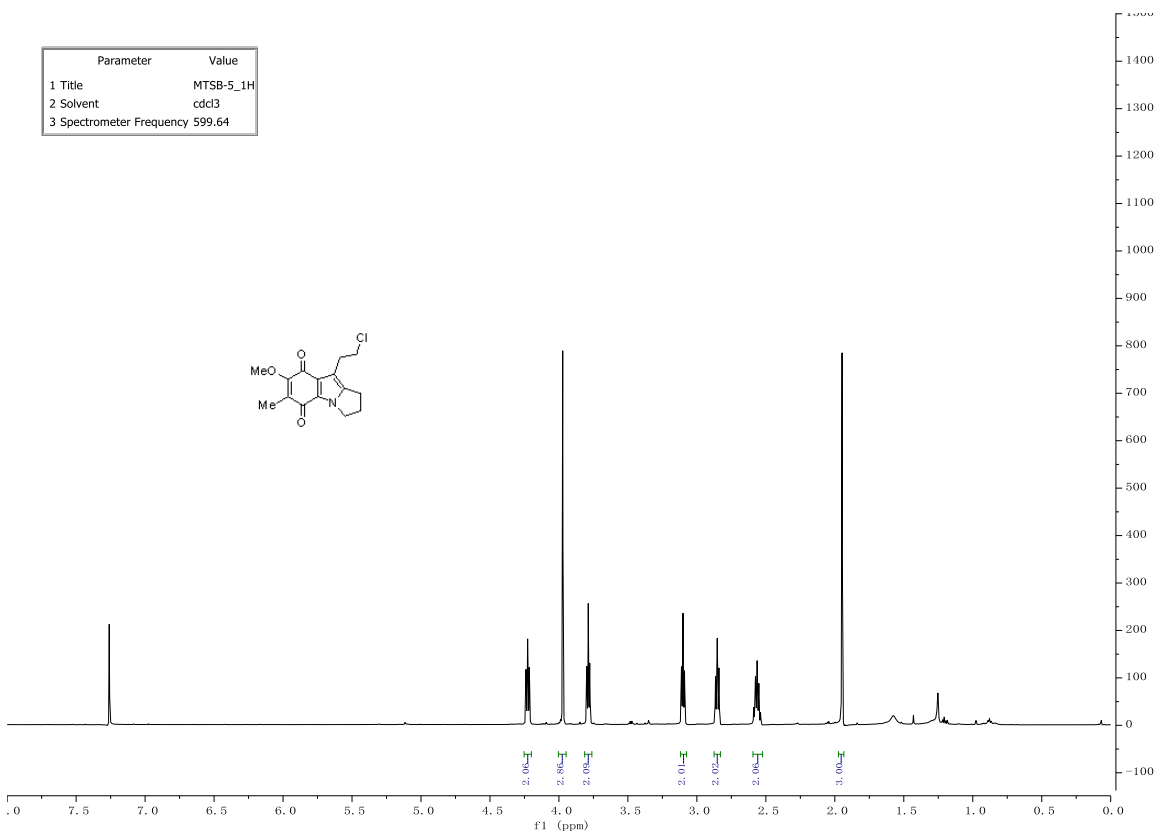
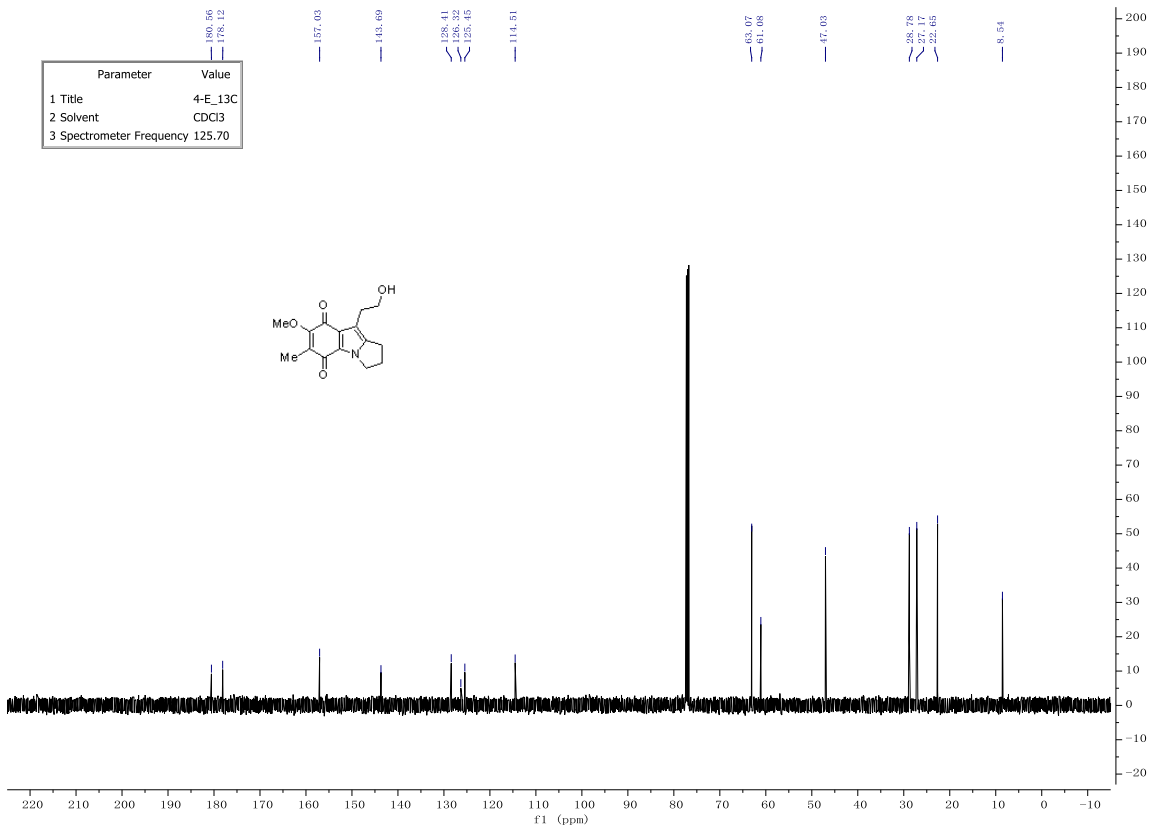


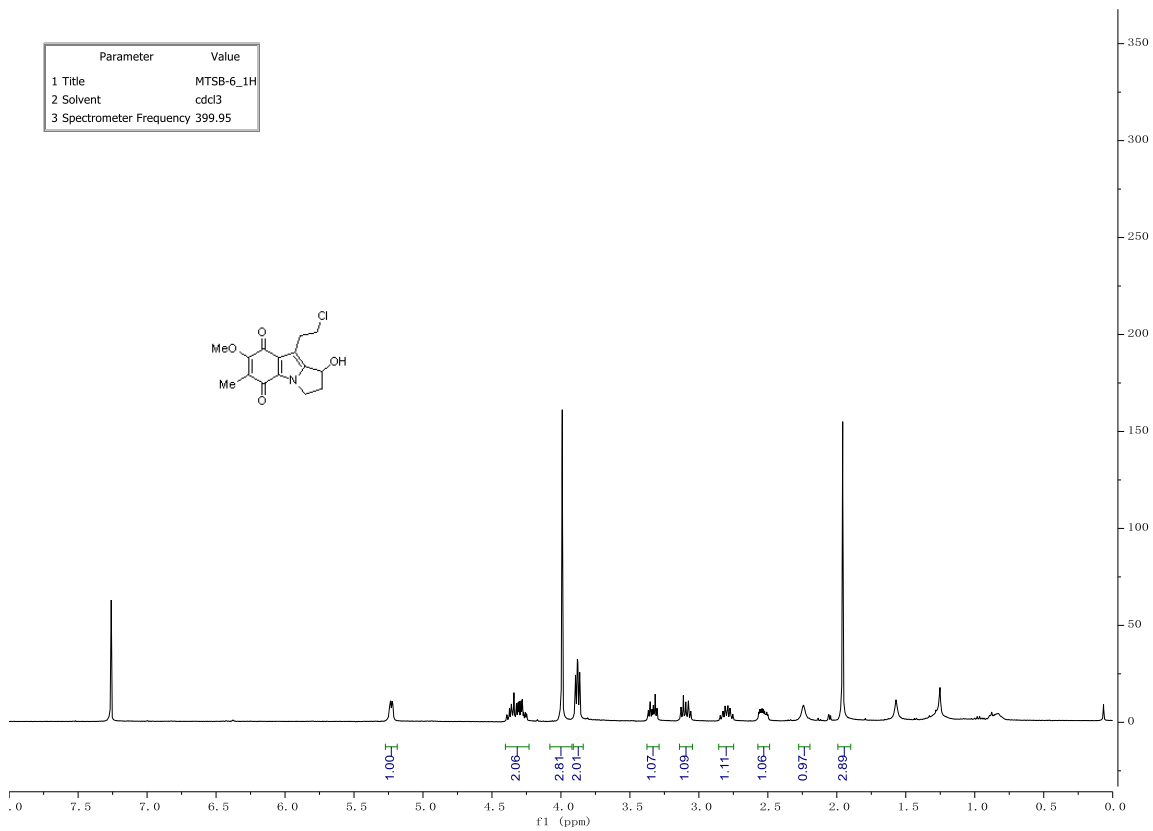
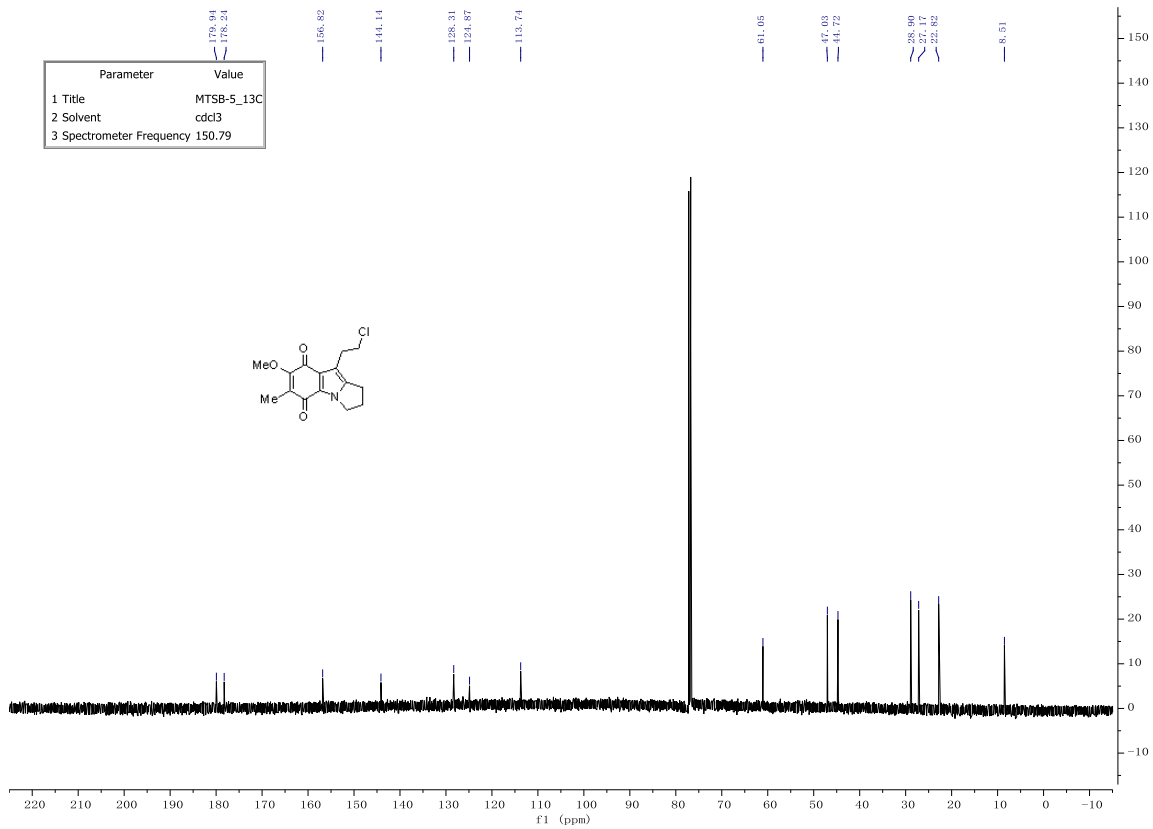


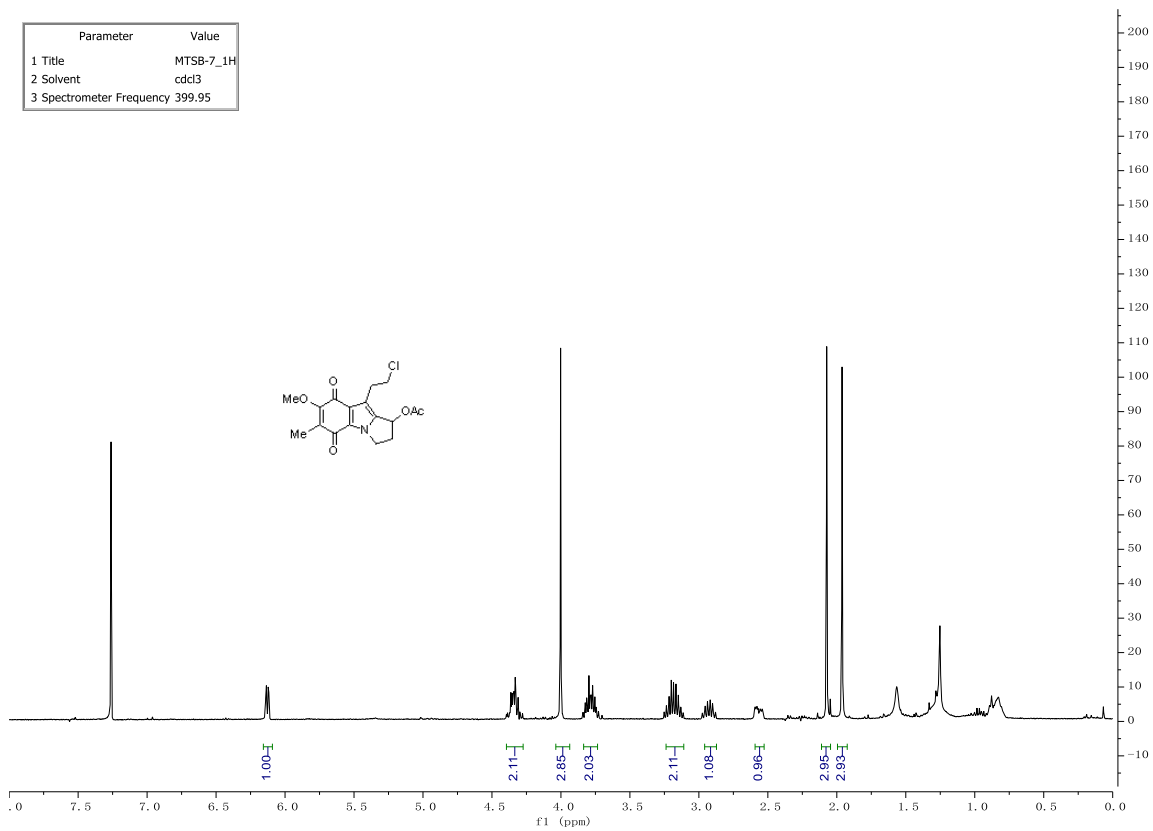
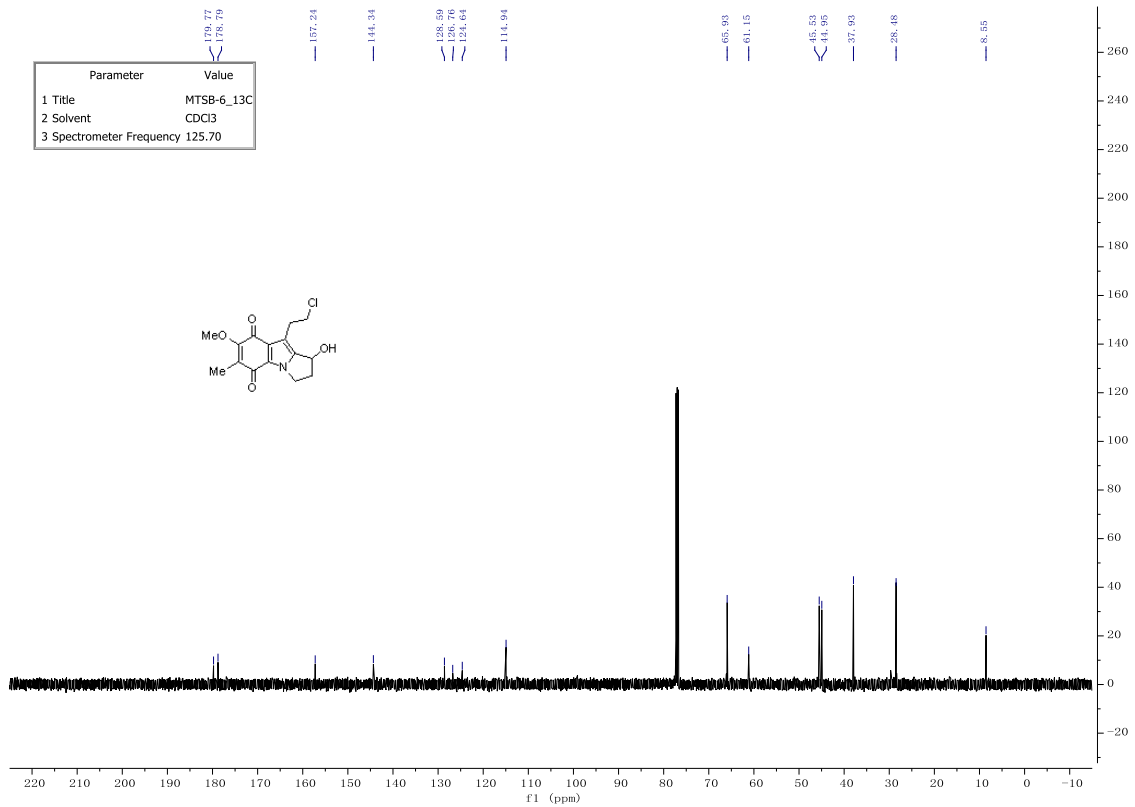


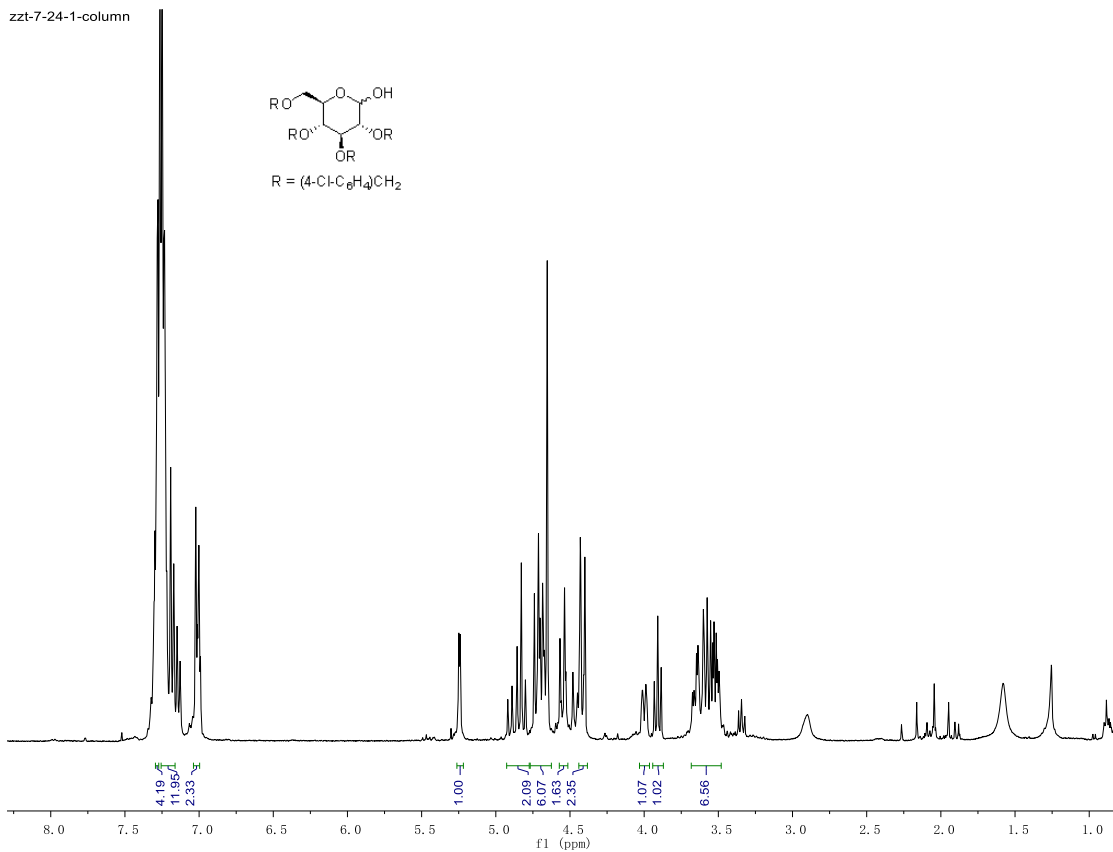
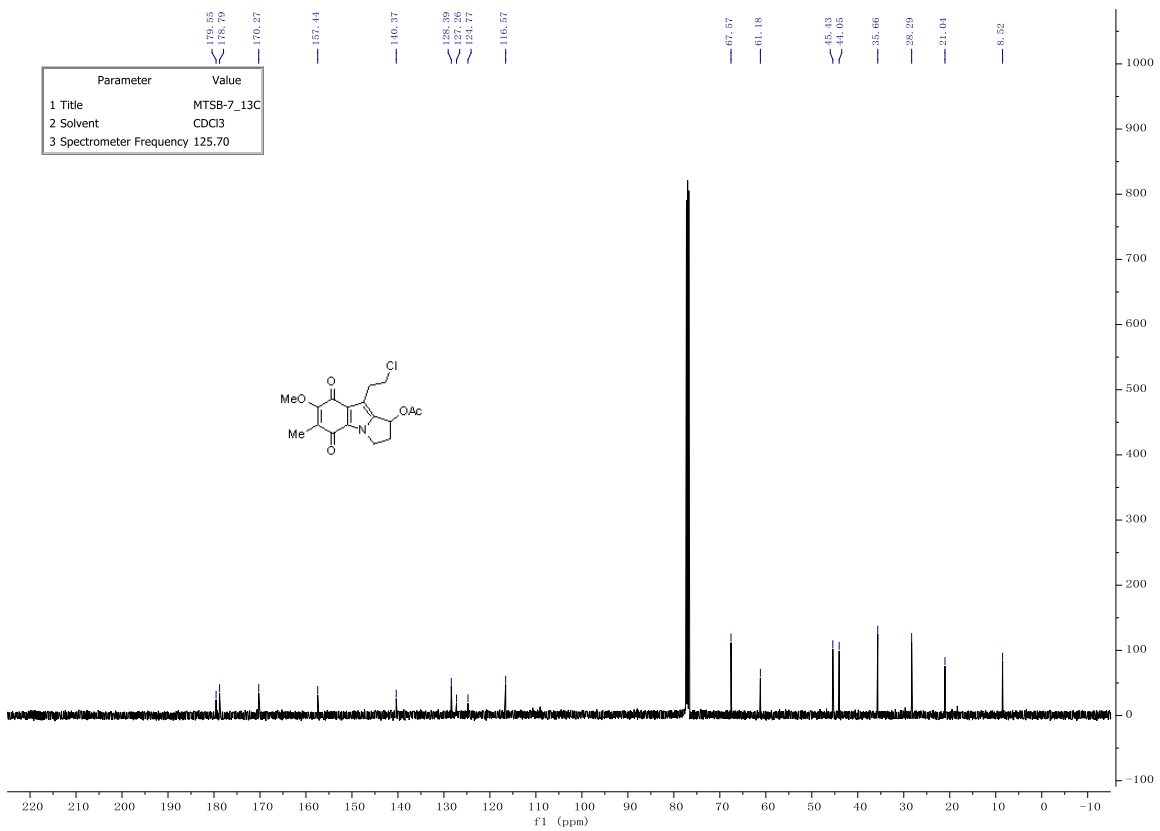




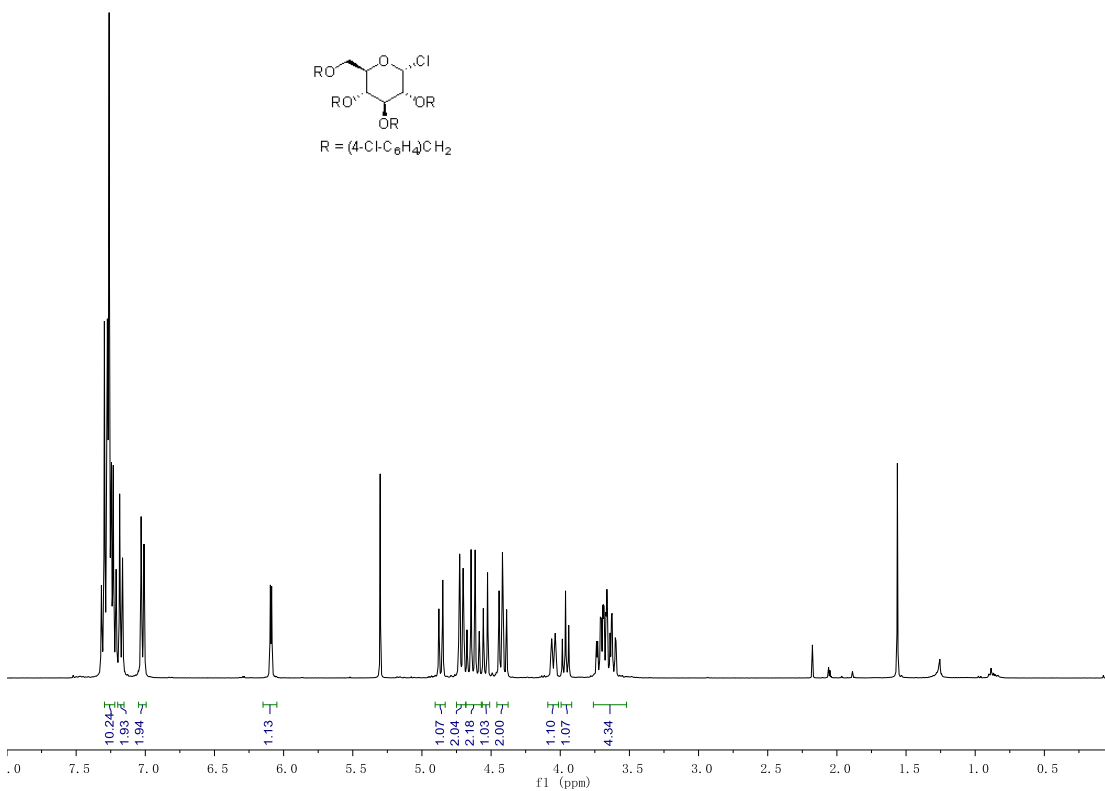




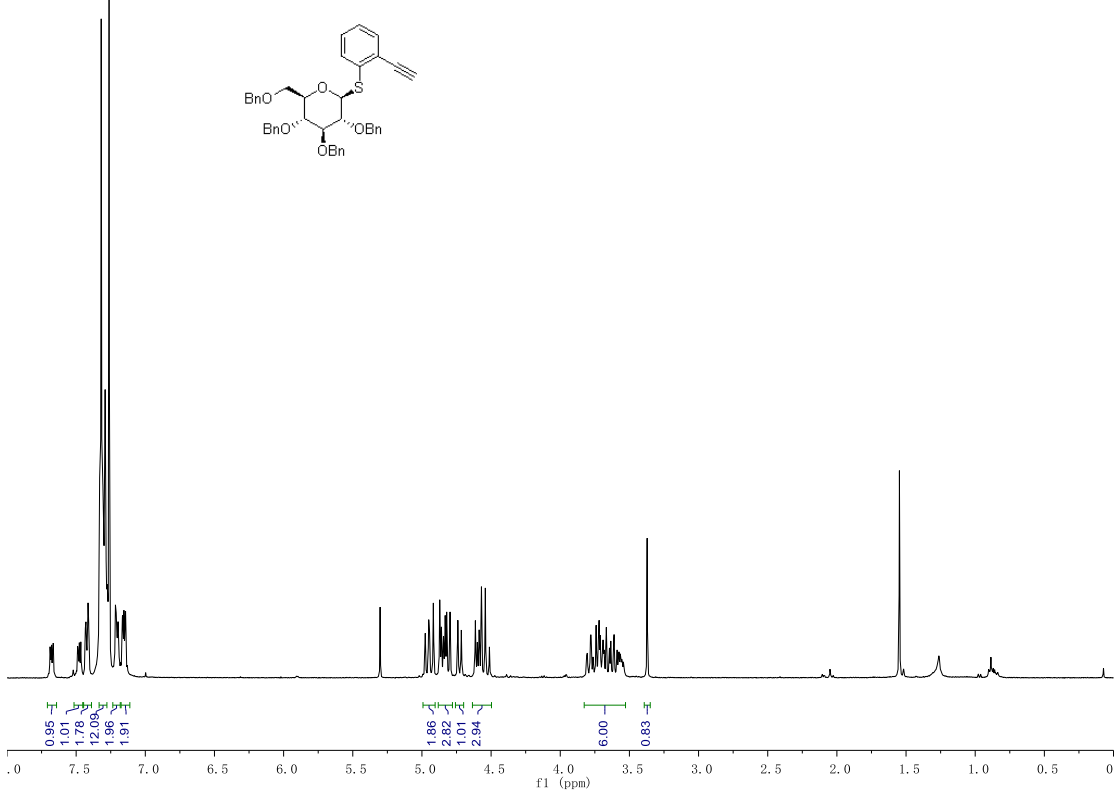




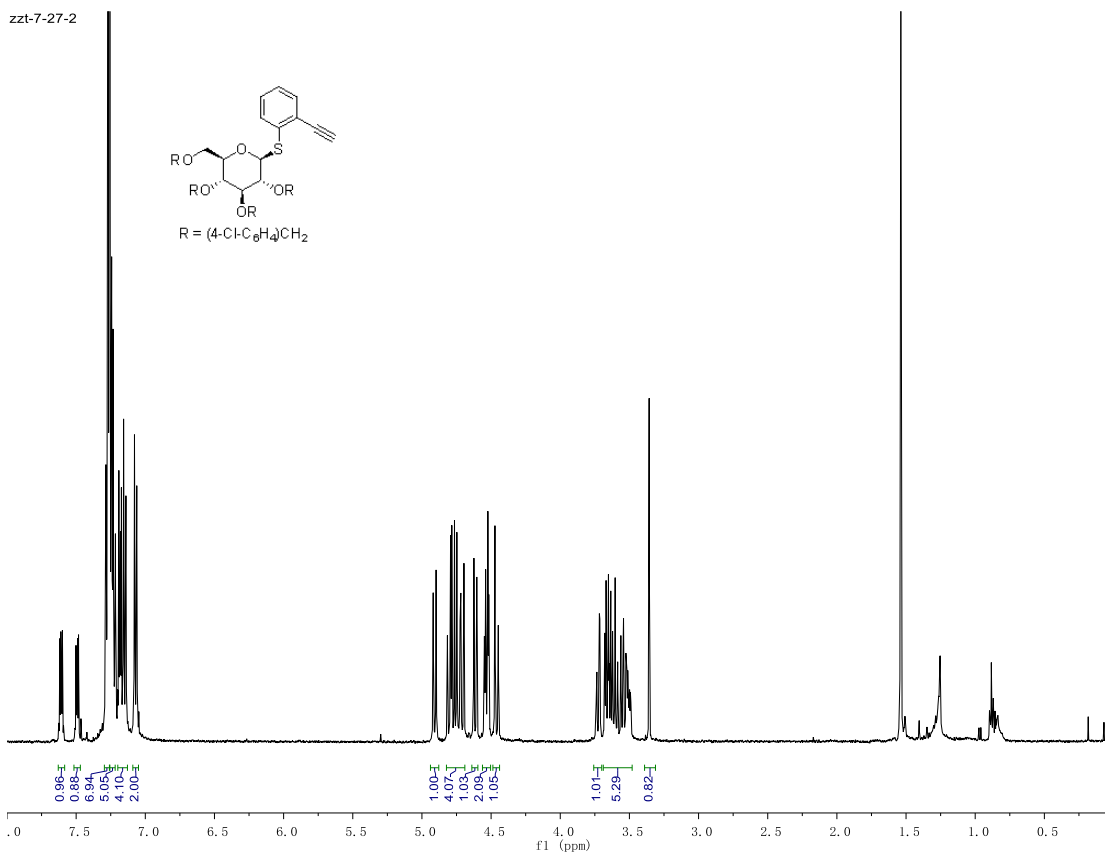
zzt-7-26-1-column



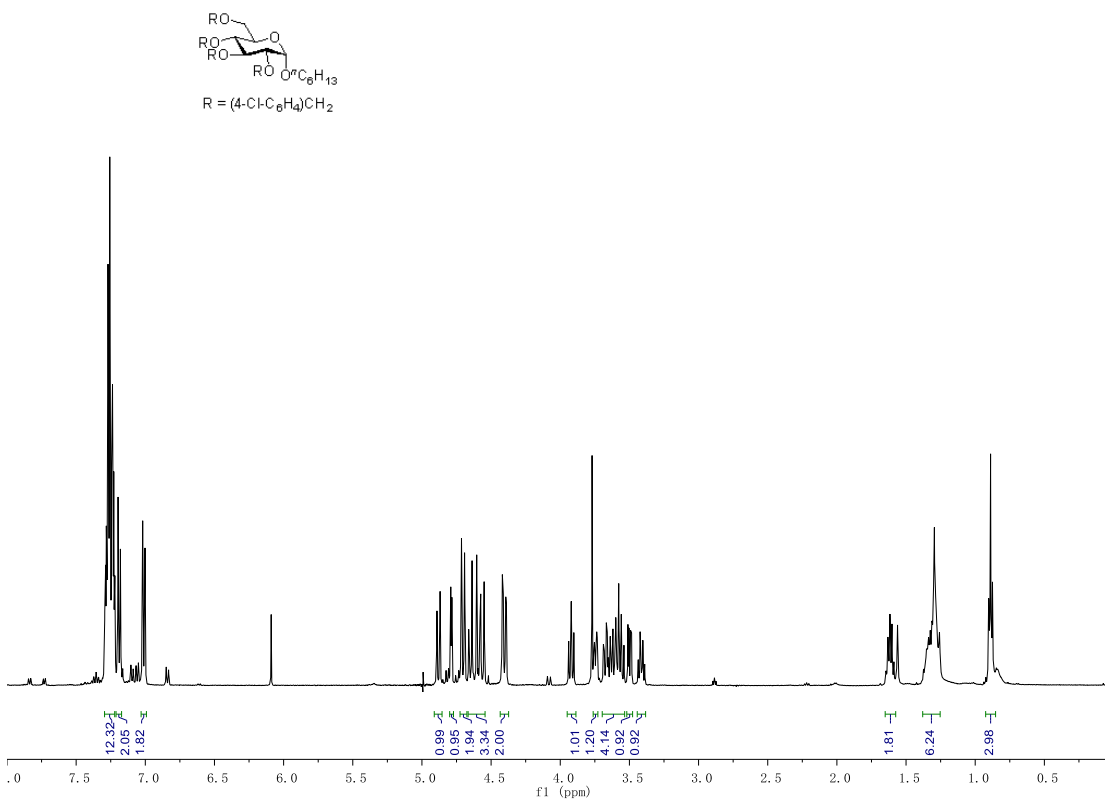
zzt-7-11-1-column

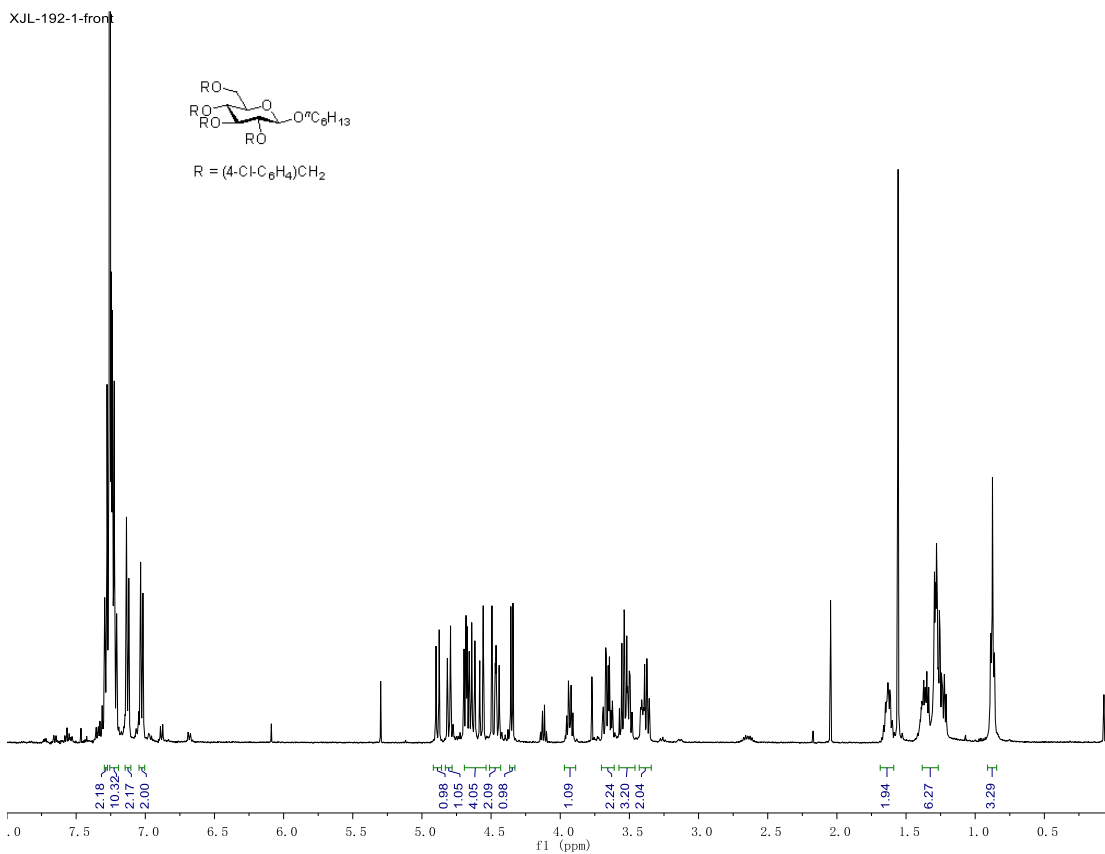


zzt-7-27-2

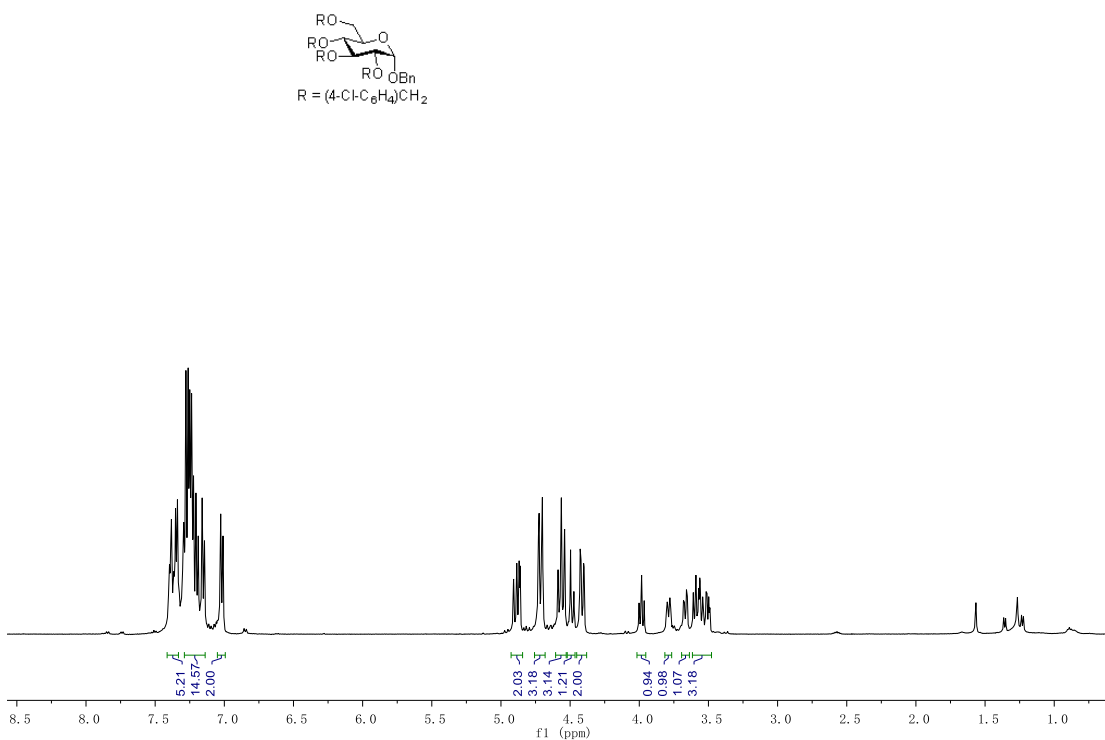


zzt-7-60-1-alpha-not_good

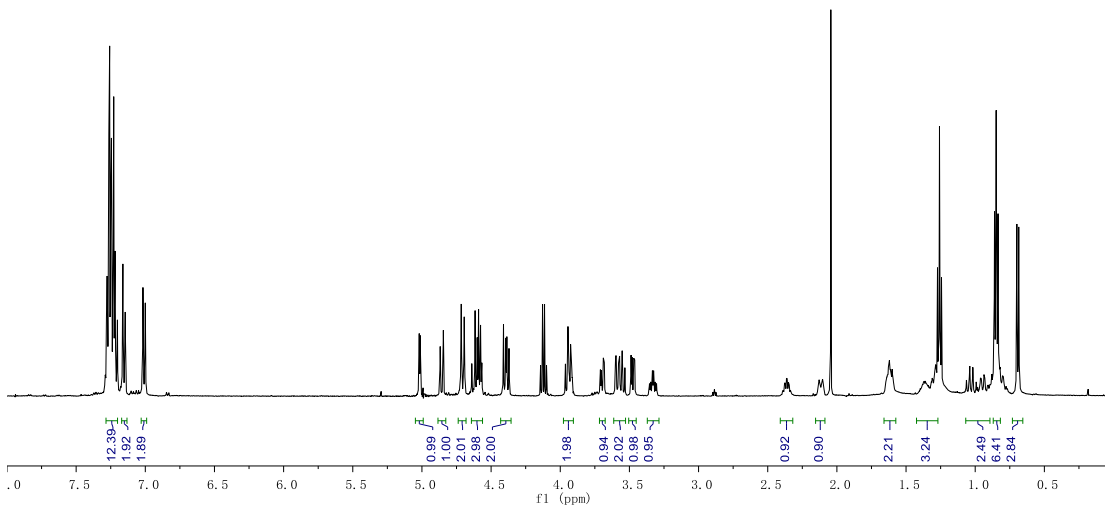
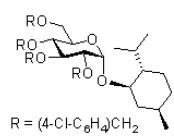




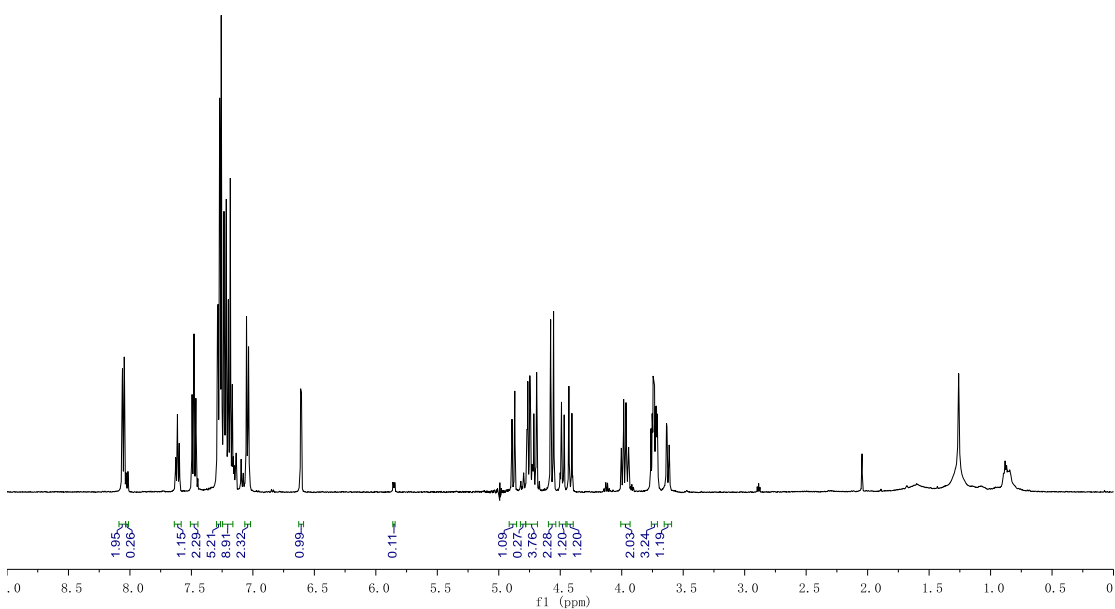
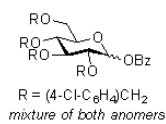
zzt-7-68-3-column



zzt-7-68-1



zzt-7-68-4



zzt-7-81-2-column

